Effects of Structures and Practices on the Circulation and Salinity Patterns of Galveston Bay, Texas

Junji Matsumoto
Principal Investigator

Gary L. Powell
David A. Brock
Christopher Paternostro

Texas Water Development Board
1700 North Congress Avenue
Austin, Texas 78711-3231

February 2005

TABLE OF CONTENTS

FIGURES

TABLES

EXECUTIVE SUMMARY

Purpose

The purpose of the Galveston Bay Modeling Project is to study the effect of structures and practices on the circulation and salinity in Galveston Bay. Five cases were studied: the *no diversion* case examined the effect of diverting flow from the Trinity River to the San Jacinto River; the *no power* case examined the effect of power plant withdrawal and discharge of bay water; the *Texas City Dike removal* case examined the effect of the Texas City Dike; the *Houston Ship Channel* (HSC) *removal* case examined the effect of the Houston Ship Channel; and the *natural* case examined a condition in which all these practices and structures were removed.

Model Simulation

TxBLEND-2D model was used to simulate the circulation and salinity pattern in Galveston Bay over an eight year period from 1989 to 1996. The results of simulations for the 1992 wet period and the 1996 dry period were closely examined by comparing each of the five cases to existing condition. Residual water velocity vectors were computed to determine net movement of bay water. Net flows through sections and passes were computed to find major pathways of freshwater through the bay system. Due to a calibration error this type of computer model cannot provide exact estimates of salinity and flow but can provide fair estimates on the system's response to different scenarios.

Net flows for Existing Condition

Total annual freshwater inflow averages 17.0 million ac-ft over the eight year period, of which 5% flows through Rollover Pass, 20% through San Luis Pass and 75% through the entrance channel to the Gulf. Approximately 92% of freshwater flows down to Bolivar Roads, then 9% goes into West Bay through the Texas City Dike section (mainly the City Channel) and 8% through Galveston Channel. These latter two make up the 17% that goes through West Bay.

No Diversion

The effect of diverting water between river basins on bay circulation is minimal because of the relatively small volume transferred between basins (from 1990-2000, on average 624 thousand ac-ft was diverted out of 9.4 million ac-ft Trinity River inflow, roughly 7%). The diversion's effect on salinity is insignificant during wet periods. During dry periods it has a greater influence but it is mostly local in effect. When river flow is not diverted, salinity decreases by 2.0 ppt near the mouth of Trinity River and by 0.7 ppt in Trinity Bay, but increases by 0.6 ppt in the upper HSC area (salinity differences are given on a monthly average basis, while percent differences in net flow are compared to total annual inflow).

No Power

The *no power* scenario removes the impact of the power plants which results in a 7% reduction in flow in the mid section (Eagle Point-Smith Point section), but the impact on flows through the entrance channel, San Luis Pass, and Rollover Pass is minimal. The

power plant operation has a salinity-leveling effect in that the process of withdrawing and discharging the cooling water promotes mixing of bay water. This leveling is more pronounced during dry periods than in wet periods. During wet periods it mostly affects salinity in the vicinity of the water intake and discharge sites. In Trinity Bay, the reduction in salinity is nearly zero but in mid-Galveston Bay near Redfish Reef and off Clear Lake salinity is about 0.5 ppt lower. The effect of the *no power* case during dry periods results in salinity increases of 2.5 ppt in Trinity Bay and 1 ppt Galveston Bay.

Texas City Dike Removal

Contrary to expectations, flow in West Bay will not increase noticeably if the Texas City Dike is removed. However, its composition will change. In the *dike removal* case, net flow through the entrance channel will decrease by 1% and net flow through West Bay, San Luis Pass, and Rollover Pass will increase by 0.6%. The composition of the West Bay flow changes from the existing condition of 8% Galveston Channel and 9% Texas City Dike section to 7% Galveston Channel and 11% Galveston Bay following dike removal. Removal also has an effect on salinity in both wet and dry periods. The major effect occurs in and near the Texas City Ship Channel and in West Bay. Salinity decreases by 4 ppt in the turning basin and by 2 ppt in mid-West Bay. Salinity in Galveston Bay and Trinity Bay also decreases by 0.6 ppt.

Houston Ship Channel Removal

Removal of the Houston Ship Channel increases net flow through the entrance channel by 5%, decreases West Bay and San Luis Pass flows by 4%, and decreases Rollover Pass by 1.5%. Because more Gulf water is carried into the upper estuary through the HSC, it also acts as a salinity-leveling device. Without the HSC, low salinity during wet periods lasts longer and high salinity during dry periods tends to get higher. Removal of the HSC has the greatest effect on upper Galveston Bay and the upper HSC area. During wet periods, salinity decreases by as much as 4 ppt near the Bay Tunnel, by 3 ppt near Morgan's Point, and by 1 to 2 ppt in Galveston Bay and Trinity Bay. During dry periods, salinity increases 1 to 2 ppt higher in both Galveston Bay and Trinity Bay.

Natural

The *natural* scenario brings the Galveston Bay system to a state where the above mentioned human activities have no impact. This case removes the salinity-leveling mechanisms of the power plant operation and the ship channel, as well as the Texas City Dike and stops river diversion. The combined effects result in the largest changes in salinity compared to existing conditions. As in the HSC removal case, salinity decreases much as 4 ppt near the Bay Tunnel, 3 ppt near Morgan's Point, and 1 to 2 ppt in Galveston Bay and Trinity Bay during wet periods. During dry periods, salinity is higher than as demonstrated in the HSC removal case. Under the natural scenario, salinity increases 2 to 3 ppt higher in Galveston Bay and Trinity Bay.

1. INTRODUCTION

Background

Among the issues concerning the bays and estuaries of the Galveston Bay area are the effects of natural and man-made perturbations on the circulation and salinity patterns of the associated estuarine ecosystems. Computer models based on fundamental physical principals of water movement and mixing can be used to simulate the hydrodynamics of bays and estuaries under conditions of interest to scientists, engineers, and decision-makers.

The initial effort at model development and use by the State of Texas focused on the influence of freshwater inflows on the Trinity-San Jacinto Estuary (TDWR 1981) and the need to analyze bay segment boundaries (TDWR 1982). These early models were coarse-grid, two-dimensional, finite difference, hydrodynamic and conservative mass transport models that were applied to show net circulation and salinity patterns under static monthly conditions. New modeling techniques are now available that utilize computationally fast, fine-grid, two-dimensional, finite element procedures to produce high-resolution, dynamic simulations of estuarine conditions for a year or longer (Longley 1994).

A similar modeling study was conducted for the Corpus Christi Bay National Estuary Program (Matsumoto, et al. 1997). A computer model, TxBLEND-2D, was used to examine the effect of cooling water used for the power plants located in Laguna Madre and Nueces Bay, the effect of the JFK Causeway, the effect of Corpus Christi Ship Channel, and the effect of freshwater diversion taken from the Nueces River. The periods 1988-1989 for dry conditions and 1991-1992 for wet conditions were simulated to compare with the existing condition.

Objectives

The objective of this project is to characterize the effects of existing structures (dike, navigation channels, and Gulf passes) and practices (recirculation of bay waters for industrial cooling and diversion of freshwater inflows) on the circulation and salinity patterns in Galveston Bay. These structures and practices can potentially alter estuarine circulation and mixing processes, influencing the transport of salts, sediments, nutrients, and plankton within the estuary.

To objectively characterize the effects of structures and practices, TWDB's hydrodynamic and salinity model was calibrated to simulate water movements and salinity gradients in Galveston Bay. The model was then applied to five case studies: (a) the effect of recirculating large volumes of bay water used for cooling of electric power generating plants, (b) the effect of the Texas City Dike on water exchange and circulation in adjacent bay areas, (c) the effect of the Houston Ship Channel on bay-wide circulation and salinity patterns, (d) the effect of freshwater inflow diversions taken from the Trinity River, and (e) the effect of impacts from these four cases combined.

It would be appropriate to use a three-dimensional model to study the localized effects of the Houston Ship Channel in greater detail, to adequately represent the interaction of deep channel waters with shallow bay areas in the context of stratified flow and salinities. However, implementing a three-dimensional model would require dramatically increased costs at the current stage of hardware and software development. In addition, more data collection would be required in order to calibrate the model. For a good first analysis and understanding of this very large estuarine system, the TWDB's two-dimensional model is more than adequate. For practical reasons, this analysis does not focus on a detailed study of the Houston Ship Channel's localized effects at this time; rather, this modeling study presents an overall picture of estuarine circulation and salinity patterns, based on a two-dimensional representation of the generally shallow, vertically well-mixed, Galveston Bay.

Galveston Bay Study Area

The Galveston Bay area (Figure 1.1) is a complex system of bays and waterways. It includes Trinity Bay, Galveston Bay, West Bay, East Bay, and other secondary bays. The Trinity River enters Trinity Bay at the northeast side of the system. San Jacinto River and Buffalo Bayou meet near the San Jacinto Monument and enter Galveston Bay at the northwest side of the system via the Houston Ship Channel (HSC). The bay system narrows at the mid point where Eagle Point lies at the west side and Smith Point at the east side. The Bolivar Roads area is situated between Galveston Island and Bolivar Peninsula. This is a busy intersection of ship channels with dike and spoil island. The main channel is the Houston Ship Channel that extends from the Gulf of Mexico, entrance channel, through Galveston Bay, to the Houston Harbor along Buffalo Bayou. The Gulf Intracoastal Waterway (GIWW) intersects with HSC at the Bolivar Roads. Galveston Channel connects the entrance channel to West Bay. The Texas City Ship Channel branches off of HSC at Bolivar Roads. The Texas City Dike lies at the east side of the city channel. West Bay is situated behind Galveston Island; and San Luis Pass connects the bay and the Gulf at its west end. Christmas Bay is located at the west end of the Galveston Bay system. East Bay is located behind Bolivar Peninsula and it is linked to the Gulf through Rollover Pass. The GIWW crosses the bay system through the East Bay and West Bay. The HSC is 40 to 45 feet deep and 400 feet wide. Galveston Channel is 40 feet deep and 300 feet wide. The Texas City Ship Channel is 40 feet deep and 200 feet wide, and the GIWW is 15 deep and 150 feet wide. The open bay part of Galveston Bay is 6 to 12 feet deep.

Previous Studies

Texas A&M University developed a 2D finite difference model for Galveston Bay to study storm surges in the bay (Reid et al 1968). University of Texas Hydraulic Engineering Laboratory developed a 2D finite difference model for the Galveston Bay to simulate the tidal hydrodynamics in shallow well mixed irregular systems (Masch et al 1969). Tracor developed a 2D finite difference model for Galveston Bay to study the water quality in the bay (Espey et al 1971). TWDB adapted the Masch's 2D finite difference model in the series of freshwater inflow needs studies of the major estuaries. One such application was on the Trinity-San Jacinto Estuary (TDWR 1981). Wang (1993) developed a 3D Galveston Bay model based on a curvilinear grid. The model was run for a month as part of an investigation of the influence of

freshwater inflow on salinity in the bay. The US Army Corps of Engineers, Waterway Experiment Station, modeled Galveston Bay to study the effect of the Houston Ship Channel expansion (Burger et al. 1995). They used the RMA10-WES model, a finite element 3D model. The impact of increased salinity intrusion was the primary concern. WES calculated water velocity and salinity using the model and this data was used to run an oyster model. The TxBLEND model was used in the Galveston Bay freshwater inflow needs study (TPWD 2001). The model was run to examine salinity conditions under selected monthly inflows to maintain the health of ecological system. TxBLEND is currently used on a daily base for predicting current over the next two days to be fed into an oil-spill model in case a spill occurs. The National Oceanic and Atmospheric Administration (NOAA) developed a 3D finite difference Galveston Bay model to complement the Physical Oceanographic Real Time System (PORTS) to nowcast and forecast currents along the Houston Ship Channel (Schmalz 1997).

The 3D models sited here were not run for long-term simulations. Wang's model ran for 29 days, and Schmalz' model runs for a 24 hour nowcast and a 36 hour forecast. RMA10 ran for nine and 12 months, a relatively long period of time, but was simulated using a super computer. In spite of technological advancement, it is still too much of a computational burden to run a 3D model for multiple year simulations such as we have done in this study. Given these limitations and a lack of additional data to support verification of a 3D model, we have chosen to use a 2D model to address the goals of this study.

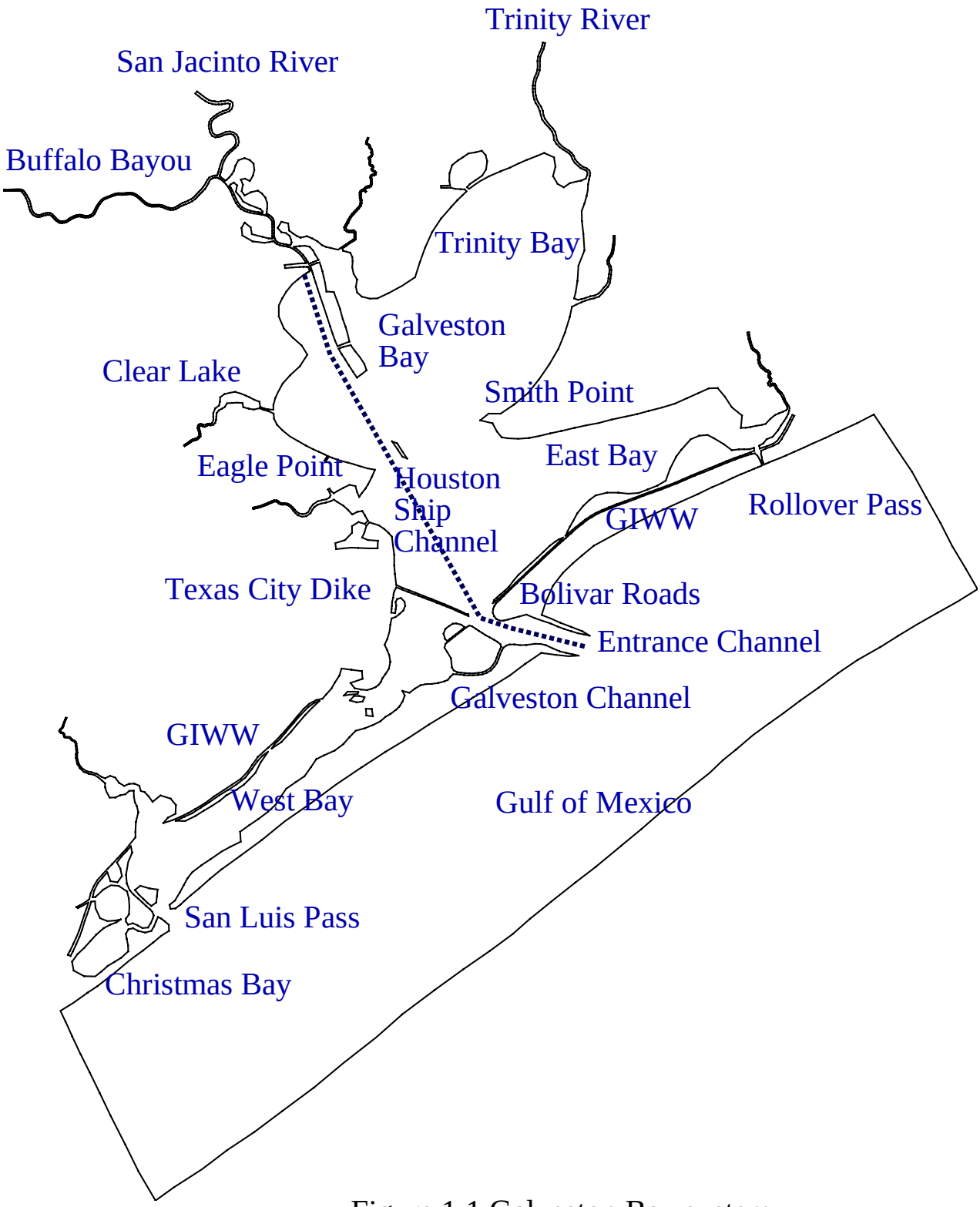

Figure 1.1 Galveston Bay system

2. TxBLEND MODEL AND INPUT DATA

TxBLEND-2D Model

TxBLEND-2D is a two-dimensional finite element model for simulating water circulation and salinity distribution in bays and estuaries. The model is a modification of the BLEND model developed by Dr. William Gray of Notre Dame University. BLEND is based on the wave continuity equation (Lynch and Gray 1979) with linear triangular elements. The wave continuity equation has particularly desirable characteristics that suppress numerical noise. The wave equation evolved into a generalized continuity equation (Kinnmark 1986; Kolar, et al. 1992) which contains a numerical parameter G (or bigG) to enhance the mass conservation property. TxBLEND is based on the generalized wave continuity equation, with various options and modifications added for estuarine application. The model is computationally efficient mostly due to the use of linear triangular elements and the sparse matrix solver. With TxBLEND, a high resolution grid consisting of ten thousand elements or more can be employed to represent bay regions and simulate multiple years with run times of 20 to 30 hours on a PC.

For the Galveston Bay application discussed herein simulations took approximately 27 CPU hours to simulate 8 years, 1989-1996, on a Dell workstation with 2.2 GHz processor. This model has been successfully used to simulate Texas bays and estuaries including San Antonio Bay (Longley 1994), Galveston Bay (Solis 1994), and Corpus Christi Bay National Estuary Program area (Matsumoto et al 1997). A mathematical description of TxBLEND and the numerical procedure are presented in Appendix I.

Input Data Preparation

Inputs to TxBLEND include data on the finite element grid and nodal coordinates, bathymetry, tides, wind, evaporation, precipitation, river inflow, and salinity. This section describes the sources of information and how data were prepared.

Computational Grid

Figure 2.1 shows the computational grid for the existing condition. It was prepared using the grid generation program SMS (Surfacewater Modeling System from ems-i). The software produces an incidence list that describes the connectivity of the triangular elements, nodal coordinates, and bathymetries. The computational grid went through many modifications prior to final model application. The grid employed in this study consists of 5,070 nodes and 8,041 (linear triangular) elements. Figure 2.2 is a close-up of the computational grid showing the Bolivar Roads area. The finite element grid is well suited to model complicated places, such as at the intersection of major and minor ship channels, spoil islands and the dike.

Bathymetry

Bathymetric information was obtained from the NGDC (National Geophysical Data Center, NOAA) Coastal Relief Model. Figure 2.3 shows bathymetry in the model and Figure 2.4 shows bathymetry of the Bolivar Road area.

Tide

Tide at Galveston Pleasure Pier was obtained from NOAA/NOS/CO-OPTS Water Level Data. The data was adjusted to MSL (4.61 ft) for the model application. After test runs, to account for attenuation between the Gulf boundary and the shore where tides were recorded, tides were amplified by 10% to apply at the model's Gulf boundary. Tide gages inside the bays are part of the Texas Coastal Ocean Observation Network (TCOON) administered by the Texas General Land Office and the TWDB. Tide data from TCOON gages in the Galveston Bay area were made available by the Conrad Blucher Institute for Surveying and Science (CBI), Texas A&M University-Corpus Christi.

Wind and Temperature

Meteorological data (wind speed, wind direction, air temperature, dew point temperature) collected at Galveston Island, Scholes Fields from 1980 to September 2001 were obtained from the National Climatic Data Center (NCDC).

Precipitation

Precipitation data from the TWDB hydrology data sets from 1960 to 2000 for the lower Galveston Bay area were used to prepare input data to the TxBLEND model. Recent data in the database were originally obtained from Hydrosphere, Inc. and includes the NCDC Summary of the Day - Climate data. (Precipitation data were calculated by Thiessen's polygon method. The data for Galveston Airport contributes the most.)

Evaporation

Recorded daily evaporation data applicable to Galveston Bay areas is not available. Therefore, appropriate daily evaporation rates were estimated by the Harbeck equation as implemented by Brandes and Masch (1972),

$$Evap = N \cdot wspd \cdot (\phi_s - \phi_a)$$

where *Evap* is evaporation in inches per day, *N* is a mass transfer coefficient, *wspd* is wind speed in miles per hour at some height above the water surface, ϕ_s is saturation vapor pressure in millibars, and ϕ_a is actual vapor pressure of air in millibars. Vapor pressure terms ϕ_s and ϕ_a are computed by

$$\phi_s = 3.28 \cdot \exp(0.0314 \cdot T_a - 0.0164) \text{ and } \phi_a = 3.28 \cdot \exp(0.0304 \cdot T_d)$$

where T_a is air temperature and T_d is dew point temperature. The mass transfer coefficient is computed as

$$N = 0.00338 / A^{0.05}$$

where *A* is the water surface area in acres. In application of the relationships to San Antonio Bay, Brandes and Masch used 0.00186 for *N*.

Evaporation data were computed from the NCDC temperature and wind data. First, hourly evaporations were computed, and then they were averaged to compute daily evaporation. These daily values were tabulated to compute monthly evaporations and average monthly evaporations as well as yearly average evaporation. This yearly average value was compared with earlier estimates (TWDB Evaporation database, 2003) for the Galveston Bay area. The ratio of these annual averages was used to adjust the generated evaporation. Also checked was the monthly distribution of the generated evaporation.

Figure 2.5 illustrates the net evaporation-or the difference of evaporation and precipitation-for the Galveston Bay area for 1992 and 1996. In the earlier part of 1992 there were many large precipitation events, while in the earlier part of 1996 there were very few precipitation events.

River Inflow

Ungaged inflows were estimated using a TWDB rainfall-runoff model TxRR (Matsumoto 1992). Diversion and return flow data were compiled from TCEQ records. The combined inflow is the sum of gaged inflow, ungaged inflow, return flow and diversion (which is treated as negative). The gaged inflows are the USGS streamflow data. For the Galveston Bay it is USGS Streamflow Gage 08066500 at Romayor.

Data from years 1989-1996 were used for model calibration as well as for test cases. Table 2.1 lists monthly and annual total inflows from 1941 to 1999 and the ranking from driest to the wettest years. Figure 2.6 graphically presents 59 annual inflows. Year 1996 was a dry year, ranked 14th in the 59 year period; 1992 was a wet year, the wettest in the 59 year period. Figure 2.7 shows monthly inflows from 1984 through 1999. Figure 2.8 shows monthly inflows in 1992, 1996, and the average monthly inflows. Large inflows occurred in the earlier part of 1992, while in the earlier part of 1996 inflows are low. These two years, 1992 representing a wet year and 1996 representing a dry year, are used in model simulations to compare each of the five scenarios to existing conditions for wet and dry years.

Table 2.2 lists summary statistics of the annual inflows. In the table it should be noted that total surface inflow is 11.1 million ac-ft, evaporation is 1.4 million ac-ft, and precipitation is 1.5 million ac-ft. The volume of evaporation is about the same as precipitation, and they are roughly 13% of the total surface inflow.

Salinity Data

Salinity data is an important tool for model calibration. Salinity data has been collected by TWDB, TDH, and TCEQ at sites within the study area over many years. The TPWD also collects salinity data at each location sampled for fisheries species biomass. Since 1987, through deployment of HydroLab Datasondes at strategic locations, TWDB has collected a fairly continuous record of environmental variables including salinity, temperature, dissolved oxygen, and pH.

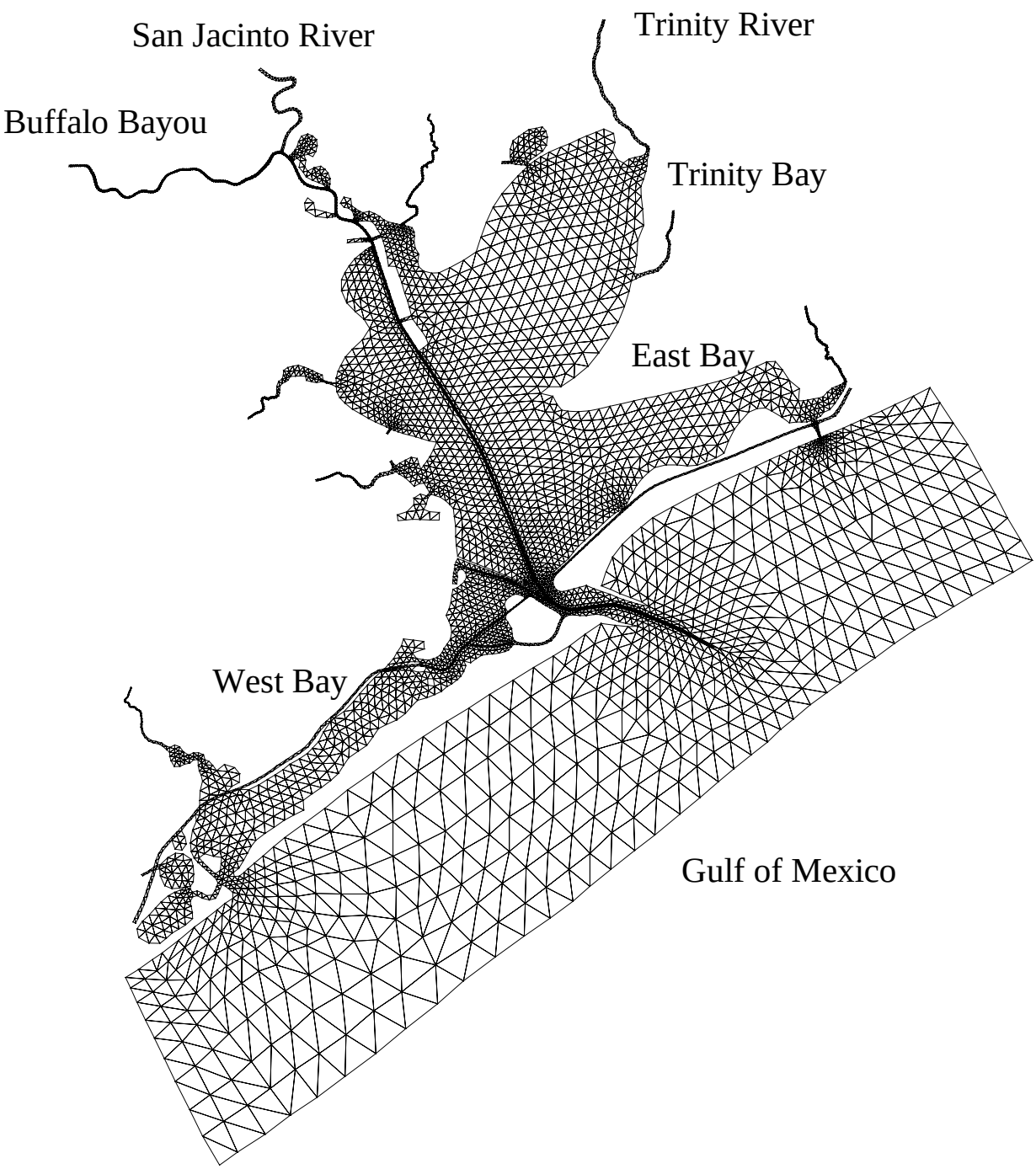

Figure 2.1 Computational grid for Galveston Bay Model
number of nodes: 5070, number of elements: 8041

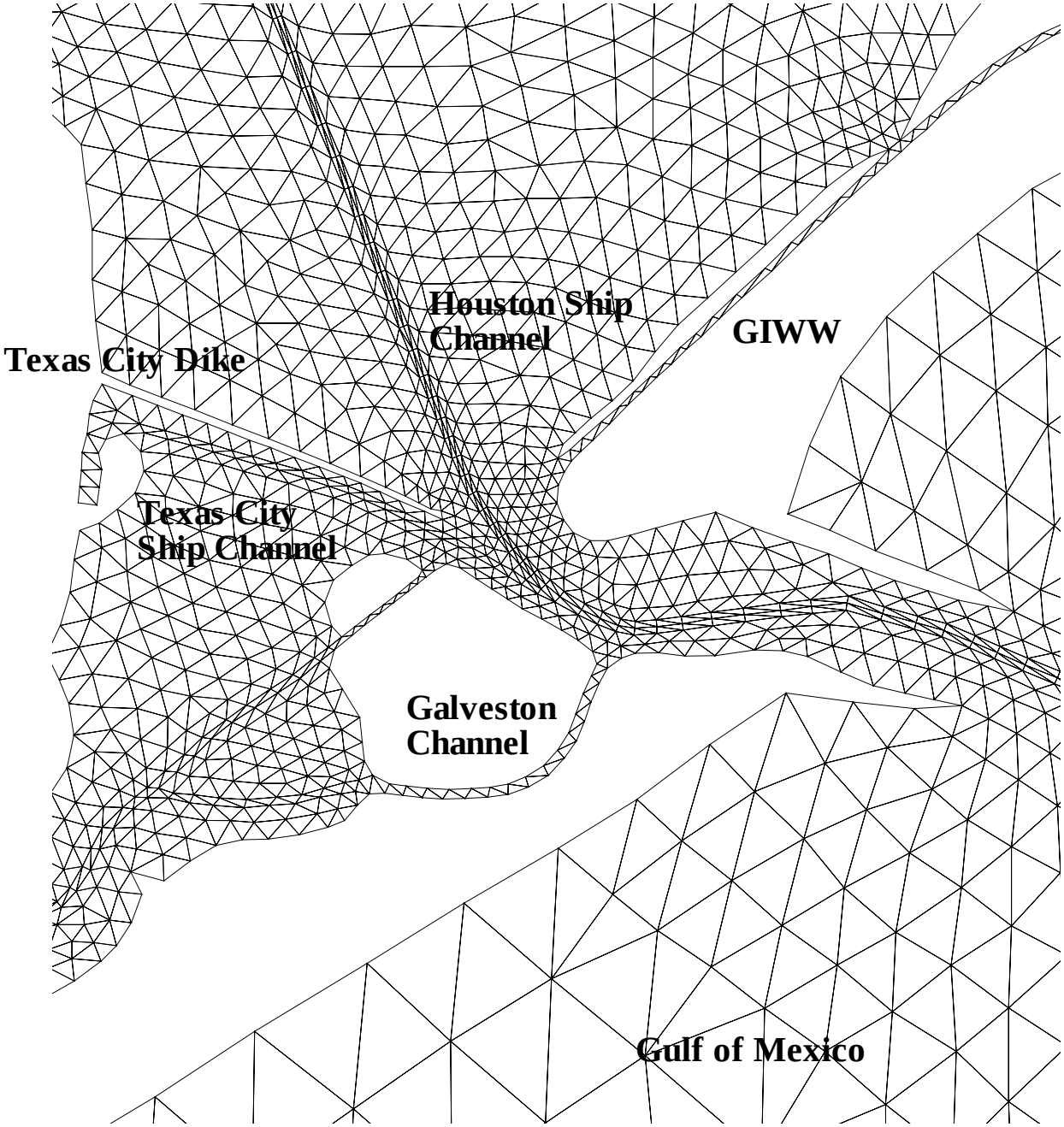

Figure 2.2 Computational grid for Galveston Bay Model
Entrance Channel and Bolivar Roards Area

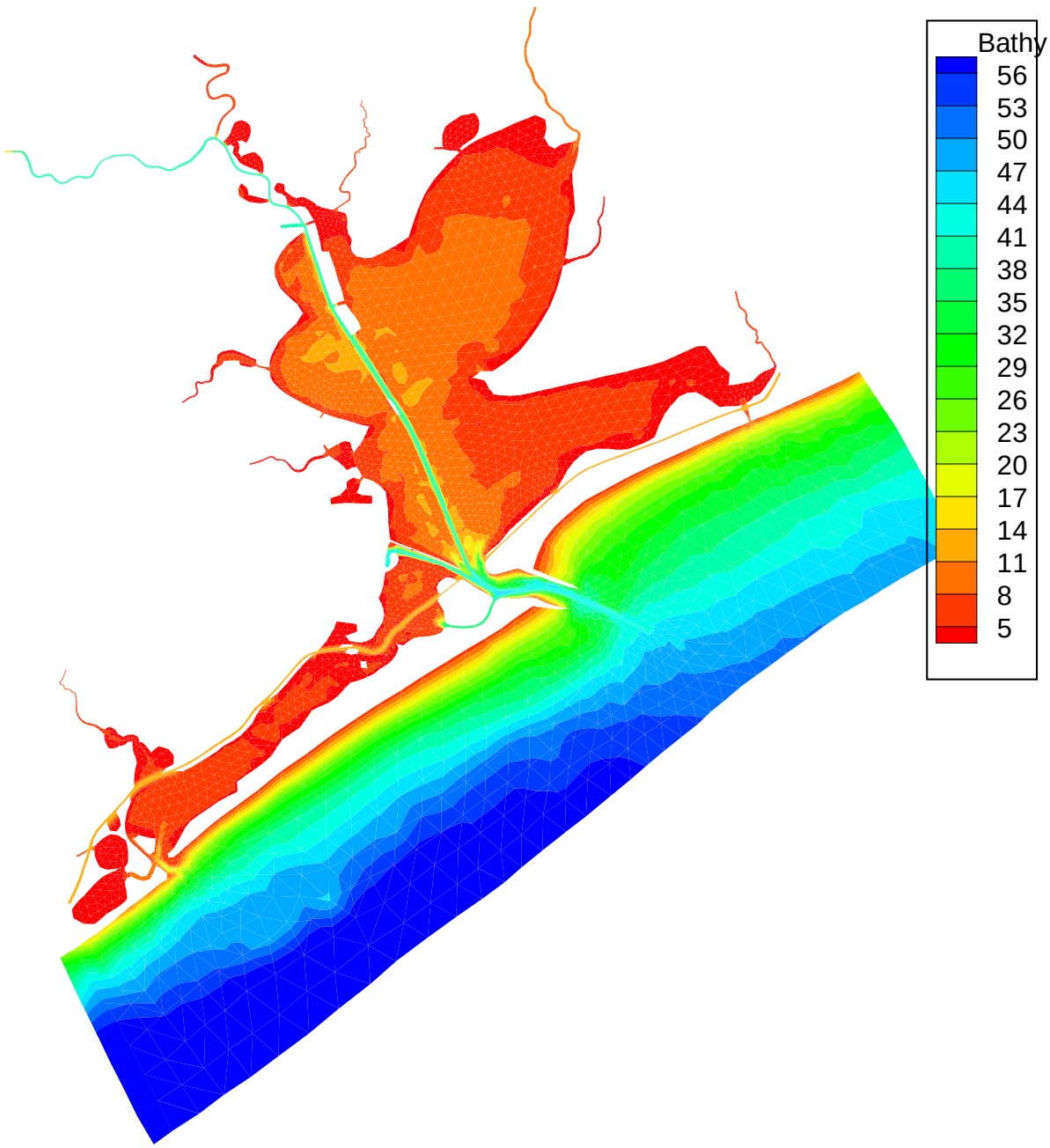

Figure 2.3 Bathymetry (ft) of Galveston Bay Model

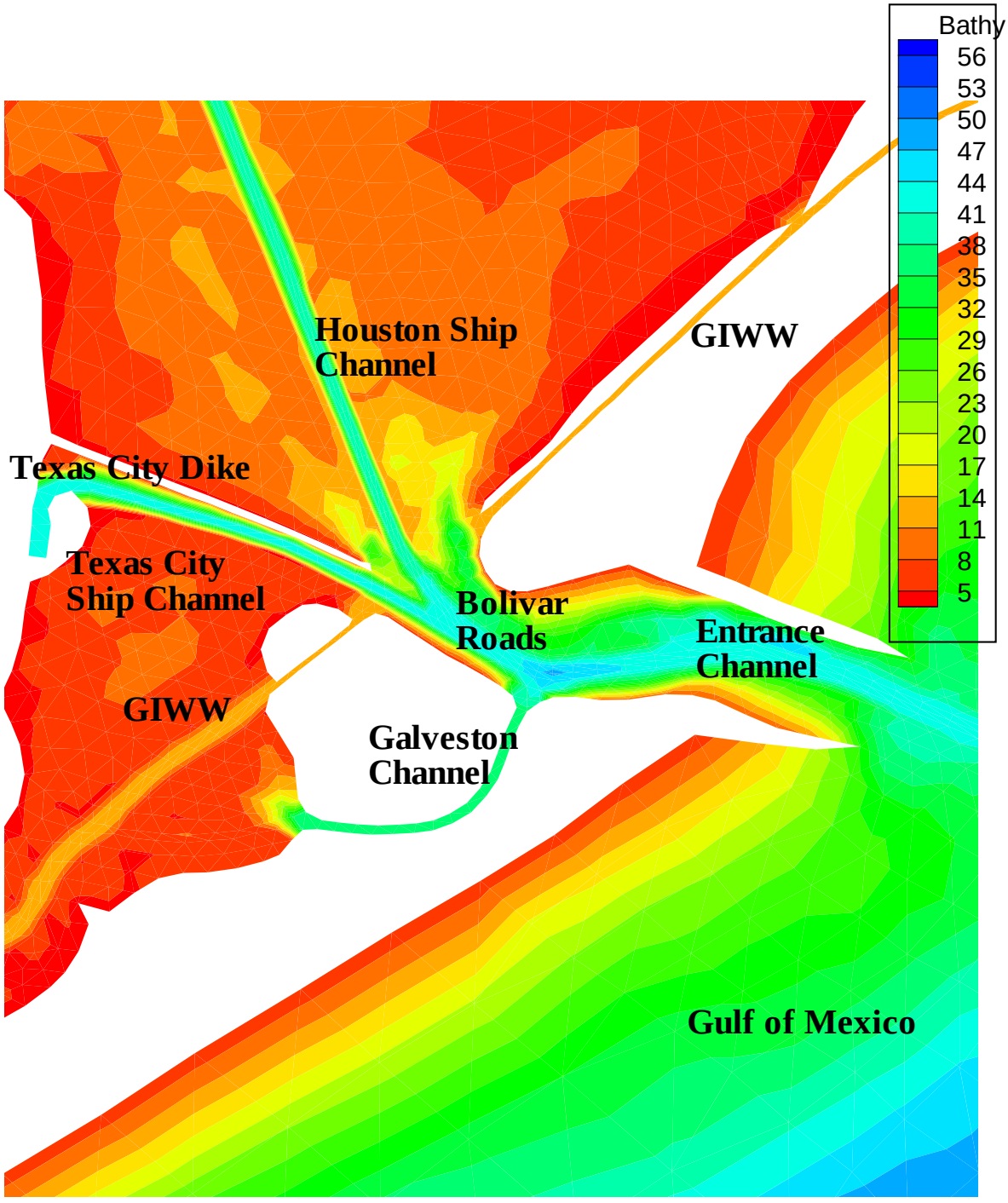

Figure 2.4 Bathymetry (ft) in the Entrance Channel and Bolivar Roards Area

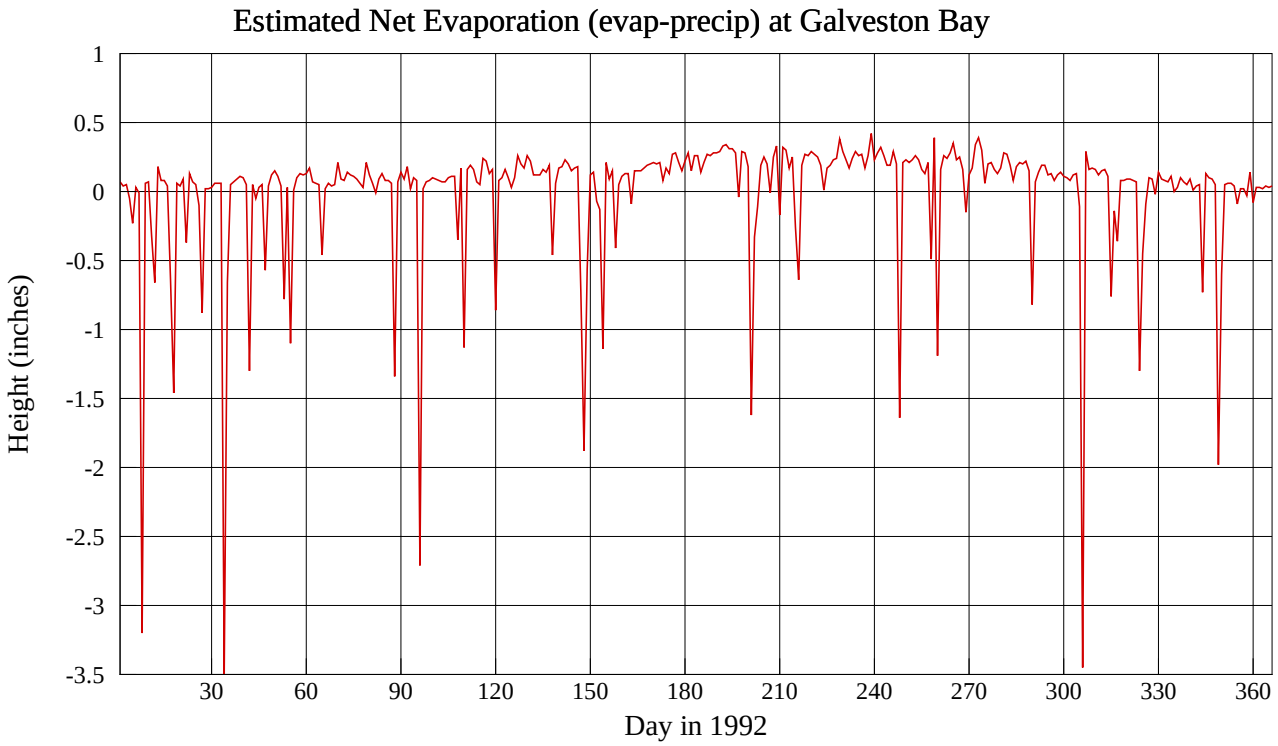

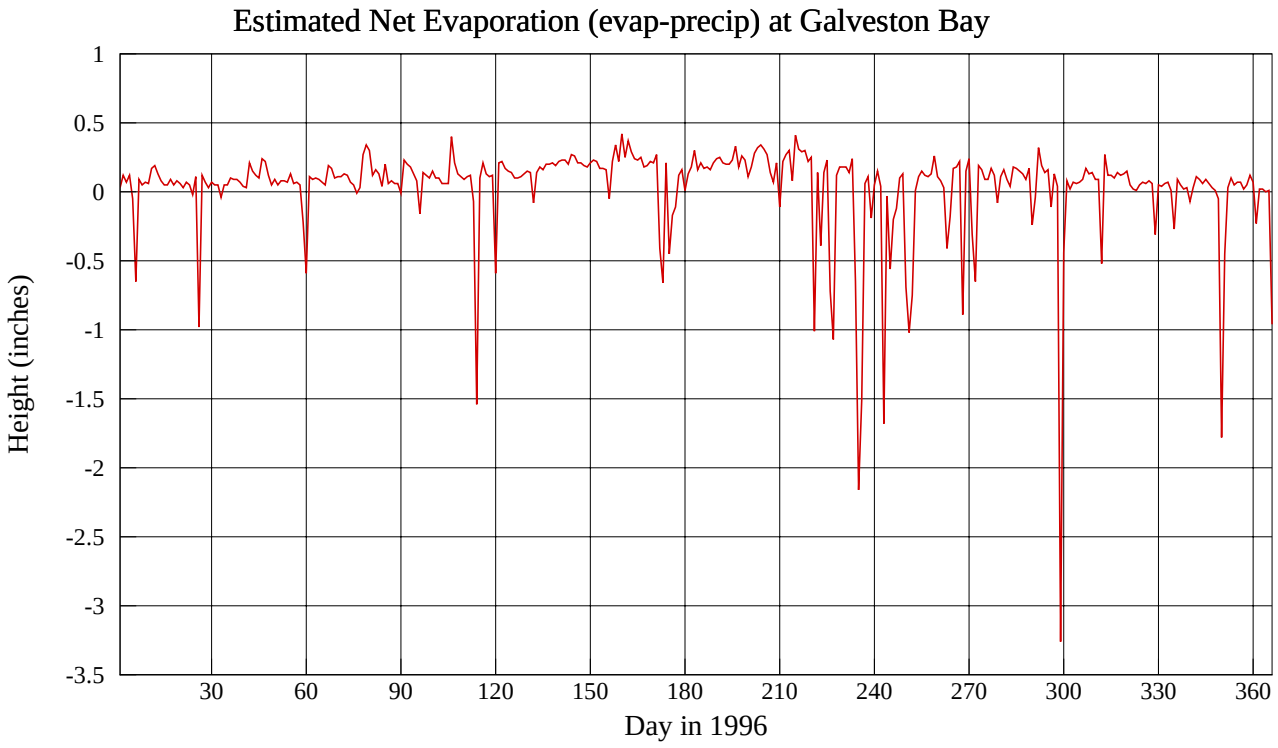

Figure 2.5 Estimated net evaporation at Galveston Bay for 1992 (wet period) and 1996 (dry period)

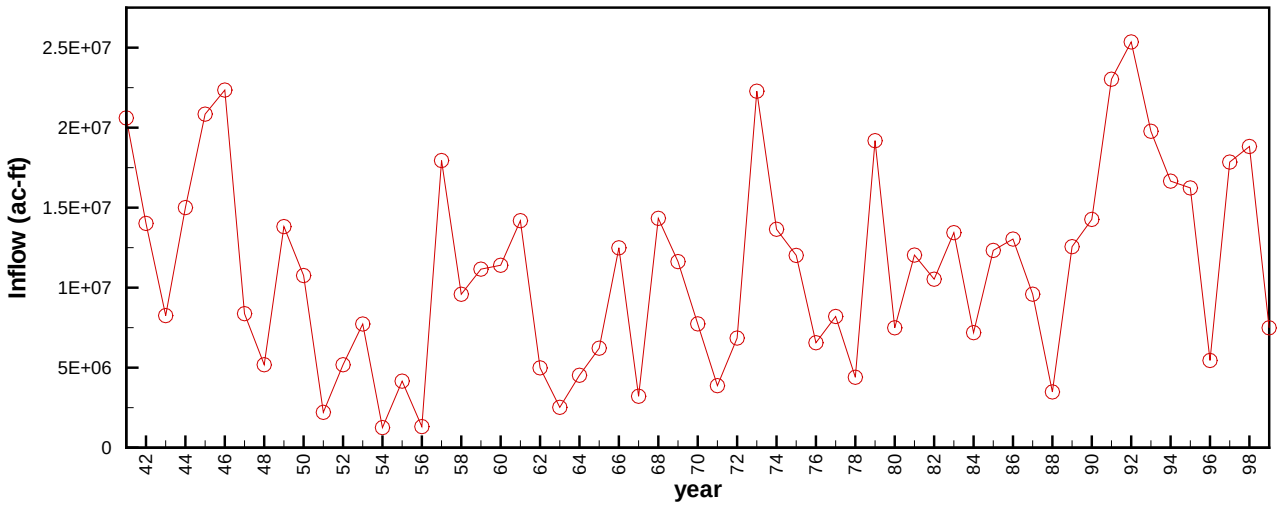

Figure 2.6 Galveston Bay annual inflows 1941-1999

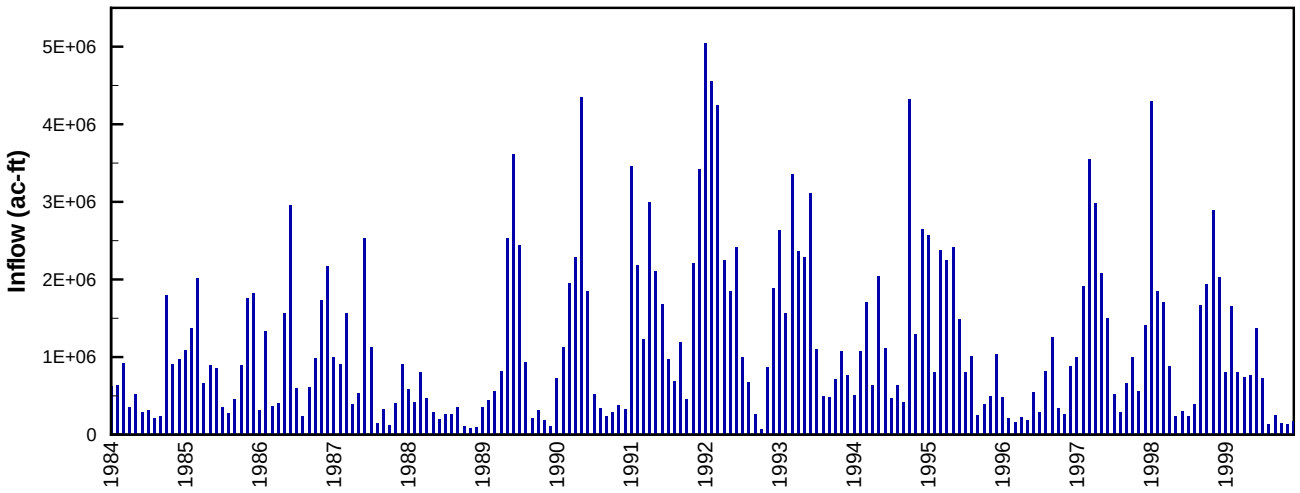

Figure 2.7 Galveston Bay monthly inflows 1984-1999

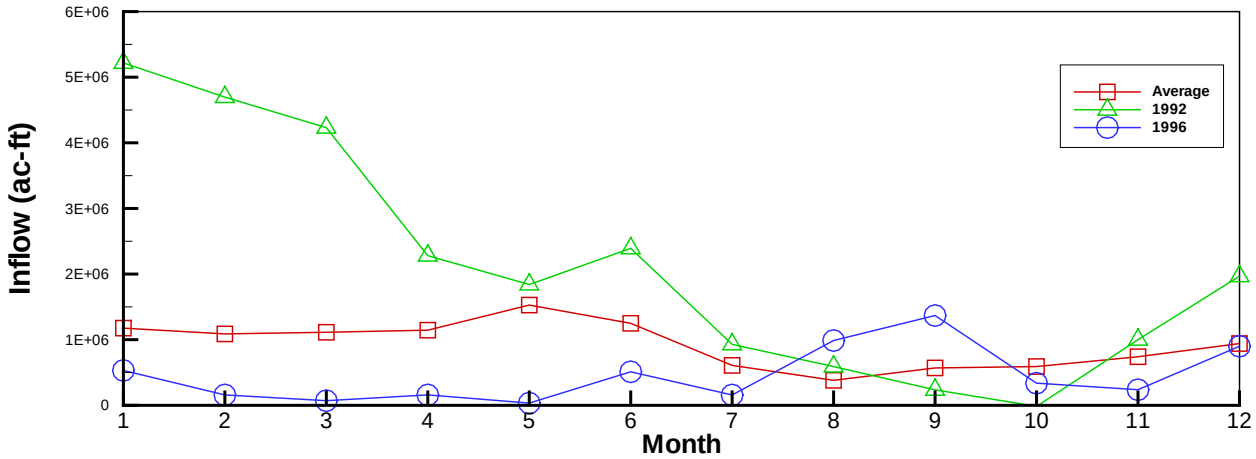

Figure 2.8 Average monthly inflows, 1992 and 1996 inflows

Table 2.1 Galveston Bay inflows (ac-ft) 1941-1999

Year	January	February	March	April	May	June	July	August	September	October	November	December	Total	Year	Flow	Rank	**Year**
41	1775641	1283346	2493074	1734134	2453469	2686074	2364663	145841	1766755	1991167	1551385	360407	20605956	1941	1254190	1	54
42	290998	369133	618367	2839775	3792425	1952343	1791005	650254	576476	174916	408551	553949	14018192	1942	1316888	2	56
43	1172044	315898	641483	783469	668003	843741	2191709	126456	218525	147334	609053	536353	8254068	1943	2210323	3	51
44	2643227	1437767	2462447	384230	4608566	754003	-58305	120199	460304	234080	413719	1544556	15004793	1944	2521798	4	63
45	2213119	1521117	2690425	5411186	1108846	985065	846578	2550254	644992	987056	374340	1510541	20843519	1945	3214281	5	67
46	2177086	2104224	1817328	514789	3730491	3907132	798408	124762	866341	197635	4953692	1158310	22350198	1946	3482406	6	88
47	2374179	311378	1383958	611716	1538726	334705	244419	272574	62091	-18581	267913	990997	8374075	1947	3876056	7	71
48	956256	1198167	1211873	484398	915337	149471	94203	-51337	39105	-53940	205824	34663	5184020	1948	4159476	8	55
49	493970	1566795	2057343	1673195	305278	872746	499343	142919	70307	4044920	204839	1886248	13817903	1949	4400535	9	78
50	1553930	2647753	824507	1104747	1352164	1729661	531552	141237	775145	97234	1929	-1806	10758053	1950	4526662	10	64
51	216383	135878	412405	68730	71564	532680	111992	-73831	781141	-69413	-16629	39423	2210323	1951	4988253	11	62
52	64264	910888	264307	1671954	1024937	301943	386413	-147567	-92631	-166290	247294	716852	5182364	1952	5182364	12	52
53	347798	756183	509096	206878	3468872	556747	39279	709975	-124972	-25701	469934	817122	7731211	1953	5184020	13	48
54	326855	-437	3008	122047	425776	-88035	88536	-24519	-87305	231631	228798	27835	1254190	1954	5452404	14	96
55	385401	1259853	114796	668941	245062	44455	45804	1093433	133884	-43271	-68431	279549	4159476	1955	6217387	15	65
56	230401	464815	102655	172646	337998	76251	-138859	-57342	-132588	-49572	4371	306112	1316888	1956	6560459	16	76
57	11742	159655	1551216	2130686	4105433	3414559	689701	605105	433922	2023044	2135492	685894	17946449	1957	6850039	17	72
58	1617305	1112583	505794	633894	2366112	396782	425113	-45749	2066379	365074	17673	127133	9588093	1958	7189032	18	84
59	282624	2132553	133787	2118670	1493340	283987	1692535	728443	-7566	903979	309789	1085258	11157399	1959	7492395	19	99
60	1475164	1415231	471587	278071	158639	1425064	329765	1102704	33974	1016252	974585	2720977	11402013	1960	7493285	20	80
61	2920388	2371962	772778	590494	50716	2030635	1261905	190506	2276155	-53687	1024257	750155	14186264	1961	7731211	21	53
62	436055	239300	289164	320280	453325	613354	61712	267479	266094	485689	356758	1199043	4988253	1962	7737219	22	70
63	706640	546124	138948	165430	381425	308010	70403	-53929	109536	-106684	52111	203784	2521798	1963	8198630	23	77
64	364925	661165	700219	378355	192482	97116	107080	52411	260133	231039	400033	1081704	4526662	1964	8254068	24	43
65	346378	1011812	654724	350830	1290537	929389	58994	123451	80552	336	272485	1097899	6217387	1965	8374075	25	47
66	902913	1471113	308703	1907775	4686447	790360	552879	927626	216498	301292	338557	88805	12492968	1966	9588093	26	58
67	109296	144778	100103	566222	492438	224639	289035	30695	163073	196676	466525	430801	3214281	1967	9591366	27	87
68	1618470	598655	1047751	2274022	3225559	3330141	675251	118441	332822	178993	335935	596998	14333038	1968	10531140	28	82
69	258716	1495465	1909380	2357238	3268775	869082	326147	177751	114450	134079	117655	599726	11628464	1969	10758053	29	50
70	416937	343751	2023970	744151	1468145	289019	202753	84899	685219	1248689	137591	92095	7737219	1970	11157399	30	59
71	-4003	66423	72165	190089	83888	57965	2221	329690	690168	46309	292948	2048193	3876056	1971	11402013	31	60
72	1671614	393598	246627	392413	1686870	358264	311154	26259	573024	18627	739281	432308	6850039	1972	11628464	32	69
73	1191225	1114197	2426589	3409097	1682661	4123327	967905	617961	1342087	3125813	1123928	1153398	22278188	1973	12018687	33	75
74	2844063	636074	533439	424767	1319634	126361	155321	295513	1379806	500011	3378655	2056243	13649887	1974	12037642	34	81
75	1192795	1956782	757305	1489975	2242691	1863396	540512	884558	257184	351151	275119	207219	12018687	1975	12329209	35	85
76	126295	71966	222752	526415	185267	1640832	714165	72235	342463	422706	481845	1753518	6560459	1976	12492968	36	66
77	720042	1312042	688369	2516017	716111	473403	85879	192155	338923	33950	719522	402217	8198630	1977	12562676	37	89
78	1298463	995833	356136	66318	9251	456974	134787	28586	331561	-64442	522193	264875	4400535	1978	13038795	38	86
79	1495067	1500463	1661712	3251085	1910564	1953065	2705504	599431	2675420	232984	578667	624359	19188321	1979	13437597	39	83
80	1631685	1015639	1022898	670021	1755648	143889	123272	-24314	612099	305584	97713	139151	7493285	1980	13649887	40	74
81	184313	138756	93362	160543	892249	3945933	1260835	394184	1009346	1309145	1749379	899597	12037642	1981	13817903	41	49
82	713784	702733	584275	935861	1984858	1494751	759966	438187	9079	44794	901048	1961804	10531140	1982	14018192	42	42
83	837275	1918124	1486043	282717	1682061	813961	1155564	2130636	1966390	118381	336541	709904	13437597	1983	14186264	43	61
84	666557	607551	868908	219481	488293	142159	198483	94210	185109	1892476	872972	952833	7189032	1984	14265152	44	90
85	1121405	1465383	2109415	575062	816858	820392	326893	138438	430765	921880	1780226	1822492	12329209	1985	14333038	45	68
86	274904	1308110	287366	281631	1549919	2987143	406807	172412	594626	1068530	1851731	2255616	13038795	1986	15004793	46	44
87	1042580	935444	1478195	242095	542314	2600814	1053911	12182	359575	-27116	414885	936487	9591366	1987	16234379	47	95
88	589580	389109	842279	453016	144199	103703	242646	178609	418112	-437	9827	111763	3482406	1988	16658603	48	94
89	489646	407094	532557	727213	2504677	3916080	2412793	933749	85394	290771	196838	65864	12562676	1989	17850175	49	97
90	810501	1162948	1995627	2271074	4370924	1699118	500693	180382	288737	258635	368783	357730	14265152	1990	17946449	50	57
91	3689095	2301431	1182604	3077699	2227020	1648429	929155	654620	1251126	360754	2242195	3464053	23028181	1991	18824216	51	98
92	5217431	4696104	4230400	2280320	1840669	2392115	927916	589992	235141	-16937	999255	1966499	25358905	1992	19188321	52	79
93	2786372	1575570	3435160	2385980	2256404	3167578	892470	301087	385360	765893	1085949	737452	19775275	1993	19775275	53	93
94	503705	1019739	1672421	603372	2036977	1069746	322418	664224	375486	4386321	1227417	2776777	16658603	1994	20605956	54	41
95	2602571	834426	2464720	2227630	2504583	1456210	804742	950872	192507	399890	596804	1199424	16234379	1995	20843519	55	45
96	531181	158253	70798	158747	34084	510488	157771	987720	1368346	337443	237879	899694	5452404	1996	22278188	56	73
97	1143588	1971254	3679814	3073658	2106134	1433740	401822	138851	751525	1040844	625147	1483798	17850175	1997	22350198	57	46
98	4505339	1932173	1664624	754534	64157	298354	64646	433450	1916677	2057213	3071704	2061345	18824216	1998	23028181	58	91
99	818229	1636912	793886	640057	794891	1387032	759212	21700	235814	60323	89045	255294	7492395	1999	25358905	59	92
Average	1176007	1088323	1113146	1145014	1527369	1249599	608466	380860	569333	590601	740060	941039	11129816				

Table 2.2 Galveston Bay annual inflow statistics for 1941-1999, ac-ft

Flow	Min	Median	Mean	Max
Gage	1053280	7834912	8044305	20799544
Model	356000	2574000	2850690	6407018
Divert	106000	240000	268200	619245
Return	122000	477594	425830	695000
Evap	1031000	1459612	1438164	1684177
Precip	798840	1481391	1515355	2885848
Surface Inflow	1871280	11061380	11052624	25150552
Balance	1254190	11157400	11129816	25358904

Surface Inflow=Gage+Model-Divert+Return
Balance=Surface Inflow-Evap+Precip

3. MODEL CALIBRATION

TxBLEND simulates hydrodynamics (circulation patterns) and salinity distribution. The model was first calibrated to hydrodynamic data and then to salinity data. Data collected during TWDB's Galveston Bay intensive inflow studies were used to calibrate model hydrodynamics. Figure 3.1 shows intensive inflow survey sites used for velocity calibration and Figure 3.2 shows tide gages used to calibrate tidal elevations. Because salinities change much more slowly within a bay system than velocities and tidal elevations, long-term salinity data is desirable for model calibration. Salinity data from the TWDB's Ambient Bay Water Quality Data Collection Program supplied time series long enough to realistically demonstrate model performance. Figure 3.3 shows the water quality data collection sites used for salinity calibration. (See the TWDB web site for the 1989 Galveston Bay intensive inflow study: http://hyper20.twdb.state.tx.us/data/bays_estuaries/studies/gal89main.html.)

There is no established procedure for model calibration, but the essence of the process is the comparison of observed data and simulated data. By adjusting model parameters the user tries to make the model trace observed values as closely as possible. For TxBLEND application to Texas bays, model parameters that require adjustment to achieve calibration most often include bigG, Manning's n, and dispersion. The non-physical parameter bigG is used to enhance mass conservation and usually ranges 0.001 to 0.1. The most important parameter for hydrodynamic calibration is Manning's n, representing bottom roughness. A larger n slows water movement and vice versa. Similarly, the dispersion coefficient, which embodies physical mixing processes, is the key parameter for salinity calibration; the larger the parameter, the faster dissolved salt disperses. At a more structural level, the finite element grid often needs to be modified to better represent flow conditions in areas where shoreline geometry or bathymetry is complicated. In most cases, calibration involves a trial and error approach, the user modifying appropriate parameters until room for improvement is exhausted.

Velocity Calibration

TWDB conducted an intensive inflow study of Galveston Bay and surrounding area from May 7 to May 10, 1989. Figure 3.4 (part A through part C) shows observed and simulated velocities at sites in the Galveston Bay area. Velocities were measured at two-tenths, five-tenths, and eight-tenths of depth. The Army Corps of Engineers conducted an intensive inflow study in July 1990. Their data was used as an independent data set for calibration (i.e., model verification). Figure 3.5 shows the comparison of observed data and simulated data.

Tide Calibration

Since the long-term tide data is available through the Texas Coastal Ocean Observation Network (TCOON) Program, four yearly simulations, 1993 through 1996, were compared and statistics were calculated at five locations as listed in Table 3.1. Figures 3.6, 3.7 and 3.8 are the time series plots for parts of 1993, 1995, and 1996 for the simulated and observed tides. Both

the figures and statistics indicate that the comparison is generally good. It is better near the passages to the Gulf and gradually degrades toward the upper estuary.

Table 3.1 Simulated observed and tides comparison statistics

Location	Year	Days	N_Data	R-square	RMS(ft)
Pleasure Pier	93	364	8732	0.96	0.21
Pier 21	93	360	8645	0.93	0.22
Eagle Point	93	257	6164	0.89	0.23
Morgan's Point	93	363	8720	0.86	0.29
Anahuac	93	358	8592	0.77	0.34
Pleasure Pier	94	365	8751	0.99	0.13
Pier 21	94	365	8751	0.97	0.14
Eagle Point	94	358	8596	0.81	0.29
Morgan's Point	94	364	8740	0.87	0.27
Anahuac	94	365	8749	0.68	0.42
Pleasure Pier	95	360	8637	0.85	0.39
Pier 21	95	365	8750	0.95	0.20
Eagle Point	95	356	8548	0.88	0.25
Morgan's Point	95	363	8701	0.87	0.29
Anahuac	95	364	8723	0.82	0.34
Clear Lake	95	360	8640	0.89	0.26
Lynchburg	95	210	5047	0.88	0.27
Alligator Point	95	364	8732	0.91	0.27
Pleasure Pier	96	364	8738	0.98	0.17
Pier 21	96	366	8777	0.98	0.14
Eagle Point	96	342	8197	0.92	0.23
Morgan's Point	96	344	8245	0.89	0.29
Anahuac	96	348	8354	0.84	0.31
Clear Lake	96	358	8587	0.93	0.21
Lynchburg	96	354	8483	0.89	0.30
Alligator Point	96	351	8417	0.83	0.36

Note: RMS stands for root mean square.

$$RMS = \sqrt{(Tide_{obsrvd} - Tide_{simultd})^2} \; / \; N\_data$$

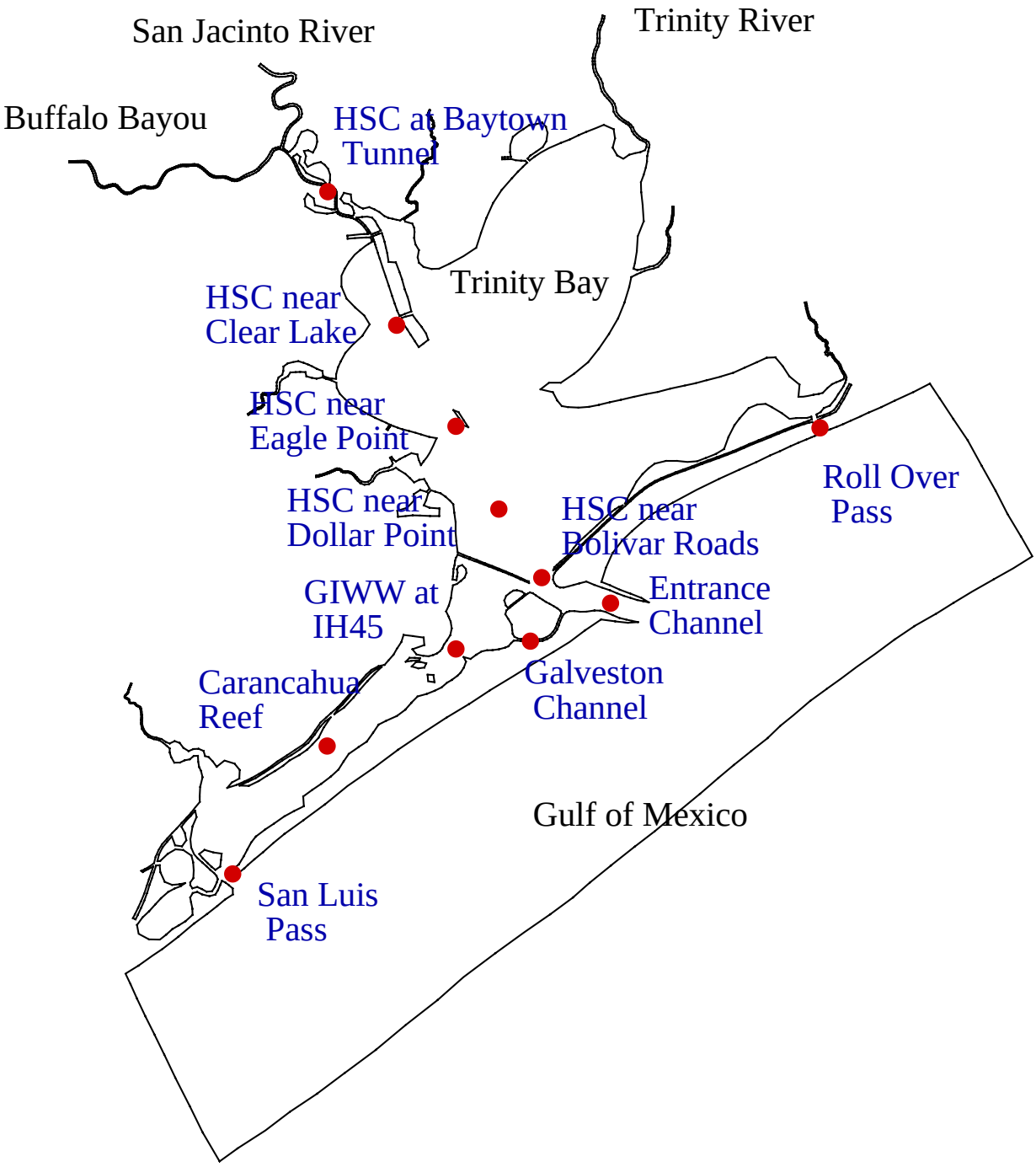

Figure 3.1 Velocity survey sites for Galveston Bay area

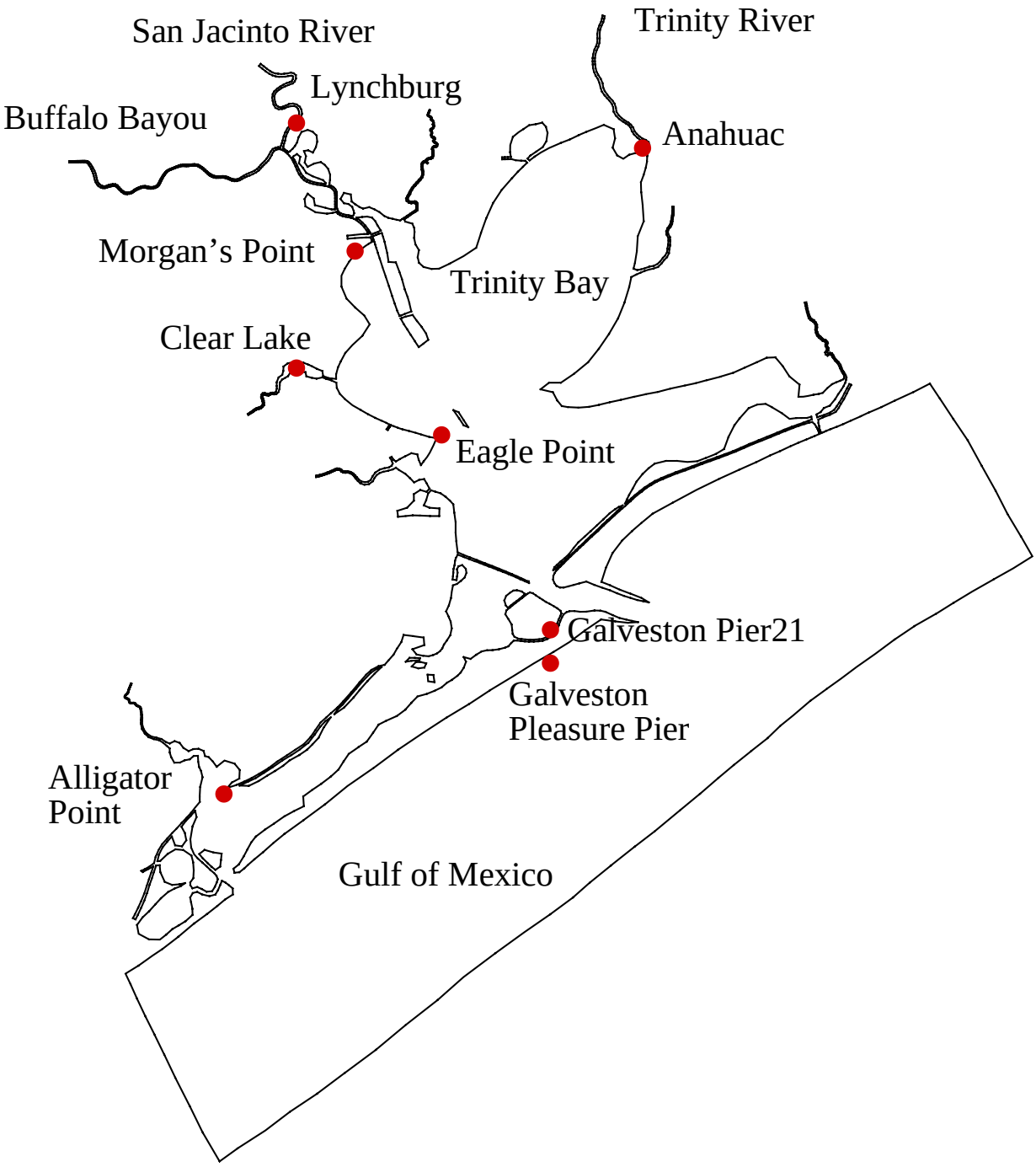

Figure 3.2 Tide gage stations in Galveston Bay area

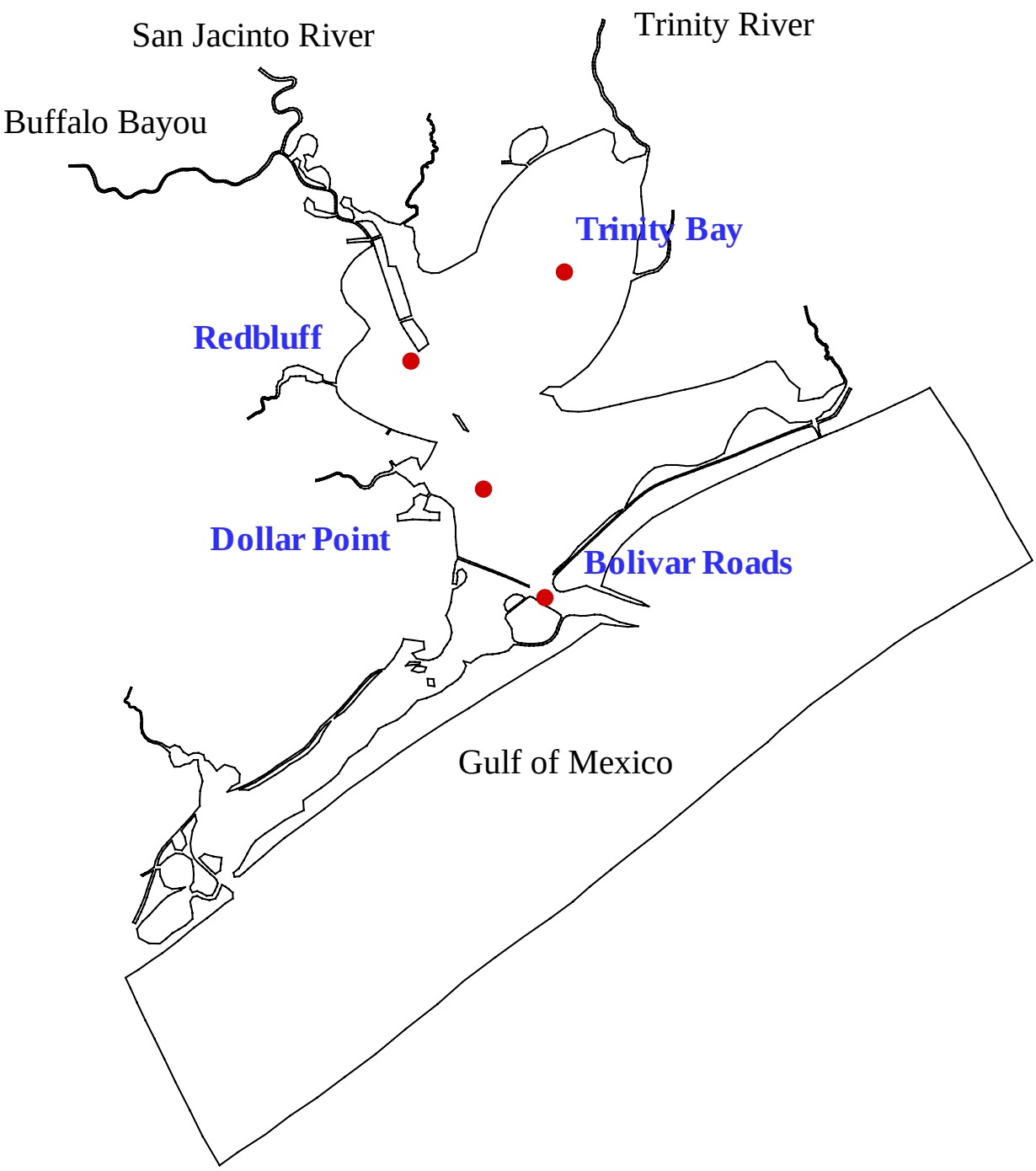

Figure 3.3 Datasonde sites (long-term water quality data collection sites) in Galveston Bay

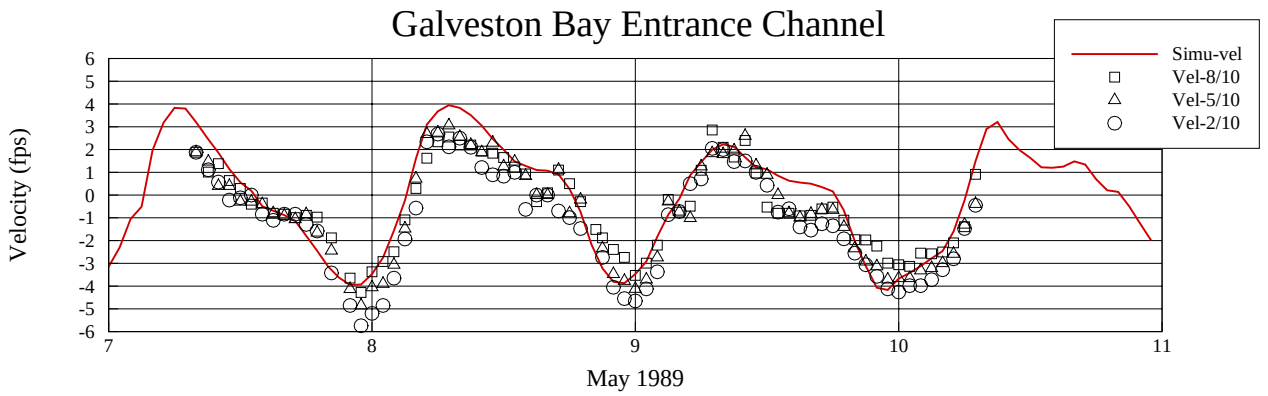

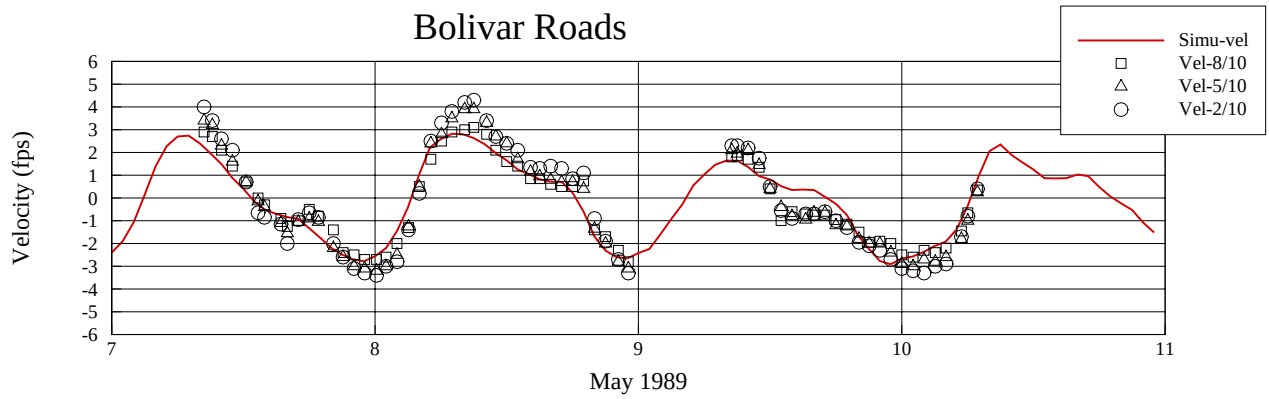

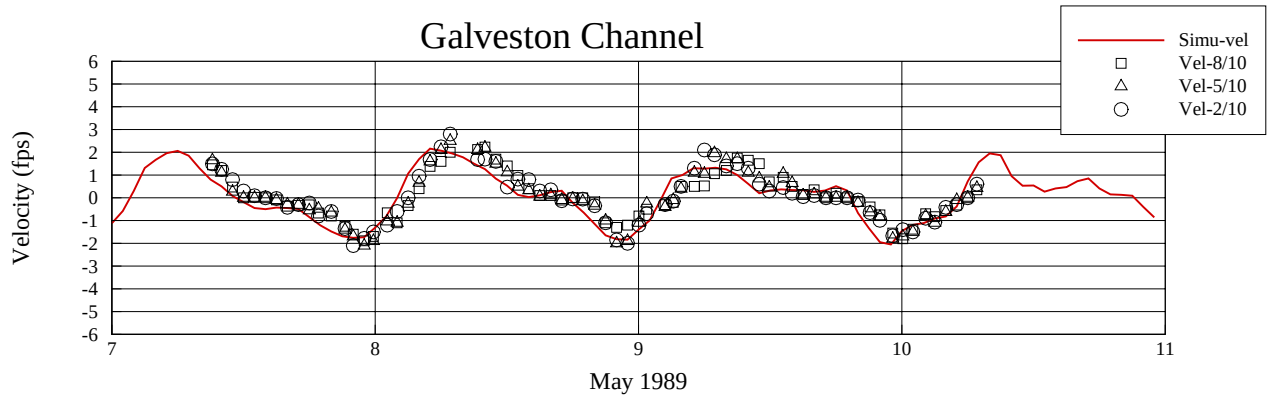

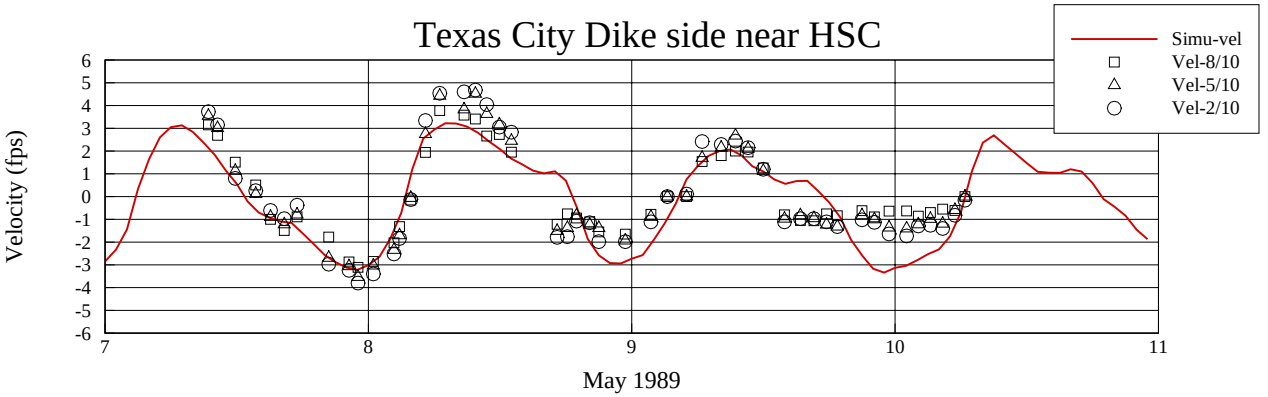

Figure 3.4 Simulated and observed velocities in May 1989 (part A)

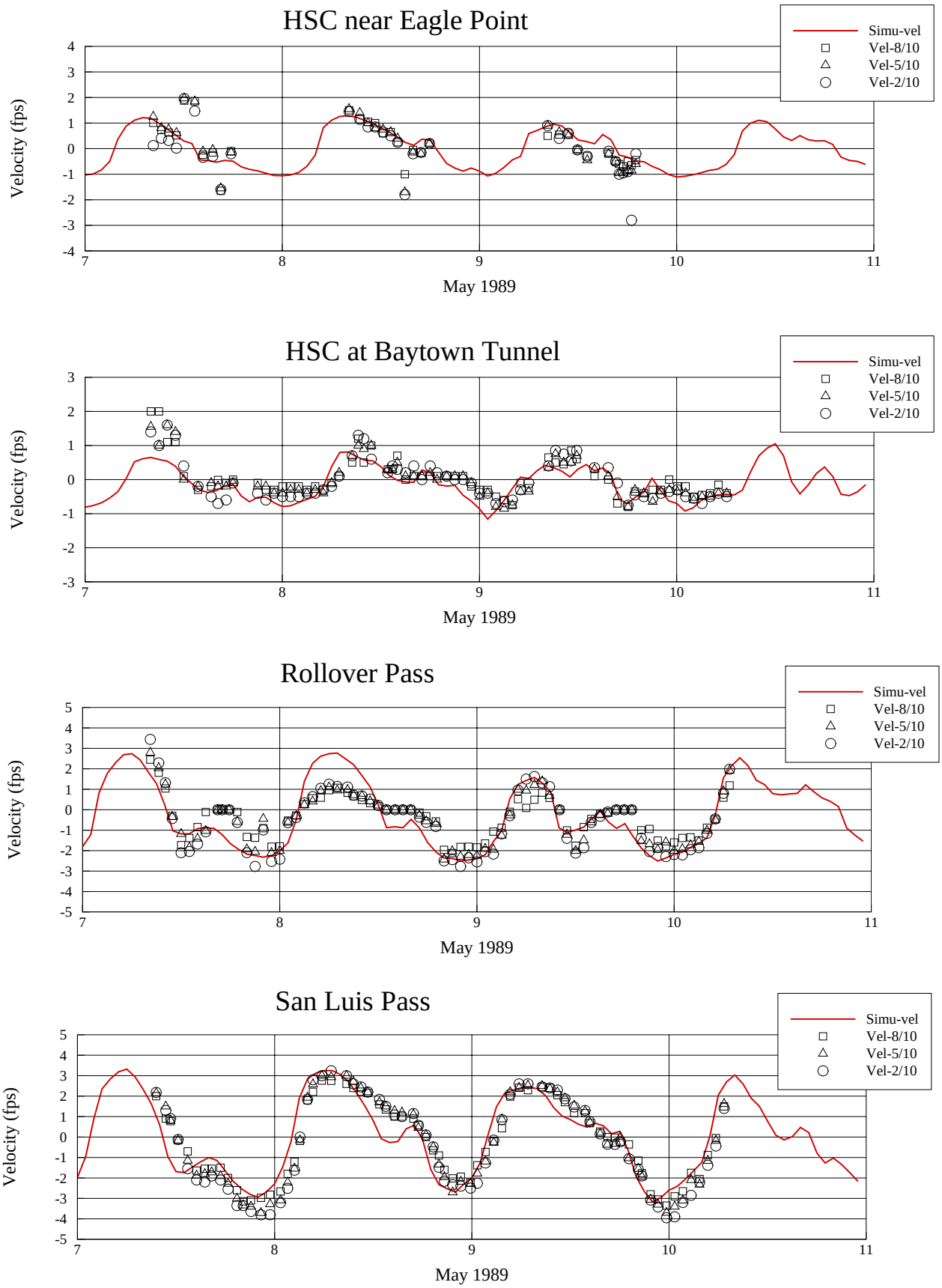

Figure 3.4 Simulated and observed velocities in May 1989 (part B)

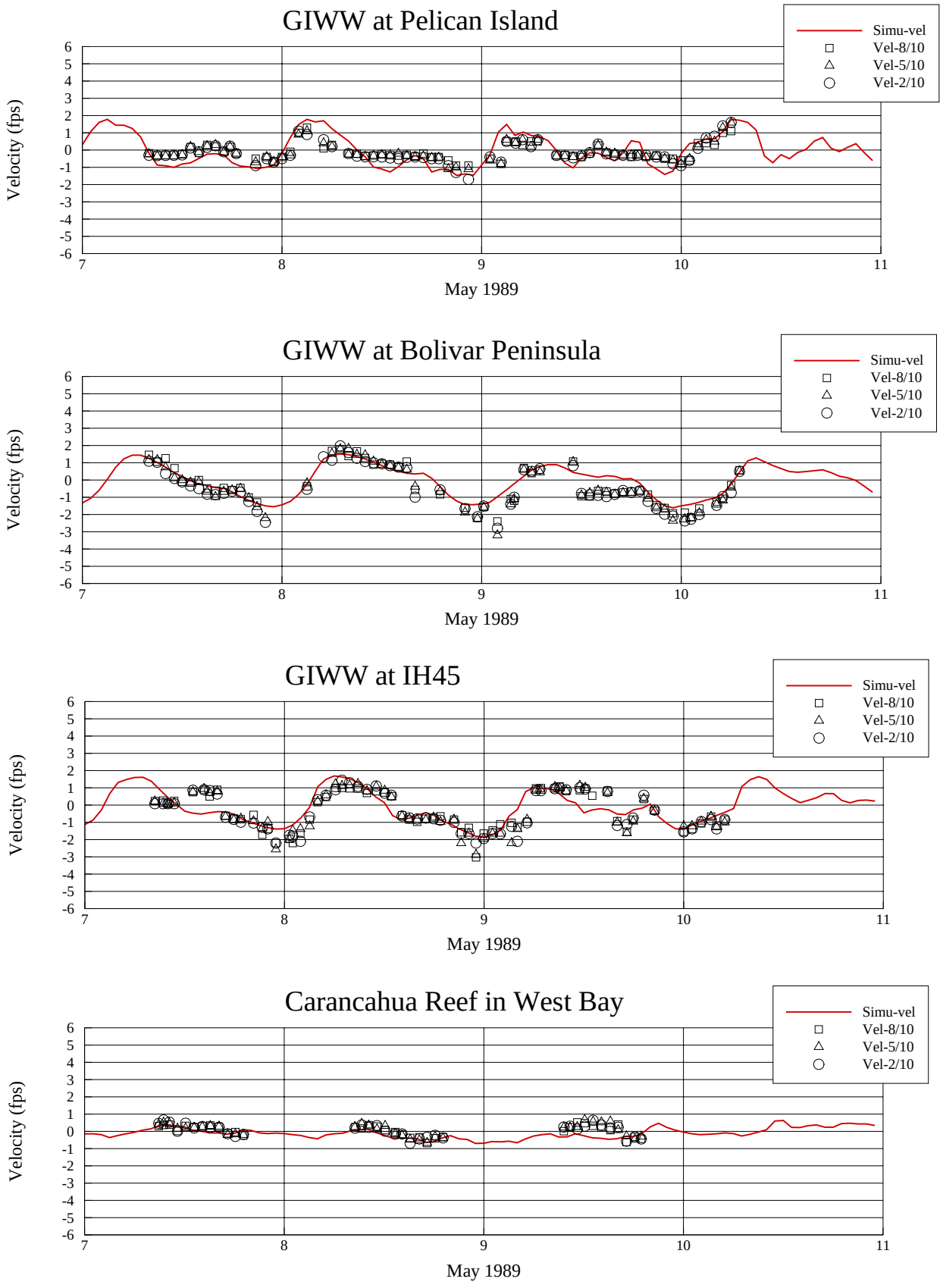

Figure 3.4 Simulated and observed velocities in May 1989 (part C)

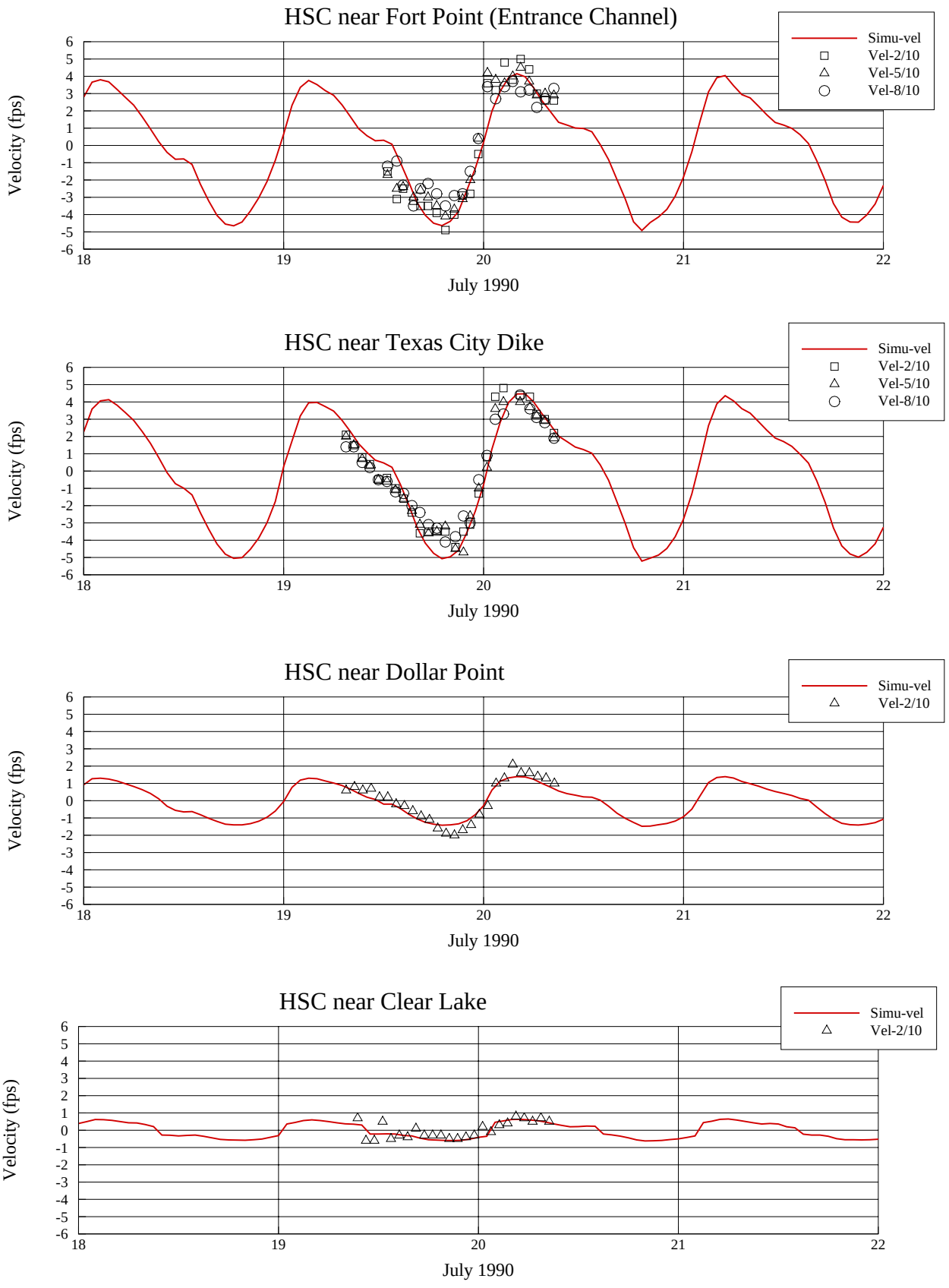

Figure 3.5 Simulated and observed velocities in July 1990

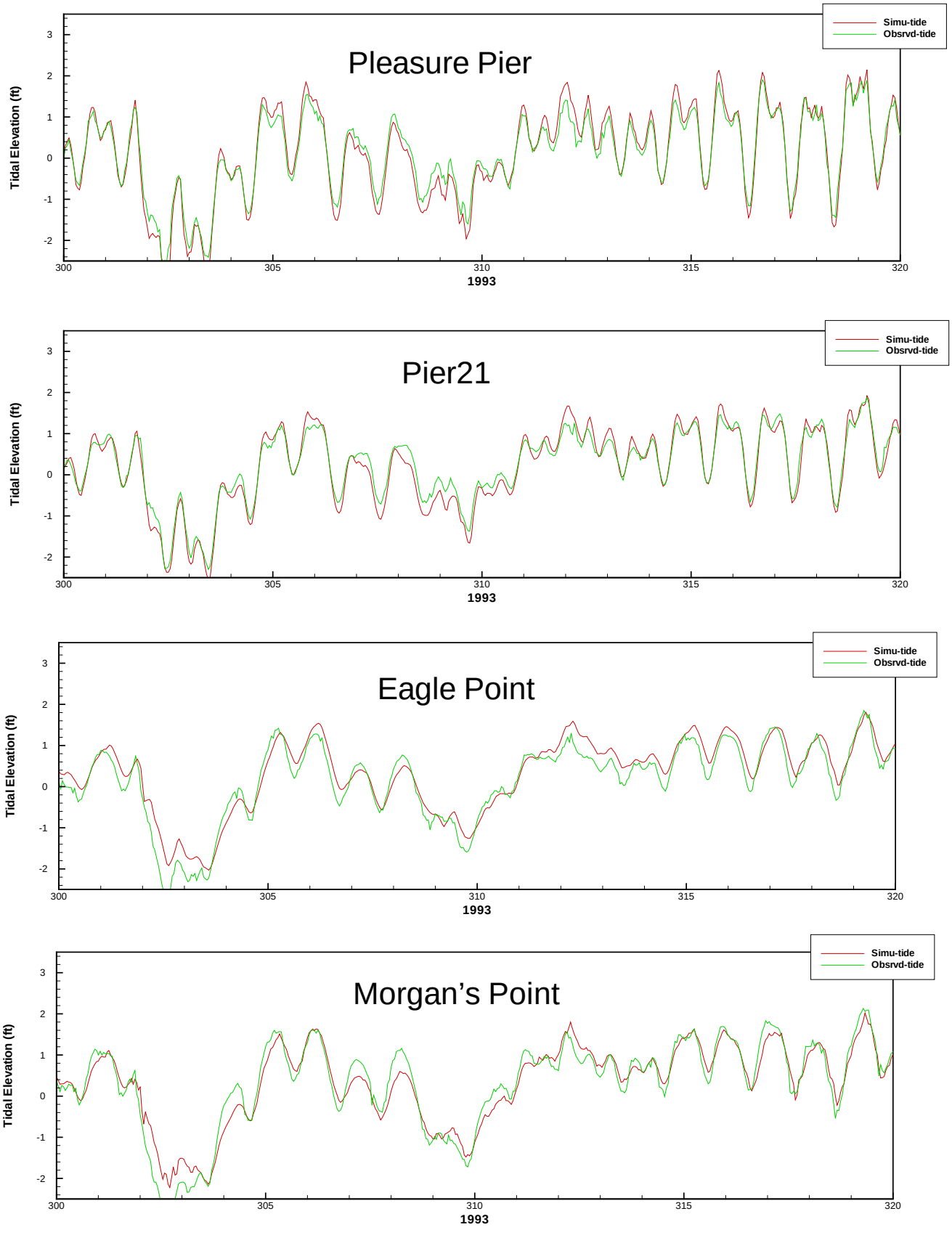

Figure 3.6 Simulated and observed tides in 1993

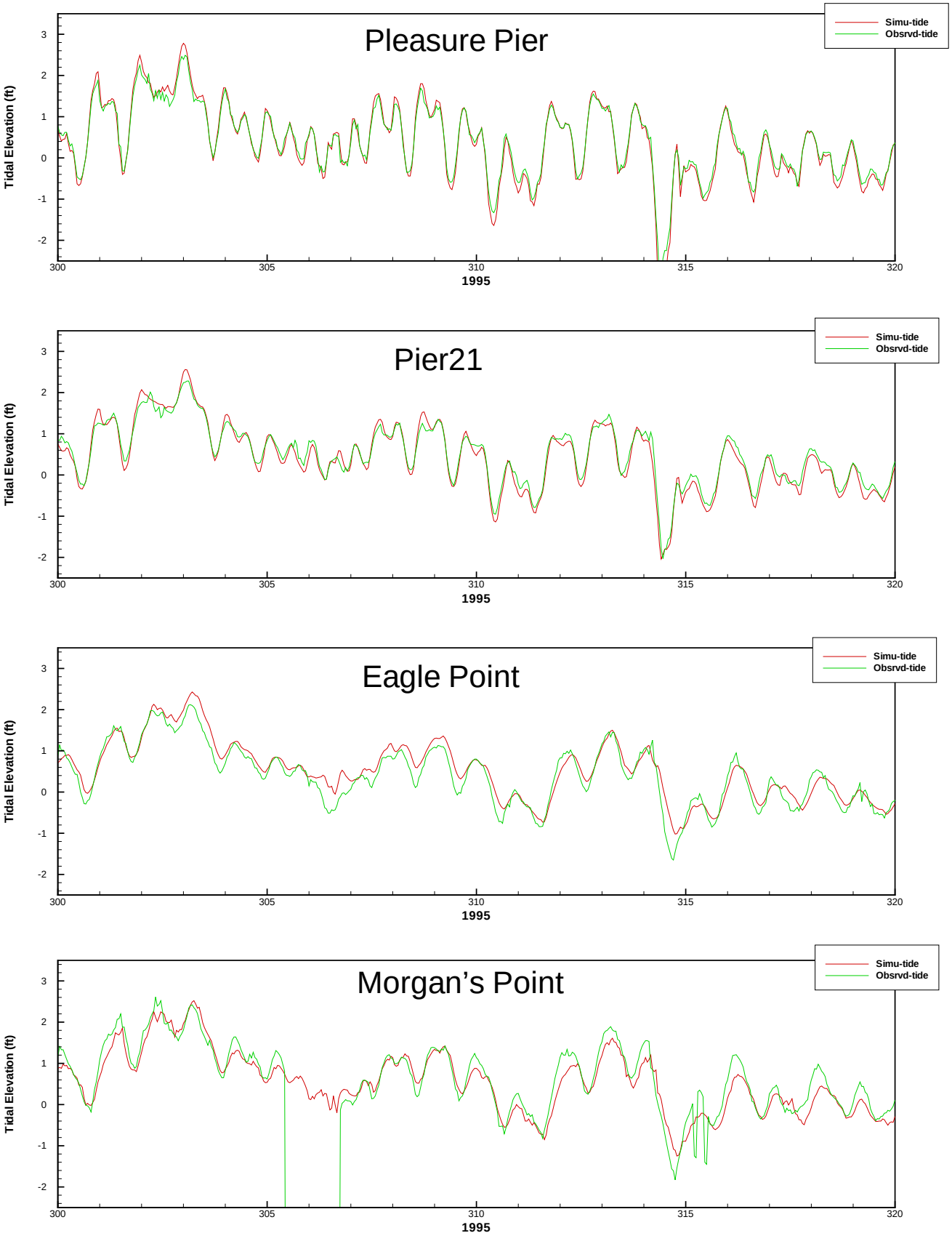

Figure 3.7 Simulated and observed tides in 1995 (part A)

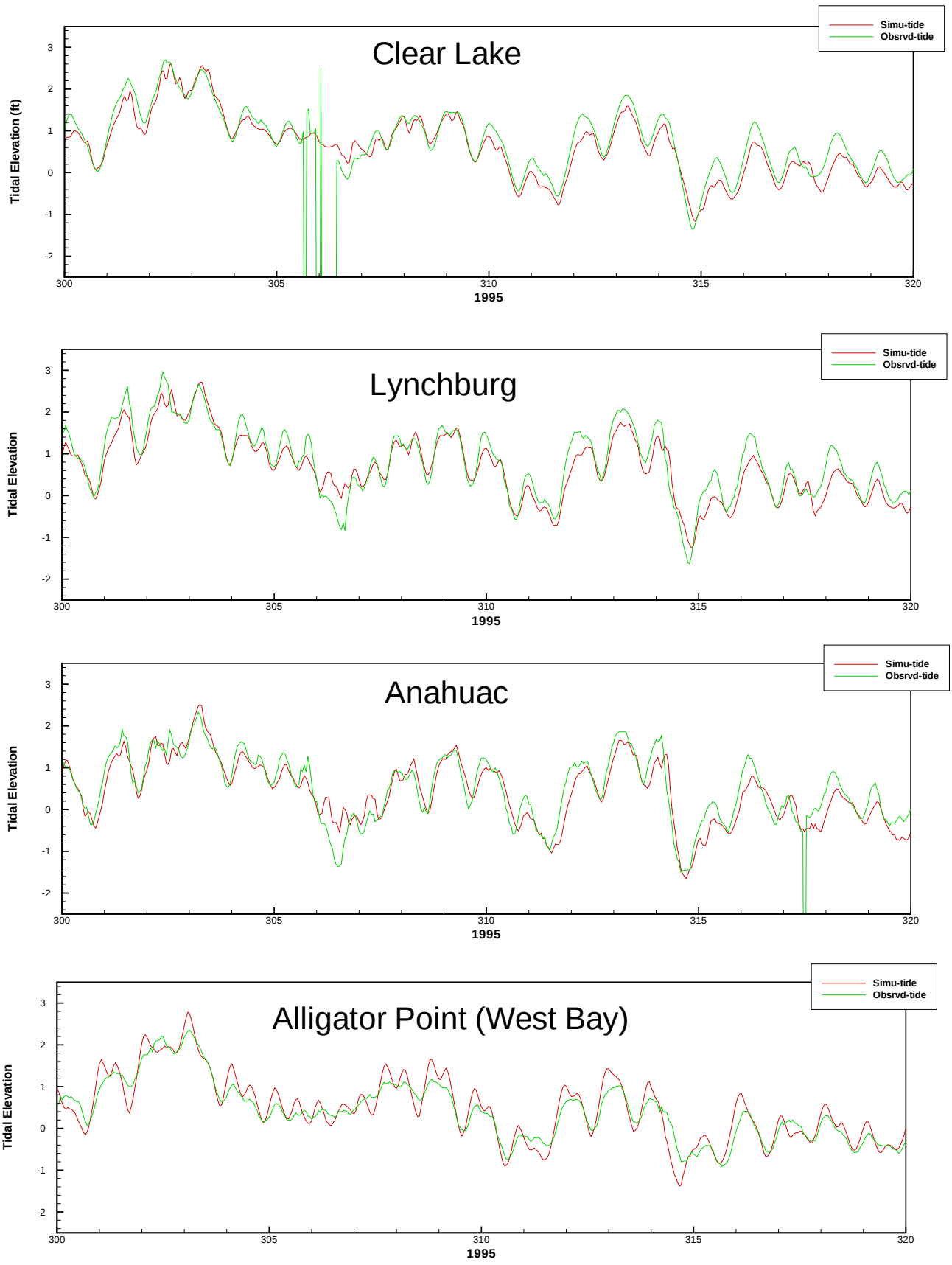

Figure 3.7 Simulated and observed tides in 1995 (part B)

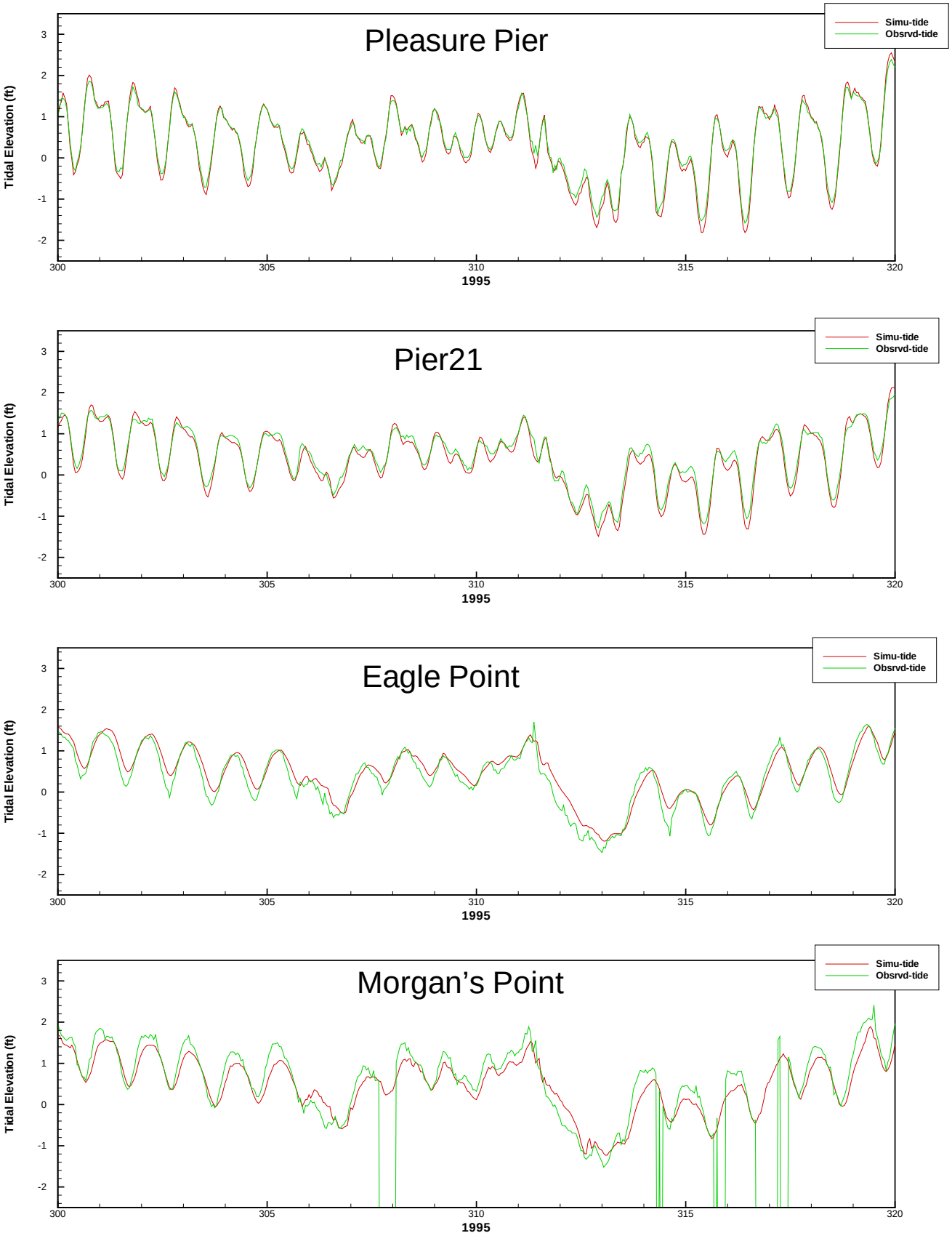

Figure 3.8 Simulated and observed tides in 1996 (part A)

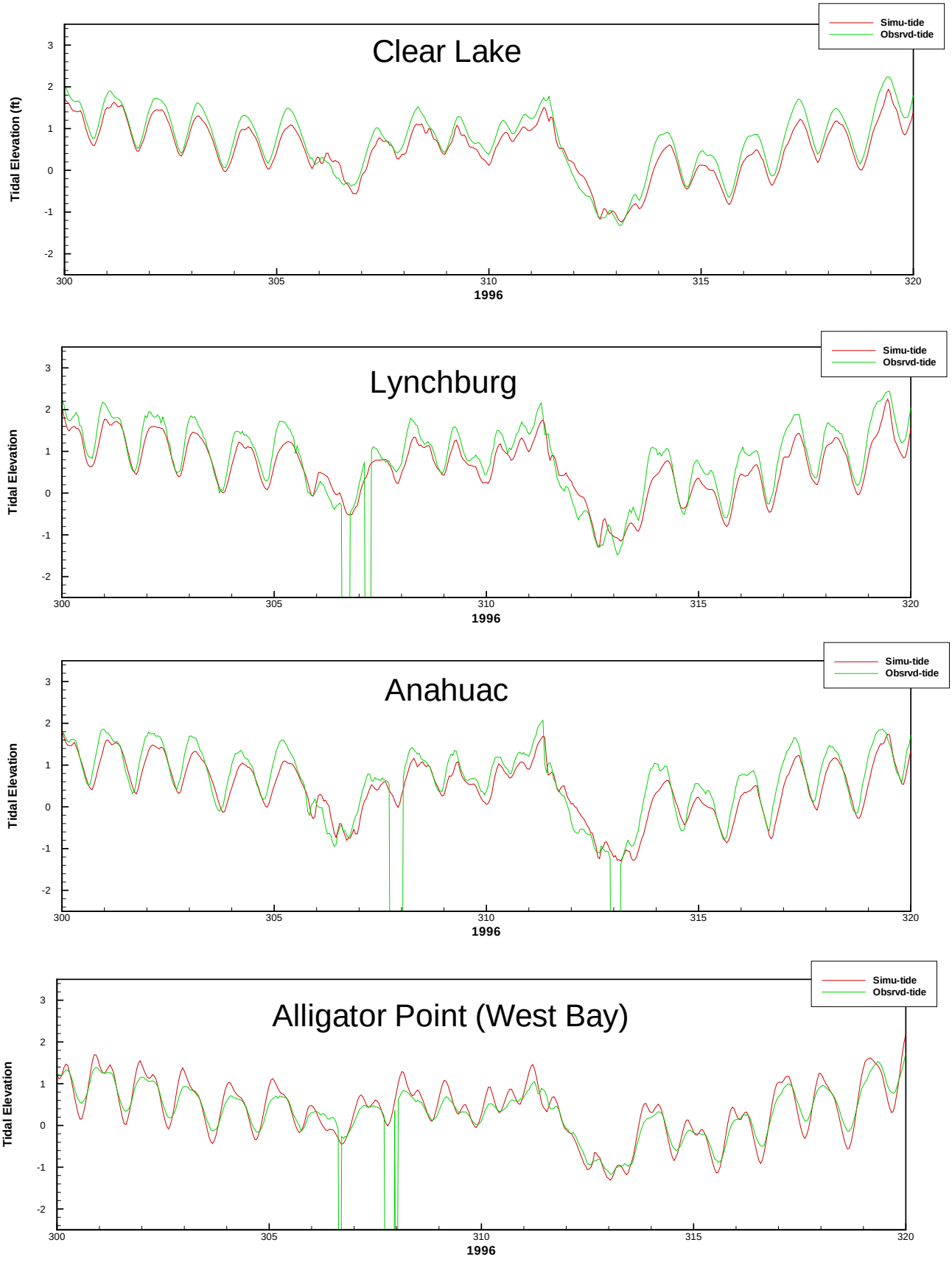

Figure 3.8 Simulated and observed tides in 1996 (part B)

Salinity Calibration

Unlike results of hydrodynamic calibrations, we have to accept that agreement between simulated and observed salinities may not be as good as we would like. There are a few reasons for disagreement between observed and simulated salinities in a properly working model. For instance, the model and observed salinities may represent different things. Salinity measured near the surface may be different than measurements made near the bottom. Fixed salinity recording meters (e.g., Datasondes), an important source of data in this study, may record values in only one of a multi-layered water mass. The model, on the other hand, is a depth-averaged model and may not compute salinities strictly comparable to observed values. The major parameter for salinity calibration is the dispersion coefficient. The value of this parameter is adjusted so that the simulated data fit the observed data. Values ranging from 10 ft^2/sec to 15,000 ft^2/sec are reported in the literature (Ippen 1971, Officer 1976, Fischer 1980). Large values of 5,000 ft^2/sec to10,000 ft^2/sec are assigned in the deeper areas, including the ship channels and the Gulf, and smaller values from 200 ft^2/sec to 1,000 ft^2/sec are assigned in the shallow areas of the system.

Another difficulty in salinity calibration arises from the lack of salinity data at the Gulf tidal boundary. There are no consistent observed salinity data to represent the near-shore Gulf of Mexico. For modeling, a constant value of 34 ppt can be set along the tidal boundary. Generally this works well, but for extreme cases, such as during very wet or very dry climatic conditions, simulations with a constant boundary value may produce results which deviate from observed values. For this modeling project the boundary salinity values were estimated from observed salinity values at the Bolivar Roads site. Given this and the above problems, the most productive approach to salinity calibration is to produce results which follow the overall pattern of observed salinity changes.

It is fortunate that there is a wealth of salinity data for Galveston Bay. However, data availability is inside of the bay, not the outside of the bay. Observed salinity data for 1990 through 1996 were compared to simulated salinity in time series plots as in Figures 3.9 through 3.15. Of particular interest is October 1994 in which a large flood event occurred (estimated daily inflow is 244,000 cfs from Trinity River on October 19, 1994) that caused a sudden drop in salinity. As shown in Figure 3.13 the salinity drop was registered at all four sites. The salinity simulation also emulated the drop fairly well. Other periods of interest are the wet period during 1991 and 1992-especially the first half of 1992-and the dry period of 1996.

Some of the salinity data are extremely high, such as at Red Bluff site in the later months of 1995 or at all four sites during 1996, which was a highly dry period. It is not certain if the salinity was as high as shown in these figures. Some observed salinities could be instrument malfunction and some of them could be true value. Because the main purpose is model calibration and plenty data exist for evaluating model performance, the extremely high salinity data were left alone. (Datasondes were maintained on a monthly basis. A crew would visit the site and replace the instrument with a newly calibrated one. Salinity was then measured by a

separate water quality meter at the time of replacement. This value was used for data correction.)

Figures 3.16 shows scatter plots comparing the daily observed salinity and simulated salinity values over 1990-1996 period. Table 3.2 lists the statistics. For these plots and statistics, extreme data points were excluded. These plots and statistics indicate that the two interior salinity sites, Dollar Point and Red Bluff, are more consistent than the Bolivar Roads site and the Trinity Bay site where the data points are more spread.

Table 3.2. Statistics between the simulated and observed daily salinity

Site	N_data	R-square	RMS(ppt)
Bolivar Roads	1438	0.73	3.3
Dollar Point	1767	0.88	2.9
Red Bluff	1604	0.87	2.6
Trinity Bay	1572	0.74	4.2

Note: salinity data greater than 35 ppt were excluded for Bolivar Roads, 30 ppt for Dollar Point, 26 ppt for Red Bluff, 35 ppt for Trinity Bay for this analysis.

$$RMS = \sqrt{(Salt_{obsrvd} - Salt_{simultd})^2} \; / \; N\_data$$

Table 3.3 lists observed and simulated daily mean salinity at four Datasonde sites between 1989 and 1996, the same period as the simulation period, and removing the anomalous data as done in Table 3.2. The difference in mean salinity is less than 2 ppt. However, as the root mean square (RMS) in Table 3.2 indicates, daily salinity may vary between 2 to 4 ppt.

Table 3.3. Simulated and observed mean daily salinity

Site	N_data	ObsvdMean	SimltdMean	Diffrnce(ppt)
Bolivar Roads	1438	20.8	20.1	0.7
Dollar Point	1767	16.0	14.5	1.5
Red Bluff	1604	11.7	10.3	1.4
Trinity Bay	1572	6.9	7.9	-1.0

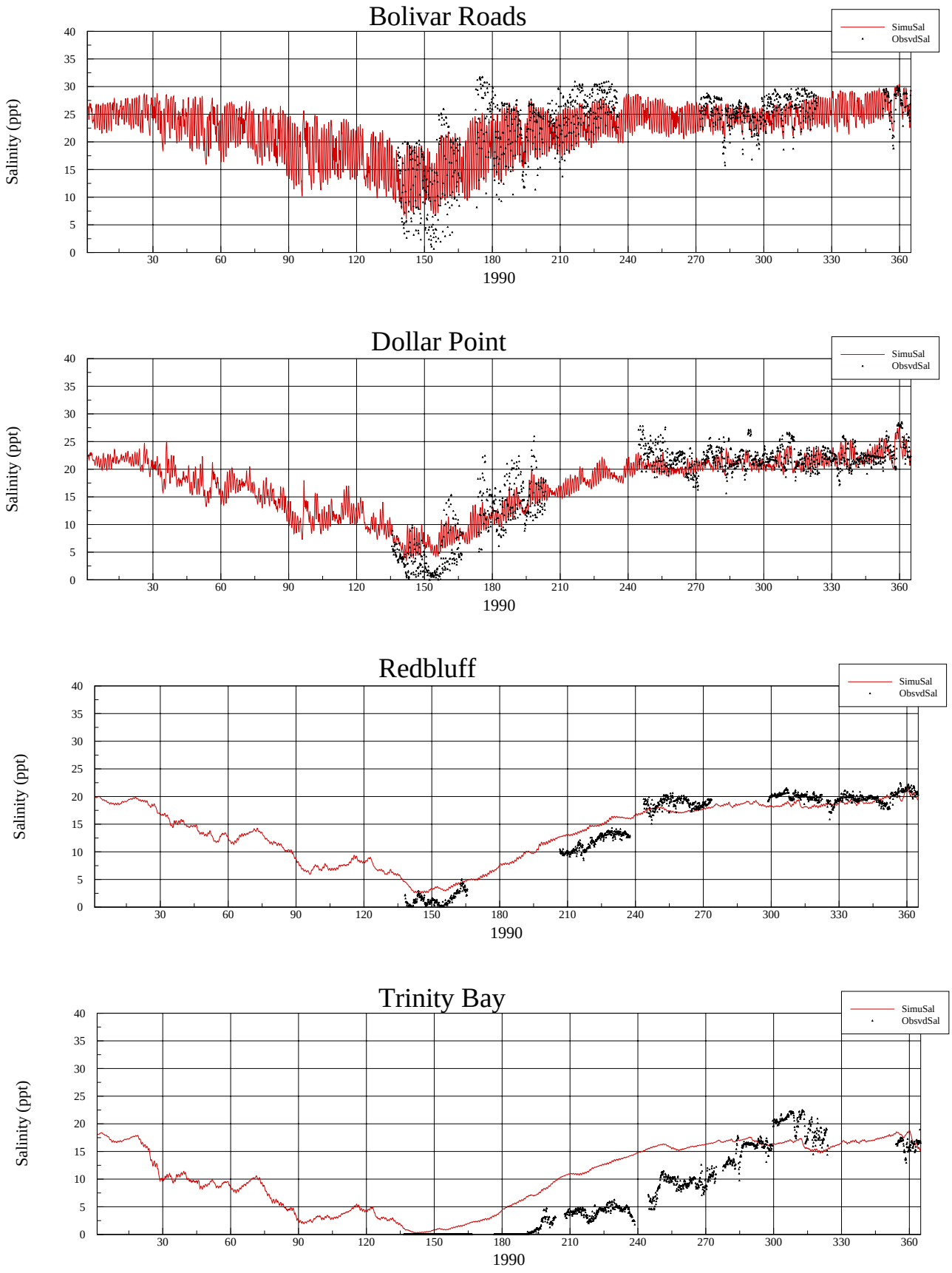

Figure 3.9 Simulated and observed salinities in 1990

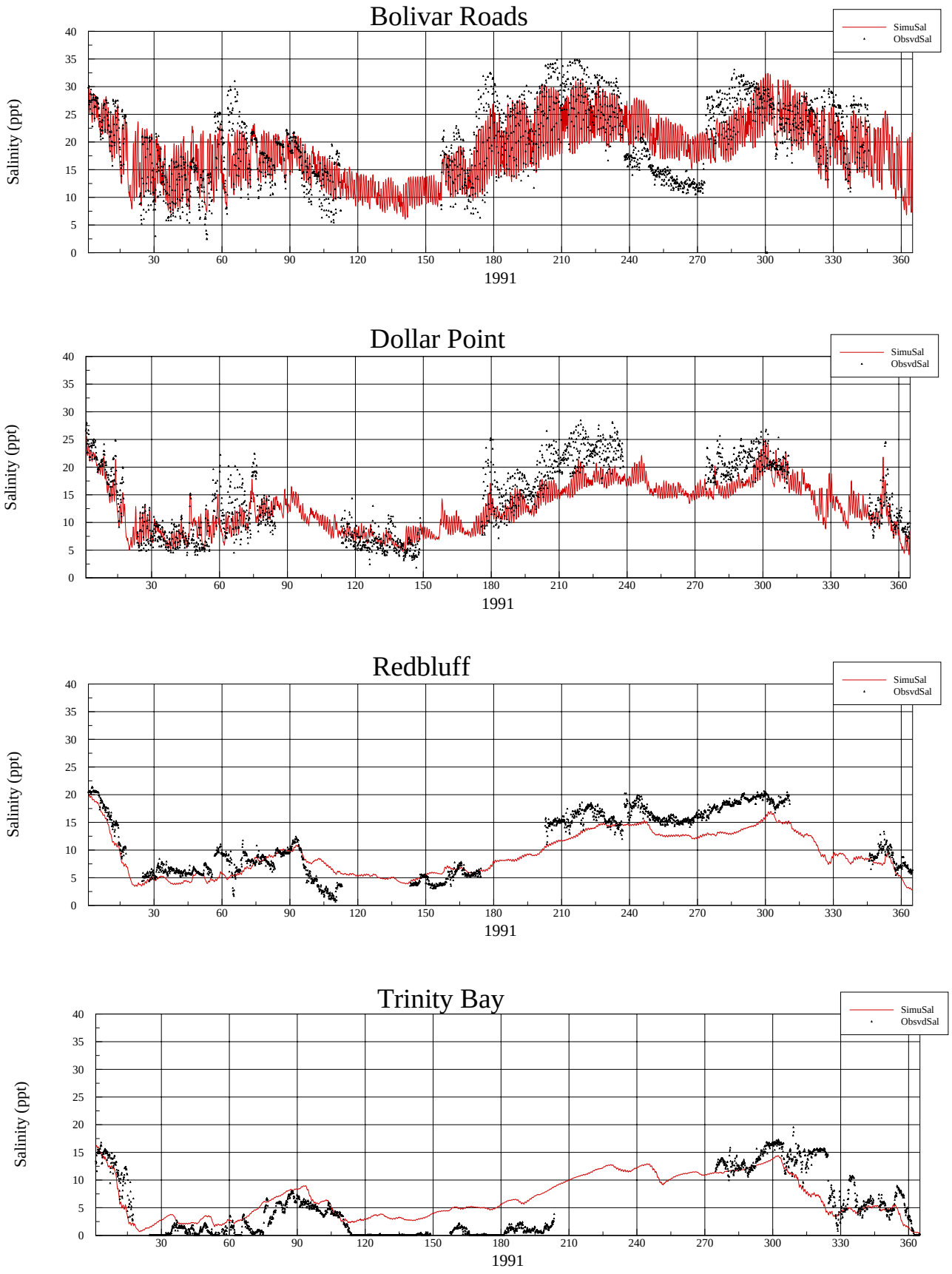

Figure 3.10 Simulated and observed salinities in 1991

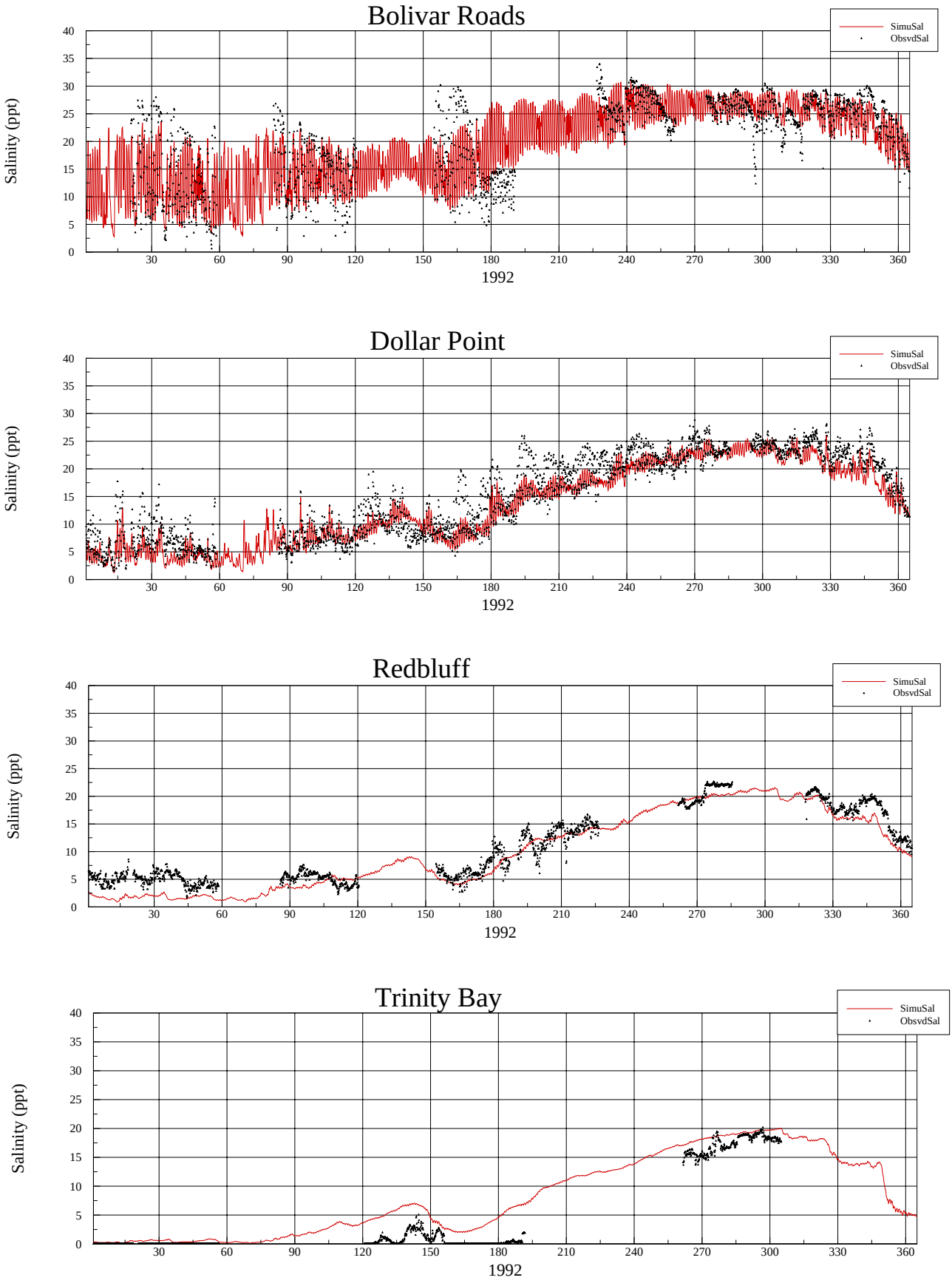

Figure 3.11 Simulated and observed salinities in 1992

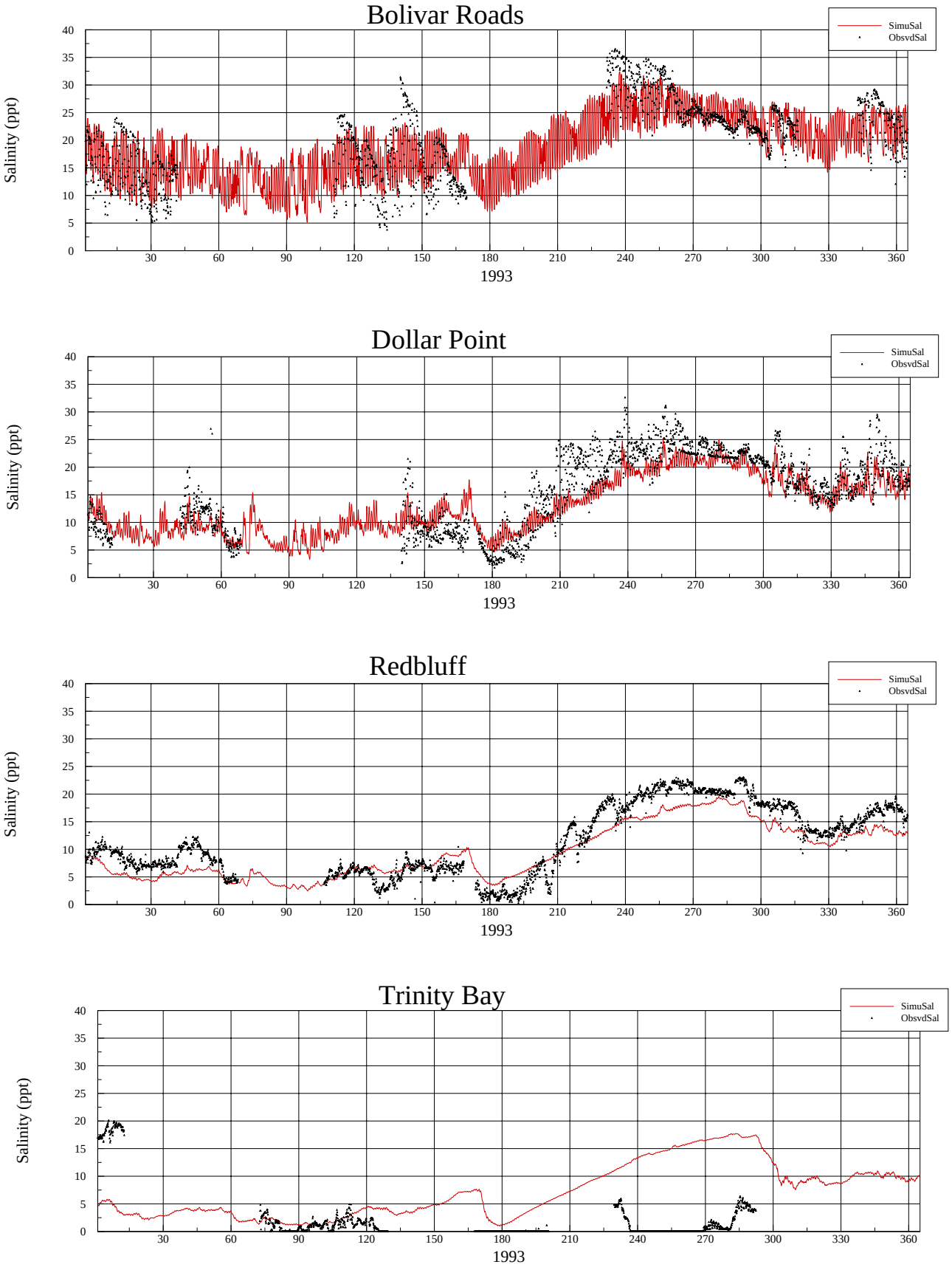

Figure 3.12 Simulated and observed salinities in 1993

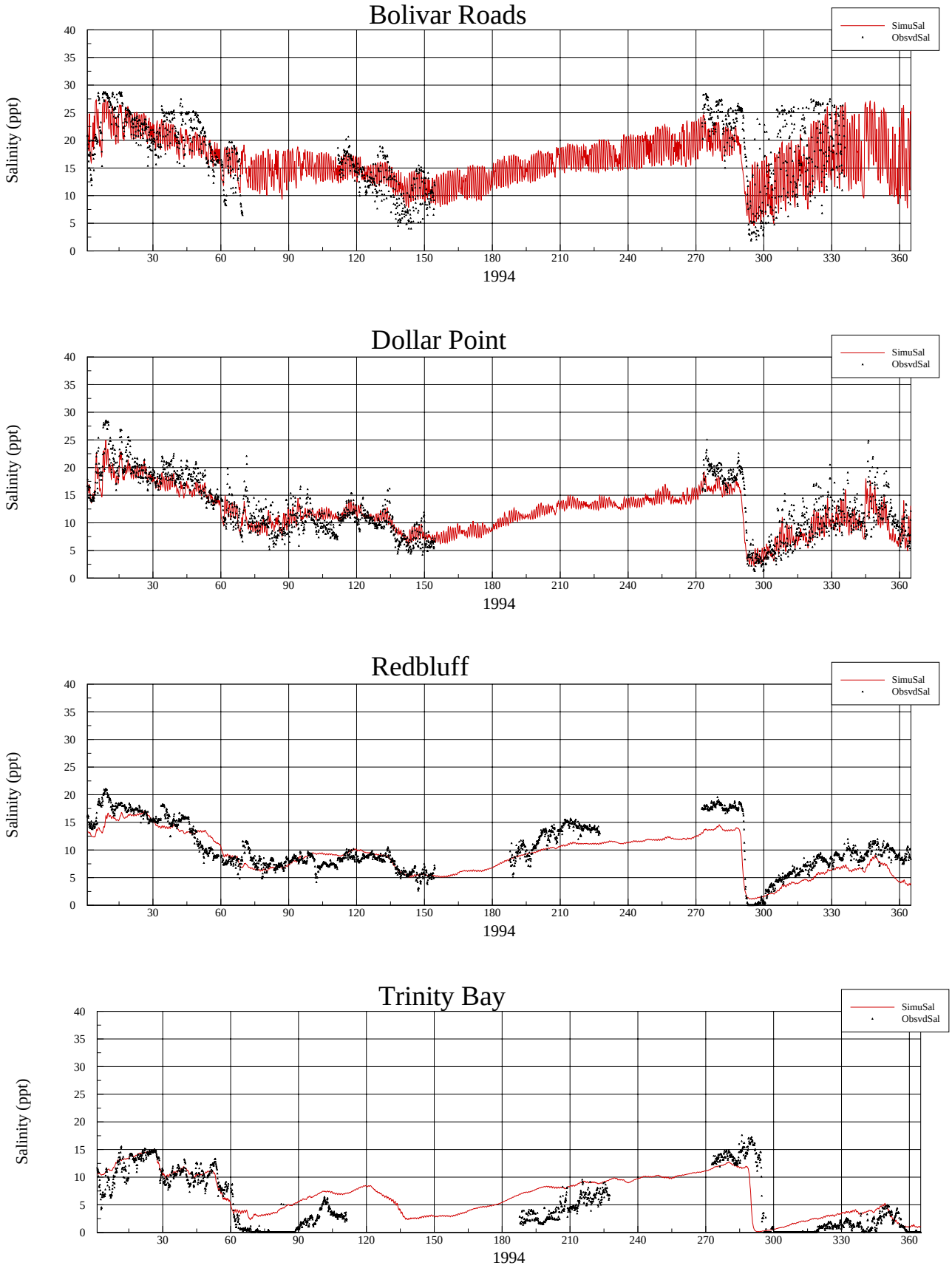

Figure 3.13 Simulated and observed salinities in 1994

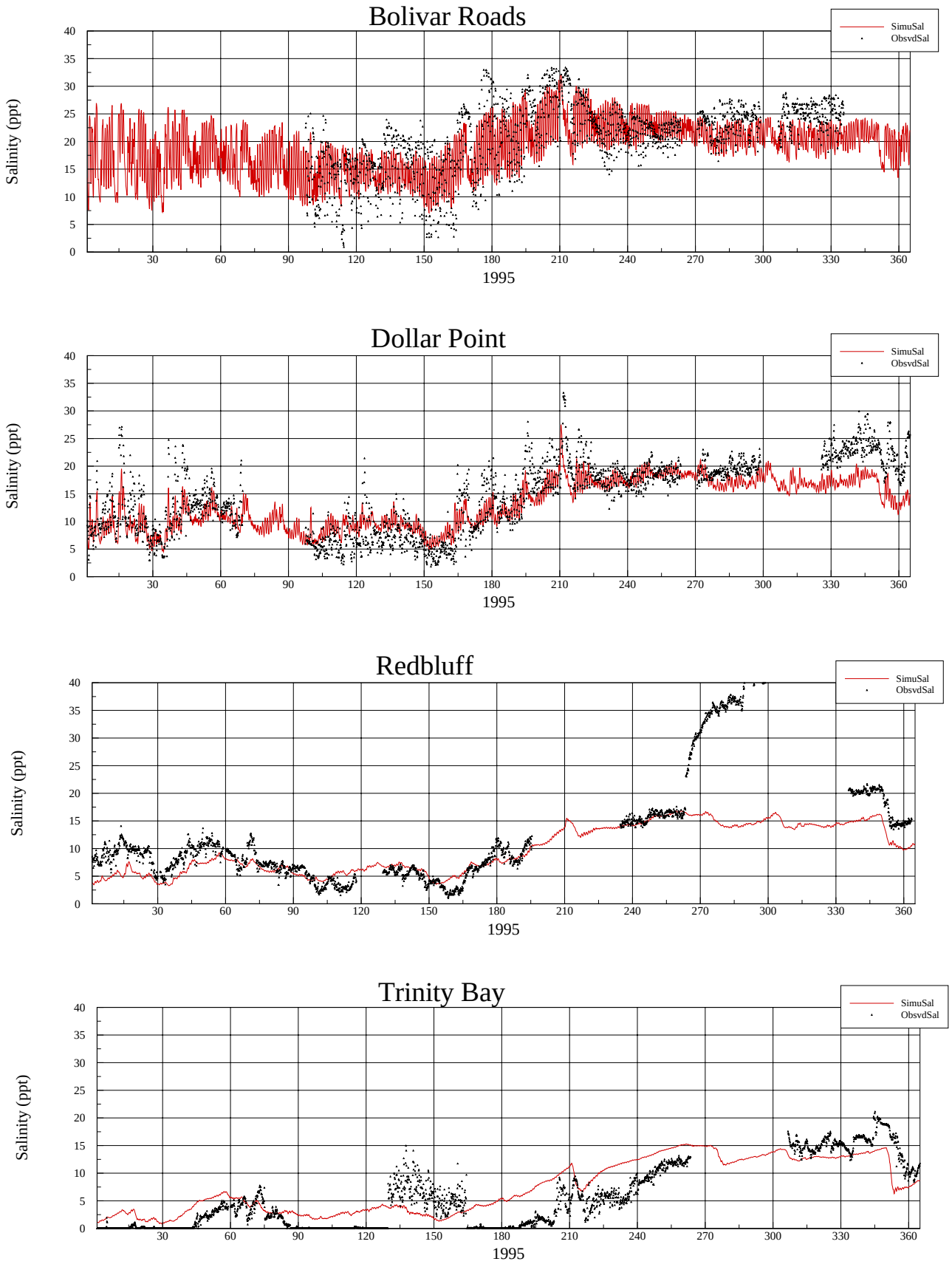

Figure 3.14 Simulated and observed salinities in 1995

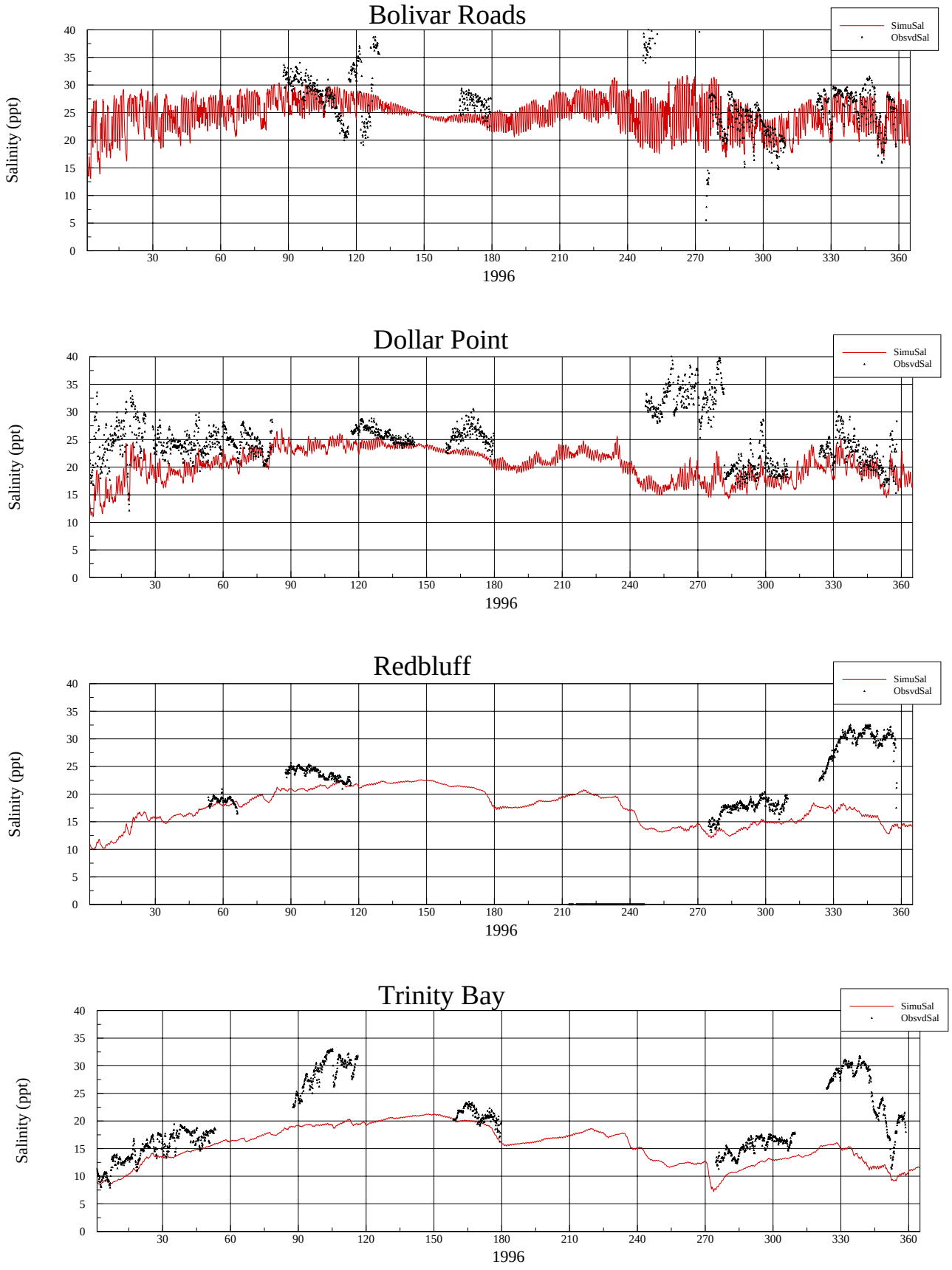

Figure 3.15 Simulated and observed salinities in 1996

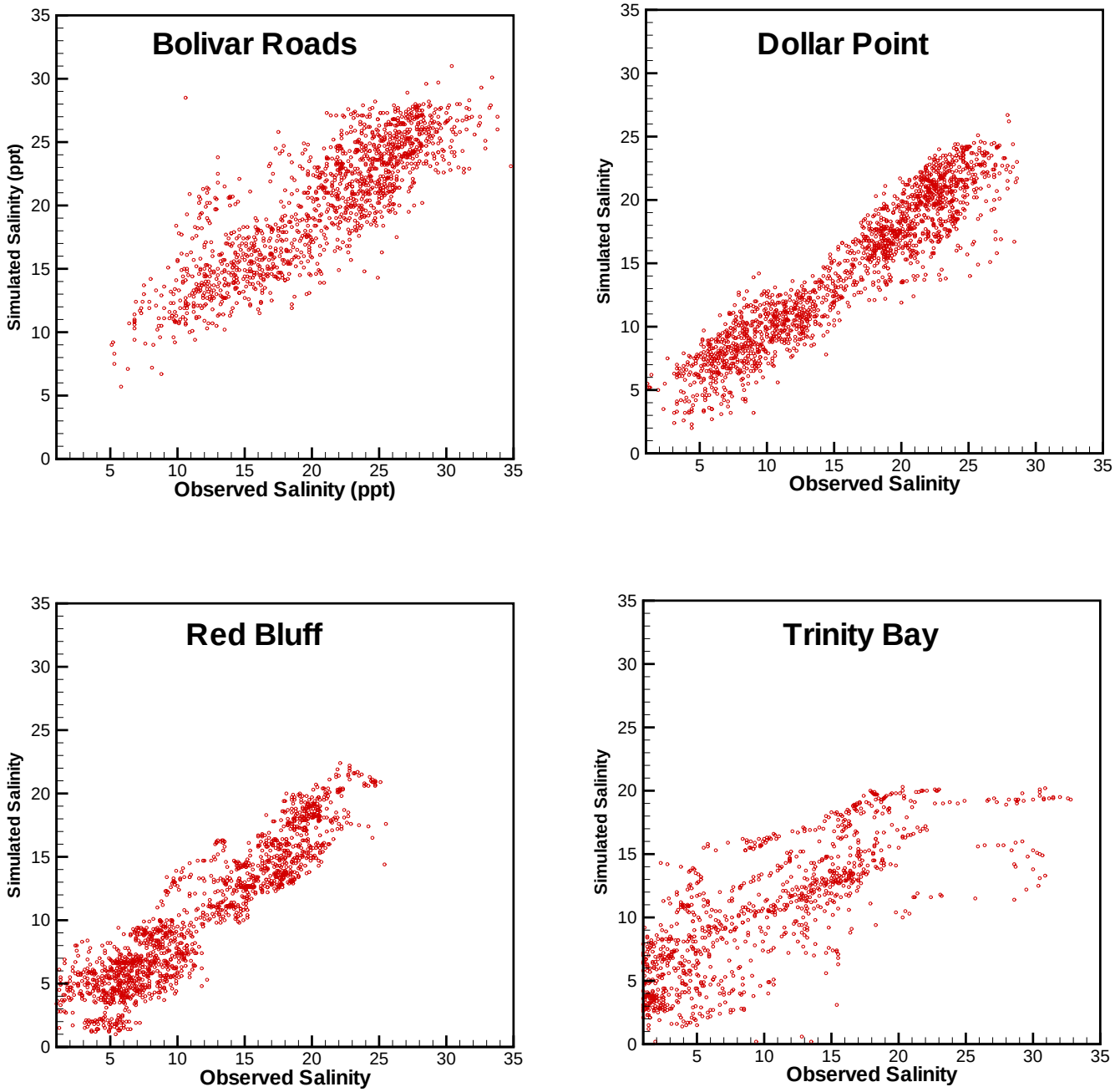

Figure 3.16 Simulated and observed daily salinities at four Datasonde sites

4. MODEL SIMULATION

The calibrated model was applied for three cases to show some of the characteristics of the bay system. Computer animations are included in the CD which accompanies this report.

January 18, 1989

The tide at Pleasure Pier in January through March of 1989 is shown in Figure 4.1. Day 17 through Day 21 (January 17th through January 21st) are a typical diurnal tide. Figure 4.2 shows vector plots in Bolivar Roads area for flood tide and ebb tide.

February 24, 1989

During Day 52 through Day 53 (near the end of February) in Figure 4.1 the water level was depressed by a northerner (low-pressure system) and recovered quickly. Figure 4.3 shows a simulated salinity pattern in the recovery period. It exhibits the leading edge (or tongue) along the HSC.

October 19, 1994

The flood of October 1994 was simulated by the model. A few selected plots are shown in Figure 4.4, which demonstrate how the bay water is pushed out by a large flood. The inflows from the Buffallo/San Jacinto side are 61 thousand cfs (kcfs), 170 kcfs, 159 kcfs, 94 kcfs on October 17, 18, 19, and 20, respectively. From Trinity River inflows are 56 kcfs, 164 kcfs, 244 kcfs, 193 kcfs from October 17 through 20, respectively.

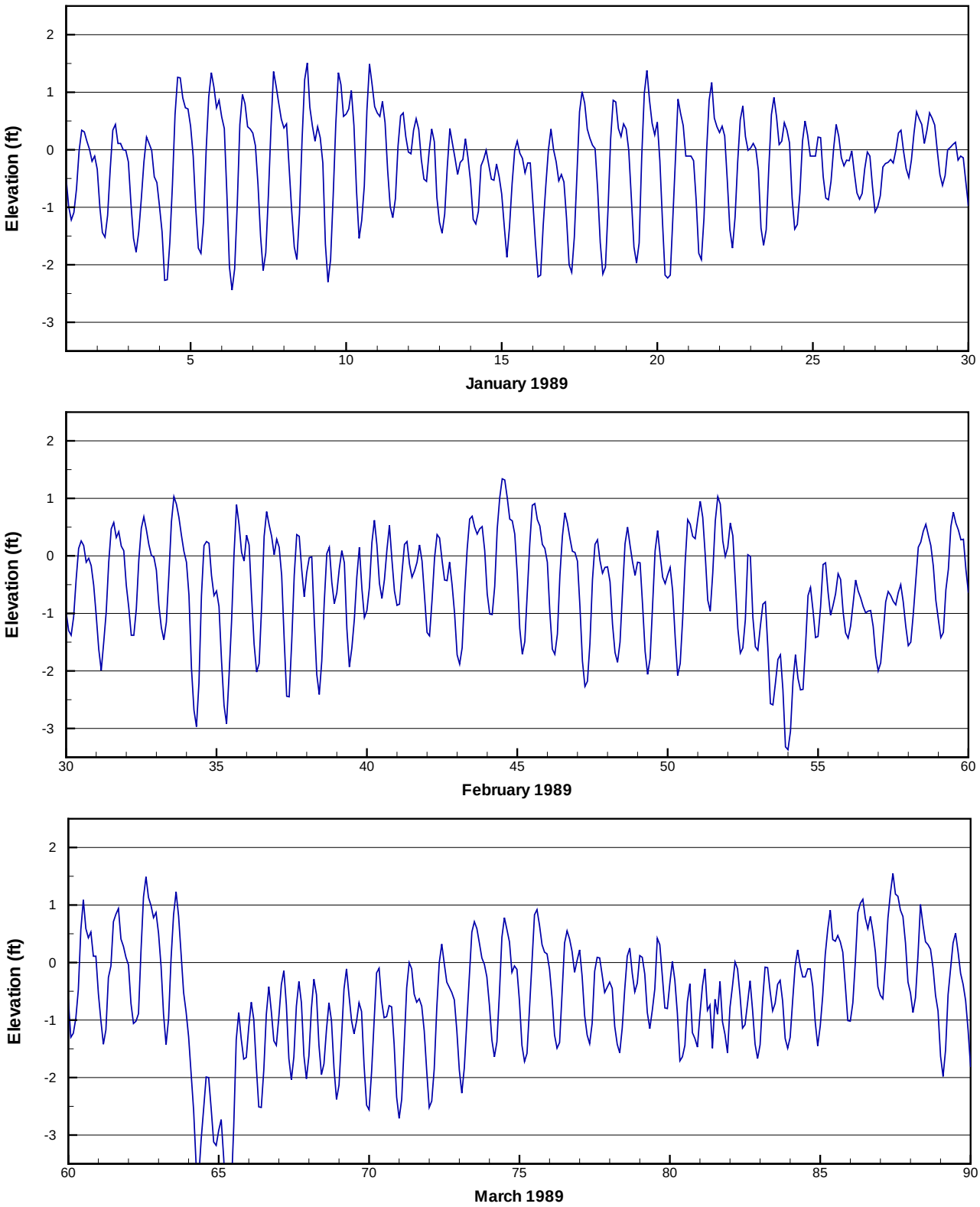

Figure 4.1 Tides at Galveston Pleasure Pier in January, February, March 1989.
A 28-day period from Day 13 through Day 40 was used for residual vector calculation

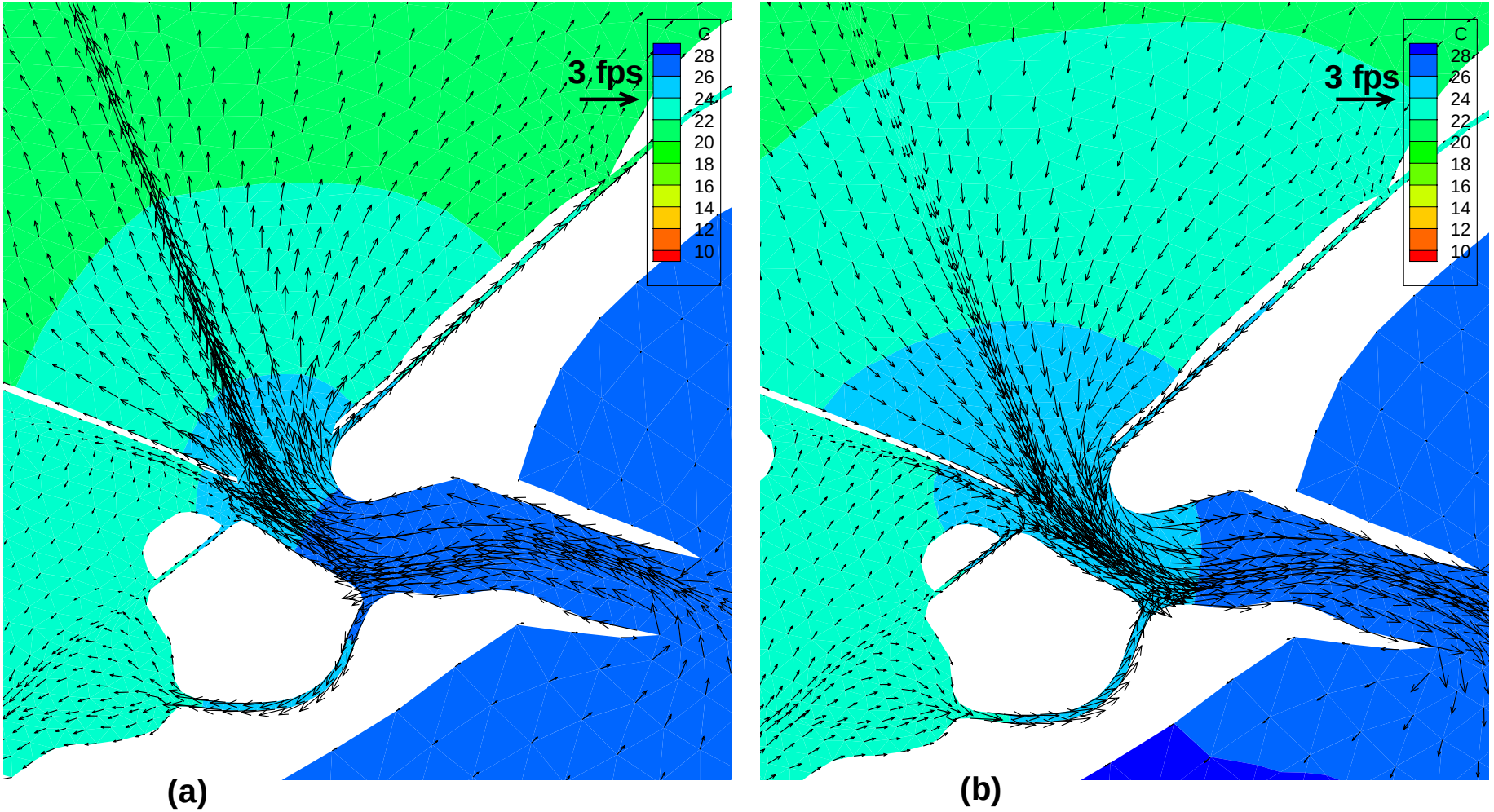

Figure 4.2 Velocity vectors in Bolivar Roads area during a typical diurnal tide,
(a) flood tide of January 17, (b) ebb tide of January 18, 1989
Color scale represents the salinity in ppt.

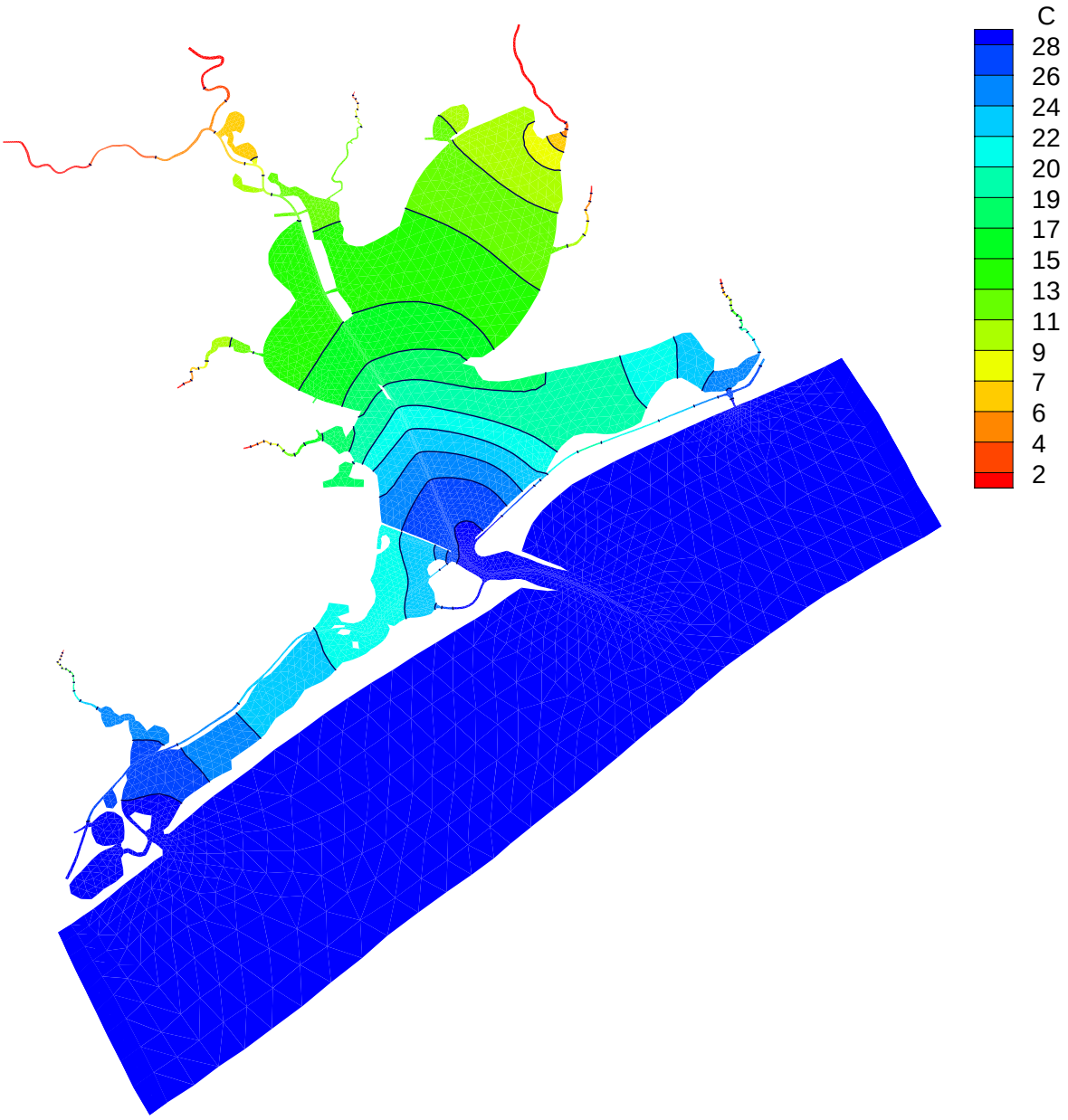

Figure 4.3 Flood tide and salinity on February 24, 1989.
Notice that the HSC is the leading edge of the salinity contours

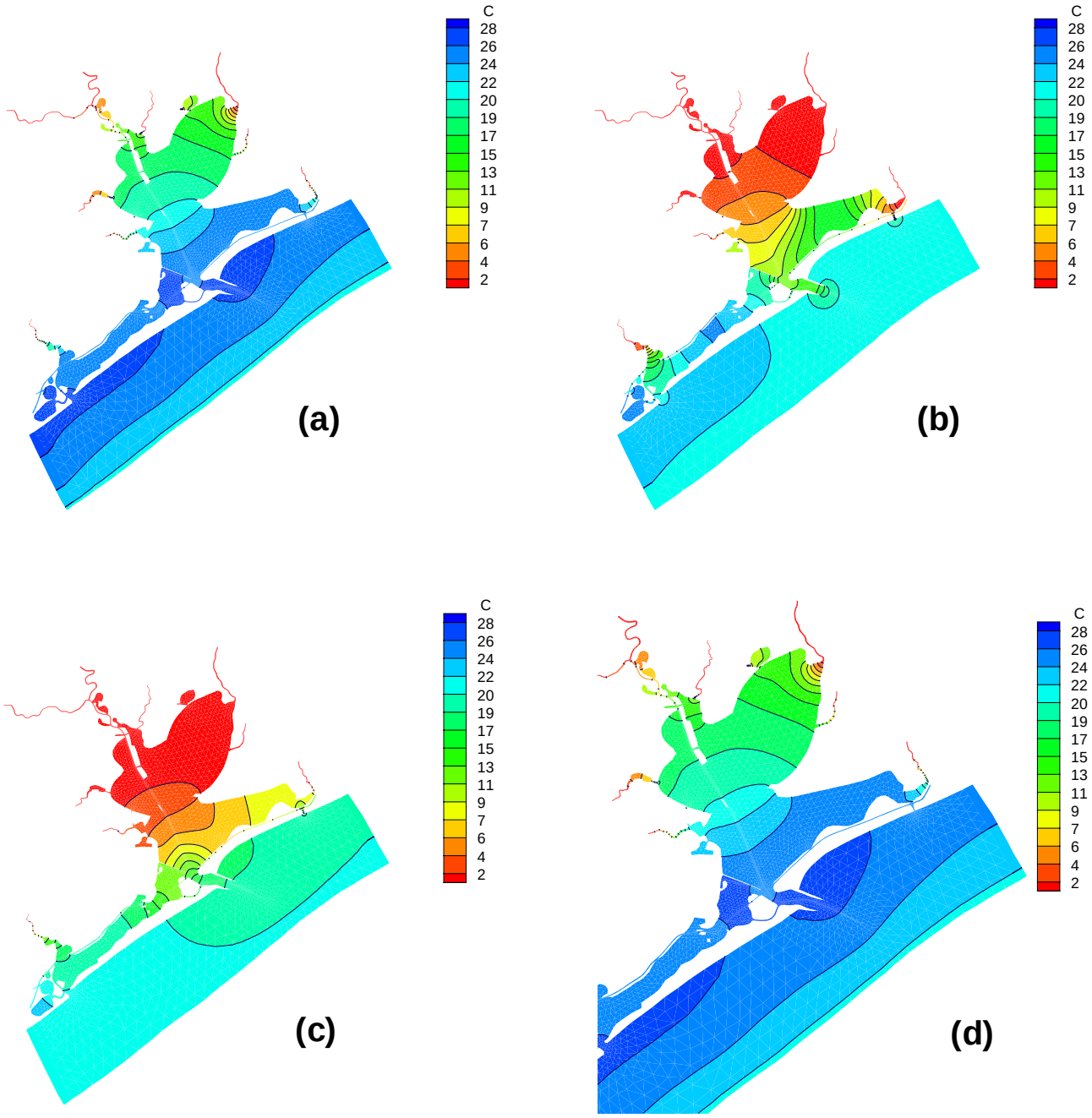

Figure 4.4 Flooding event of October 1994,
(a) October 17, (b) October 18, (c) October 19, (d) October 20

5. NET FLOW CALCULATION

In this section the detailed calculation of net flows through passes and sections are presented. In the context of flow balance, inflow and net flow (net outflow) can be used interchangeably because the difference between the incoming flow and outgoing flow at passes should be the same as the inflow from the rivers and creeks, since the evaporation and direct precipitation are close to each other. We calculated net flow (net outflow) because flows at the Gulf passes and chosen cross sections are so strongly influenced by tides that it is unclear from the hourly discharges what portion of river inflows exits from the passes.

Entrance Channel Area Sections

Figure 5.1 shows the sections in the Entrance Channel area where the flows going out of the system and coming into the system are computed. TxBLEND computes hourly flow volumes at specified sections. In earlier test runs the EntrCh1 and EntrCh2 sections were specified for the outflow calculation. It was realized that there is a significant difference between those two sections. To investigate the difference, an additional six sections, EntrX1 through EntrX6 were added. Table 5.1 lists monthly in/out flows through the Entrance Channel sections as well as through Rollover Pass and San Luis Pass for 1989. The yearly sum near the end of the table shows the difference between the in/out flows. These net flows are added to the net flows through Rollover Pass and San Luis Pass to compute the total outflow from the Galveston Bay system. These estimated outflows are compared with observed total inflows and the differences are computed and shown in the last line of the table. From this error calculation the EntrX2 was selected to represent the entrance channel section because it has the smallest error.

There may be various reasons as to why variability exists among those sections. The sections could be taken along straight lines by adding more elements (by dividing elements into two to make straight lines), although theoretically it should give the same result with those sections taken along the edge of the elements because the normal component of the velocity to the element edge is the same as taking the component of the edge normal to the flow direction. Another reason is coarseness of the computational grid. Finer computational grids should give better estimates. Also, related to the resolution, is the complex flow pattern in the Entrance Channel area. There can be a reverse flow along the jetties. In spite of the differences, since the model is not intended to study the detail flow pattern in the Entrance Channel area, it is decided the estimated outflows are accurate enough to calculate the overall balance of inflow and outflow of the Galveston Bay system.

Total Outflow and Error

Table 5.2 lists the simulated outflows from the Galveston Bay system at Rollover Pass, San Luis Pass, and the entrance channel represented by EntrX2 for the 8-year period of 1989-1996. The simulated total outflows are compared with the observed total inflows and the percent errors are computed. It ranges from 0.1 % to 5.7% in absolute value and the average error is 2.3%. These calculations are based on the assumption that yearly inflow equals yearly net outflow.

West Bay Net Flow
Table 5.2 also lists the corrected outflows through Rollover Pass, San Luis Pass, and the EntrX2. The error is distributed according to the percent error. The last column in Table 5.2 is West Bay net flows. These were calculated by subtracting the Chocolate Creek inflow from the corrected San Luis Pass outflow.

Texas City Dike Section
Table 5.3 shows how the net flow in the Texas City Dike section was computed (see Figure 6.1 for the locations of the sections). The second and the third columns list simulated net flows through the Texas City Dike section and the Galveston Channel section. Because the flow pattern in the Texas City Dike section is complex including the reverse flow along the Pelican Island near the GIWW, the net flow calculated by the sectional average velocity may not be accurate. On the other hand, the flow in Galveston Channel is more uniform (and uni-directional) and the flow volume calculation should give an accurate estimate. Therefore, instead of correcting the flows by the ratio between the Galveston Channel and Texas City Dike, the simulated Galveston Channel flow was taken as the net flow and the Texas City Dike section net flow was computed by subtracting the Galveston Channel net flow from the corrected West Bay net flow.

The net flow through the Bolivar1 section was computed by adding the calculated Texas City Dike net flow, the Galveston Channel net flow, and the EntrX2 net flow. The net flow through the Bolivar2 section was computed by subtracting the calculated Texas City Dike net flow from the Bolivar1 net flow.

River Inflows
Table 5.4 lists the river inflows from rivers and creeks around the Galveston Bay system for the 8 year period. It also lists the average inflows and the averages in percent. The bottom half of the table lists the percent inflows to show the variability among the rivers and creeks. The DickinsnIn is the intake at Reliant Power Plant near Dickinson Bay. It is listed in the table for comparison and is not a part of the total inflow.

Eagle Point and Smith Point
Table 5.5 lists the calculation of net flows through the Eagle Point section and the Smith Point section. Because the Reliant Power Plant near Dickinson Bay discharges cooling water to Galveston Bay near Bacliff, total net flow through the Eagle Point – Smith Point section should be the sum of the discharge and inflows from rivers and creeks. The RivrA includes Trinity River, San Jacinto River, Buffalo Bayou, Cedar Bayou, Clear Creek and Double Bayou. The corrected net flows through Eagle Point section and Smith Point section were calculated so that the sum of the RivrA inflow and the power plant discharge equals the net flow through the Eagle Point – Smith Point section.

Net Flows at Passes for the Existing Condition
Table 5.6 is a summary table for the net flows at passes for the existing condition. The flows were summarized as percent of average 8-year flows (Figure 6.2). The bottom half

of Table 5.6 lists the percent net flows at passes to indicate the variation among the passes.

Net Flows at Passes for the Scenarios

Table 5.7 is a summary table for the *no diversion* case. Those net flows were computed as for the existing case. Tables 5.8 through 5.11 are summary tables for the no-power case, the Texas City Dike removal case, the HSC removal case, and the natural case.

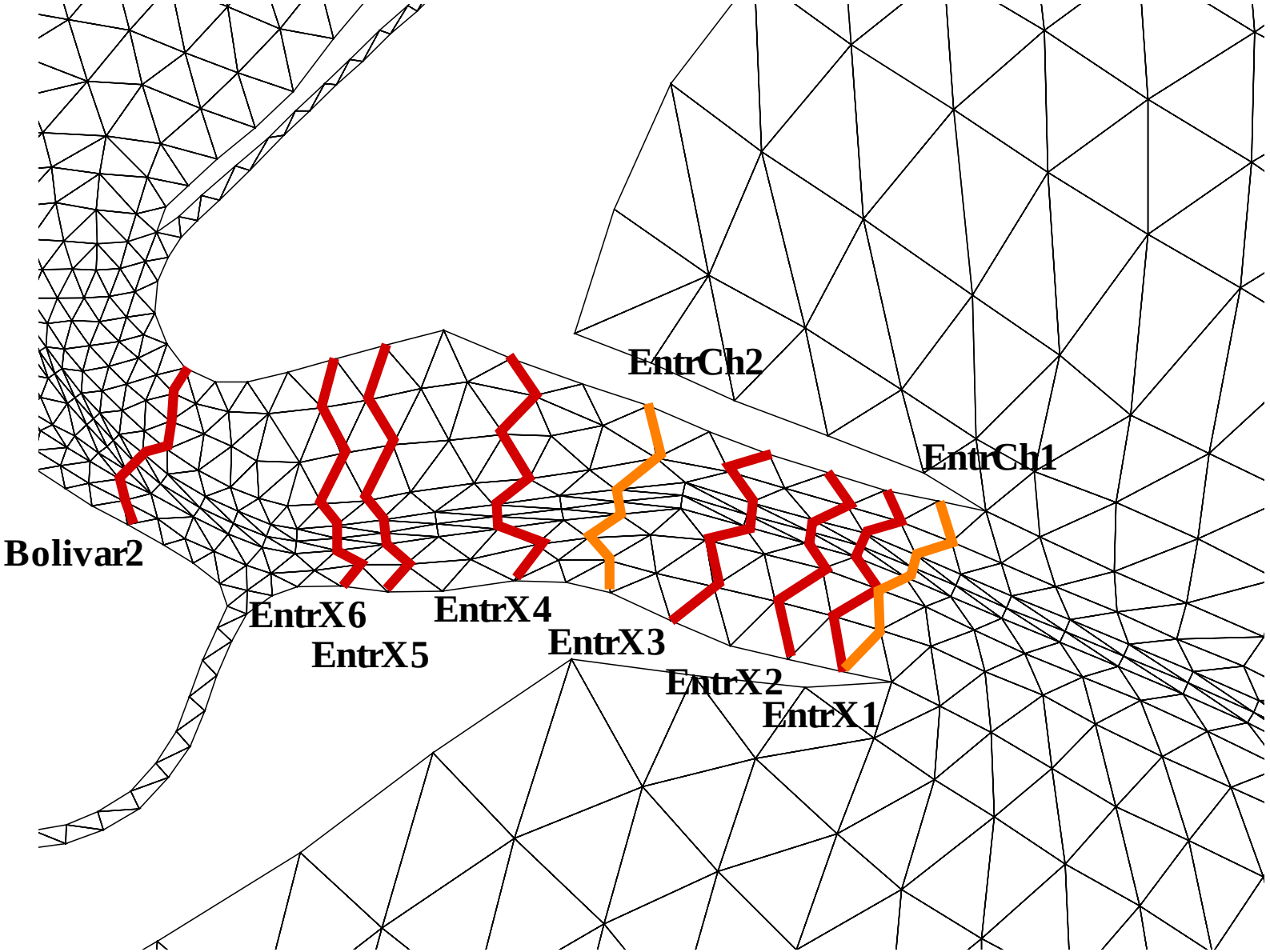

Figure 5.1 Cross sections at the Entrance Channel
Orange: original two sections, red: addtional 5 sections

Table 5.1 Flow comparison at cross-sections in the entrance channel area, flow in 1000 ac-ft

Year	Month	Days	In/Out	Rollover	SanLuis	EntrCh1	EntrCh2	EntrX1	EntrX2	EntrX3	EntrX4	EntrX5	EntrX6
1989	1	31	in	288	1788	12102	11770	11826	11833	11857	11820	11864	11673
1989	1	31	out	-258	-2190	-11976	-11641	-11717	-11705	-11738	-11690	-11765	-11529
1989	2	28	in	242	1571	10583	10302	10354	10347	10370	10350	10395	10230
1989	2	28	out	-229	-1927	-10602	-10310	-10360	-10364	-10398	-10356	-10425	-10218
1989	3	31	in	247	1734	11224	10938	10986	10984	11010	10978	11023	10850
1989	3	31	out	-273	-1934	-11978	-11636	-11694	-11698	-11737	-11696	-11775	-11540
1989	4	30	in	259	1829	11002	10728	10770	10771	10798	10774	10827	10651
1989	4	30	out	-273	-1962	-11253	-10936	-10968	-10990	-11029	-10989	-11078	-10862
1989	5	31	in	237	2018	10179	9935	9972	9976	10001	9959	10005	9843
1989	5	31	out	-326	-1930	-13096	-12706	-12766	-12776	-12815	-12774	-12875	-12620
1989	6	30	in	247	2066	11164	10893	10949	10940	10964	10923	10971	10790
1989	6	30	out	-401	-2109	-15078	-14613	-14697	-14706	-14748	-14698	-14806	-14500
1989	7	31	in	221	1960	11495	11244	11327	11278	11294	11269	11311	11146
1989	7	31	out	-366	-2077	-13300	-12886	-12924	-12965	-13015	-12962	-13074	-12798
1989	8	31	in	224	1894	10975	10754	10817	10773	10792	10783	10827	10676
1989	8	31	out	-353	-2206	-12010	-11637	-11655	-11709	-11756	-11703	-11809	-11561
1989	9	30	in	271	1817	11291	11020	11065	11057	11080	11068	11120	10949
1989	9	30	out	-297	-2298	-10685	-10391	-10401	-10445	-10486	-10439	-10531	-10321
1989	10	31	in	300	1993	12025	11721	11767	11771	11798	11772	11828	11633
1989	10	31	out	-308	-2379	-12065	-11724	-11765	-11787	-11828	-11779	-11876	-11638
1989	11	30	in	287	1858	12133	11807	11869	11867	11892	11860	11910	11709
1989	11	30	out	-271	-2191	-12037	-11695	-11763	-11762	-11797	-11742	-11816	-11582
1989	12	31	in	237	1599	11932	11608	11677	11665	11688	11656	11702	11508
1989	12	31	out	-229	-1993	-11897	-11563	-11641	-11629	-11664	-11607	-11666	-11433
Yearly sum			in	3060	22126	136105	132719	133377	133261	133543	133213	133782	131657
Yearly sum			out	-3585	-25195	-145977	-141737	-142352	-142534	-143011	-142434	-143495	-140603
Yearly sum			difference	-525	-3069	-9872	-9018	-8975	-9274	-9468	-9221	-9713	-8946
Rollover+SanLuis+Entr						-13466	-12613	-12569	-12868	-13062	-12815	-13307	-12540
Observed total inflow						12855	12855	12855	12855	12855	12855	12855	12855
Difference=Obseved -(Rollover+SanLuis+Entr)						-611	243	286	-13	-207	40	-452	315

Table 5.2 Simulated total outflow and calculated West Bay net flow in 1000 ac-ft for the existing condition

Year	Simultd Rollover	Simultd SanLuisP	Simultd EntrX2	Simultd Sum	Observed inflow	%Error	Correctd Rollover	Correctd SanLuis	Corrected EntrX2	Corrected Sum	Chocorate Creek	Calculated WestBay
1989	525.7	3003.7	9337.2	12866.5	12854.9	0.09	525.2	3001.0	9328.8	12855.0	367.0	2634.0
1990	697.2	2260.7	10873.4	13831.3	14621.2	-5.71	737.0	2389.8	11494.4	14621.2	218.4	2171.4
1991	979.5	4279.7	18135.9	23395.0	23077.7	1.36	966.2	4221.7	17889.9	23077.8	600.7	3621.0
1992	1115.4	4325.7	20912.5	26353.5	25457.1	3.40	1077.5	4178.6	20201.2	25457.2	801.6	3377.0
1993	957.7	3945.9	15315.0	20218.6	20282.3	-0.32	960.7	3958.3	15363.3	20282.3	624.5	3333.9
1994	683.3	3263.4	12644.6	16591.2	17196.2	-3.65	708.2	3382.4	13105.7	17196.3	320.3	3062.1
1995	750.6	4387.9	11537.3	16675.8	16310.8	2.19	734.2	4291.9	11284.8	16310.8	597.1	3694.8
1996	491.3	2176.1	3117.0	5784.3	5905.6	-2.10	501.6	2221.7	3182.4	5905.7	329.4	1892.4

Note: %Error=(Simultd-Obsrvd)/Simultd*100
Correction: Simultd*(1-%Error/100)
Calculatd WestBay=Correctd SanLuis-ChocorateCreek

Table 5.3 Calculated Texas City Dike section net flow in 1000 ac-ft for the existing condition

Year	Simulated TxCtyDike	Simulated GalvestnChnl	Calculated WestBay	Calculatd TxCtyDk	Corrected EntrX2	Calculatd Bolivar2	Calculatd Bolivar1
1989	782.2	1386.6	2634.0	1247.4	9328.8	10715.4	11962.8
1990	95.2	1735.9	2171.4	435.5	11494.4	13230.3	13665.8
1991	1376.4	1347.7	3621.0	2273.3	17889.9	19237.6	21510.9
1992	1110.1	1333.5	3377.0	2043.5	20201.2	21534.7	23578.2
1993	1300.2	1312.6	3333.9	2021.3	15363.3	16675.9	18697.1
1994	1130.3	1355.8	3062.1	1706.3	13105.7	14461.5	16167.8
1995	1611.6	1513.6	3694.8	2181.2	11284.8	12798.4	14979.5
1996	284.4	1475.1	1892.4	417.3	3182.4	4657.5	5074.7

CalculatedTxCtyDk=CalculatedWestBay-Simulated GalvestonChannel
CalculatedBolivar1=CorrectedEntr2+CalculatdTxCtyDk+SimulatdGalvestnChnnl
CalculatdBolivar2=CalculatdBolivar1-CalculatdTxCtyDk

Table 5.4 River inflows in 1000 ac-ft, 1989-1996

Year	Buffalo	Cedar	Chocolate	Clear	Dickinson	Double	Oyster	SanJacinto	Trinity	DicknsnIn	TotalInflw
1989	1485.3	237.6	367.0	337.5	293.4	269.2	752.7	1171.3	7940.9	1495.9	12854.9
1990	1026.2	130.3	218.4	242.7	214.3	191.4	547.7	896.2	11154.0	1528.6	14621.2
1991	2111.1	359.3	600.7	572.4	498.9	399.0	1158.6	7007.9	10369.9	1525.2	23077.7
1992	2346.1	406.2	801.6	546.2	551.7	243.1	638.6	6507.7	13415.9	1437.4	25457.1
1993	1886.8	372.8	624.5	439.9	343.1	275.2	742.8	5938.7	9658.5	1339.0	20282.3
1994	1658.7	479.3	320.3	347.9	195.8	258.1	687.5	2385.4	10863.2	1535.8	17196.2
1995	1410.1	426.8	597.1	423.8	502.9	312.1	875.3	2069.8	9692.8	1437.6	16310.8
1996	982.0	232.6	329.4	237.3	361.2	167.6	439.4	927.9	2228.2	1270.6	5905.6
average	1613.3	330.6	482.4	393.5	370.2	264.5	730.3	3363.1	9415.4	1446.3	16963.2
ave(in%)	9.5	1.9	2.8	2.3	2.2	1.6	4.3	19.8	55.5	8.5	
1989	11.6	1.8	2.9	2.6	2.3	2.1	5.9	9.1	61.8	11.6	
1990	7.0	0.9	1.5	1.7	1.5	1.3	3.7	6.1	76.3	10.5	
1991	9.1	1.6	2.6	2.5	2.2	1.7	5.0	30.4	44.9	6.6	
1992	9.2	1.6	3.1	2.1	2.2	1.0	2.5	25.6	52.7	5.6	
1993	9.3	1.8	3.1	2.2	1.7	1.4	3.7	29.3	47.6	6.6	
1994	9.6	2.8	1.9	2.0	1.1	1.5	4.0	13.9	63.2	8.9	
1995	8.6	2.6	3.7	2.6	3.1	1.9	5.4	12.7	59.4	8.8	
1996	16.6	3.9	5.6	4.0	6.1	2.8	7.4	15.7	37.7	21.5	
avearge	10.1	2.1	3.0	2.5	2.5	1.7	4.7	17.8	55.5	10.0	

For Figure 6.2 the average inflow in percent based on the annual average inflow is used instead of the average of the annual percent inflow. DickinsnIn is the intake at the Reliant Power Plant near Dickinson Bay; it is listed here for comparison. It is not a part of the total inflow.

Table 5.5 Calculated net flow in 1000 ac-ft at Eagle Point section and Smith Point section for the exisiting condition

	EaglePt	Simulatd SmithPt	Simulatd DicknsnIn	Simulatd EglSmth	RatioE	RatioS	Sum of RivrA	Calculatd EglSmth	Percent Error	Correctd EaglePt	Correctd SmithPt
1989	3912.1	8448.2	1495.9	12360.3	0.32	0.68	11441.8	12937.7	4.5	4094.9	8842.9
1990	3659.6	10441.4	1528.6	14101.0	0.26	0.74	13640.8	15169.4	7.0	3936.9	11232.5
1991	5509.5	15690.5	1525.2	21200.0	0.26	0.74	20819.5	22344.7	5.1	5807.0	16537.7
1992	5564.0	18305.5	1437.4	23869.5	0.23	0.77	23465.2	24902.6	4.1	5804.8	19097.8
1993	5194.4	13513.6	1339.0	18708.0	0.28	0.72	18572.0	19911.0	6.0	5528.4	14382.6
1994	4288.4	12089.0	1535.8	16377.4	0.26	0.74	15992.6	17528.4	6.6	4589.8	12938.6
1995	4261.5	10693.4	1437.6	14954.9	0.28	0.72	14335.5	15773.1	5.2	4494.6	11278.4
1996	2716.3	2931.6	1270.6	5647.9	0.48	0.52	4775.7	6046.3	6.6	2907.9	3138.4
avearge	4388.2	11514.2	1446.3	15902.4			15380.4			4645.5	12181.1
%of total			8.5				90.7			27.4	71.8

Simulated EglSmith is the sum of EaglePt and SmithPt
Calculated EglSmth is the sum of RvrA and DikinsonIntake
Sum of RivrA includes Buffalo Bayou, Cedar Bayou, Clear Creek, Double Bayou, San Jacinto River, and Trinity River
Total inflow is the average of 8 year inflows: 16,963*1000 ac-ft

Table 5.6 Net flows for the existing condition in 1000 ac-ft

	Correctd EaglePt	Correctd SmithPt	Calculated WestBay	Calculatd TxCtyDk	Simulatd GalChnl	Calculatd Bolivar2	Calculatd Bolivar1	Correctd Rollover	Correctd SanLuis	Corrected EntrX2	Obsrvd Total_Inflw
1989	4094.9	8842.9	2634.0	1247.4	1386.6	10715.4	11962.8	525.2	3001.0	9328.8	12854.9
1990	3936.9	11232.5	2171.4	435.5	1735.9	13230.3	13665.8	737.0	2389.8	11494.4	14621.2
1991	5807.0	16537.7	3621.0	2273.3	1347.7	19237.6	21510.9	966.2	4221.7	17889.9	23077.7
1992	5804.8	19097.8	3377.0	2043.5	1333.5	21534.7	23578.2	1077.5	4178.6	20201.2	25457.1
1993	5528.4	14382.6	3333.9	2021.3	1312.6	16675.9	18697.1	960.7	3958.3	15363.3	20282.3
1994	4589.8	12938.6	3062.1	1706.3	1355.8	14461.5	16167.8	708.2	3382.4	13105.7	17196.2
1995	4494.6	11278.4	3694.8	2181.2	1513.6	12798.4	14979.5	734.2	4291.9	11284.8	16310.8
1996	2907.9	3138.4	1892.4	417.3	1475.1	4657.5	5074.7	501.6	2221.7	3182.4	5905.6
average	4645.5	12181.1	2973.3	1540.7	1432.6	14163.9	15704.6	776.3	3455.7	12731.3	16963.2
%	27.4	71.8	17.5	9.1	8.4	83.5	92.6	4.6	20.4	75.1	100.0
Annual net flow in percent											
1989	31.9	68.8	20.5	9.7	10.8	83.4	93.1	4.1	23.3	72.6	
1990	26.9	76.8	14.9	3.0	11.9	90.5	93.5	5.0	16.3	78.6	
1991	25.2	71.7	15.7	9.9	5.8	83.4	93.2	4.2	18.3	77.5	
1992	22.8	75.0	13.3	8.0	5.2	84.6	92.6	4.2	16.4	79.4	
1993	27.3	70.9	16.4	10.0	6.5	82.2	92.2	4.7	19.5	75.7	
1994	26.7	75.2	17.8	9.9	7.9	84.1	94.0	4.1	19.7	76.2	
1995	27.6	69.1	22.7	13.4	9.3	78.5	91.8	4.5	26.3	69.2	
1996	49.2	53.1	32.0	7.1	25.0	78.9	85.9	8.5	37.6	53.9	
aveargе	29.7	70.1	19.2	8.9	10.3	83.2	92.0	4.9	22.2	72.9	

Table 5.7 Net flows for the No Diversion case in 1000 ac-ft

	Correctd EaglePt	Correctd SmithPt	Calculated WestBay	Calculatd TxCtyDk	Simulatd GalChnl	Calculatd Bolivar2	Calculatd Bolivar1	Correctd Rollover	Correctd SanLuis	Corrected EntrX2	Obsrvd Total_Inflw
1989	4094.8	8842.9	2634.0	1247.4	1386.6	10715.3	11962.7	525.2	3001.0	9328.7	12854.9
1990	3942.7	11226.7	2190.9	450.5	1740.4	13208.8	13659.3	743.6	2409.3	11468.4	14621.2
1991	5792.1	16552.6	3637.6	2285.1	1352.5	19220.3	21505.4	971.6	4238.3	17867.8	23077.7
1992	5792.8	19109.8	3393.9	2056.1	1337.8	21516.2	23572.3	1083.2	4195.5	20178.4	25457.1
1993	5514.1	14396.9	3350.0	2032.9	1317.1	16658.9	18691.7	966.1	3974.4	15341.8	20282.3
1994	4590.7	12937.6	3085.6	1723.6	1362.0	14436.0	16159.6	716.4	3405.9	13074.0	17196.2
1995	4489.1	11284.0	3716.1	2196.5	1519.6	12776.1	14972.6	741.2	4313.2	11256.5	16310.8
1996	2927.3	3119.0	1929.6	446.6	1483.0	4614.3	5060.9	515.2	2259.0	3131.3	5905.6
average	4642.9	12183.7	2992.2	1554.8	1437.4	14143.2	15698.1	782.8	3474.6	12705.9	16963.2
ave(%)	27.4	71.8	17.6	9.2	8.5	83.4	92.5	4.6	20.5	74.9	
Annual net flow in percent											
1989	31.9	68.8	20.5	9.7	10.8	83.4	93.1	4.1	23.3	72.6	
1990	27.0	76.8	15.0	3.1	11.9	90.3	93.4	5.1	16.5	78.4	
1991	25.1	71.7	15.8	9.9	5.9	83.3	93.2	4.2	18.4	77.4	
1992	22.8	75.1	13.3	8.1	5.3	84.5	92.6	4.3	16.5	79.3	
1993	27.2	71.0	16.5	10.0	6.5	82.1	92.2	4.8	19.6	75.6	
1994	26.7	75.2	17.9	10.0	7.9	83.9	94.0	4.2	19.8	76.0	
1995	27.5	69.2	22.8	13.5	9.3	78.3	91.8	4.5	26.4	69.0	
1996	49.6	52.8	32.7	7.6	25.1	78.1	85.7	8.7	38.3	53.0	
avearge	29.7	70.1	19.3	9.0	10.3	83.0	92.0	5.0	22.3	72.7	

Table 5.8 Net flows for the No Power case in 1000 ac-ft

	Correctd EaglePt	Correctd SmithPt	Calculated WestBay	Calculatd TxCtyDk	Simulatd GalChnl	Calculatd Bolivar2	Calculatd Bolivar1	Correctd Rollover	Correctd SanLuis	Corrected EntrX2	Obsrvd Total_Inflw
1989	3801.6	7640.2	2597.3	1215.4	1381.9	10753.0	11968.4	519.6	2964.3	9371.1	12854.9
1990	3655.5	9985.3	2156.8	422.3	1734.5	13248.0	13670.4	732.6	2375.2	11513.5	14621.2
1991	5550.3	15269.2	3605.9	2260.6	1345.3	19251.7	21512.2	964.8	4206.6	17906.4	23077.7
1992	5530.5	17934.8	3355.4	2025.5	1329.9	21557.6	23583.0	1072.6	4156.9	20227.7	25457.1
1993	5339.3	13232.6	3332.6	2017.6	1315.0	16677.4	18695.0	962.9	3957.1	15362.4	20282.3
1994	4337.2	11655.4	3045.5	1691.4	1354.1	14476.3	16167.7	708.2	3365.8	13122.2	17196.2
1995	4220.9	10114.6	3662.5	2148.9	1513.6	12834.6	14983.5	730.2	4259.6	11321.0	16310.8
1996	2504.0	2271.6	1752.0	299.9	1452.1	4819.2	5119.1	457.2	2081.4	3367.1	5905.6
average	4367.4	11013.0	2938.5	1510.2	1428.3	14202.2	15712.4	768.5	3420.9	12773.9	16963.2
ave(%)	25.7	64.9	17.3	8.9	8.4	83.7	92.6	4.5	20.2	75.3	
Annual net flow in percent											
1989	29.6	59.4	20.2	9.5	10.7	83.6	93.1	4.0	23.1	72.9	
1990	25.0	68.3	14.8	2.9	11.9	90.6	93.5	5.0	16.2	78.7	
1991	24.1	66.2	15.6	9.8	5.8	83.4	93.2	4.2	18.2	77.6	
1992	21.7	70.5	13.2	8.0	5.2	84.7	92.6	4.2	16.3	79.5	
1993	26.3	65.2	16.4	9.9	6.5	82.2	92.2	4.7	19.5	75.7	
1994	25.2	67.8	17.7	9.8	7.9	84.2	94.0	4.1	19.6	76.3	
1995	25.9	62.0	22.5	13.2	9.3	78.7	91.9	4.5	26.1	69.4	
1996	42.4	38.5	29.7	5.1	24.6	81.6	86.7	7.7	35.2	57.0	
avearge	27.5	62.2	18.8	8.5	10.2	83.6	92.1	4.8	21.8	73.4	

Table 5.9 Net flows for the Texas City Dike Removal case in 1000 ac-ft

	Correctd EaglePt	Correctd SmithPt	Calculated WestBay	Calculatd TxCtyDk	Simulatd GalChnl	Calculatd Bolivar2	Calculatd Bolivar1	Correctd Rollover	Correctd SanLuis	Corrected EntrX2	Obsrvd Total_Inflw
1989	4045.6	8892.2	2876.5	1654.6	1221.9	10214.3	11868.9	619.0	3243.5	8992.4	12854.9
1990	3926.7	11242.7	2221.7	649.1	1572.6	12890.7	13539.8	862.9	2440.1	11318.1	14621.2
1991	5744.1	16600.6	3663.7	2607.6	1056.1	18786.4	21394.0	1083.2	4264.3	17730.3	23077.7
1992	5779.3	19123.3	3416.9	2406.6	1010.3	21064.9	23471.5	1184.0	4218.5	20054.6	25457.1
1993	5449.3	14461.6	3359.2	2242.9	1116.3	16330.9	18573.8	1084.0	3983.7	15214.6	20282.3
1994	4571.6	12956.7	2950.0	1814.5	1135.5	14242.1	16056.7	819.3	3270.3	13106.6	17196.2
1995	4444.0	11329.1	3844.9	2550.6	1294.3	12317.9	14868.5	845.2	4442.0	11023.6	16310.8
1996	2892.1	3154.1	2250.9	792.9	1458.0	4213.0	5005.9	570.3	2580.3	2755.0	5905.6
average	4606.6	12220.0	3073.0	1839.9	1233.1	13757.5	15597.4	883.5	3555.3	12524.4	16963.2
ave(%)	27.2	72.0	18.1	10.8	7.3	81.1	91.9	5.2	21.0	73.8	
Annual net flow in percent											
1989	31.5	69.2	22.4	12.9	9.5	79.5	92.3	4.8	25.2	70.0	
1990	26.9	76.9	15.2	4.4	10.8	88.2	92.6	5.9	16.7	77.4	
1991	24.9	71.9	15.9	11.3	4.6	81.4	92.7	4.7	18.5	76.8	
1992	22.7	75.1	13.4	9.5	4.0	82.7	92.2	4.7	16.6	78.8	
1993	26.9	71.3	16.6	11.1	5.5	80.5	91.6	5.3	19.6	75.0	
1994	26.6	75.3	17.2	10.6	6.6	82.8	93.4	4.8	19.0	76.2	
1995	27.2	69.5	23.6	15.6	7.9	75.5	91.2	5.2	27.2	67.6	
1996	49.0	53.4	38.1	13.4	24.7	71.3	84.8	9.7	43.7	46.7	
avearge	29.4	70.3	20.3	11.1	9.2	80.2	91.3	5.6	23.3	71.1	

Check-1: Rollover+SanLuisPass+EntrX2
Calculated TxCty Dike: Clculated West Bay - Simulated Galveston Channel
Calculated Bolivar1: Calculated Bolivar2+Calculated TxCtyDike

Table 5.10 Net flows for the HSC Removal case in 1000 ac-ft

	Correctd EaglePt	Correctd SmithPt	Calculated WestBay	Calculatd TxCtyDk	Calculatd GalChnl	Calculatd Bolivar2	Calculatd Bolivar1	Correctd Rollover	Correctd SanLuis	Corrected EntrX2	Obsrvd Total_Inflw
1989	3335.2	9602.5	2015.9	2015.9		10184.1	12200.0	287.9	2382.9	10184.1	12854.9
1990	3834.8	11334.6	1376.4	1376.4		12529.1	13905.5	497.4	1594.8	12529.1	14621.2
1991	5724.7	16620.0	3068.5	3068.5		18656.4	21724.9	752.2	3669.2	18656.4	23077.7
1992	6278.7	18623.9	2892.7	2892.7		20907.9	23800.5	855.0	3694.2	20907.9	25457.1
1993	5132.5	14778.5	2701.8	2701.8		16252.9	18954.7	703.3	3326.2	16252.9	20282.3
1994	4444.7	13083.7	2561.2	2561.2		13842.5	16403.6	472.3	2881.4	13842.5	17196.2
1995	3956.6	11816.5	2939.0	2939.0		12339.9	15278.9	434.8	3536.1	12339.9	16310.8
1996	1694.1	4352.2	1070.8	1070.8		4267.0	5337.8	238.3	1400.1	4267.0	5905.6
average	4300.2	12526.5	2328.3	2328.3		13622.5	15950.7	530.1	2810.6	13622.5	16963.2
ave(%)	25.3	73.8	13.7	13.7		80.3	94.0	3.1	16.6	80.3	
Annual net flow in percent											
1989	25.9	74.7	15.7	15.7		79.2	94.9	2.2	18.5	79.2	
1990	26.2	77.5	9.4	9.4		85.7	95.1	3.4	10.9	85.7	
1991	24.8	72.0	13.3	13.3		80.8	94.1	3.3	15.9	80.8	
1992	24.7	73.2	11.4	11.4		82.1	93.5	3.4	14.5	82.1	
1993	25.3	72.9	13.3	13.3		80.1	93.5	3.5	16.4	80.1	
1994	25.8	76.1	14.9	14.9		80.5	95.4	2.7	16.8	80.5	
1995	24.3	72.4	18.0	18.0		75.7	93.7	2.7	21.7	75.7	
1996	28.7	73.7	18.1	18.1		72.3	90.4	4.0	23.7	72.3	
avearge	25.7	74.1	14.3	14.3		79.6	93.8	3.1	17.3	79.6	

Calculated TxCty Dike is the same as the Calculated West Bay
Calculated Bolivar2 is the same as the Corrected EntrX2
Calculated Bolivar1 is the sum of Calculated Bolivar2+Calculated TxCtyDike

Table 5.11 Net flows for the Natural case in 1000 ac-ft

	Correctd EaglePt	Correctd SmithPt	Calculated WestBay	Calculatd TxCtyDk	Calculatd GalChnl	Calculatd Bolivar2	Calculatd Bolivar1	Correctd Rollover	Correctd SanLuis	Corrected EntrX2	Obsrvd Total_Inflw
1989	2878.1	8563.7	1988.6	1988.6		10214.5	12203.1	284.7	2355.6	10214.5	12854.9
1990	3356.8	10283.9	1372.4	1372.4		12535.9	13908.3	494.5	1590.8	12535.9	14621.2
1991	5247.7	15571.8	3055.3	3055.3		18671.6	21726.8	750.2	3655.9	18671.6	23077.7
1992	5825.8	17639.5	2876.1	2876.1		20929.0	23805.1	850.6	3677.6	20929.0	25457.1
1993	4720.5	13851.5	2695.0	2695.0		16259.8	18954.9	703.0	3319.5	16259.8	20282.3
1994	3960.0	12032.6	2550.8	2550.8		13851.5	16402.3	473.7	2871.1	13851.5	17196.2
1995	3499.5	10835.9	2913.3	2913.3		12368.0	15281.2	432.6	3510.4	12368.0	16310.8
1996	1277.1	3498.5	995.1	995.1		4364.8	5359.9	216.4	1324.5	4364.8	5905.6
average	3845.7	11534.7	2305.8	2305.8		13649.4	15955.2	525.7	2788.2	13649.4	16963.2
ave(%)	22.7	68.0	13.6	13.6		80.5	94.1	3.1	16.4	80.5	
Annual net flow in percent											
1989	22.4	66.6	15.5	14.7		79.5	94.9	2.2	18.3	79.5	
1990	23.0	70.3	9.4	8.4		85.7	95.1	3.4	10.9	85.7	
1991	22.7	67.5	13.2	12.8		80.9	94.1	3.3	15.8	80.9	
1992	22.9	69.3	11.3	10.8		82.2	93.5	3.3	14.4	82.2	
1993	23.3	68.3	13.3	12.7		80.2	93.5	3.5	16.4	80.2	
1994	23.0	70.0	14.8	14.2		80.5	95.4	2.8	16.7	80.5	
1995	21.5	66.4	17.9	17.3		75.8	93.7	2.7	21.5	75.8	
1996	21.6	59.2	16.9	15.2		73.9	90.8	3.7	22.4	73.9	
avearge	22.5	67.2	14.0	13.3		79.8	93.9	3.1	17.1	79.8	

Calculated TxCty Dike is the same as the Calculated West Bay
Calculated Bolivar2 is the same as the Corrected EntrX2
Calculated Bolivar1 is the sum of Calculated Bolivar2+Calculated TxCtyDike

6. FLOWS THROUGH PASSES

In this section we present simulation results on circulation in terms of flow volumes that go through sections and passes. First we describe flows in the existing condition, then we compare between the existing condition and each scenario.

Existing Condition

Table 5.6 presents the summary of an eight year simulation for the existing condition. Figure 6.1 shows the passes where the net flows are calculated. Figure 6.2 shows percent inflows and net flows. There are three passes connected to the Gulf: Rollover Pass, Entrance Channel, and San Luis Pass. Total inflow is averages 17.0 million ac-ft over the eight years from 1989 through 1996. For the existing condition net outflows are 0.8 million ac-ft for Rollover Pass, 12.7 million ac-ft for the Entrance Channel, and 3.5 million ac-ft for San Luis Pass, which are 4.6%, 75.1% and 20.4%, respectively.

The inflows from Trinity River, San Jacinto River, Buffalo Bayou, Cedar Bayou, Double Bayou, and Clear Creek (RivrA in Table 5.5) make up 90.7% of the total inflow and they pass through the mid Galveston Bay at the Eagle Point - Smith Point section. The power plant discharge from Robinson Power Plant which is 8.5% is added to the 90.7% from the upper part of the bay and thus 99.2% go through the mid section. Of that, 27.4% passes on Eagle Point side and 71.8% on Smith Point side.

After going through the mid section, 2.2% is added from Dickinson Creek and 8.5% is subtracted for the power plant intake for Robinson Power Plant. Then 92.9% goes toward the Gulf passes of which 92.6% goes to the Bolivar1 section and 0.3% goes to East Bay. That 0.3% net flow from East Bay is added to 4.3% from Oyster Bayou to give 4.6% going through Rollover Pass to the Gulf.

The section designated as Bolivar1 extends from the tip of Texas City Dike to Port Bolivar and captures 92.6% of the total inflow. The Texas City Dike section extends from the tip of the dike to Pelican Island. The Bolivar2 section extends between Pelican Island and Bolivar Peninsula (Figure 6.1). The inflow that comes to Bolivar1 is divided into 9.1% going through Texas City Dike section and 83.5% through Bolivar2 section. The net flow at Bolivar2 is further divided into Galveston Channel, 8.4%, and the Entrance Channel, 75.1%.

Model simulation for the existing condition indicates that 17.5% of the net flow moves through West Bay toward San Luis Pass, of which 9.1% comes from the Texas City Dike section and 8.4% from the Galveston Channel.

No Diversion

Table 6.1 presents a summary of flow comparisons among the scenarios. Table 6.2 lists monthly diversions from Trinity River to San Jacinto River from 1990 through 2000. The average annual diversion is 624 thousand ac-ft. The annual Trinity River inflow is 9.4 million ac-ft over 8-year period 1989-1996, see Table 5.4. Therefore the diversion is about 7%. (Although the base periods are not the same, these numbers still convey useful

information). Model simulation indicates that the impact of the diversion to flows through the passes is minimal, all less than 0.6%(Table 6.1).

No Power

There are two power plants on the periphery of Galveston Bay: Cedar Bayou Power Plant located in Baytown and Robinson Power Plant located near Bacliff. These power plants withdraw bay water for cooling and discharge the water back into the bay. We are interested in how water withdrawal and discharge affect the circulation and salinity. In this sub-section we discuss the simulation results for circulation. The Cedar Bayou Power Plant withdraws water from Cedar Bayou and routes the discharge into a cooling pond and releases it into upper Trinity Bay. Table 6.3 lists the daily average discharge and monthly averages. The average annual discharge over 19 years is 1.25 million ac-ft, or it is 7% compared to the total inflow of 16.93 million ac-ft. (Similar to diversion statistics these numbers are based on different time periods but they still contain useful information.)

Robinson Power Plant withdraws water from Dickinson Bay and discharges into Galveston Bay near Bacliff. The average annual discharge over 16 years is 1.59 million ac-ft, which is 9% compared to the total inflow, see Table 6.4.

The *no power* scenario examines the case in which there is no cooling water withdrawal and discharge. For the existing condition the flow through the Eagle Point - Smith Point Section includes the re-circulation of cooling water from Robinson Power Plant. Without power plant operation the reduction is 8.5% (1.6% at Eagle Point side and 6.9% at Smith Point side, Table 6.1). This is consistent with the 9% withdrawal/discharge at Robinson Power Plant. (The influence of cooling water of Cedar Bayou Power Plant on the flow at the mid section is not estimated here.)

The influence on flows through the Gulf passes is very small. The net flow will be increased by 0.3% at Entrance Channel, decreased by 0.2% at San Luis Pass and no change at Rollover Pass (Table 6.1).

Texas City Dike Removal

Contrary to the expectation, the influence of Texas City Dike on the flow through West Bay is rather small. The simulation indicates only a 0.6% increase in the net flow through West Bay and San Luis Pass (Table 6.1) when the dike is removed. The flow through the City Dike section toward West Bay will be increased by 1.8% but the flow through Galveston Channel will be decreased by 1.2% and as a result the net increase is 0.6%. The flow through Rollover Pass will be increased by 0.6% and the flow through Entrance Channel will be decreased by 1.2%.

The inference that the impact is rather small is based on the percent increase of net flow through West Bay compared to total inflow. The net flow volume through West Bay is 2.97 million ac-ft for the existing condition and 3.07 million ac-ft for the dike removal case. The increase is 0.10 million ac-ft or 3.3% increase compared to the West Bay net inflow which still appears to be small. It may be that the change in flow pattern bringing

flow from upper Galveston Bay through West Bay is more significant than the increase in volume following dike removal.

Houston Ship Channel Removal

This scenario removes the Houston Ship Channel, Galveston Channel, GIWW, and Texas City Dike. (Without the HSC, the Galveston Channel and Texas City Ship Channel will not function as designed. Therefore, they too are removed for modeling this scenario). However, the diversion and power plant operations are kept as in the existing condition. The simulation indicates that the net flow in the mid section near Smith Point increases by 2.0% whereas the section of Eagle Point side that contains Houston Ship Channel decreases by 2.0%. The net flow through West Bay and San Luis Pass is reduced by 3.8%; the net flow through Rollover Pass is decreased by 1.5%; while the net flow through Entrance Channel is increased by 5.3% (Table 6.1).

Natural

For the *natural* scenario, all ship channels and the dike are removed and the diversion and power plant operations are ceased. The simulation indicates that net flow through Eagle Point section decreases by 4.7% and flow through Smith Point section also decreases by 3.8%. Flows through Rollover Pass, San Luis Pass and Entrance Channel are similar to the HSC removal case (Table 6.1). As expected, change in net flow (and thus bay circulation) for the natural case is the largest among the five scenarios.

Summary

Overall changes between the existing condition and the scenarios are relatively small with the same basic pattern: 74 to 80% of inflows exit from the Entrance Channel, 16 to 21% exit from San Luis Pass, and 3 to 5% exit from Rollover Pass. Figure 6.3 shows average annual net flows through major passes for all cases. Figure 6.4 shows the difference of average net flows in percent between the existing condition and the five cases.

Among the scenarios, the *no diversion* case has the smallest effect on circulation. The *no power* case reduces flow in the mid section (Eagle Point-Smith Point) by 8.5% but the impact on the entrance channel, San Luis Pass, and Rollover Pass is minimal. The *Texas City Dike removal* case reduces flow through the entrance channel by 1%, and increases net flow through West Bay, San Luis Pass, and Rollover Pass by 0.6%. The composition of the West Bay flow will change from 8% Galveston Channel and 9% Texas City Dike in the *existing condition* to 7% Galveston Channel and 11% Galveston Bay if the dike is removed. *Removal of the Houston Ship Channel* increases flow through the entrance channel by 5%, and decreases flow in the West Bay and San Luis Pass by 4% and the Rollover Pass by 1.5%. The *natural* case is similar to the *HSC removal* case regarding the changes in the Gulf passes, but at the mid section the net flow through Eagle Point-Smith Point will be reduced by 4%.

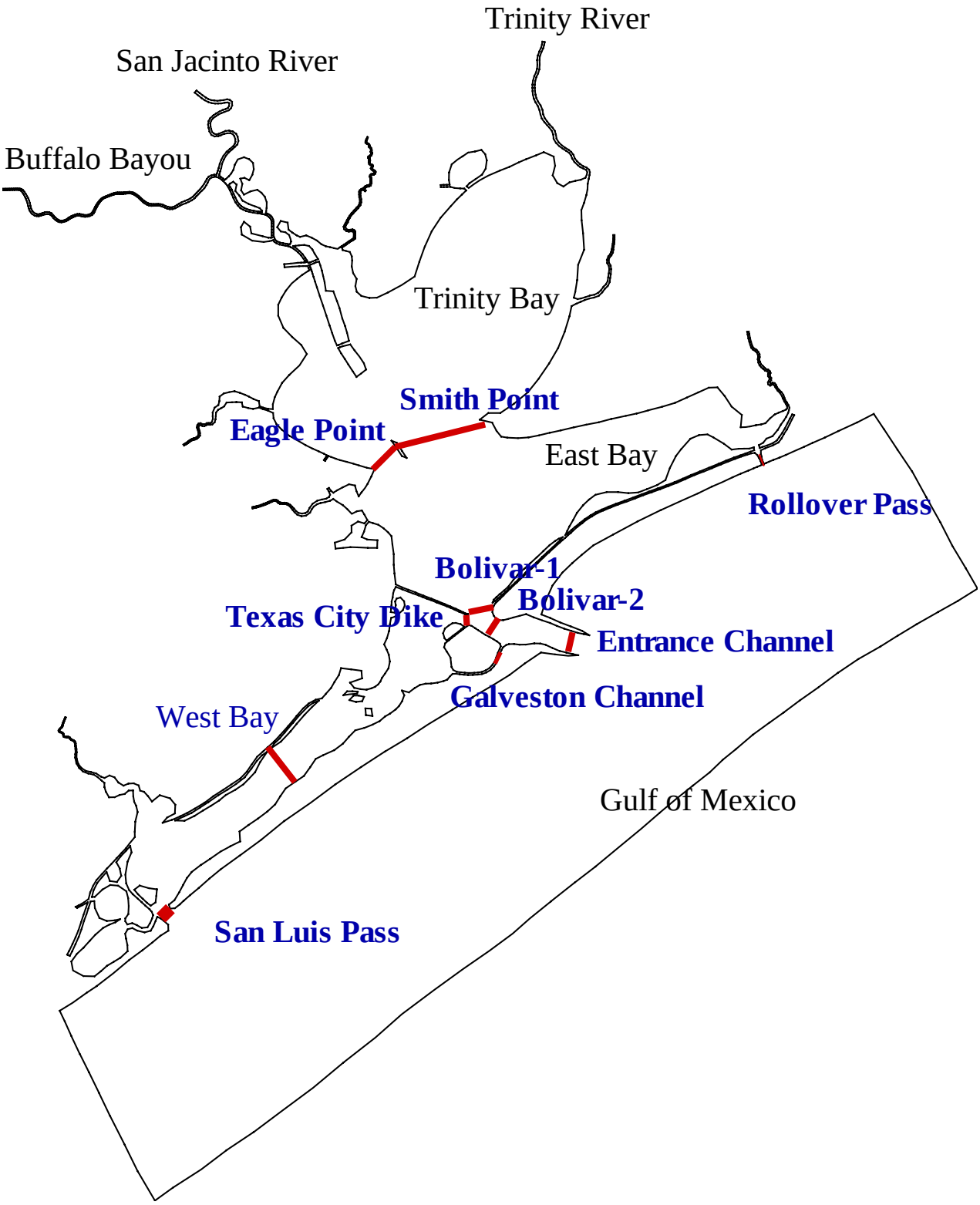

Figure 6.1 Passes and cross sections used for net flow calculation

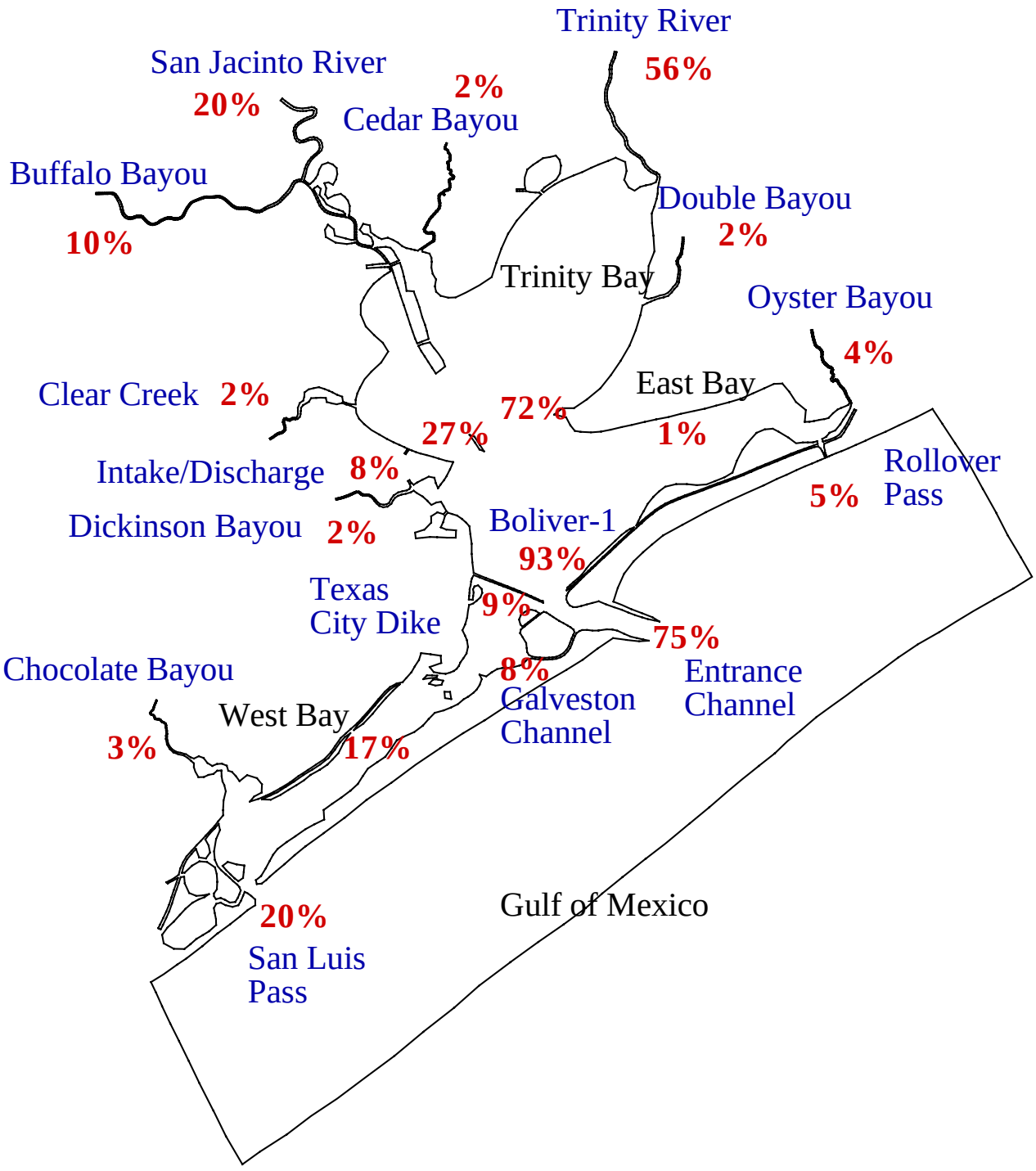

Figure 6.2 Inflows and net flows in percent, average of 8 years 1989 - 1996

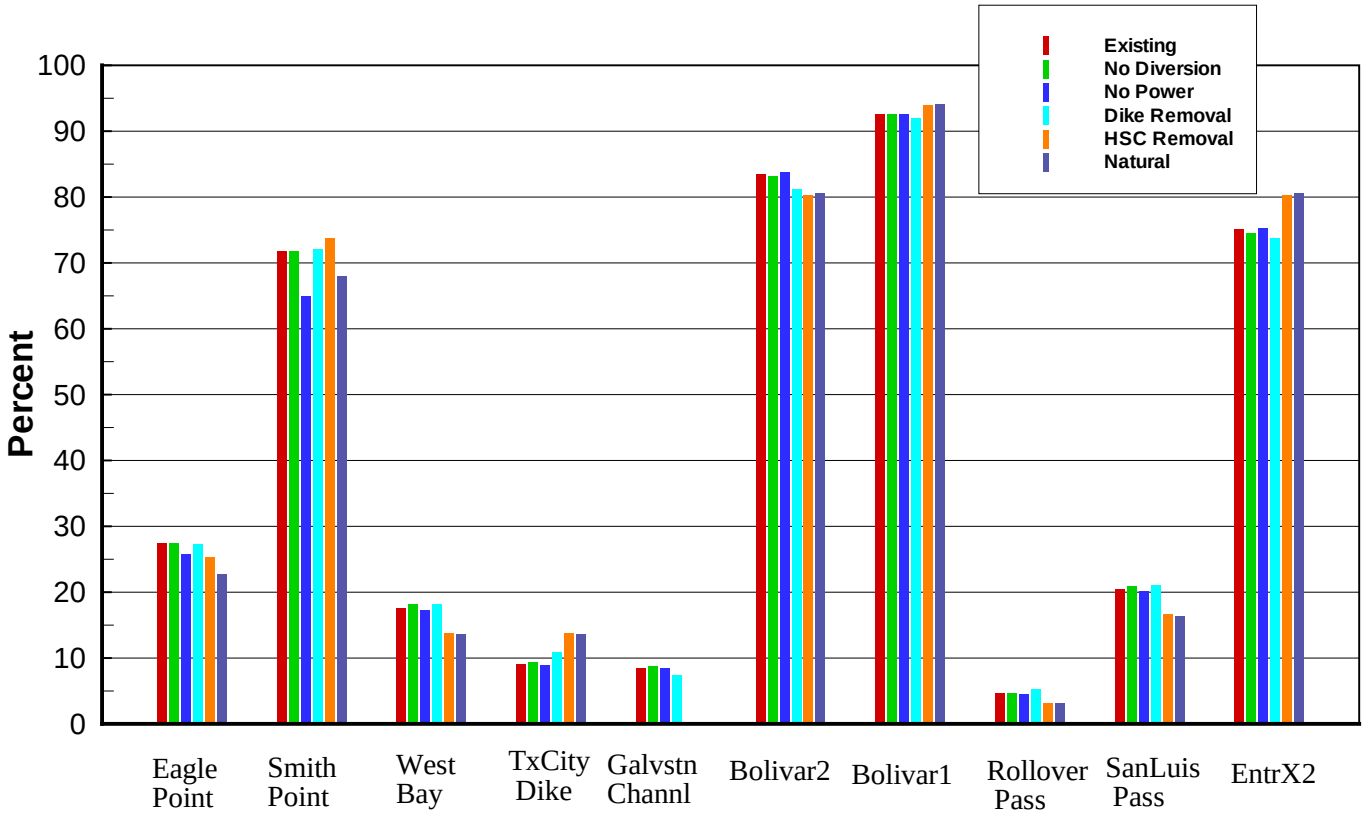

Figure 6.3 Simulated average annual net flows (%)

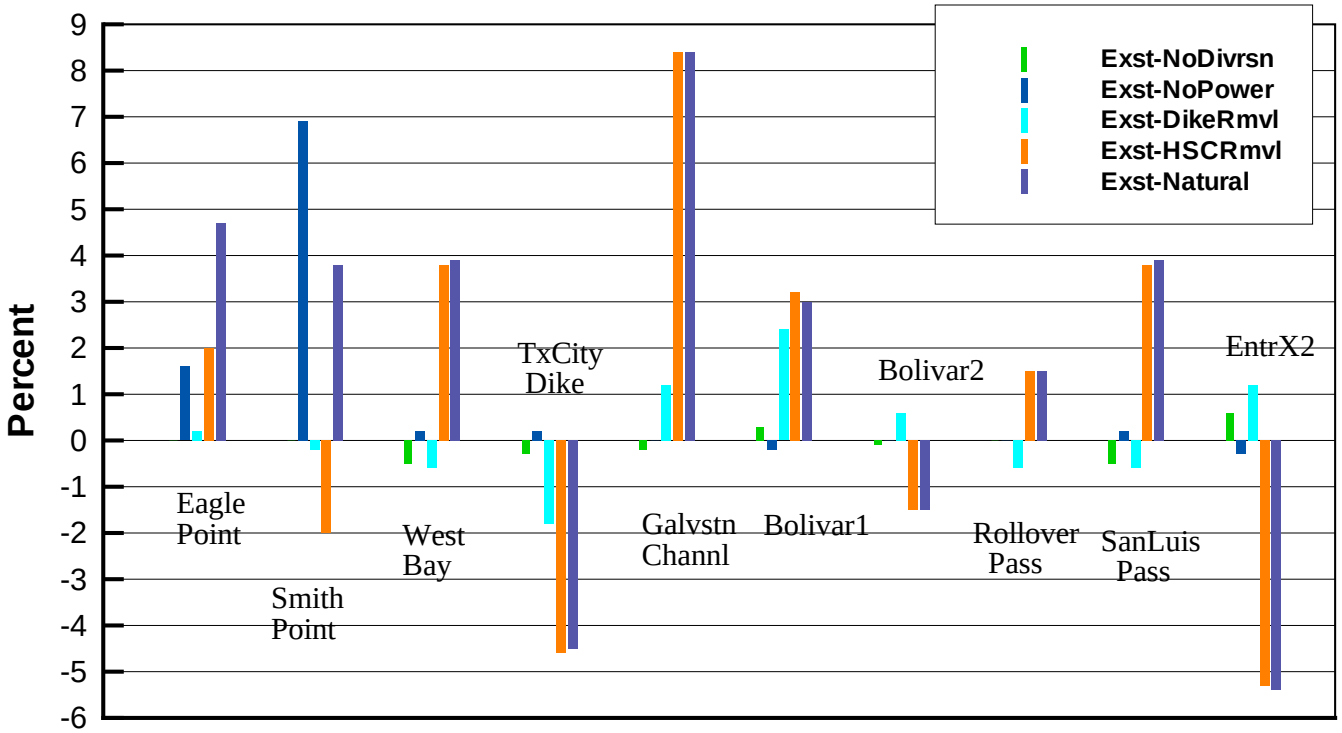

Figure 6.4 Differences (%) in simulated average annual net flows

Table 6.1 Simulated average annual net flows at passes

Annual net flow in 1000 ac-ft

Condition	EaglePt	SmithPt	WestBay	TxCtyDk	GalChnl	Bolivar2	Bolivar1	Rollover	SanLuis	EntrX2
Existing	4645.5	12181.1	2973.3	1540.7	1432.6	14163.9	15704.6	776.3	3455.7	12731.3
No Diversion	4642.9	12183.7	2992.2	1554.8	1437.4	14143.2	15698.1	782.8	3474.6	12705.9
No Power	4367.4	11013.0	2938.5	1510.2	1428.3	14202.2	15712.4	768.5	3420.9	12773.9
Dike Removal	4606.6	12220.0	3073.0	1839.9	1233.1	13757.5	15597.4	883.5	3555.3	12524.4
HSC Removal	4300.2	12526.5	2328.3	2328.3		13622.5	15950.7	530.1	2810.6	13622.5
Natural	3845.7	11534.7	2305.8	2305.8		13649.4	15955.2	525.7	2788.2	13649.4

Annual net flow in percent

Existing	27.4	71.8	17.5	9.1	8.4	83.5	92.6	4.6	20.4	75.1
No Diversion	27.4	71.8	18.1	9.4	8.7	83.2	92.6	4.6	20.9	74.5
No Power	25.7	64.9	17.3	8.9	8.4	83.7	92.6	4.5	20.2	75.3
Dike Removal	27.2	72.0	18.1	10.8	7.3	81.1	91.9	5.2	21.0	73.8
HSC Removal	25.3	73.8	13.7	13.7		80.3	94.0	3.1	16.6	80.3
Natural	22.7	68.0	13.6	13.6		80.5	94.1	3.1	16.4	80.5

Difference in 1000 act-ft: Existing-Scenario

Exst-NoDivrsn	3	-3	-19	-14	-5	21	7	-6	-19	25
Exst-NoPower	278	1168	35	31	4	-38	-8	8	35	-43
Exst-DikeRemvl	39	-39	-100	-299	199	406	107	-107	-100	207
Exst-HSCRemvl	345	-345	645	-788	1433	541	-246	246	645	-891
Exst-Natural	800	646	667	-765	1433	515	-251	251	667	-918

Difference in percent: Existing-Scenario

Exst-NoDivrsn	0.0	0.0	-0.5	-0.3	-0.2	0.3	-0.1	0.0	-0.5	0.6
Exst-NoPower	1.6	6.9	0.2	0.2	0.0	-0.2	0.0	0.0	0.2	-0.3
Exst-DikeRemvl	0.2	-0.2	-0.6	-1.8	1.2	2.4	0.6	-0.6	-0.6	1.2
Exst-HSCRemvl	2.0	-2.0	3.8	-4.6	8.4	3.2	-1.5	1.5	3.8	-5.3
Exst-Natural	4.7	3.8	3.9	-4.5	8.4	3.0	-1.5	1.5	3.9	-5.4

Table 6.2 Diversion from Trinity River to San Jacinto River, in ac-ft

Month	1990	1991	1992	1993	1994	1995	1996	1997	1998	1999	2000
1	29132	34841	47490	40167	45569	37541	56337	60069	61651	63539	48446
2	26182	30888	43824	41013	40643	38242	55766	52069	54616	58608	44912
3	28509	38520	48495	48362	45887	45415	58761	58446	61957	63659	48671
4	27368	35301	48709	40958	48370	48561	58072	58138	61968	64000	48679
5	28217	40669	53822	46495	52570	59513	63367	61423	71643	67384	52884
6	29263	42281	53106	43962	54529	56921	62965	63148	76086	66304	54460
7	32017	45916	57586	55983	57908	58569	68105	68808	75907	67170	59045
8	31873	45590	56187	57387	48412	57234	67772	67678	75282	76285	57735
9	32008	49623	53397	54196	50237	54970	57236	64665	67711	69744	56660
10	33336	51027	49274	52440	48855	55880	55478	63506	66961	70745	54051
11	31998	46359	46123	31272	34923	49075	54463	61296	61798	69292	47734
12	32808	45868	46127	33790	26900	46886	55801	61595	63251	68795	46268
sum	362711	506883	604140	546025	554803	608807	714123	740841	798831	805525	619545
annual ave	623839										

Table 6.3 Reliant Cedar Bayou Power Plant Discharge(daily average ac-ft/day)

1980	1981	1982	1983	1987	1988	1989	1990	1991	1992	1993	1994	1995	1996	1997	1998	1999	2000	2001	no of data	Average
3288.1	2448.7	2474.7	2053.8	n/a	2145.9	2777.2	3218.8	2575.2	4278.7	3499.8	3363.9	3615.4	1706.7	1640.7	1607.9	2279.4	2758.1	2850.6	18	2699.1
2848.9	2224.9	3161.4	2107.6	n/a	2145.9	2145.9	3219.2	2668.5	2521.6	4291.8	3207.9	2486.3	3149.6	2097.3	n/a	1321.8	2847.1	2146.1	17	2623.0
2232.4	2128.6	2803.5	2232.4	n/a	2231.0	2158.9	3171.0	2578.2	2693.2	3917.3	1863.6	3412.3	2650.3	2549.5	3218.8	1259.5	1989.7	2009.9	18	2505.6
3218.8	4408.2	3102.6	2294.9	n/a	3123.5	2259.7	4054.1	2650.5	n/a	2683.9	2574.0	2327.2	2776.2	2653.3	4291.8	2516.1	1687.2	2088.5	17	2865.3
4430.2	4387.0	4811.0	4258.2	3999.0	3500.8	4340.8	4156.0	3479.2	n/a	3672.6	3185.0	3765.2	4035.1	2597.2	4291.8	3184.8	3048.7	2634.1	18	3765.4
4828.3	4828.3	4828.3	4819.1	4823.8	4582.7	4798.5	4477.5	4713.2	n/a	4209.1	4410.7	3862.6	4127.1	4142.5	4828.2	4000.3	4280.3	3432.8	18	4444.1
4779.6	4828.3	4828.3	4733.1	3898.1	4653.8	4513.7	4828.3	4828.3	4644.4	4387.7	4828.2	4753.2	4433.6	4793.6	4828.2	4283.5	4291.8	4732.6	19	4624.6
4724.4	4828.3	4724.4	n/a	4733.6	4681.9	4776.0	4779.3	n/a	n/a	n/a	4780.4	4828.2	4143.4	4828.2	4828.2	4291.8	4291.8	4825.1	15	4671.0
4700.1	4828.3	n/a	n/a	4406.5	4828.3	n/a	n/a	4810.4	3701.3	4729.6	3392.5	3204.1	4521.8	4810.1	4828.2	4122.4	3908.0	4386.7	15	4345.2
3178.5	4154.8	4291.8	n/a	3170.2	3472.7	n/a	4675.7	4068.9	3685.8	4828.2	3011.8	1995.1	1795.7	3739.3	4828.2	2414.2	2888.9	2863.4	17	3474.3
2604.9	2691.3	1895.5	n/a	2729.1	2733.0	n/a	3016.6	4165.5	n/a	4042.9	3050.4	2182.0	1580.9	3079.2	1865.5	2032.6	1753.5	2851.6	16	2642.2
2367.9	2421.3	2094.0	n/a	1804.1	2626.1	n/a	2412.8	n/a	4255.8	3747.8	2954.6	1609.4	1116.5	1563.9	2257.3	1954.8	2151.7	1419.8	16	2297.4
Monthly in ac-ft																				
101930	75911	76716	63669		66523	86093	99784	79830	132641	108492	104281	112077	52907	50862	49844	70663	85501	88367		83672
79768	62298	88518	59012		62231	60085	90138	74717	73127	120170	89820	69616	91337	58725		37009	82565	60090		73445
69205	65986	86909	69205		69161	66925	98301	79924	83488	121436	57772	105780	82159	79033	99783	39043	61681	62306		77672
96565	132246	93078	68848		93704	67792	121623	79514		80516	77220	69817	83285	79598	128753	75482	50617	62655		85960
137338	135996	149140	132004	123970	108524	134566	128835	107854		113851	98736	116722	125089	80513	133044	98730	94511	81658		116727
144848	144848	144848	144572	144714	137480	143954	134326	141396		126273	132320	115878	123813	124275	144847	120008	128409	102985		133322
148168	149677	149677	146726	120841	144267	139924	149677	149677	143976	136020	149675	147348	137443	148602	149675	132790	133044	146710		143364
146458	149677	146458		146743	145139	148056	148157				148192	149675	128444	149675	149675	133044	133044	149577		144801
141004	144848			132196	144848			144312	111040	141889	101776	96122	135655	144302	144847	123672	117240	131600		130357
98533	128799	133046		98275	107653		144947	126136	114260	149675	93367	61848	55666	115918	149675	74841	89557	88766		107704
78147	80739	56866		81874	81991		90499	124965		121287	91513	65459	47427	92376	55966	60979	52606	85547		79265
73405	75062	64913		55928	81410		74798		131930	116181	91593	49892	34611	48482	69977	60598	66702	44012		71218
																			annual	1247506
																			monthAve	103958.8

Table 6.4 Reliant Robinson Power Plant Discharge (ac-ft/day)

1980	1981	1987	1988	1989	1990	1991	1992	1993	1994	1995	1996	1997	1998	1999	2000	2001	no of data	Average
3162.8	4135.2	n/a	n/a	3564.0	2953.2	3973.3	2522.4	2422.8	n/a	3243.1	1883.0	2249.0	5778.4	2765.2	2614.4	2092.7	14	3097.1
3636.0	3038.8	n/a	3692.0	3513.4	2944.8	4002.2	2024.2	1833.5	n/a	2388.9	3116.5	1155.0	n/a	2244.9	4011.6	813.0	14	2743.9
5035.0	2689.4	n/a	3041.3	2717.4	3404.4	3363.3	n/a	2077.0	4202.6	2512.0	2760.7	1280.6	8472.0	3423.9	4391.2	2475.2	15	3456.4
5157.1	3017.2	n/a	3789.8	3106.0	3522.0	3930.6	2949.2	2204.8	4032.8	3319.5	2268.9	2406.8	6962.7	4950.1	4962.5	4601.9	16	3823.9
4550.8	3273.0	3761.5	4701.2	4107.1	4350.4	4412.1	n/a	4178.7	4789.0	4109.6	4890.6	3484.5	15008.2	5116.2	5057.4	4796.4	16	5036.7
4735.8	4164.0	4189.8	4886.4	4937.9	n/a	5103.0	5152.8	4967.6	4980.9	4920.9	5184.5	4362.2	15910.3	5056.5	4978.4	4296.0	16	5489.2
4959.8	4970.4	n/a	5027.2	4846.3	n/a	n/a	4984.3	5022.1	5080.9	5066.0	4932.8	3139.6	15137.8	5183.6	5182.4	5187.2	14	5622.9
4865.2	5053.0	4832.8	5081.8	5065.3	3575.1	4064.3	5122.7	n/a	5027.1	4967.6	4981.9	3324.2	15288.5	5108.3	4919.8	5170.4	16	5403.0
4929.1	4902.6	4979.1	5124.2	5000.1	5048.3	n/a	4950.7	4071.8	4873.8	4962.0	3830.6	3511.8	11755.5	5039.1	5218.3	5126.2	16	5207.7
4732.0	4395.3	4623.3	4041.8	5028.1	4668.0	n/a	4713.8	n/a	4502.7	4533.3	3466.7	3477.9	10638.6	4598.1	4362.3	4786.7	15	4837.9
3802.0	4270.0	4127.6	4127.1	n/a	4419.6	n/a	3053.8	n/a	3830.8	4338.1	2361.0	3450.2	7245.3	3048.5	1648.0	3667.5	14	3813.5
4090.0	n/a	4345.3	3122.4	n/a	4072.9	2165.3	3172.3	n/a	3247.1	2599.9	2089.6	3088.6	6412.4	1725.1	2470.2	n/a	13	3277.0

Monthly in ac-ft																		Average
98048	128192			110485	91549	123173	78194	75107		100535	58372	69718	179131	85722	81046	64873		96010
101807	85086		107067	98374	82455	112062	58703	51339		66889	90378	32341		62856	116336	22765		76830
156085	83371		94279	84239	105536	104261		64388	130282	77871	85581	39699	262631	106140	136128	76730		107148
154712	90517		113693	93180	105659	117918	88475	66143	120983	99586	68066	72205	208881	148503	148876	138056		114716
141075	101464	116606	145737	127320	134862	136776		129541	148459	127397	151608	108018	465253	158603	156778	148687		156136
142073	124919	125695	146591	148137		153090	154584	149029	149427	147626	155536	130866	477309	151696	149352	128879		164676
153754	154084		155844	150234			154512	155686	157509	157047	152917	97327	469270	160693	160655	160804		174310
150821	156644	149817	157536	157025	110829	125993	158802		155841	153996	154439	103049	473943	158358	152514	160283		167493
152801	151981	154353	158849	155004	156497		153473	126226	151087	153822	118750	108866	364420	156211	161766	158914		161439
146692	136253	143321	125297	155870	144707		146129		139583	140531	107467	107815	329796	142543	135230	148387		149975
117862	132370	127956	127941		137007		94667		118755	134481	73189	106955	224604	94502	51087	113693		118219
126790		134705	96795		126261	67125	98340		100660	80598	64776	95746	198785	53478	76575			101587
																	Annual	1588539
																	monthAve	132378.2

7. RESIDUAL VECTORS

To study the effects of the five scenarios on bay circulation patterns, residual vectors were computed. A residual vector indicates the direction of net flow over a given period. This is useful in a tidal environment since the net movement is not apparent from the time sequence of ebb and flood tides. There are two sets of residual vectors. One set is from a short term to visualize the residual general flow pattern. The other is a residual flow over a month to see the influence of inflows.

Flow Trace

Figure 4.1 shows the observed tide at Pleasure Pier in January through March 1989. The January 18-19 period was chosen because it is a typical diurnal tide. The two day period was taken as the four Principal Lunar periods or 49.68 (=4x12.42) hours. The residual vectors were calculated by summing all vectors during the two-day period. The flow traces were created by making the residual vectors move and tracking the movement. Figure 7.1 shows the residual vector flow trace for the existing condition. It shows a few circular patterns in the mid and upper Galveston Bay and in the East Bay. It shows the pattern qualitatively but not necessarily indicative of the strength of the flows.

Figure 7.2 shows the residual flow pattern for the *no diversion* case. It is indistinguishable from the *existing* case. Figure 7.3 shows a close-up of upper and mid Galveston Bay residual flow pattern for the *existing* case to which Figure 7.4 should be compared for the *no power* case. Differences are seen at the cooling pond near Trinity Bay, in Tabbs Bay, in Dickinson Bay, and at the discharge site at Bacliff. Figure 7.5 is a close-up of the Texas City Dike area for the existing condition to which Figure 7.6 should be compared for the *dike removal* case. Because Texas City Ship Channel is operational under the dike removal case, the influence of the ship channel is seen in Figure 7.6. But, still there is more water directly coming from Galveston Bay toward West Bay. Figure 7.7 is the residual flow pattern for the *HSC removal* case and Figure 7.8 is for the *natural* case. In both figures HSC is removed and there is no influence of the HSC.

Residual Vector for the Existing Condition

Another set of residual vectors was calculated over a month period to show the influence of inflows. One lunar month from January 13 through February 9, 1989 (or Day 13 through Day 40 in Figure 4.1) was chosen. The residual vectors were calculated by summing all the vectors during the 28-day period. Table 7.1 lists the inflow from Trinity River and Table 7.2 the precipitation. Figure 7.9 shows the wind direction and wind speed in January and February 1989. All these data indicate a typical condition (not very unusual condition) in the simulation period.

Figure 7.10 shows the residual vectors in the Bolivar Roads and the entrance channel area for the *existing* condition. It shows the net flow is toward the Gulf in the entrance channel area although some vectors in deeper (channel) part show reversed direction. The vectors in the mid portion of the Bolivar Roads area are directed up-estuary while the vectors in shallower parts

are directed toward the Gulf. The residual vectors in the Texas City Ship Channel are directed toward the bay near the tip of the dike. The vectors in the Galveston Channel are directed toward the West Bay and the vectors in West Bay are directed westward toward San Luis Pass. The residual vectors in the HSC from the lower Galveston Bay through upper Galveston Bay are directed up-estuary but the vectors in the open bay along the HSC are directed down-estuary. At Trinity Bay, as shown in Figure 7.11, the residual vectors along the north shore are directed westward and the ones along the south shore are directed south-westward or down-estuary and there is a counter clockwise circulation in the upper Trinity Bay. Because of the power plant operation, the vectors in Cedar Bayou are directed toward the intake point and discharged into the cooling pond near Trinity Bay. Similarly the residual vectors in Dickinson Bay and the discharge site near Bacliff show the withdrawal and discharge for the Robinson Power Plant.

No Power. Figure 7.12 shows the residual vectors for the *no power* case. The vectors along the north shore of Trinity Bay are directed westward toward upper Galveston Bay same as the existing case, but at Cedar Bayou the net flow is down-river toward Tabbs Bay. Similarly in Dickinson Bay the net flow is down-estuary. The overall movement appears very similar to the existing condition. The residual vectors at both shorelines of Trinity Bay are similar and the circular movement in upper Trinity Bay still exists. The vectors in the HSC are similar to the existing case in that they are directed up-estuary.

Texas City Dike Removal. Figure 7.13 shows the residual vectors in the Bolivar Roads and entrance channel area for the *dike removal* case. The vectors in the Texas City Ship Channel are directed up-estuary and the neighboring vectors are directed to cross the channel indicating the net flow from Galveston Bay toward West Bay. The vectors in Galveston Channel are directed toward West Bay and the vectors in West Bay are directed westward toward San Luis Pass. The vectors in HSC are directed up-estuary even in the Bolivar Roads area.

HSC Removal and Natural Cases. Figure 7.14 shows the residual vectors for the HSC removal case and Figure 7.15 for the *natural* case. As expected, they are much different from the residual vectors for the *existing* condition. Above all, there is no trace of HSC dominance. The vectors in the HSC location look the same as their neighboring ones. From mid Galveston Bay through lower Galveston Bay they are all directed toward the entrance channel and West Bay. And at the entrance channel all vectors are directed toward the Gulf. Since there is no Texas City Ship Channel and no Texas City Dike the residual vector in the city channel area look more natural in that the flow from Galveston Bay are freely moving toward West Bay. At upper Galveston Bay there are circular movements off Clear Lake and near Morgan’s Point. However, these are artificial in that the Atkinson Island (spoil island) could have been removed for modeling the HSC removal and the natural case, but it was not removed and the figures indicate the blocking circulation by the spoil island. The figures also indicate an existence of a counter-clockwise circulation in the upper Trinity Bay.

Stream Trace

Figures 7.16 through 7.19 show the stream traces for the *existing* condition, which were plotted based on the residual vectors that were calculated for the one month period. These stream traces show possible pathways for water particles. Figure 7.16 shows the stream traces in the upper Galveston Bay and Trinity Bay for the *existing* condition. They show more clearly possible circular paths. Figure 7.17 shows the stream traces in the lower Galveston Bay and Bolivar Roads area for the *existing* condition. It shows possible circular paths along the HSC and complex flow paths in the Bolivar Roads area.

Figure 7.18 shows the stream traces for the *Texas City Dike Removal* case. The traces show how the water from Galveston Bay may move toward West Bay. Some of the traces are bent at the Texas City Ship Channel. Figure 7.19 shows the stream traces for the *natural* case. It shows more clearly the non-existence of the HSC. The main direction of the traces is more toward West Bay than along the HSC.

Summary

The residual vectors in the HSC in Galveston Bay for the *existing* condition are all directed up-estuary. This indicates, in the sense of net flow, the ship channel conveys the Gulf water into Galveston Bay and upper HSC area, whereas the bay water is carried out to the Gulf through the open bay part. Comparing the *no power* case with the existing case, the effect of power plant operation on circulation appears local. The residual vectors for the *dike removal* case indicate a net flow directly from Galveston Bay to West Bay. The *natural* case shows no clear path conveying Gulf water to the bay, instead all the residual vectors are directed toward the Gulf through the entrance channel or West Bay. There appears to be a counter-clockwise circulation in the upper Trinity Bay for all cases.

Figure 7.1 Residual flow pattern for the existing case

Figure 7.2 Residual flow pattern for the no diversion case

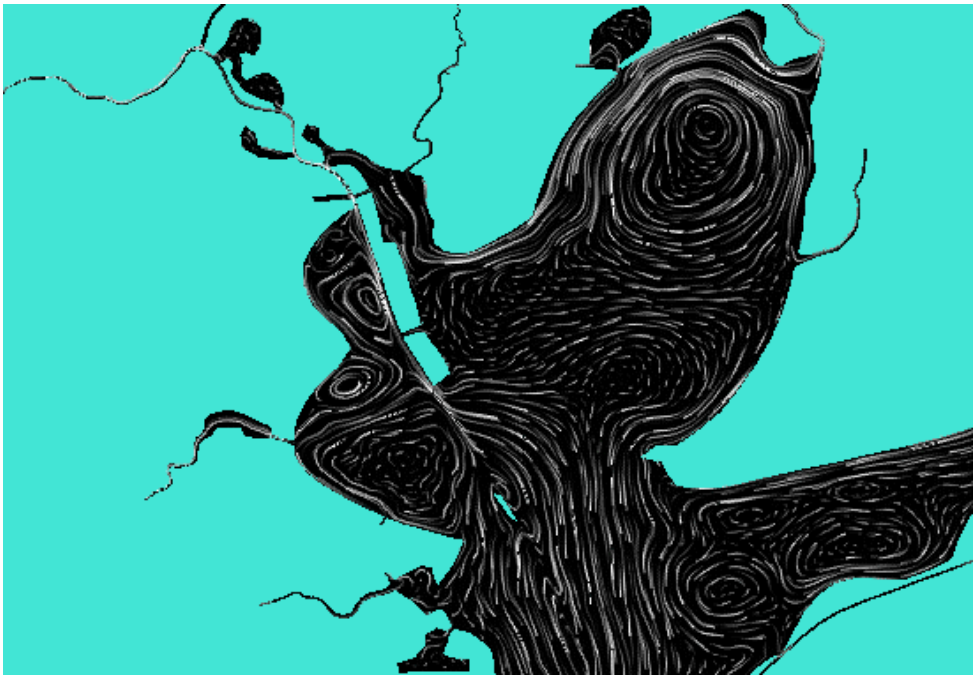

Figure 7.3 Residual flow pattern for the existing case in the mid and upper Galveston Bay; notice the influence of power plant intake and withdrawal

Figure 7.4 Residual flow pattern for the no power case,
Compare the flow traces in Dickinson Bay and the cooling pond near Trinity Bay with the ones for the existing condition (Figure 7.3)

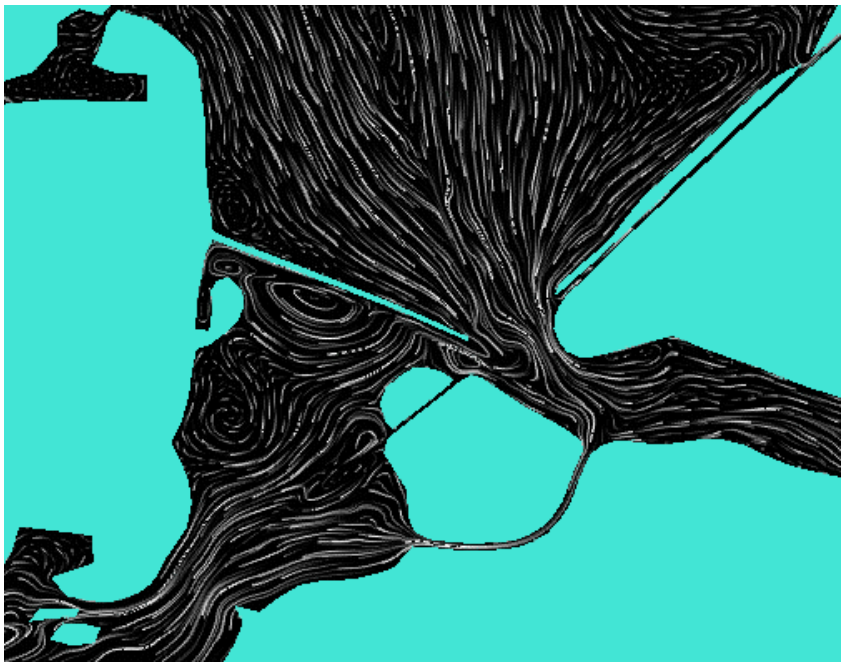

Figure 7.5 Residual flow pattern in Bolivar Roads area for the existing case

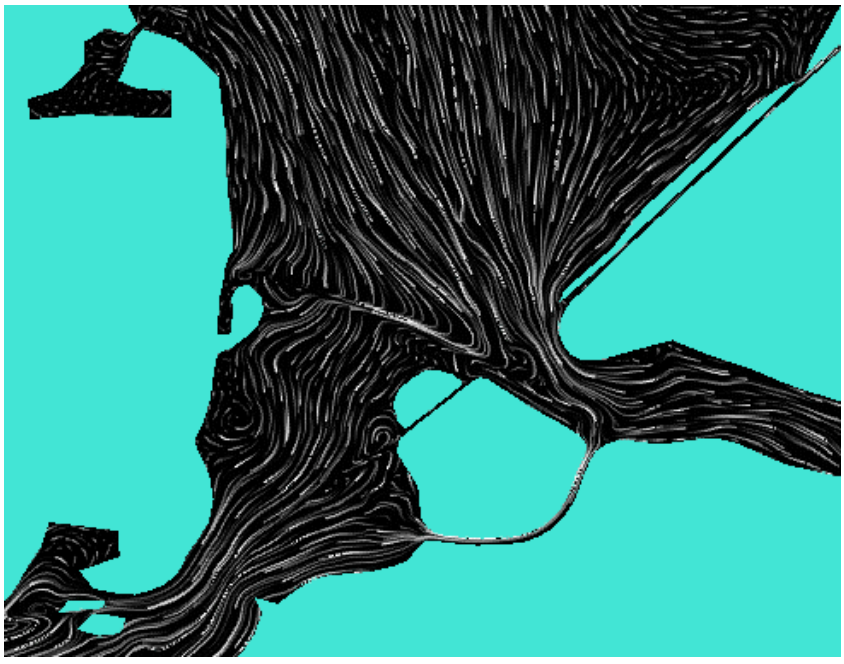

Figure 7.6 Residual flow pattern in Bolivar Roads Area for the Texas City Dike removal case

Figure 7.7 Residual flow pattern for the HSC removal case

Figure 7.8 Residual flow pattern for the natural case

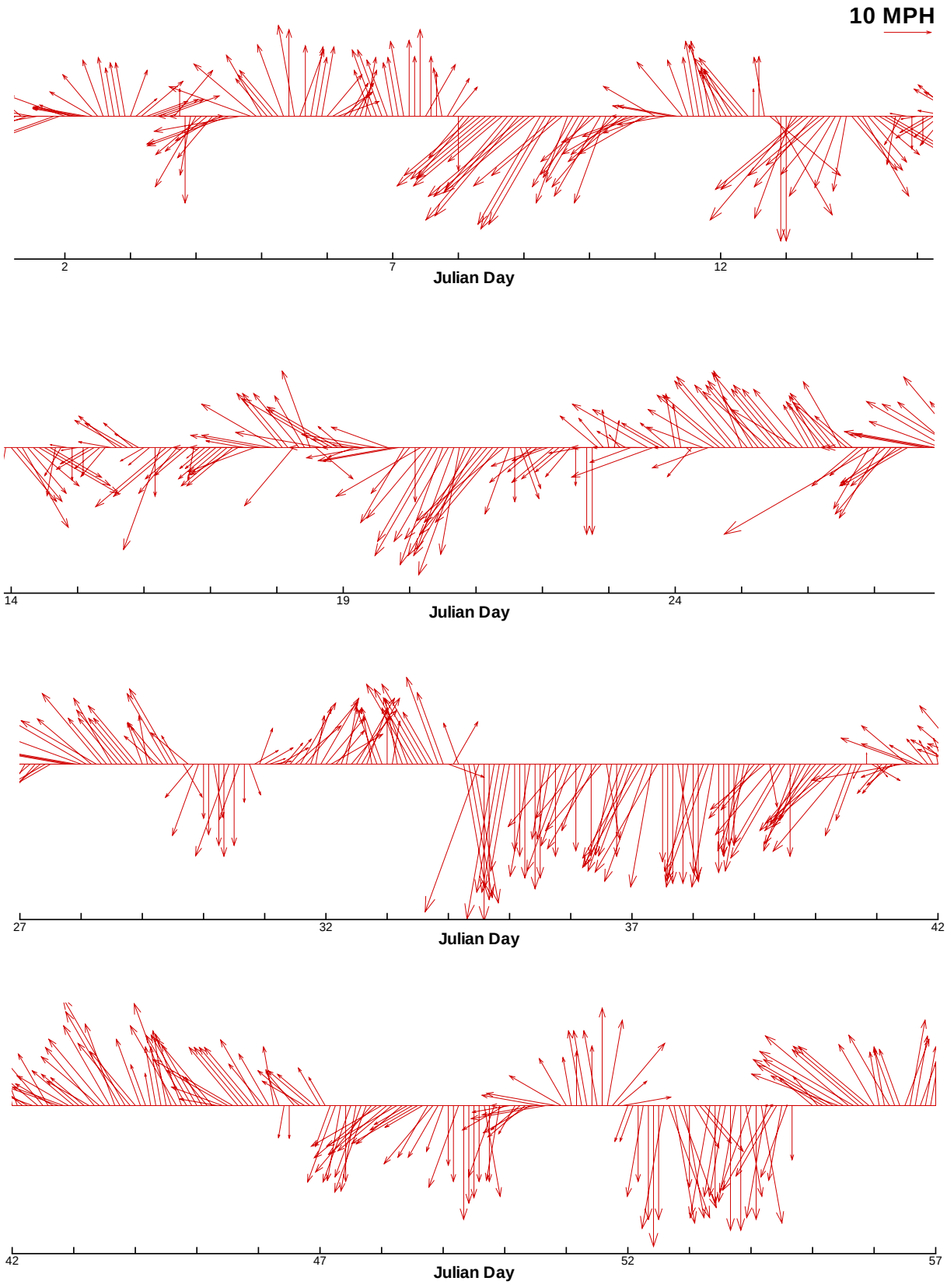

Figure 7.9 Wind speed and direction at Galveston Island, Scholes Field, 1989
The largest in this plot is 35 mph from 60 degree from north on the 27th day

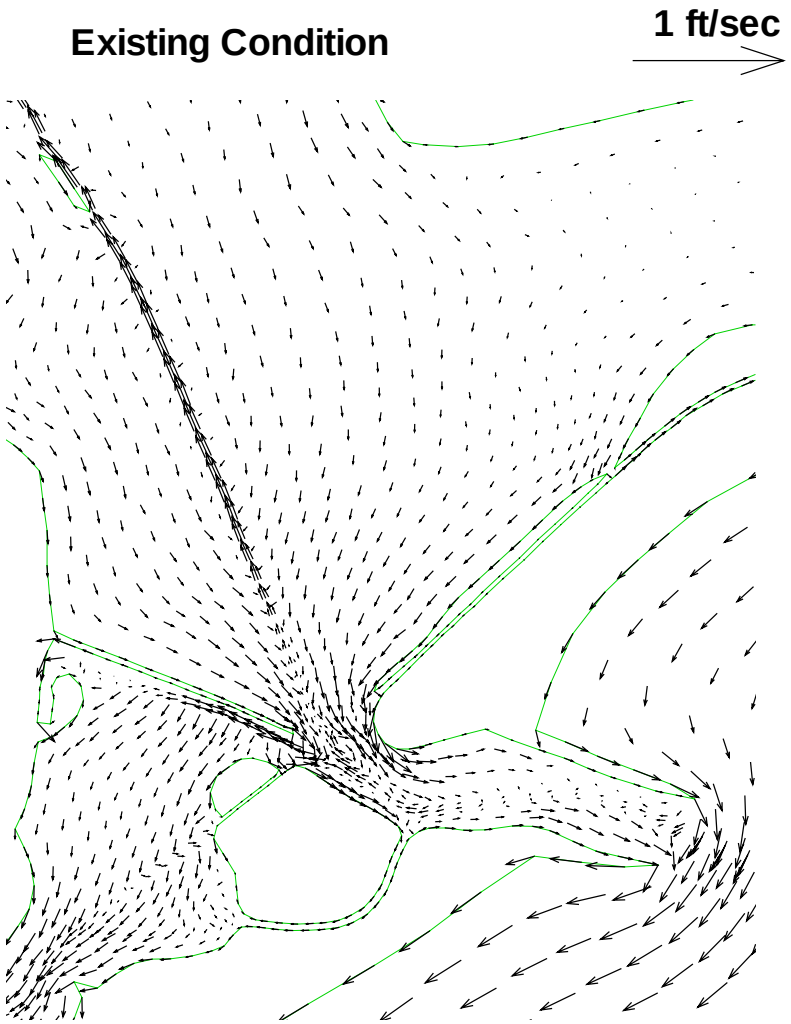

Figure 7.10 Residual vectors in Bolivar Roads area for the existing condition

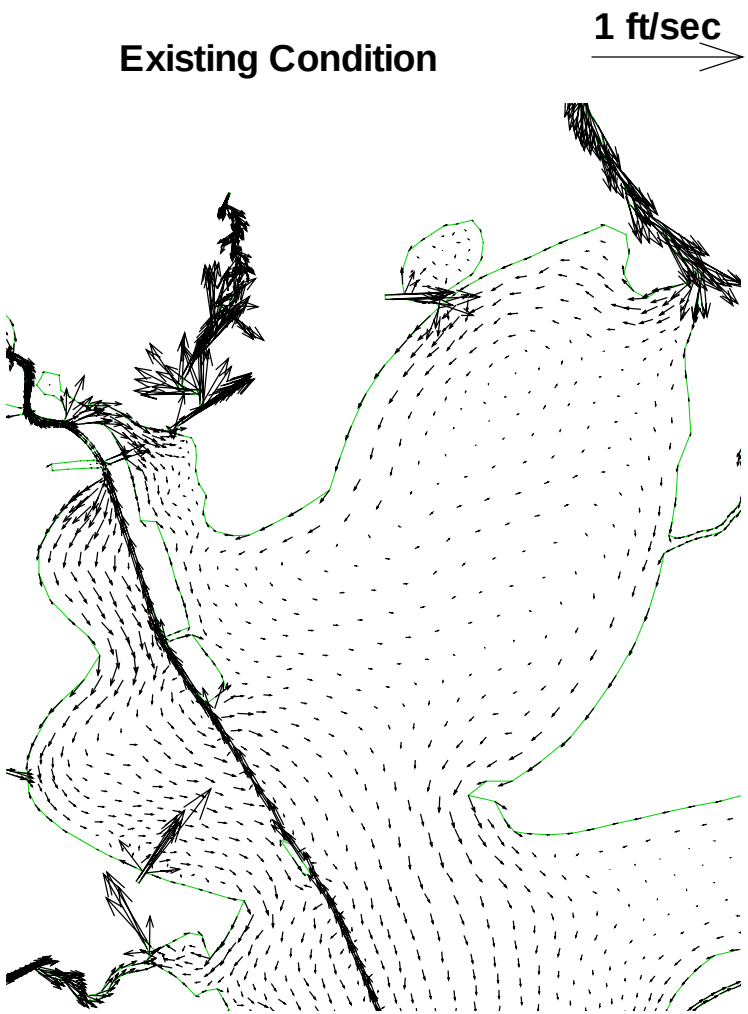

Figure 7.11 Residual vectors in mid and upper Galveston Bay for the existing condition; notice the vectors for the power plant operation

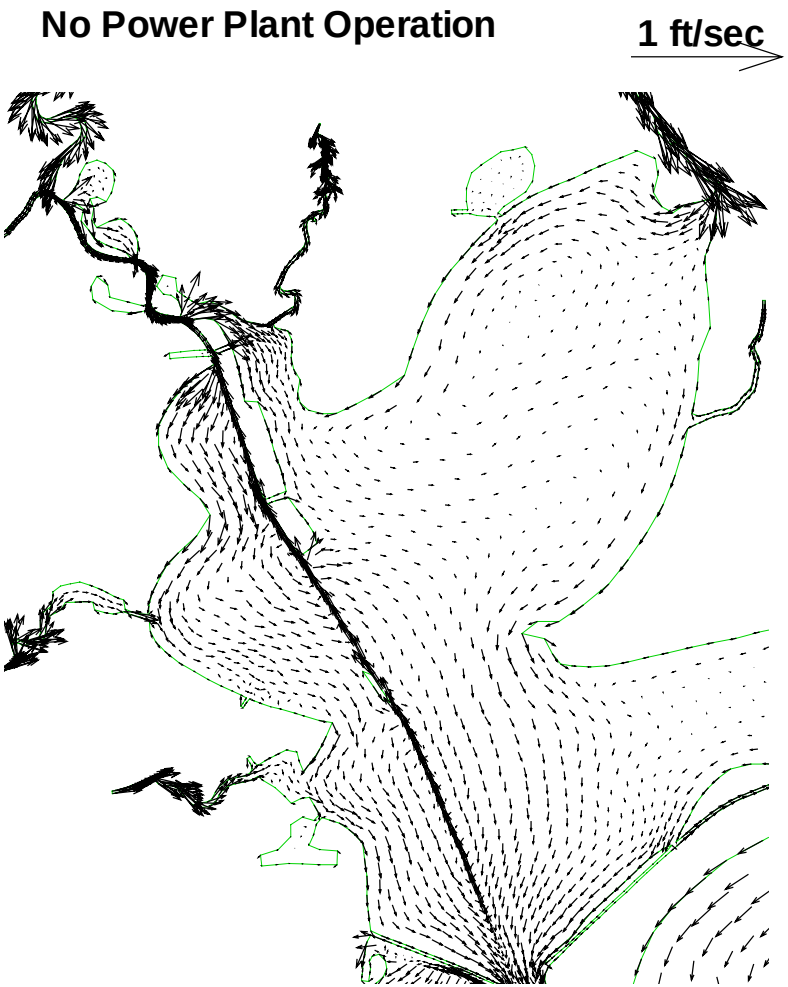

Figure 7.12 Residual vectors for the no power case

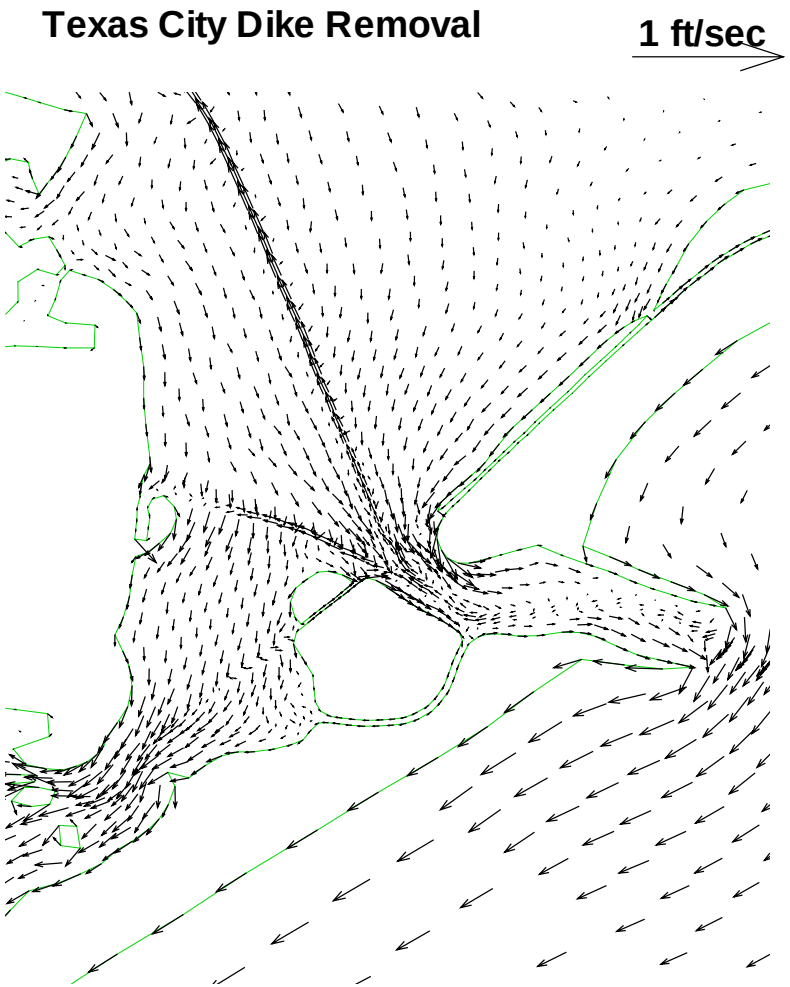

Figure 7.13 Residual vectors for the Texas City Dike removal case

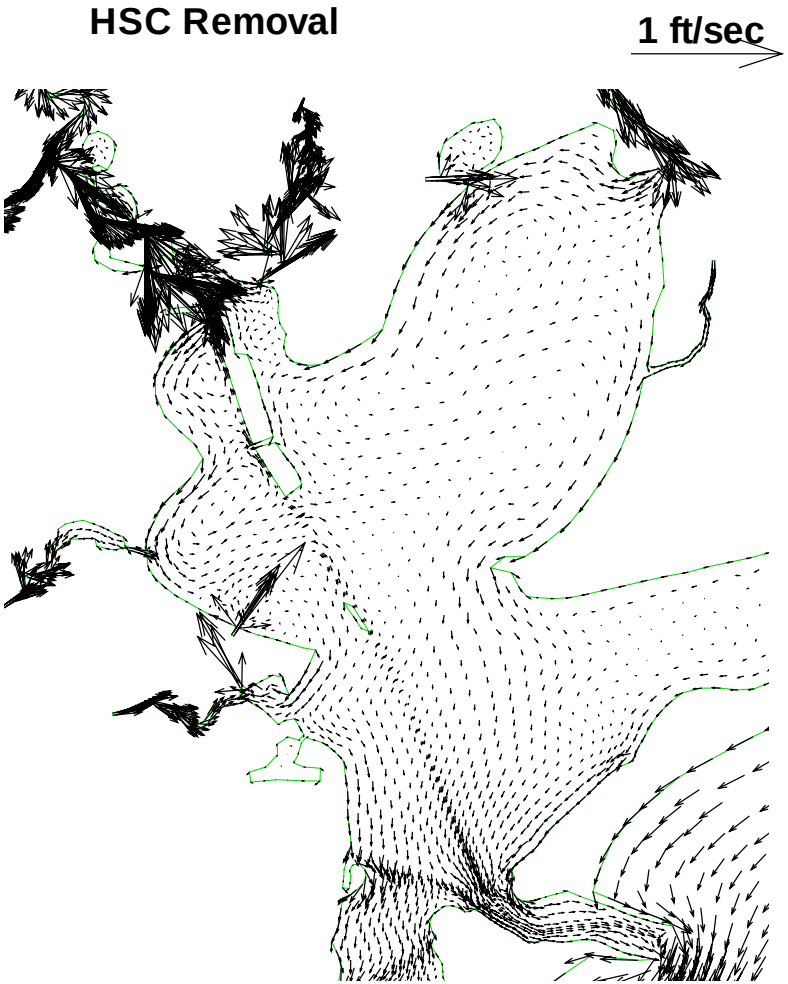

Figure 7.14 Residual vectors for the HSC removal case

Figure 7.15 Residual vectors for the natural case

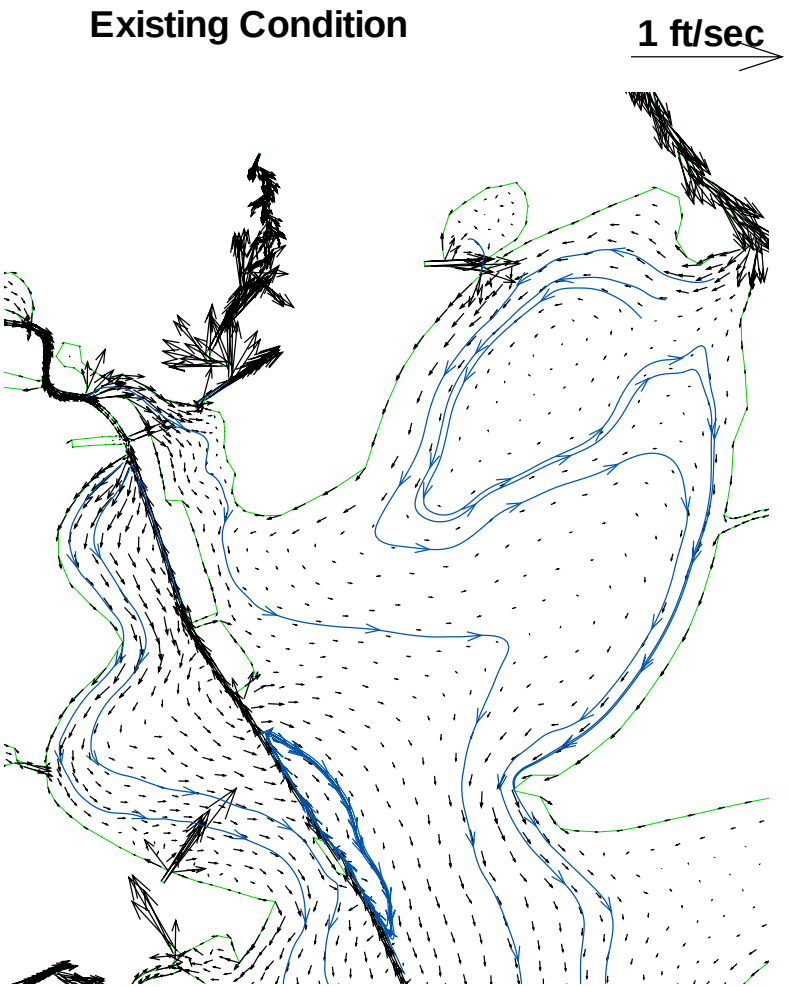

Figure 7.16 Stream traces in Trinity Bay, mid and upper Galveston Bay for the existing condition

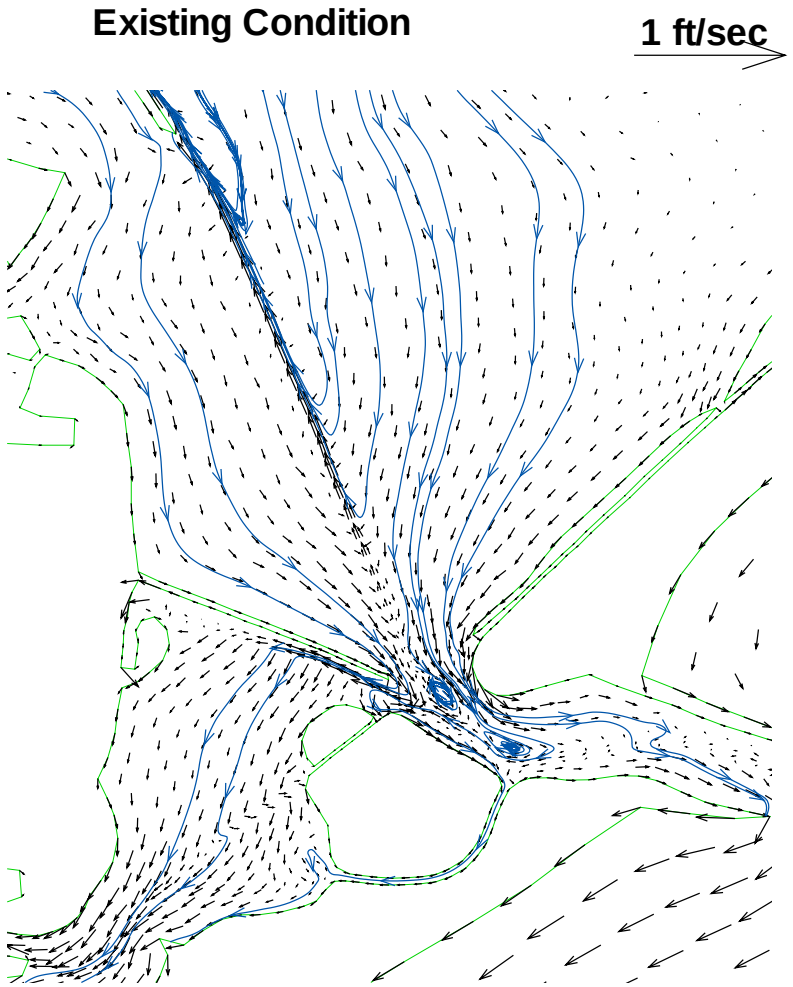

Figure 7.17 Stream traces in lower Galveston Bay and Bolivar Roads area for the existing condition

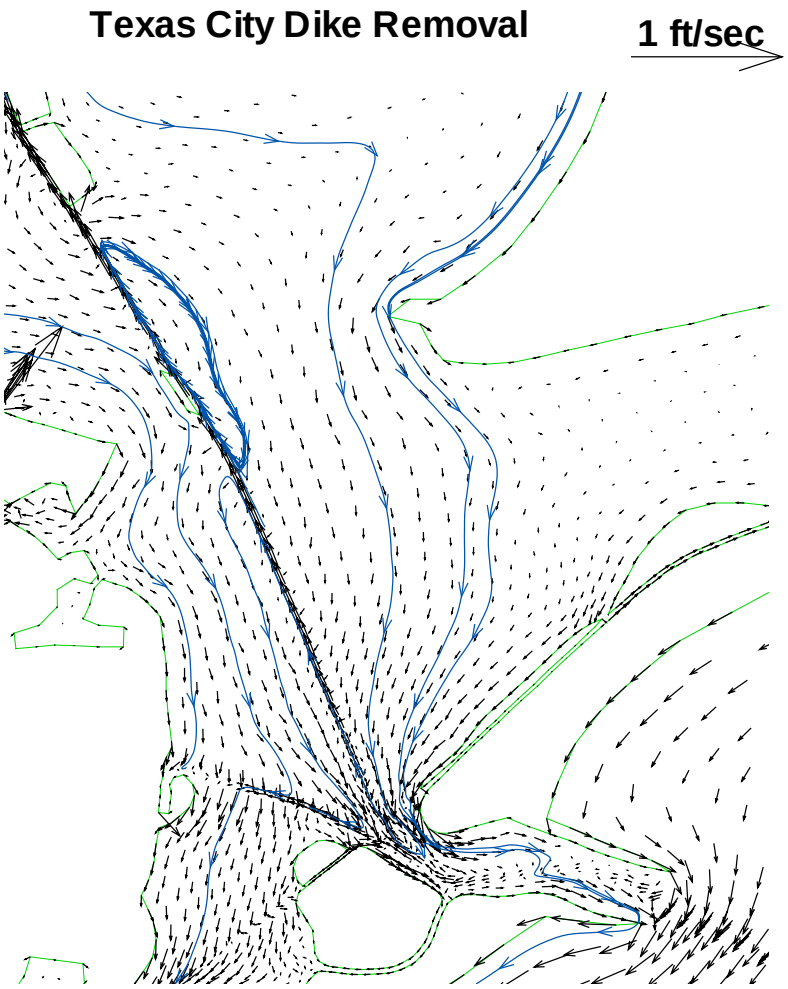

Figure 7.18 Stream traces in lower Galveston Bay and Bolivar Roads area for the Texas City Dike removal case

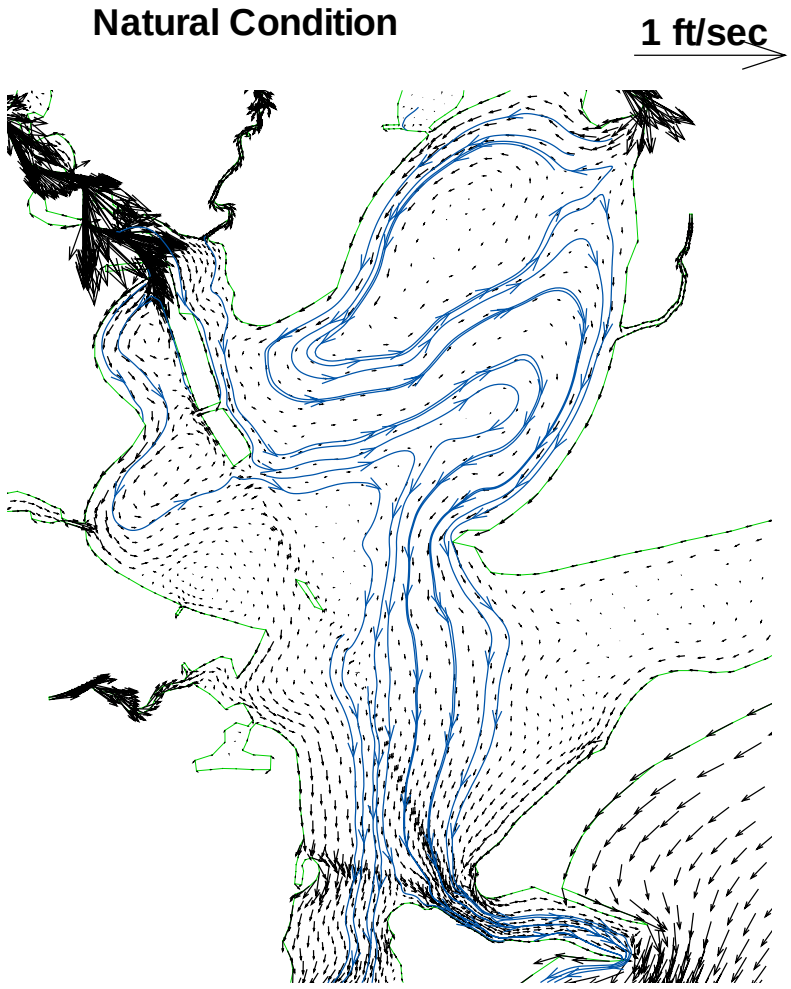

Figure 7.19 Stream traces in Galveston Bay and Bolivar Roads area for the natural case

Table 7.1 Trinity river daily inflow in cfs; part of inflow data listed here to see the inflows of early 1989.

1988,12,31											
TrinityR 12 1	479	479	479	479	479	479	487	524	590	720	
TrinityR 12 2	968	1371	1124	864	711	624	589	584	575	573	
TrinityR 12 3	579	613	653	647	624	605	616	695	679	662	806
1989, 1,31											
TrinityR 1 1	954	745	623	568	550	547	521	505	525	590	
TrinityR 1 2	566	642	1014	1914	2001	1356	1120	1159	2951	3138	
TrinityR 1 3	3440	2528	1593	1013	851	790	919	1100	1624	6492	4860
1989, 2,28											
TrinityR 2 1	3439	2123	1264	2780	4488	6013	6272	5691	5481	5310	
TrinityR 2 2	3979	3580	3540	3099	2669	1888	1668	1668	1677	1807	
TrinityR 2 3	5348	8789	9099	8815	10511	12572	13157	13051			
1989, 3,31											
TrinityR 3 1	11737	9507	8969	7870	7121	5276	3310	2517	1996	1745	
TrinityR 3 2	1665	1615	1605	1595	1553	1543	1534	1534	1514	1514	
TrinityR 3 3	2039	6637	8171	7609	6239	4667	4613	5314	10374	29184	39903
1989, 4,30											
TrinityR 4 1	40324	40487	35973	31068	20866	12966	8895	7844	7625	7544	
TrinityR 4 2	7394	7084	7286	7556	7657	7369	6058	5784	5715	5652	
TrinityR 4 3	5597	6135	6453	6462	6443	6423	6252	4722	3762	3887	

Table 7.2 Galveston Bay precipitation in inches; part of precipitation data listed here to see the precipitation of early 1989

1988,11,30												
Galvestn 11	1	0.00	0.00	0.00	0.00	0.00	0.00	0.00	0.00	0.00	0.00	
Galvestn 11	2	0.00	0.02	0.00	0.00	0.00	0.82	0.00	0.00	0.00	0.00	
Galvestn 11	3	0.00	0.00	0.00	0.00	0.00	0.05	0.00	0.00	0.04	0.00	
1988,12,31												
Galvestn 12	1	0.00	0.00	0.00	0.00	0.00	0.00	0.11	0.11	0.05	0.01	
Galvestn 12	2	0.03	0.00	0.00	0.00	0.01	0.00	0.00	0.00	0.00	0.00	
Galvestn 12	3	0.00	0.00	0.93	0.00	0.00	0.00	0.59	0.00	0.00	0.03	1.02
1989, 1,31												
Galvestn 1	1	0.00	0.00	0.00	0.00	0.00	0.00	0.00	0.29	1.80	0.00	
Galvestn 1	2	0.09	0.13	0.17	0.07	0.00	0.00	0.00	1.36	0.71	0.76	
Galvestn 1	3	0.00	0.00	0.00	0.00	0.00	0.00	0.00	0.00	0.44	0.43	0.00
1989, 2,28												
Galvestn 2	1	0.00	0.00	0.00	0.00	0.00	0.06	0.00	0.00	0.00	0.00	
Galvestn 2	2	0.00	0.00	0.00	0.00	0.00	0.08	0.00	0.01	0.00	0.00	
Galvestn 2	3	0.00	0.00	0.00	0.00	0.00	0.00	0.00	0.02			
1989, 3,31												
Galvestn 3	1	0.03	0.00	0.00	0.04	0.00	0.00	0.00	0.00	0.00	0.00	
Galvestn 3	2	0.00	0.00	0.00	0.00	0.00	0.00	0.00	0.00	0.00	0.00	
Galvestn 3	3	0.92	0.17	0.00	0.00	0.08	0.02	0.00	0.05	1.06	0.00	0.00

8. SALINITY CHANGES

To examine the effect of structures and practices on salinity, TxBLEND-2D was run for eight years from 1989 to 1996. We mainly looked at differences in salinity during the wet period represented by 1992 and during the dry period represented by 1996. In this section we describe the salinity condition in the existing case and salinity changes under each scenario.

Existing Condition

Salinity in Galveston Bay is a balance of freshwater from rivers and creeks such as the Trinity River, San Jacinto River, and Buffalo Bayou and seawater from the Gulf through the Entrance Channel, San Luis Pass, and Rollover Pass. Figure 8.1 shows eight locations where simulated salinity is tracked for comparison purposes. They are located at upper Galveston Bay, Trinity Bay, Galveston Bay off Clear Lake, Galveston Bay near Redfish Reef, East Bay, Christmas Bay, mid-West Bay, and West Bay near Texas City Channel. Eight additional salinity sites were added as shown in Figure 8.2 to obtain a better understanding of the effect. Table 8.1 lists monthly average salinity at those sixteen sites for 1992 and 1996. Figure 8.3 shows a salinity contour plot for May 1992 representing a wet period, while Figure 8.4 shows a June 1996 plot representing a dry period. From these tables and plots it is clear, maybe obvious, that the closer to the freshwater source the fresher is the bay water, and the closer to the Gulf the saltier is the bay water. At Trinity Bay and upper Galveston Bay salinity ranges from 0 to 22 ppt, at mid-Galveston Bay from 2 to 23 ppt, at mid-West Bay from 12 to 28 ppt, at East Bay from 6 to 25 ppt, and at Christmas Bay from 20 to 30 ppt.

No Diversion

Table 8.2 lists the salinity difference between the *existing* condition and the *no diversion* scenario for the sixteen sites. A negative difference indicates a rise in salinity under the no diversion scenario, and a positive difference indicates a reduction in salinity under the scenario. In general, the impact of the *no diversion* scenario is very small due to the small volume of water currently diverted (compared to the volume of inflow) from Trinity River to San Jacinto River area. Table 8.3 lists the minimum and maximum salinity differences over the entire simulation area. The minimum is –0.6 ppt that occurs at HSC in Buffalo Bayou and the Maximum is 2.1 ppt near the mouth of Trinity River.

Figure 8.5 is a salinity difference contour plot for the wet period in May 1992. It shows a limited effect near the mouth of Trinity River. Figure 8.6 shows the dry period of June 1996. The effect of not diverting water is stronger during a dry period than during a wet period, but overall the effect is mostly local. If diversion of water is withheld during a dry period, salinity in Trinity Bay is lowered by 2 ppt near the mouth of Trinity River and by 0.7 ppt in the middle of Trinity Bay. In contrast, salinity increases on the San Jacinto side by 0.6 ppt in the upper HSC area during dry periods.

Figure 8.7 is a time series plot for salinity at the upper Trinity Bay site under the *no diversion* scenario. It indicates that there is not much difference between diverting and

not diverting water during a wet period, while salinity decreases as much as 0.7 ppt during a dry period when water is not diverted.

No Power

Table 8.4 lists salinity differences for the *no power* case. Figure 8.8 is a contour plot of salinity difference for May 1992, a wet period. The impact of water withdrawal and discharge by the power plant is limited to the local area during wet periods. For the Cedar Bayou plant, mainly Cedar Bayou and the cooling pond at Trinity Bay are affected. For May 1992, the minimum difference is –1.5 ppt at the discharge site of the cooling pond and the maximum is 1.9 ppt in Cedar Bayou. The influence of Robinson Power Plant operation during a wet period is not significant. Salinity will be less than 0.5 ppt in the mid Galveston Bay near Redfish Reef and off Clear Lake.

The impact of power plant operation during a dry period is more pervasive than during a wet period. Figure 8.9 shows salinity differences in June 1996. The Minimum difference of –9.0 ppt occurs at the discharge site of the cooling pond and the maximum difference of 5.5 ppt occurs in Cedar Bayou, see Table 8.5. The impact spreads bay-wide. Salinity increases 2 to 2.5 ppt in Trinity Bay, 1 ppt in mid-Galveston Bay, and 0.5 ppt in lower Galveston Bay if the power plant is not in operation.

Figure 8.10 is a time series plot for salinity at the upper Trinity Bay site. This also indicates a similar pattern of little difference during a wet period and salinity increases (by 2 to 2.5 ppt) during a dry period.

Texas City Dike Removal

In this scenario we remove the Texas City Dike and examine the response of salinty. Table 8.6 lists the salinity difference between the *existing* condition and the *Dike removal* scenario at the sixteen sites. As expected the impact occurs in and near the Texas City Ship Channel and in West Bay. Salinity decreases as much as 4 ppt in the Texas City Ship Channel and the turning basin, 3 ppt in the adjacent area of West Bay, and 2 ppt at mid-West Bay. In mid-Galveston Bay and Trinity Bay, salinity decreases by 0.6 ppt. The reduction in salinity is consistent throughout wet and dry periods. Figure 8.11 shows the salinity difference contour plot for May 1992 and Figure 8.12 for June 1996. The plots exhibit a similar pattern in that the largest impact occurs in the city channel turning basin and spreads to West Bay. It also affects lower Galveston Bay but not upper Galveston Bay or upper Trinity Bay.

Table 8.7 lists the minimum and maximum salinity differences. The minimum is close to zero both in wet and dry periods implying dike removal will not raise salinity anywhere in the system. The maximum difference of 4.3 ppt occurs at the turning basin of the city channel.

Figure 8.13 shows a salinity time series comparing the *existing* condition and the *dike removal* scenario at West Bay near the city channel for 1992 and 1996. The dike removal case exhibits consistently lower salinity by 3 to 4 ppt for both 1992 and 1996. Another effect is an increase in daily variation of salinity (i.e., the removal case shows larger daily

variation). Figure 8.14 is a time series plot of salinity at mid-West Bay that also exhibits consistently lower salinity by 1 to 2 ppt. Figure 8.15 is a time series plot at the upper Trinity Bay site indicating a slight decrease during a high salinity period.

HSC Removal

In this scenario, the HSC channel is removed by changing the channel depth to match neighboring bay depths. Other channels such as Texas City Channel, Galveston Channel, and the GIWW are also removed as well as Texas City Dike, because these facilities lose their function without the HSC. However, the power plant operation and the diversion from Trinity River to San Jacinto River remain. Table 8.8 lists the salinity difference between the existing condition and the HSC removal case at the eight reference sites plus the eight additional sites.

Table 8.9 lists the minimum and maximum differences. In 1992 (wet period) the minimum difference of –1.3 ppt occurs at the north side of Texas City Dike and the maximum difference of 4.5 ppt occurs at the HSC near the Bay Tunnel. In 1996 (dry period) the minimum difference of –2.5 ppt occurs at the north side of Texas City Dike and the maximum difference of 3.8 ppt occurs in Burnett Bay near the San Jacinto Monument.

The removal of the HSC under 1992 conditions decreases salinity by 4.3 ppt at the HSC Bay Tunnel site, by 1.8 ppt at the upper Galveston Bay site, by 1.6 ppt at the Trinity Bay site, and by 1.1 ppt at the mid Galveston Bay. At the West Bay site salinity decreases by 1.2 ppt, and at the Texas City Channel site salinity decreases as much as 1.8 ppt. Figure 8.16 is a salinity difference contour plot for May 1992. It shows a strong influence at the HSC near the Bay Tunnel.

For 1996 conditions, salinity increases by 0.1 ppt at the HSC Bay Tunnel site, by 1.3 ppt at the upper Galveston Bay site, by 1.4 ppt at the Trinity Bay site, by 1.7 ppt at the mid-Galveston Bay site, and by 0.8 ppt at the Texas City Channel site. Figure 8.17 shows a salinity difference contour plot for June 1996. The pattern is similar to Figure 8.16 in that the upper HSC area is impacted. Figure 8.18 also shows the impact in another dry period (April 1996) and indicates that all of Galveston Bay will have higher salinity by 1 to 2 ppt during dry conditions if the HSC and associated channels are removed.

Figure 8.19 is a salinity time series plot at the Trinity Bay site. During the wet period of 1992, salinity is lower, less than 1 ppt; while during a dry period salinity increases by 1 ppt. Figure 8.20 is a salinity time series plot for the Morgan's Point site. Here, salinity decreases during a wet period by 2 to 3 ppt, and increases by 1 ppt during a dry period.

Natural

In the *natural* scenario there is no power plant operation, no diversion, no ship channels or dikes. Table 8.10 lists salinity difference between the existing condition and the *natural* scenario at the sixteen selected sites.

Table 8.11 lists minimum and the maximum differences. In 1992, the minimum difference of –8.8 ppt occurs at the discharge site of the cooling pond near upper Trinity Bay and the maximum difference of 5.7 ppt occurs at Cedar Bayou. In 1996, the minimum difference is –8.2 ppt at discharge site of the Trinity Bay cooling pond, and the maximum difference of 5.8 ppt occurs at Cedar Bayou.

Under the *natural* scenario, the 1992 wet period conditions yield lower salinity values than under existing conditions. Salinity at the HSC Bay Tunnel decreases by 4.0 ppt; at upper Galveston Bay, salinity decreases by 1.9 ppt; at Trinity Bay it decreases by 0.9 ppt; and, at mid-Galveston Bay it decreases by 1.2 ppt. At West Bay, salinity decreases by 1.3 ppt, and at the Texas City Channel site, it decreases by 1.8 ppt. At Cedar Bayou, salinity decreases by 5.4 ppt and at the cooling pond it decreases by 0.5 ppt. Figure 8.21 is a contour plot of salinity differences for May 1992. It shows a strong impact at the HSC Bay Tunnel area and Cedar Bayou.

For 1996 conditions, simulated salinity values are higher at the HSC Bay Tunnel by 1.7 ppt, at upper Galveston Bay by 2.1 ppt, at Trinity Bay by 2.7 ppt, and at mid-Galveston Bay by 2.2 ppt. Values were also higher at the Texas City Channel site by 1.0 ppt and at West Bay 1.0 ppt. Salinity decreases at Cedar Bayou by 5.7 ppt but increases at the cooling pond by 4.4 ppt. Figure 8.22 is a contour plot of salinity difference for June 1996. It shows a strong impact at Cedar Bayou and the cooling pond by Trinity Bay.

Figure 8.23 is a salinity time series plot at the Trinity Bay site assuming natural conditions. During the 1992 wet period, salinity decreases by nearly 1 ppt while during a dry period it increases by as much as 3 ppt. Figure 8.24 is a salinity time series plot for Morgan's Point site. It has a similar pattern to the Trinity Bay site. However, salinity is much lower, by as much as 3 ppt, during the wet period.

Average Daily Salinity

Table 8.12 lists the simulated average (or mean) daily salinities over the eight simulation years at the eight salinity sites, with standard deviations, difference in the mean between the existing condition and scenario cases, and the difference in the standard deviations. The number of data points is 2,922 (=8 years x 365 days + 2 days for leap years). These statistics bear out the characteristics stated in the previous subsections. For the *no diversion* scenario the overall influence is small, as shown by small differences in the means and their standard deviations. For the *existing* condition, mean salinity at Trinity Bay is 8.84 ppt, whereas it is 8.64 ppt in the *no diversion* case. Mean salinity at the Bay Tunnel at HSC is 7.74 ppt for the *existing* condition, while it is 7.79 ppt in the *no diversion* scenario. This supports the above stated results that salinity will be lower in Trinity Bay and higher on the San Jacinto side.

Under the *no power* scenario, mean daily salinity in Trinity Bay increases as well as the standard deviation. Salinity is 8.84 (±5.73) ppt in the *existing* condition and 9.37 (±6.26) ppt in the *no power* scenario. This supports the statement that power plant operation has a salinity-leveling effect due to withdrawal and discharge of the cooling water which promotes mixing of bay water.

In the *dike removal* scenario, all daily mean salinities are less than those under *existing* conditions. This implies that *dike removal* will reduce bay-wide salinities. But the major impact is in the vicinity of the dike and in West Bay, as shown by differences in the daily means. Under existing conditions, mean salinity is 21.31 ppt at the West Bay site and is 20.13 ppt in the *dike removal* scenario. At the Texas City Channel site, salinity is 18.48 ppt under *existing* conditions and 16.53 ppt with the dike removed. This is evident in Figures 8.13 and 8.14 where daily variations in salinity (or daily salinity excursion) are larger in the *dike removal* scenario.

Under the *HSC removal* scenario, the upper HSC area is most impacted. For example, mean salinity under existing conditions is 7.74 ppt near Bay Tunnel, but in the *HSC removal* scenario mean salinity drops to 6.11 ppt, the lowest among the five scenarios.

The strong impact of the *natural* scenario is evident by the largest increase in the standard deviations of salinities. Standard deviation increases approximately 0.9 ppt in the upper HSC area, Trinity Bay and upper Galveston Bay. This is another indication that the cumulative effect of the practices and structures results in less variation in salinity.

Summary

Because of the relatively small volume of water diverted, the *no diversion* case has little influence on salinity during a wet period. During a dry period it has more influence but is mostly local. *No diversion* of water reduces salinity by 2 ppt near the mouth of Trinity River and by 0.7 ppt in Trinity Bay. It raises salinity by 0.6 ppt in the upper HSC area.

The *no power* scenario has limited effect during a wet period, mostly affecting area near the water withdrawal and discharge sites. In Trinity Bay, the reduction in salinity is nearly zero but in mid-Galveston Bay near Redfish Reef and off Clear Lake salinity decreases by 0.5 ppt. The effect of power plant operation on salinity is more pervasive during a dry period. Salinity increases 2.5 ppt in Trinity Bay and 1 ppt in mid- and upper Galveston Bay. The power plant operation has a salinity-leveling effect, because the withdrawal and discharge of cooling water contributes to mixing of the bay water. This leveling is more effective during dry periods than during wet periods. Without the power plant operation, salinity in Galveston Bay including Trinity Bay will be higher by 1 to 2.5 ppt.

The *removal of Texas City Dike* has an effect in both wet and dry periods. The major effect occurs in and near the Texas City Ship Channel and in West Bay. Salinity will decrease by 4 ppt in the turning basin and by 2 ppt in mid-West Bay. Salinity in mid- and upper Galveston Bay and Trinity Bay will be lower by 0.6 ppt.

The depth of the ship channel is 40 to 45 feet, whereas open bay depths are 6 to 12 feet. The deep ship channel carries dense saltwater from the Gulf into upper Galveston Bay and the upper HSC area. The ship channel also acts as a salinity-leveling device, similar to the power plant operation. Without the HSC, low salinity during wet periods lasts

longer and high salinity during dry periods tends to increase. Because the area is directly linked by the channel that conveys salty Gulf water, the removal of the HSC has a greater effect on the upper Galveston Bay and upper HSC area. During a wet period salinity will decrease as much as 4 ppt near the Bay Tunnel and 3 ppt near Morgan's Point. Salinity will decrease by 1.8 ppt in upper Galveston Bay, by 1.6 ppt in Trinity Bay, and by 1.1 ppt in mid-Galveston Bay. During dry periods salinity will increase by 1.3 ppt in upper Galveston Bay, 1.3 ppt in Trinity Bay, and 1.7 ppt in mid Galveston Bay.

The *natural* case removes the salinity-leveling mechanism of the power plant operation and the ship channel, and opens flow to West Bay by removing the city dike. The combined effect results in the largest dry-season increases and wet-season decreases in salinity as compared to the *existing* condition. As in the *HSC removal* scenario, salinity decreases as much as 4 ppt near the Bay Tunnel and 3 ppt near Morgan's Point. Salinity also decreases by 1.9 ppt in upper Galveston Bay, by 0.9 ppt in Trinity Bay, and by 1.2 ppt in mid-Galveston Bay. Under natural conditions during a dry period, salinity is higher than in the *HSC removal* scenario, increasing by 2.1 ppt in upper Galveston Bay, by 2.7 ppt in Trinity Bay, and by 2.2 ppt in mid-Galveston Bay.

At mid-West Bay, salinity decreases by 1.3 ppt during a wet period and increases by 1 ppt during a dry period. A similar pattern occurs in West Bay near the Texas City Ship Channel, decreasing by 1.8 ppt during a wet period and increasing by 1 ppt during a dry period.

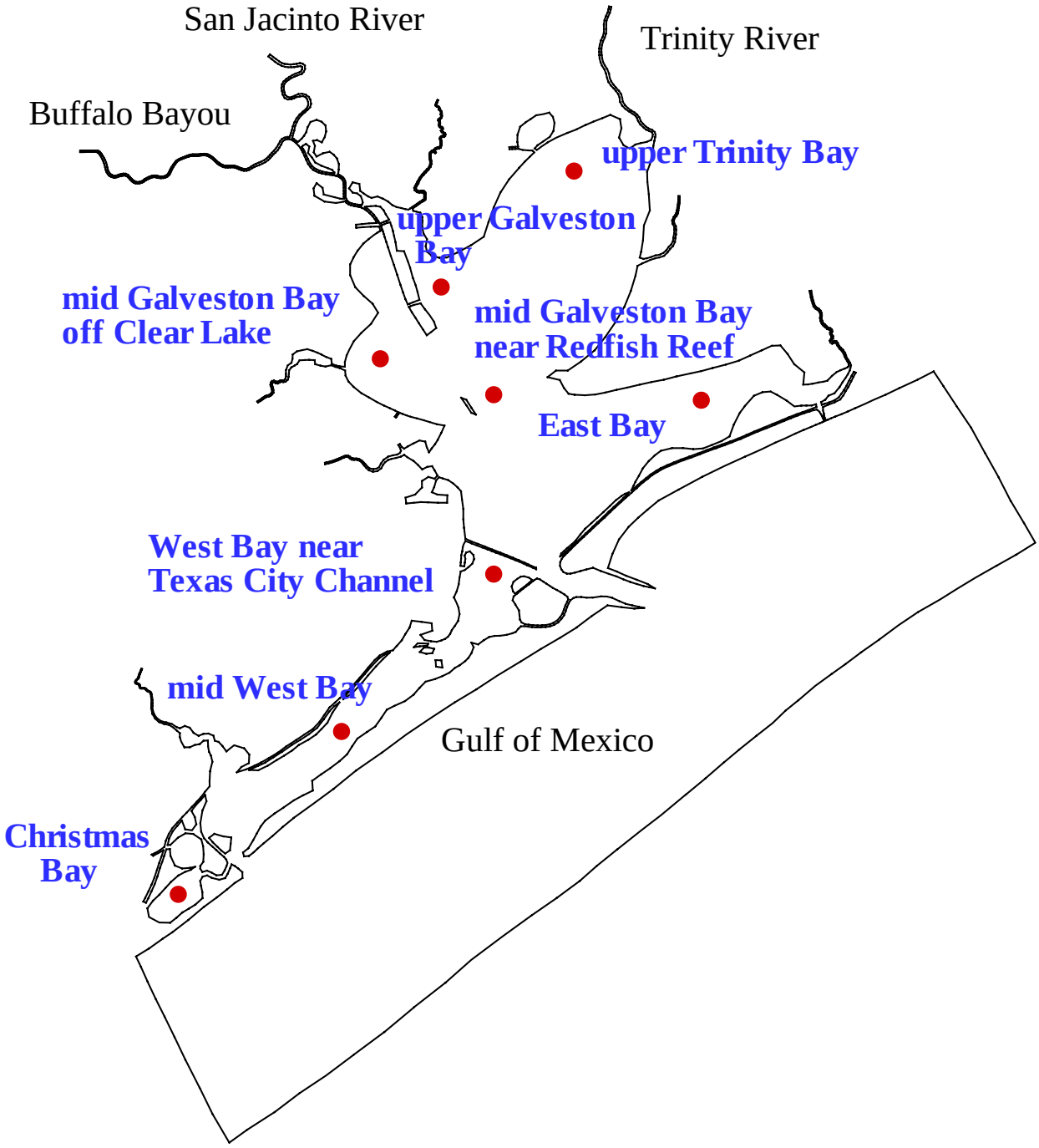

Figure 8.1 Salinity sites for Galveston Bay Model simulation

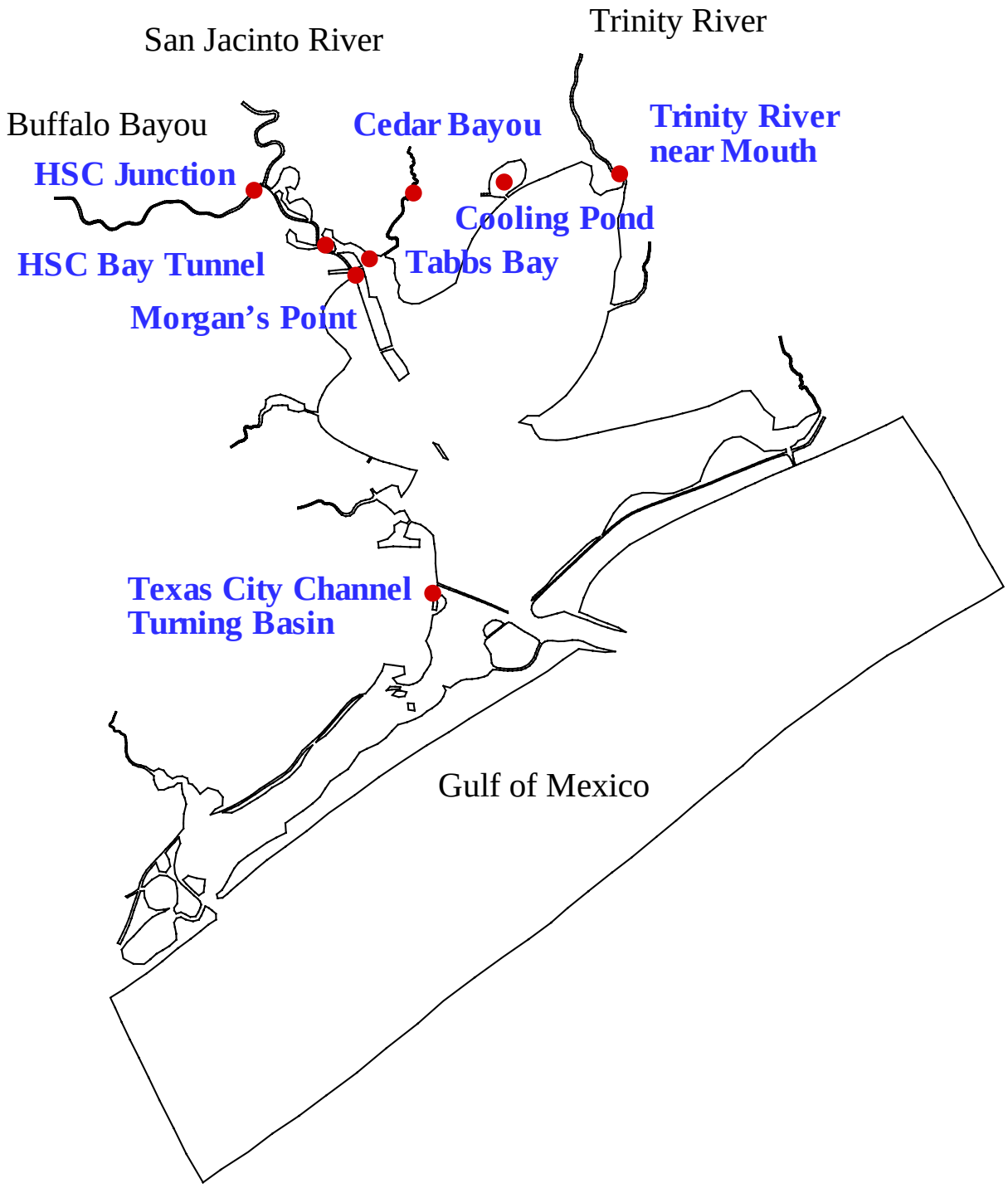

Figure 8.2 Eight additional salinity sites for Galveston Bay Model simulation

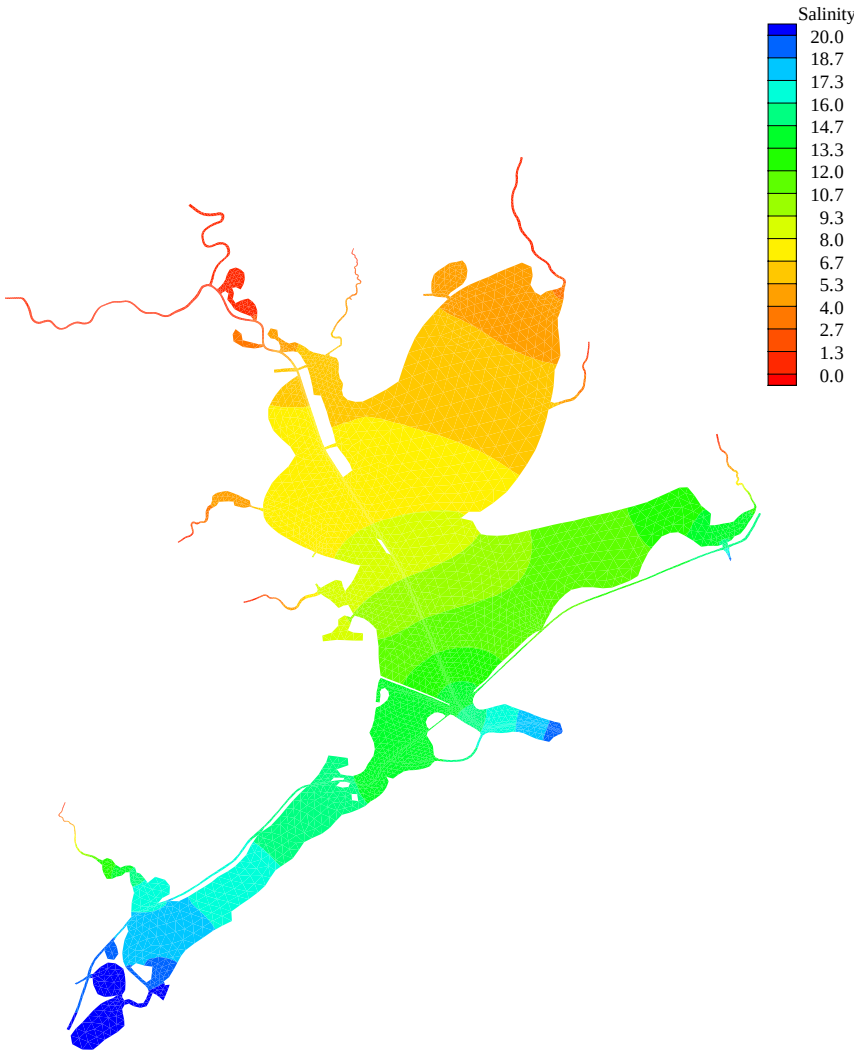

Figure 8.3 Simulated average monthly salinity in May 1992 for the existing condition

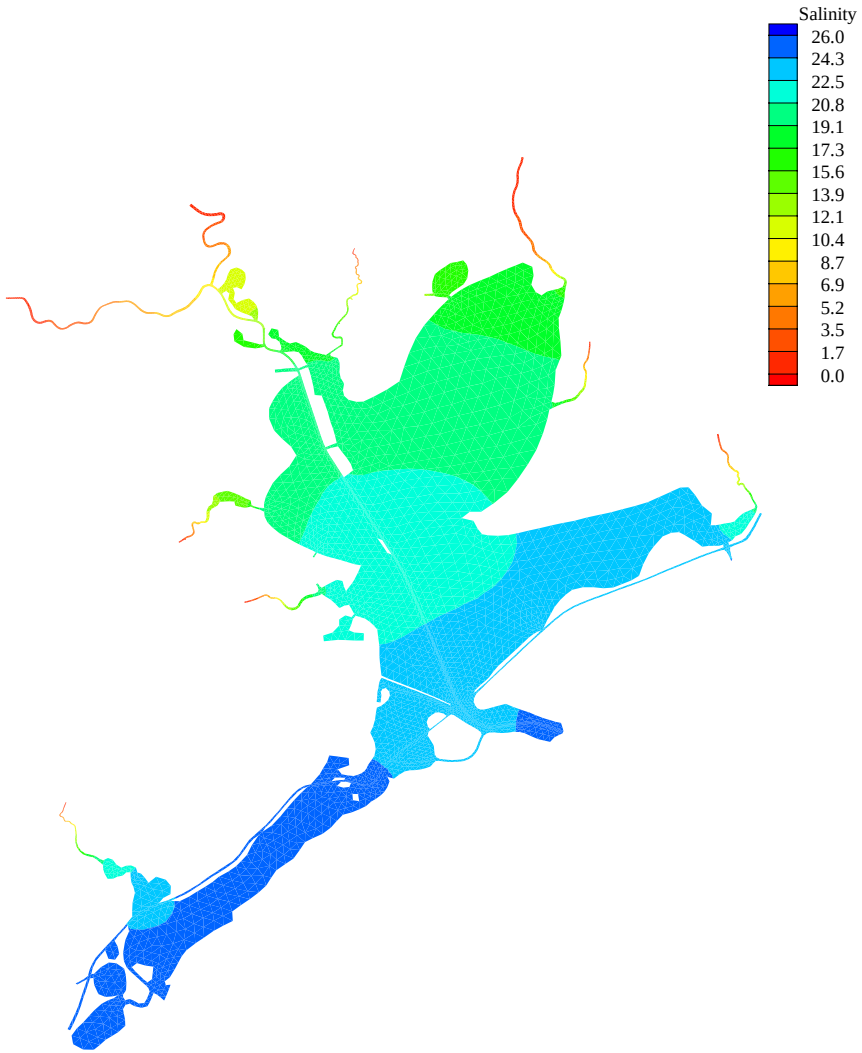

Figure 8.4 Simulated average monthly salinity in June 1996 for the existing condition

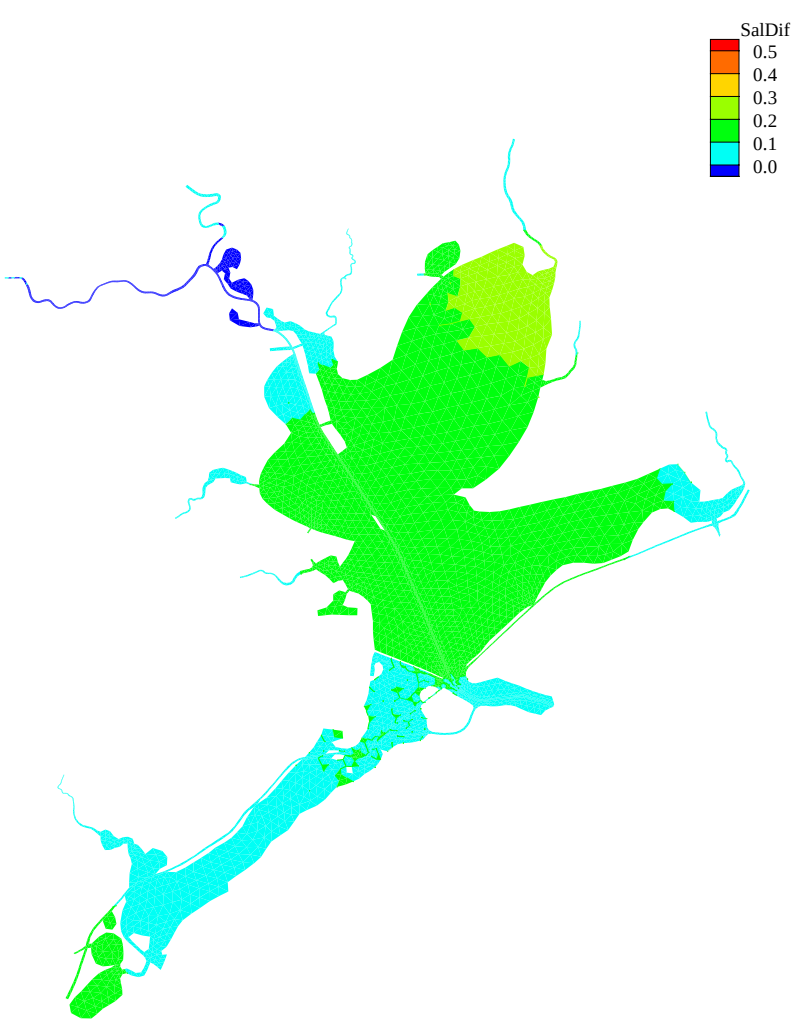

Figure 8.5 Salinity difference (ppt) in May 1992 between the existing case and the no diversion case

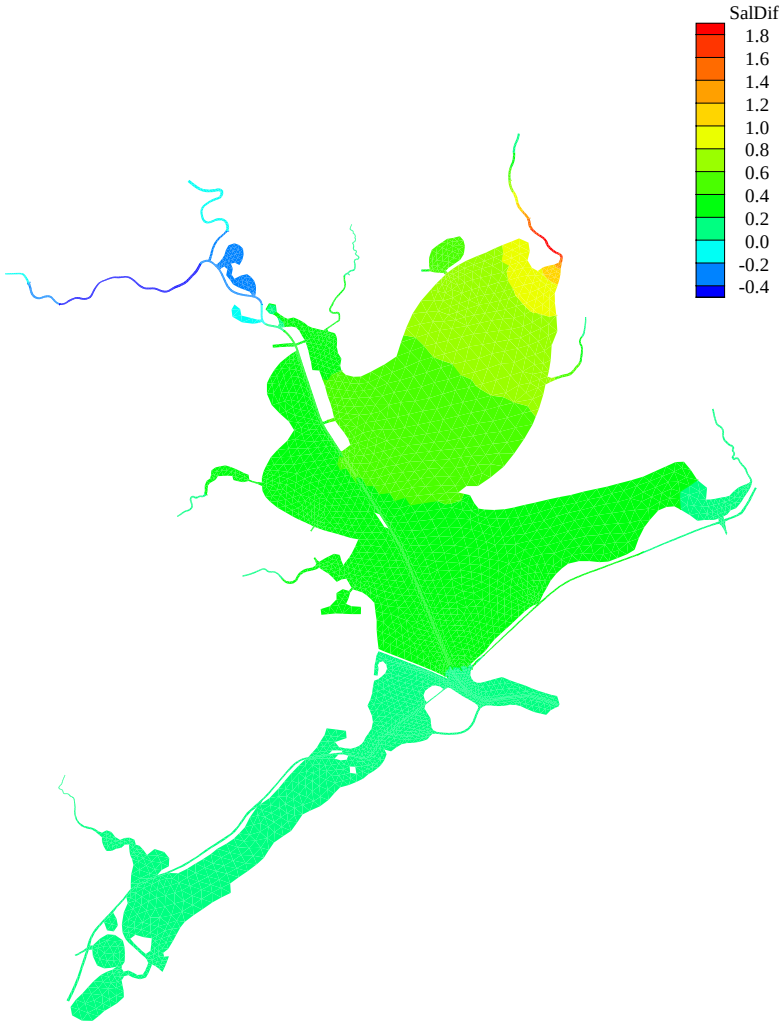

Figure 8.6 Salinity difference (ppt) in June 1996 between the existing case and the no diversion case

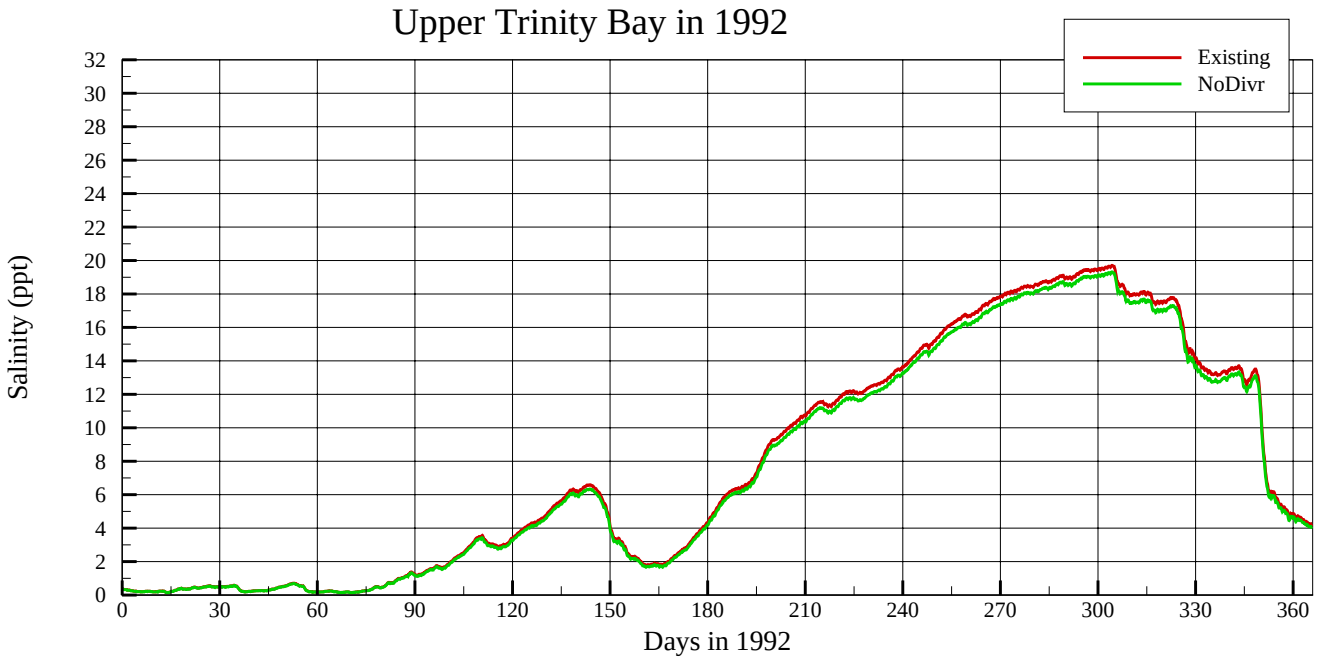

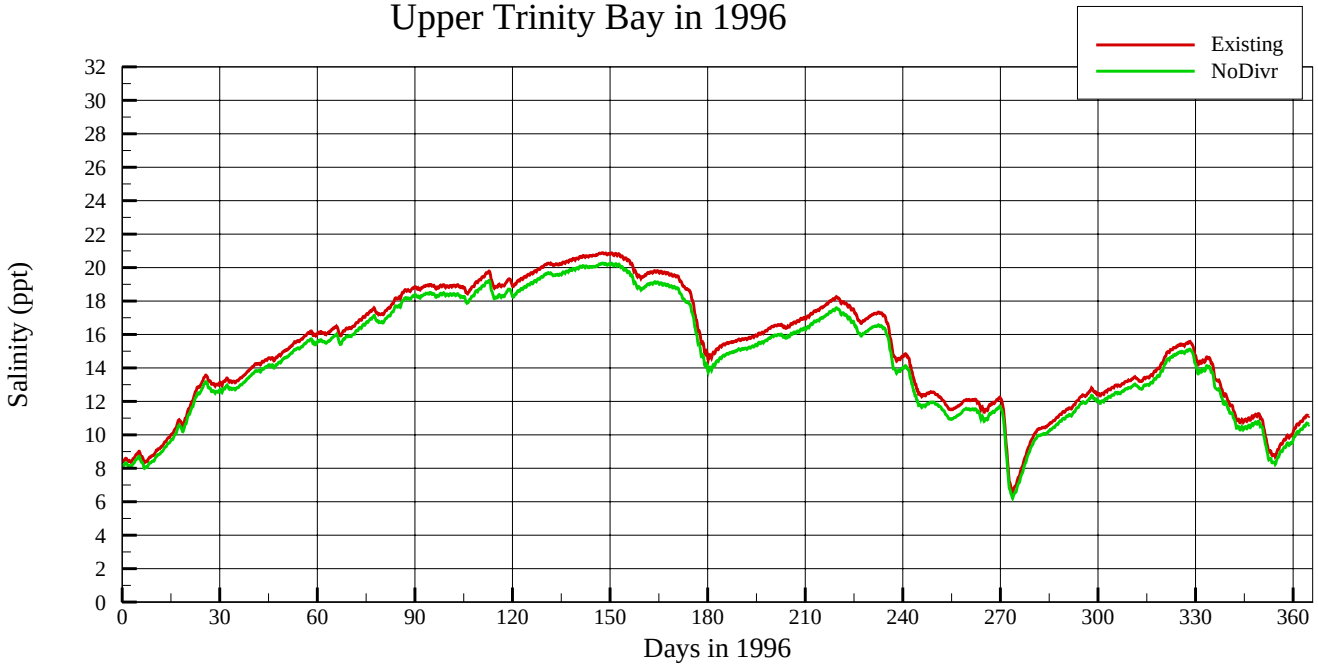

Figure 8.7 Comparison of simulated salinity at upper Trinity Bay; Existing case (red line) and no diversion case (green)

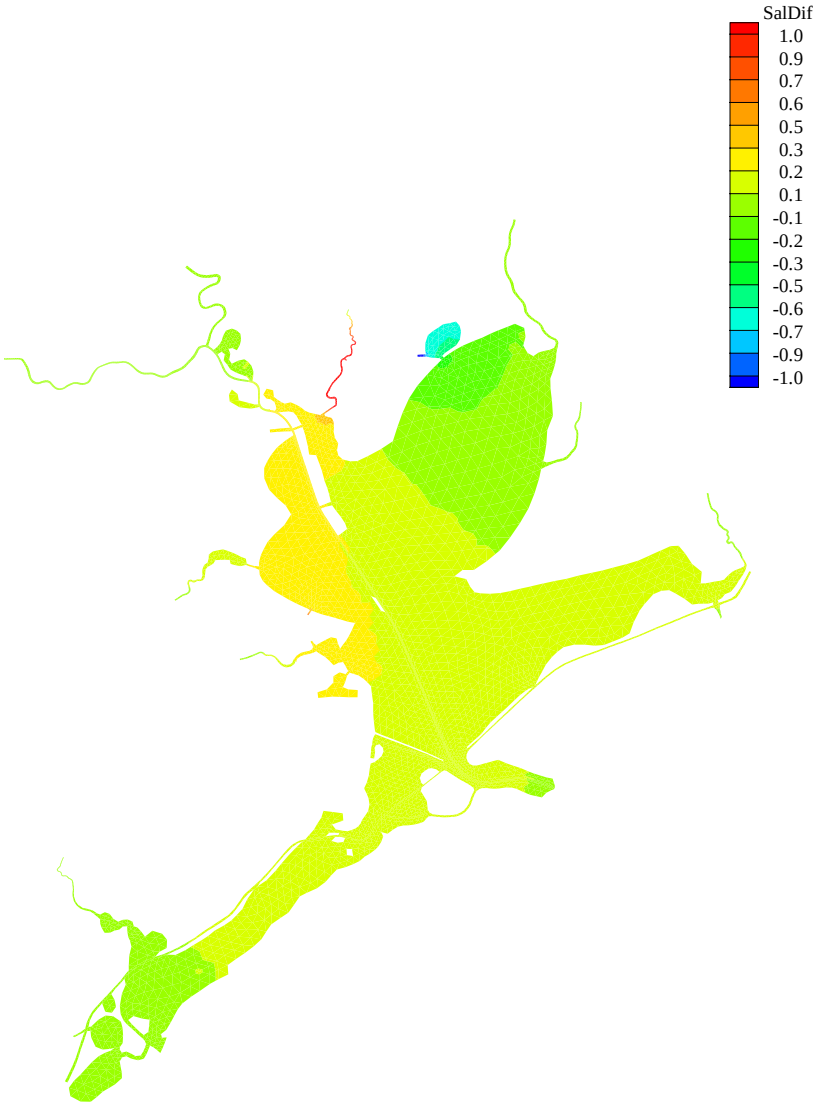

Figure 8.8 Salinity difference (ppt) in May 1992 between the existing case and the no power case

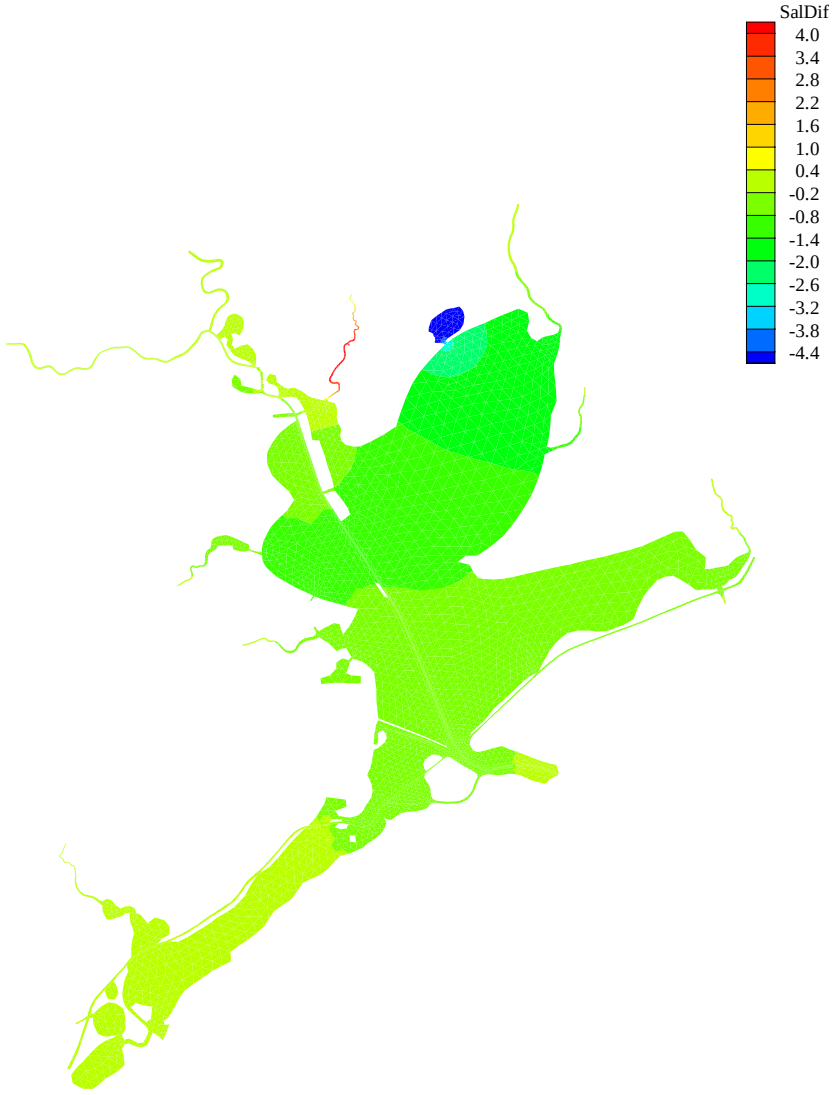

Figure 8.9 Salinity difference (ppt) in June 1996 between the existing case and the no power case

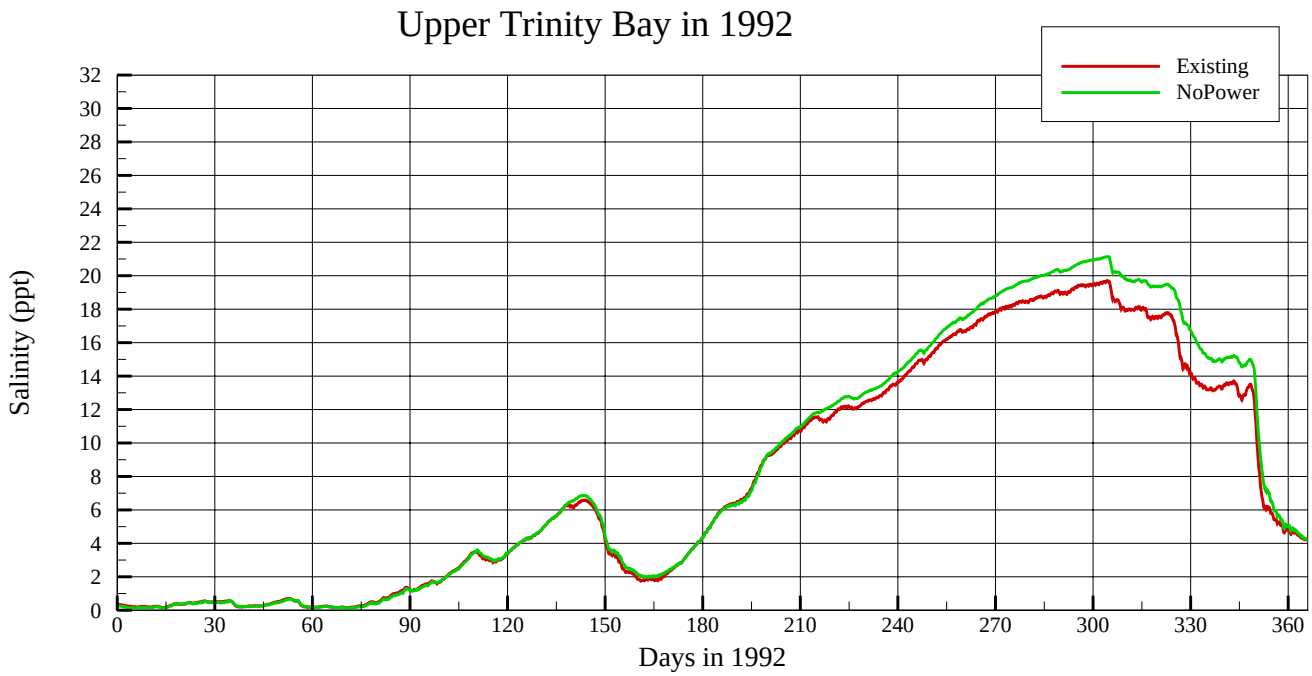

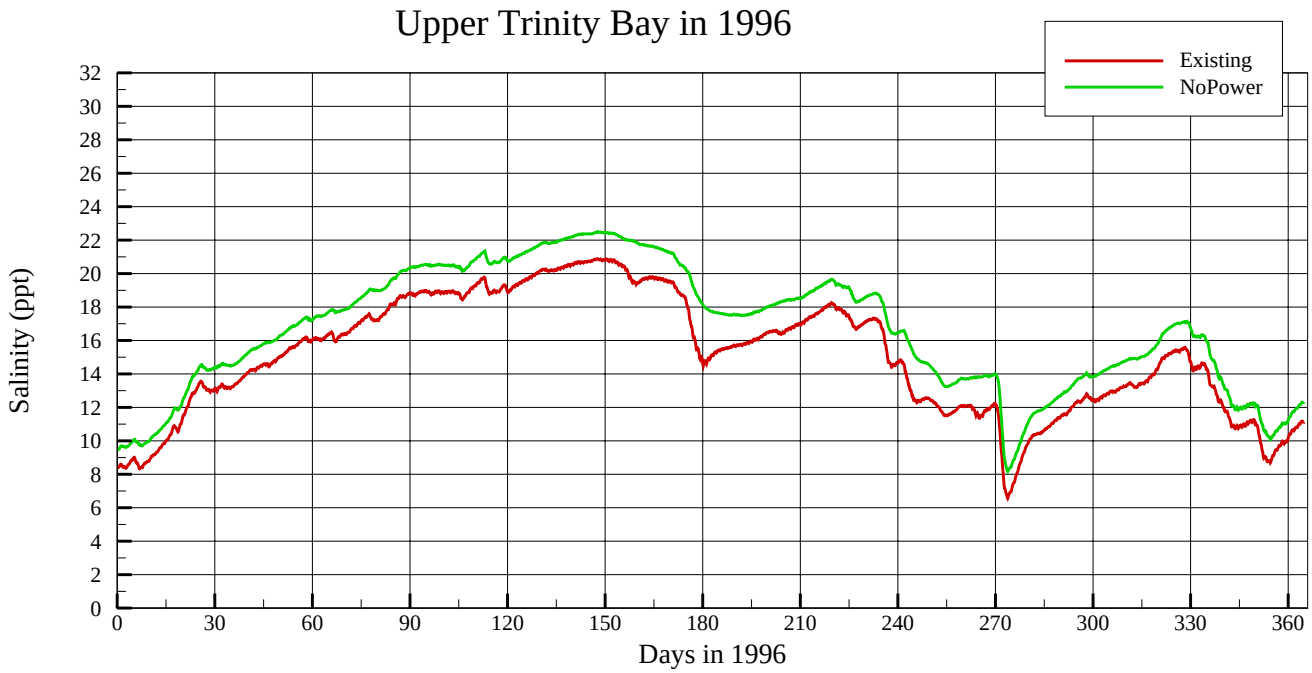

Figure 8.10 Comparison of simulated salinity at upper Trinity Bay; Existing case (red line) and no power case (green)

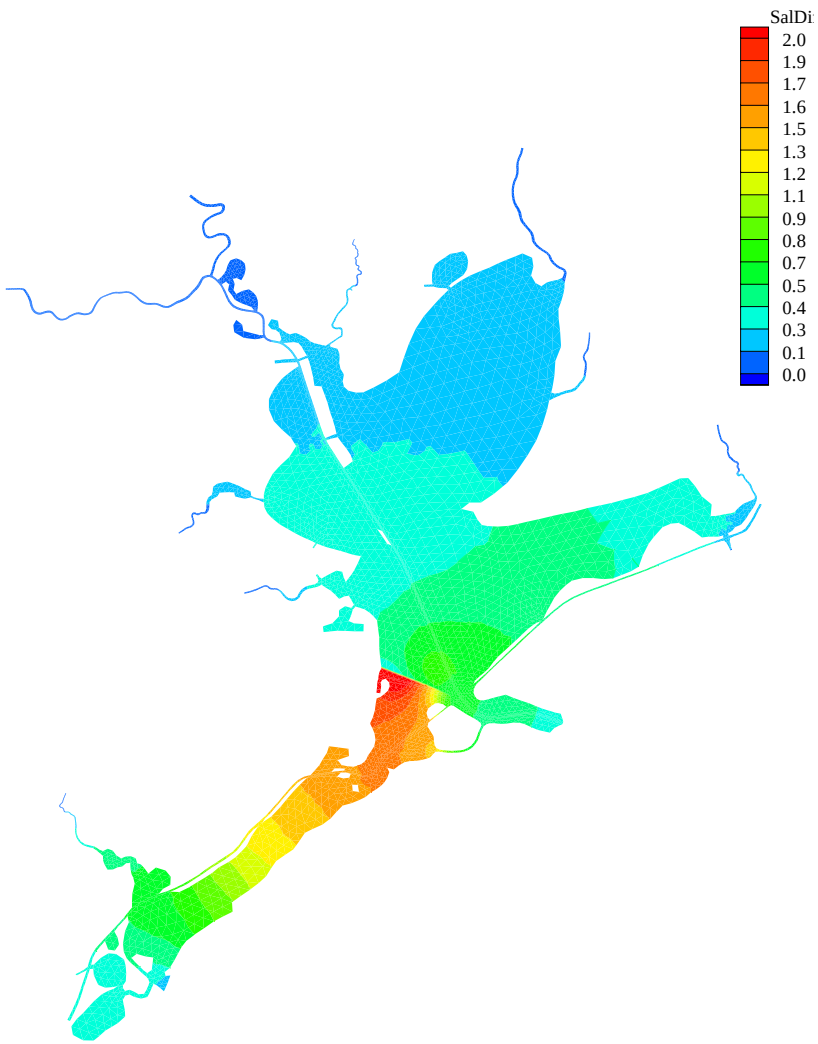

Figure 8.11 Salinity difference (ppt) in May 1992 between the existing case and the Texas City Dike removal case

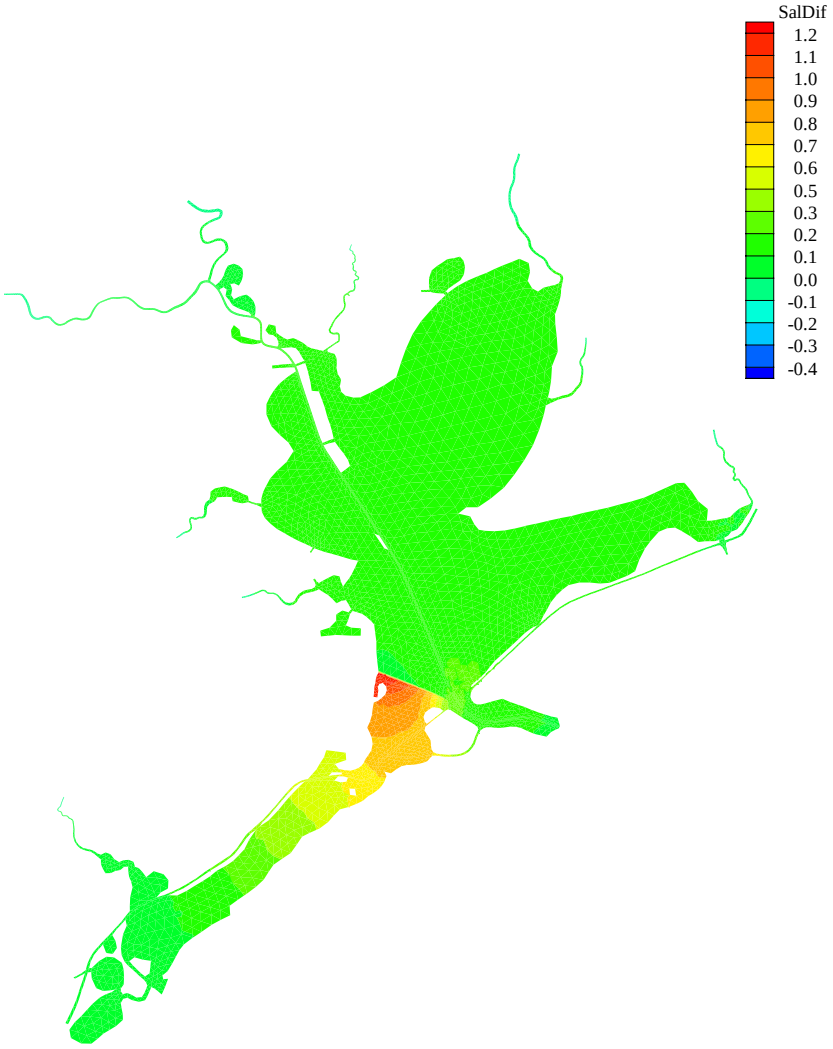

Figure 8.12 Salinity difference (ppt) in June 1996 between the existing case and the Texas City Dike removal case

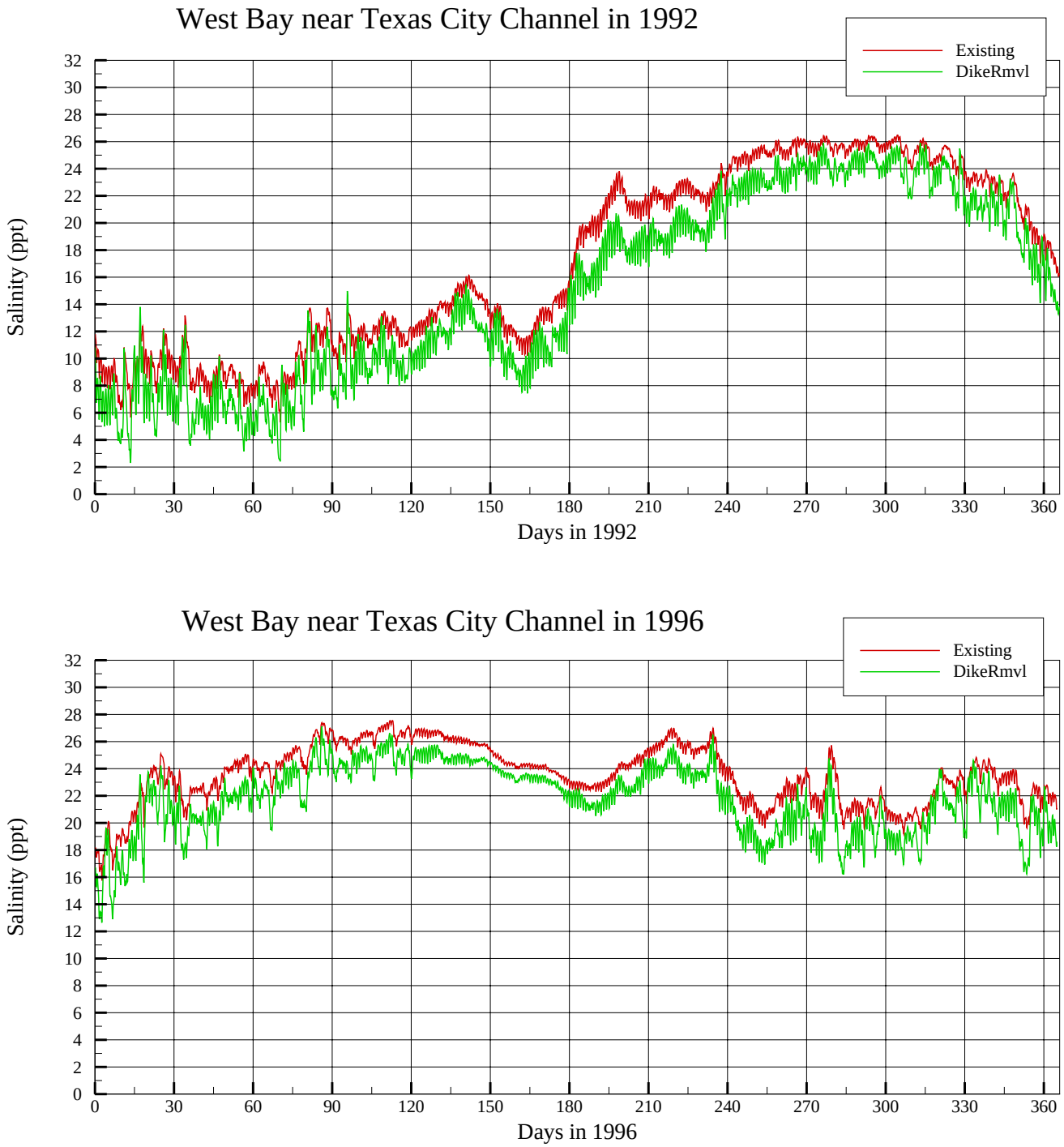

Figure 8.13 Comparison of simulated salinity at West Bay near Texas City Channel; existing case (red line) and Texas City Dike removal case (green)

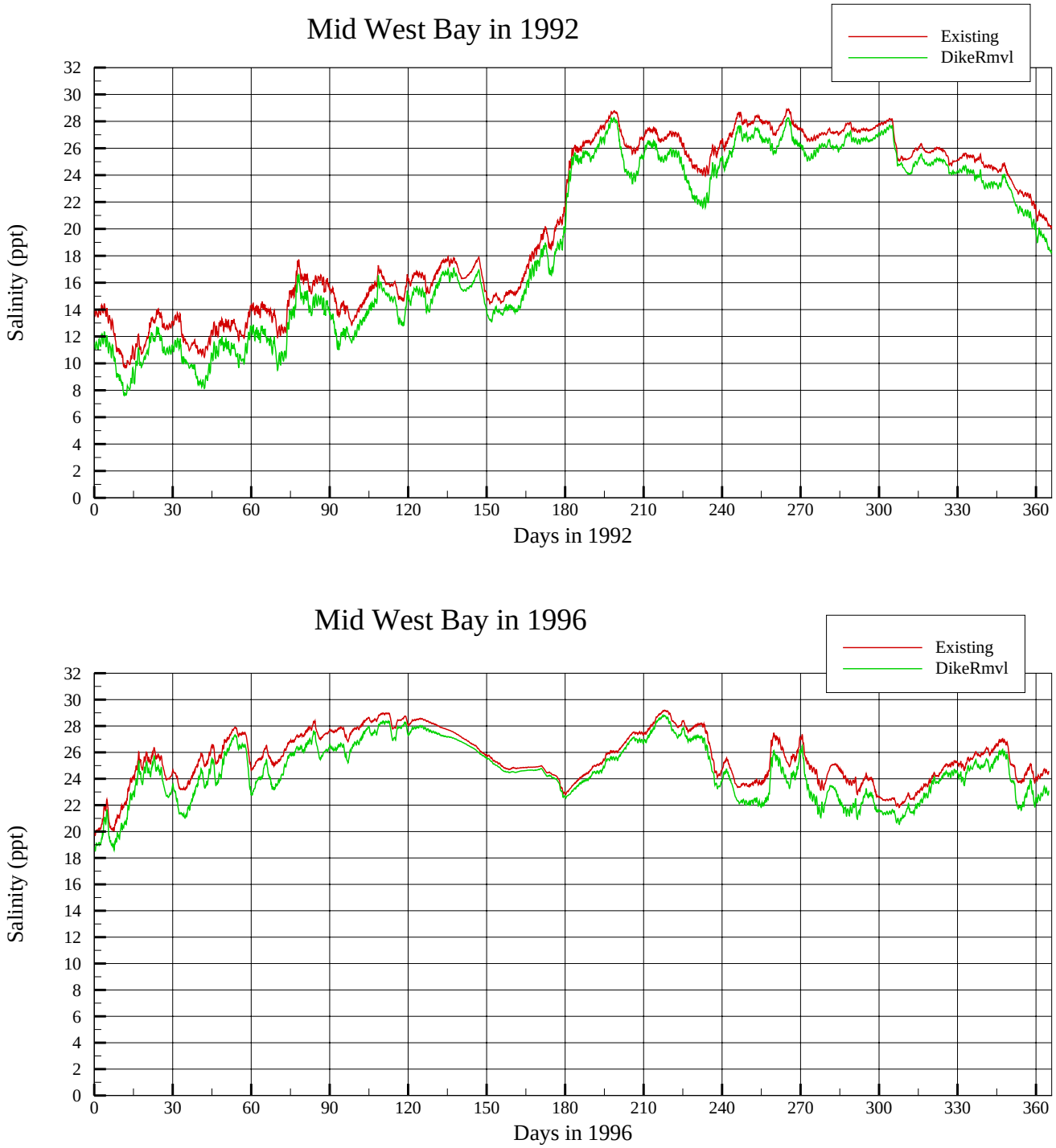

Figure 8.14 Comparison of simulated salinity at mid West Bay; Existing case (red line) and Texas City Dike removal case (green)

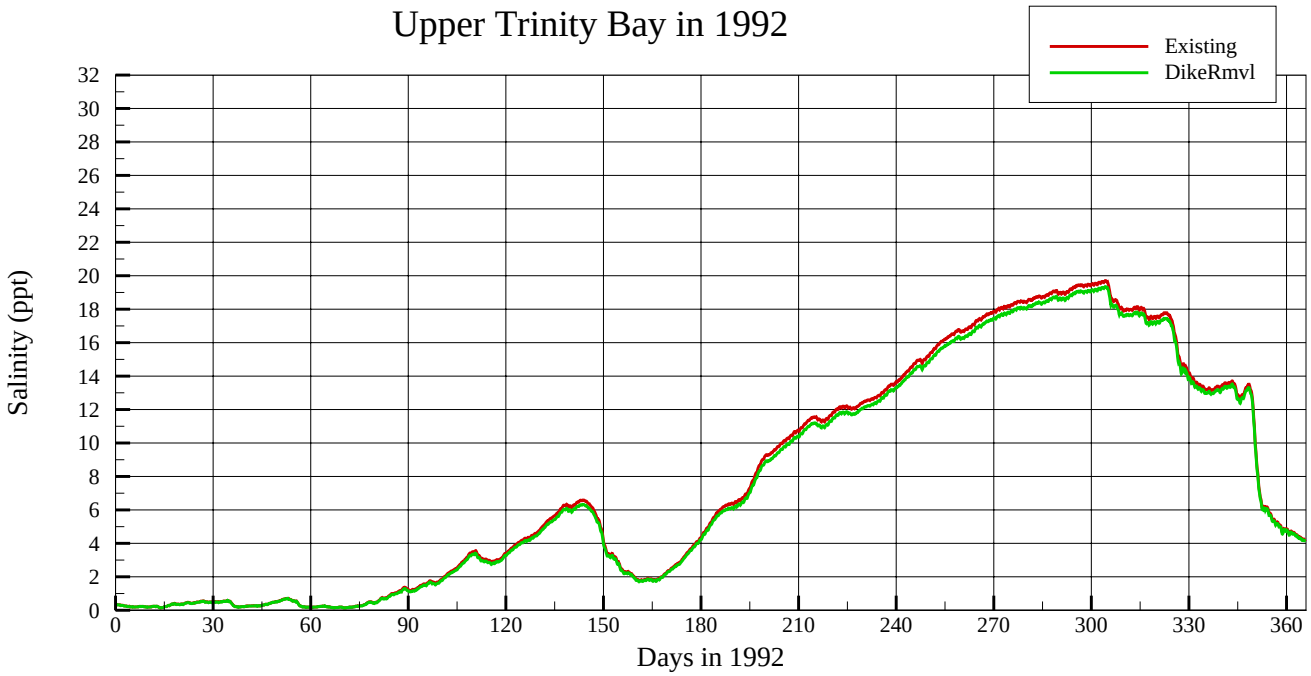

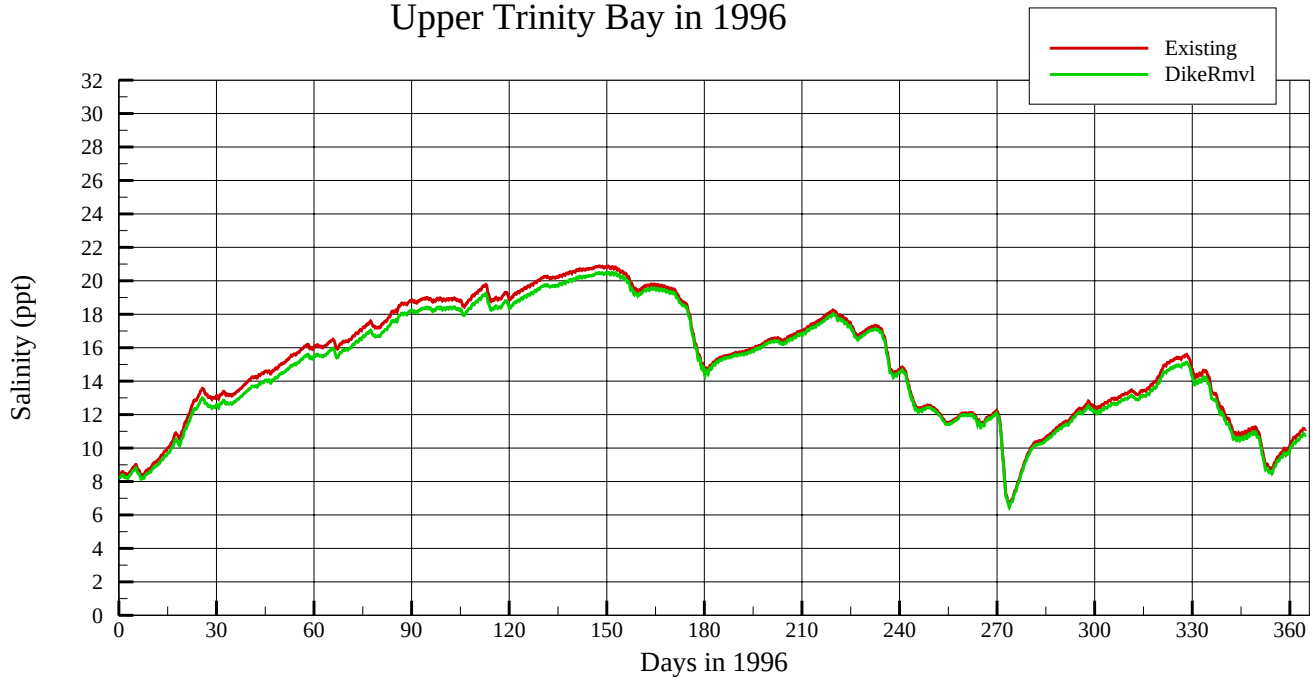

Figure 8.15 Comparison of simulated salinity at upper Trinity Bay; Existing case (red line) and Texas City Dike removal case (green)

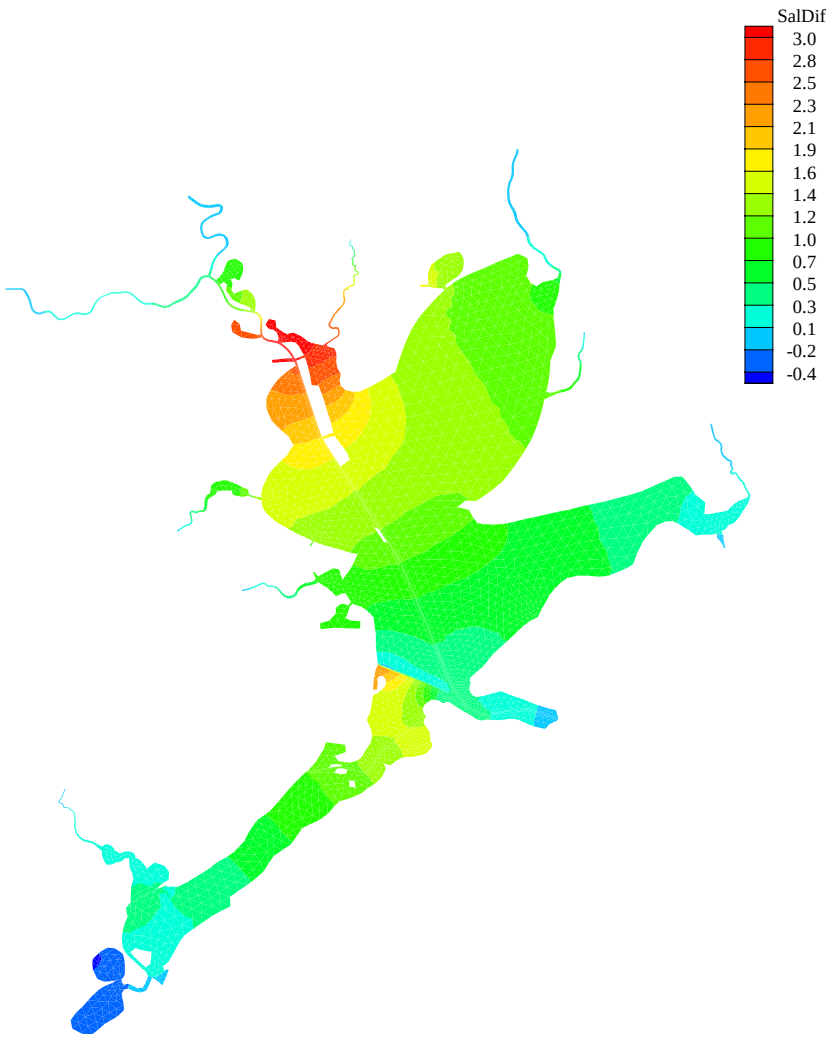

Figure 8.16 Salinity difference (ppt) in May 1992 between the existing case and the HSC removal case

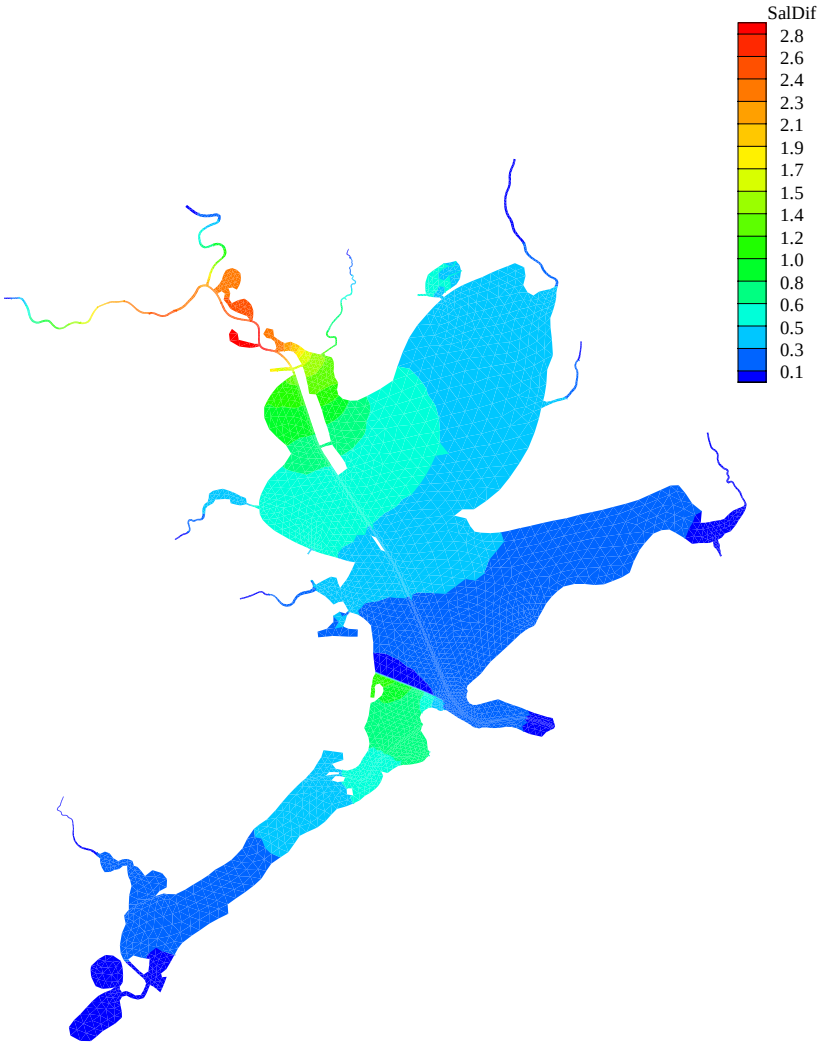

Figure 8.17 Salinity difference (ppt) in June 1996 between the existing case and the HSC removal case

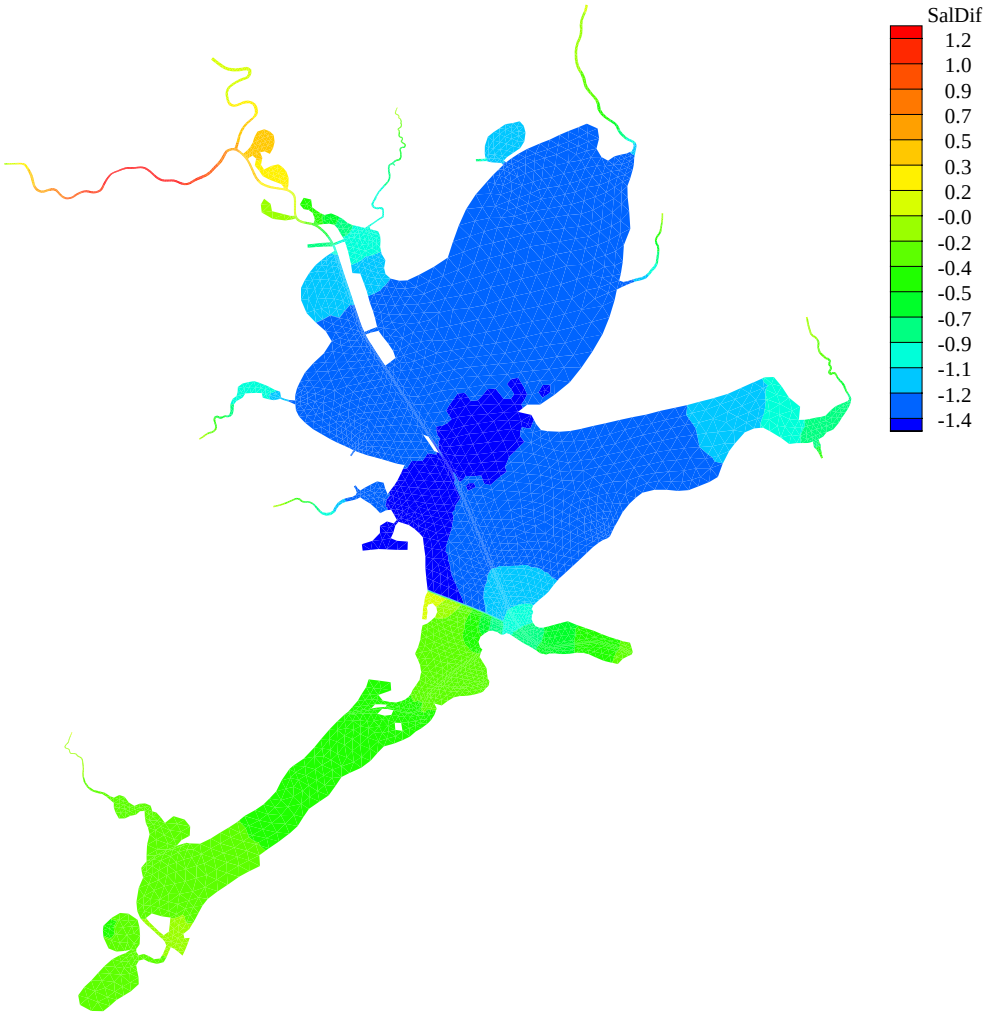

Figure 8.18 Salinity difference (ppt) in April 1996 between the existing case and the HSC removal case

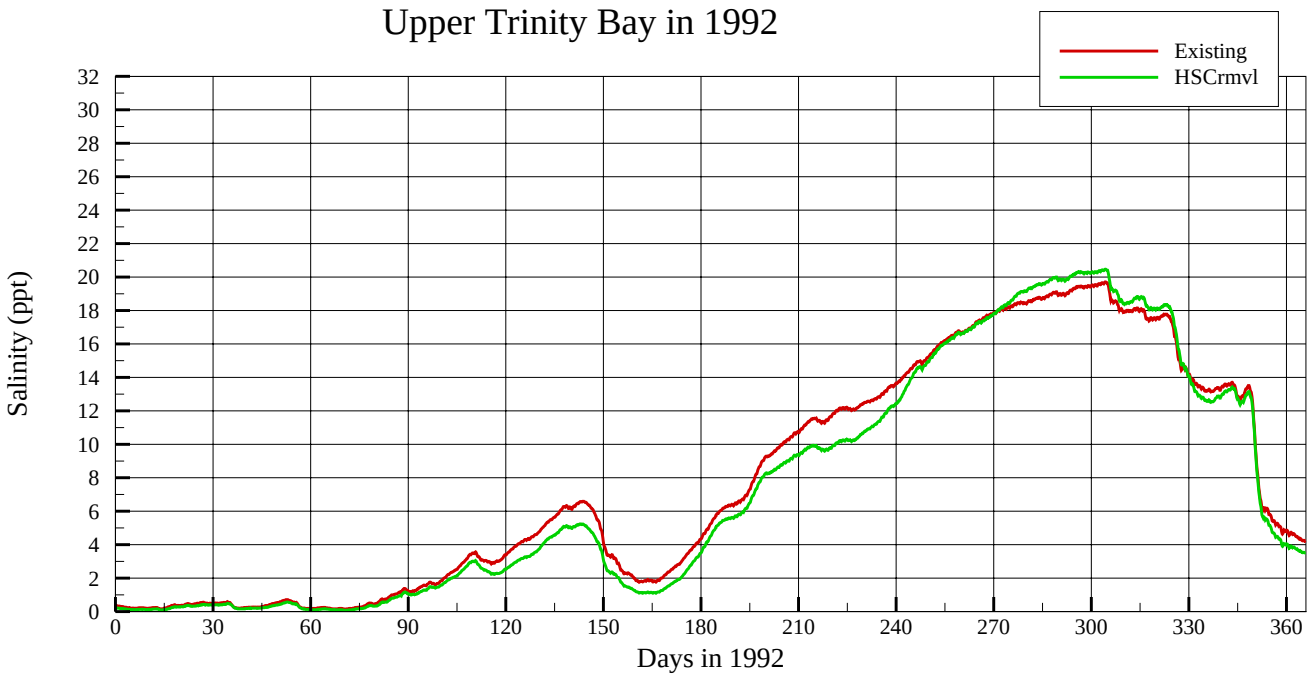

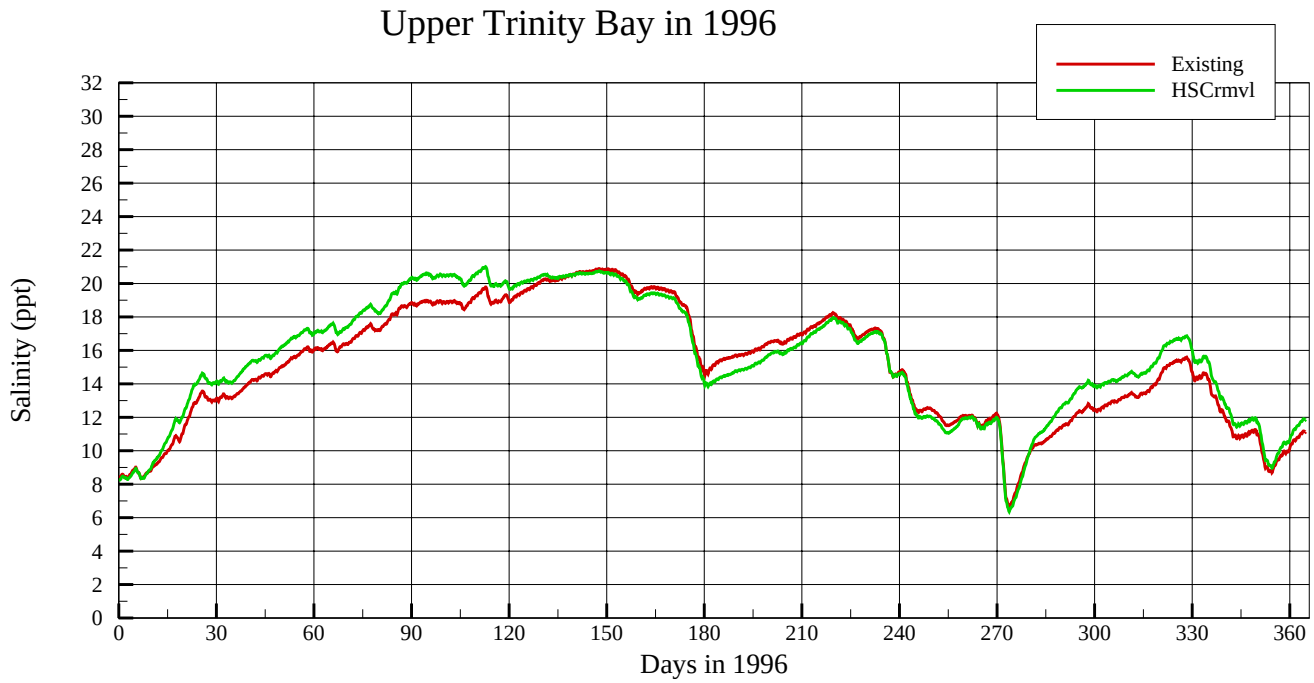

Figure 8.19 Comparison of simulated salinity at upper Trinity Bay; Existing case (red line) and HSC removal (green)

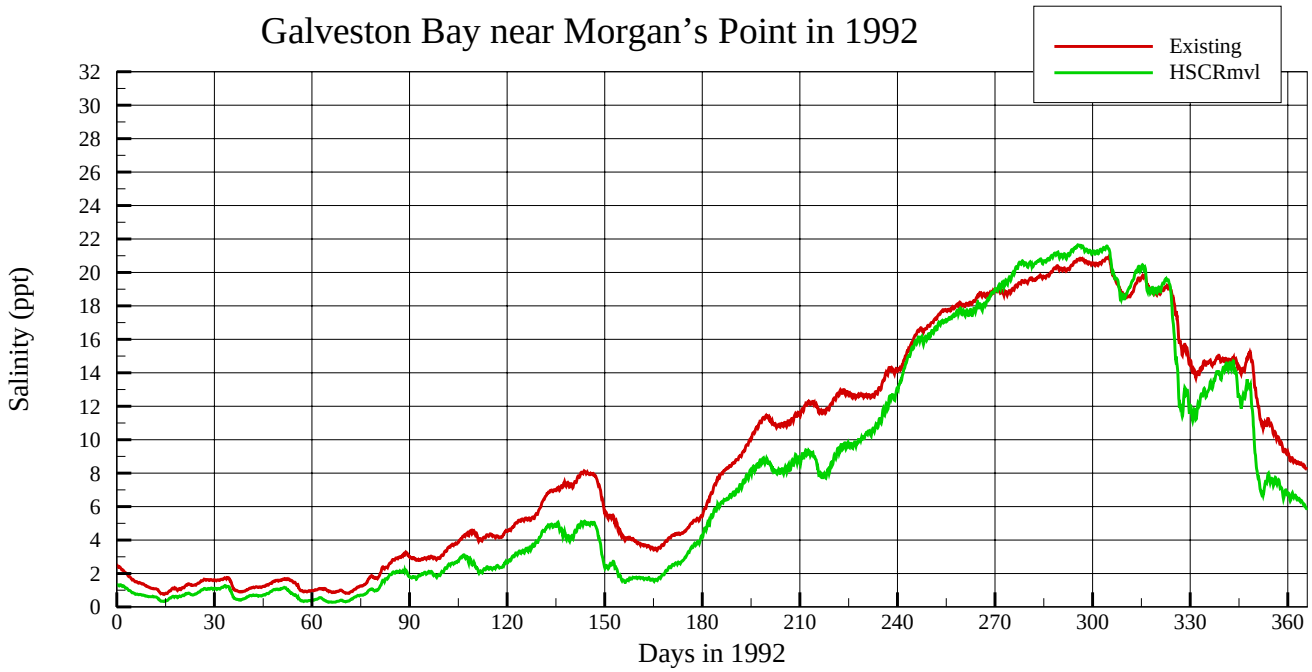

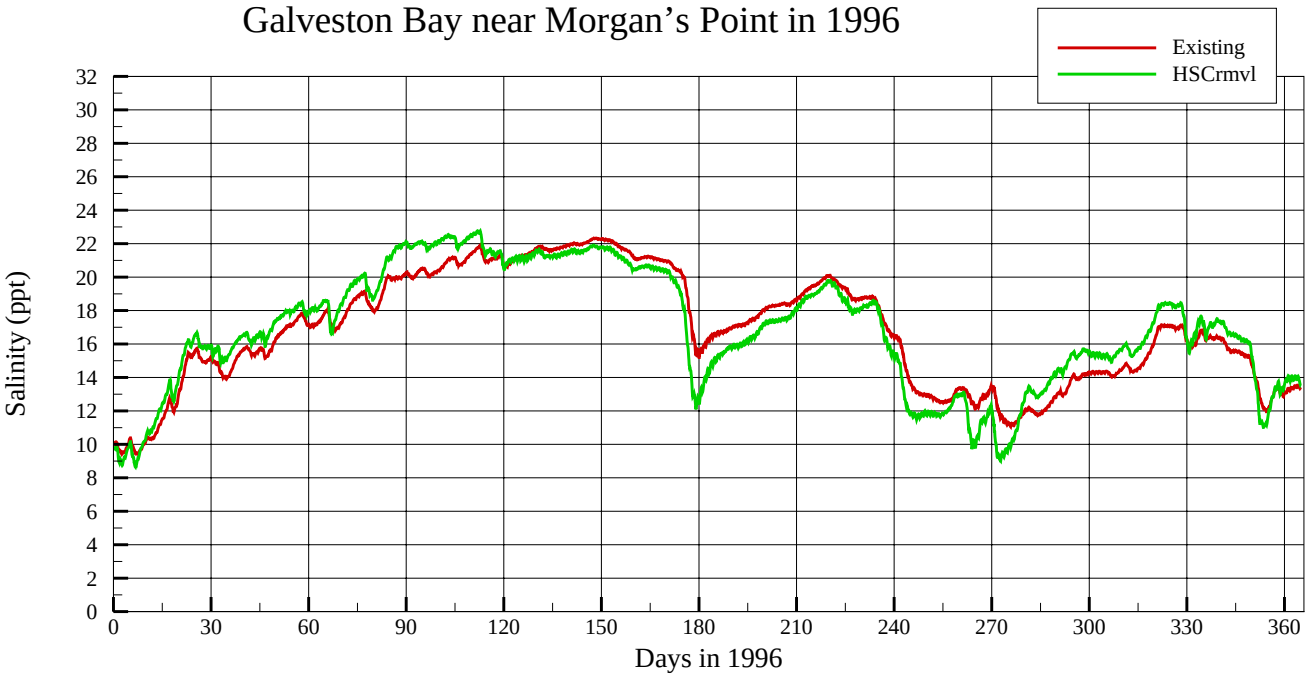

Figure 8.20 Comparison of simulated salinity near Morgan's Point; Existing case (red line) and HSC removal case (green)

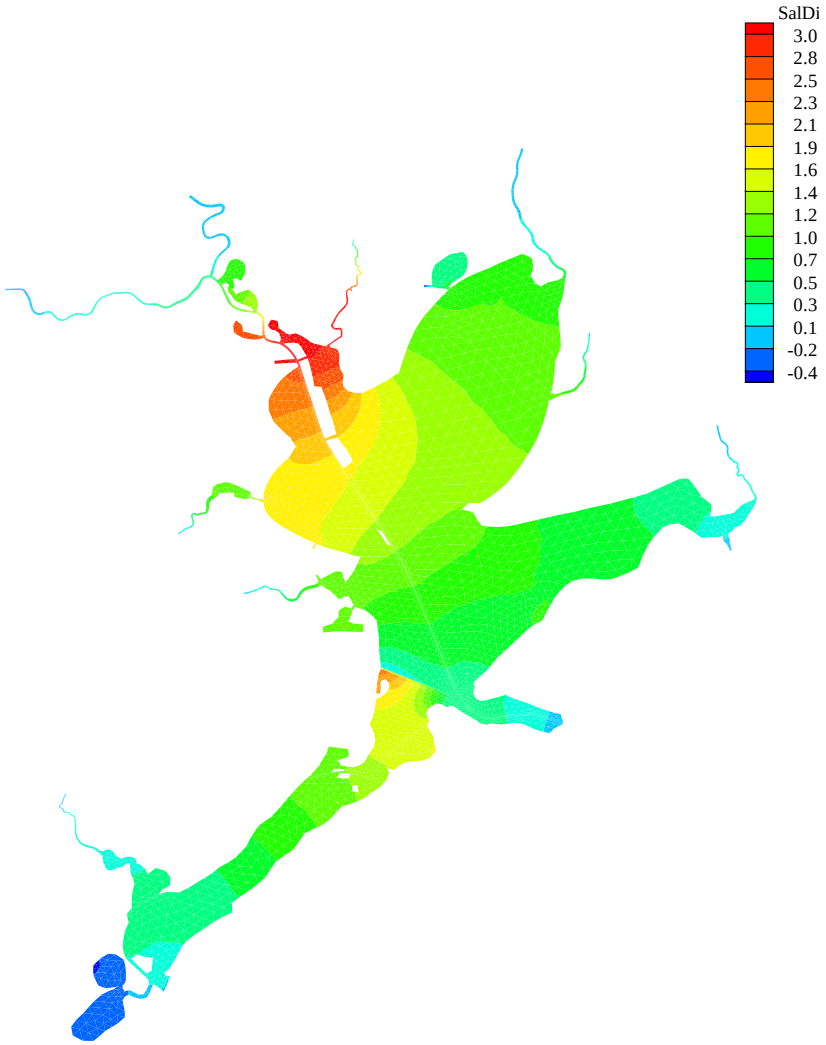

Figure 8.21 Salinity difference (ppt) in May 1992 between the existing case and the natural case

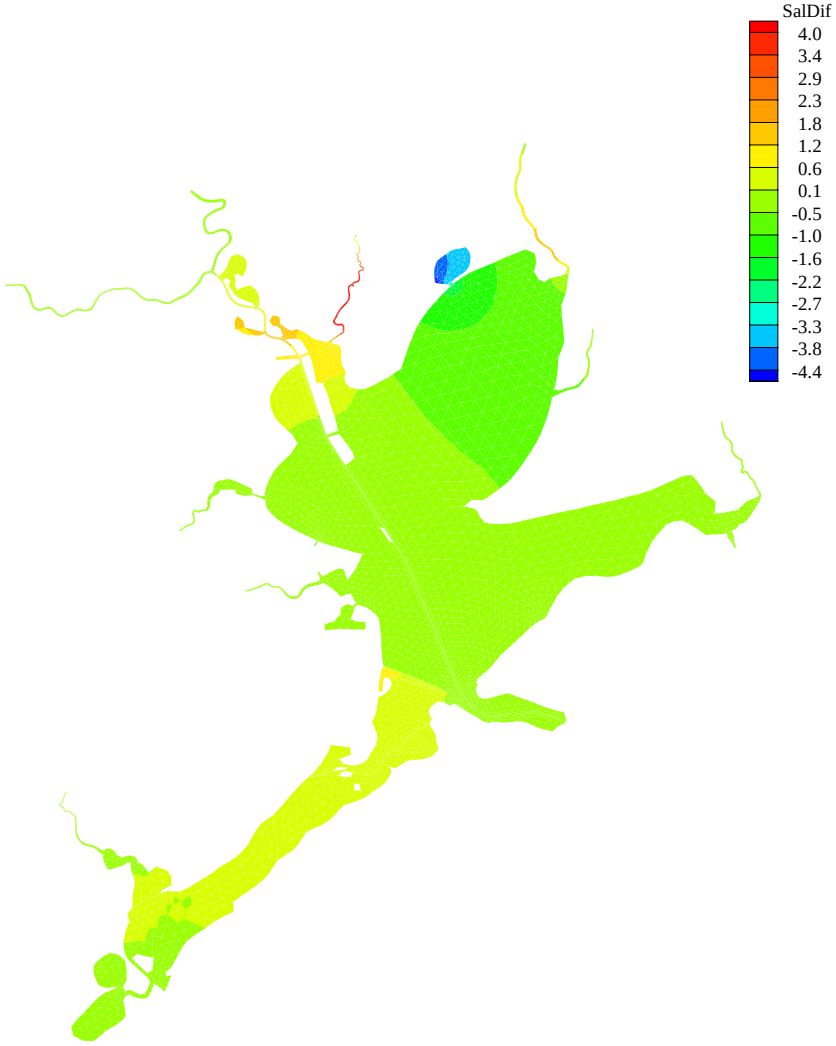

Figure 8.22 Salinity difference (ppt) in June 1996 between the existing case and the natural case

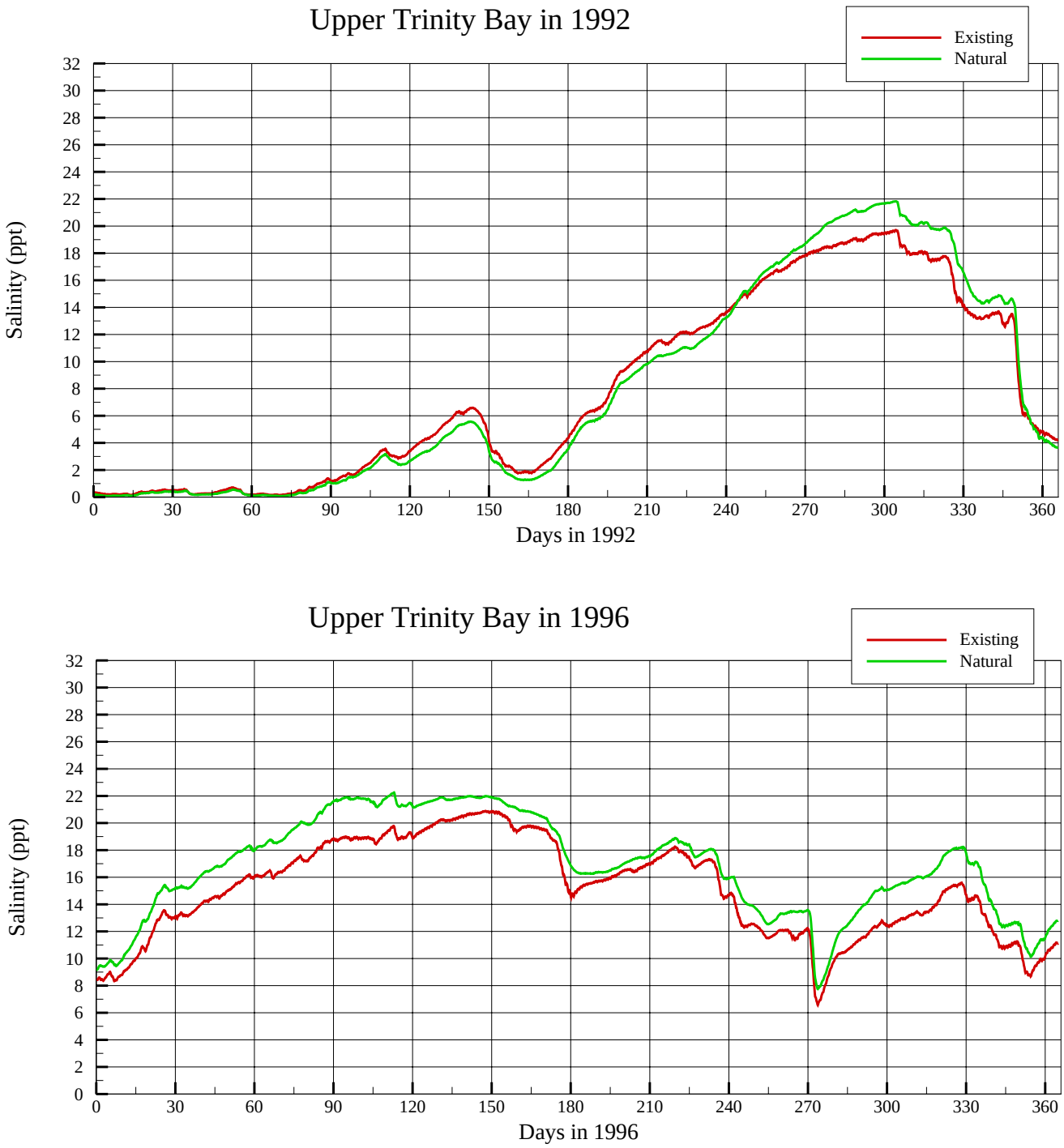

Figure 8.23 Comparison of simulated salinity at upper Trinity Bay; Existing case (red line) and Natural case (green)

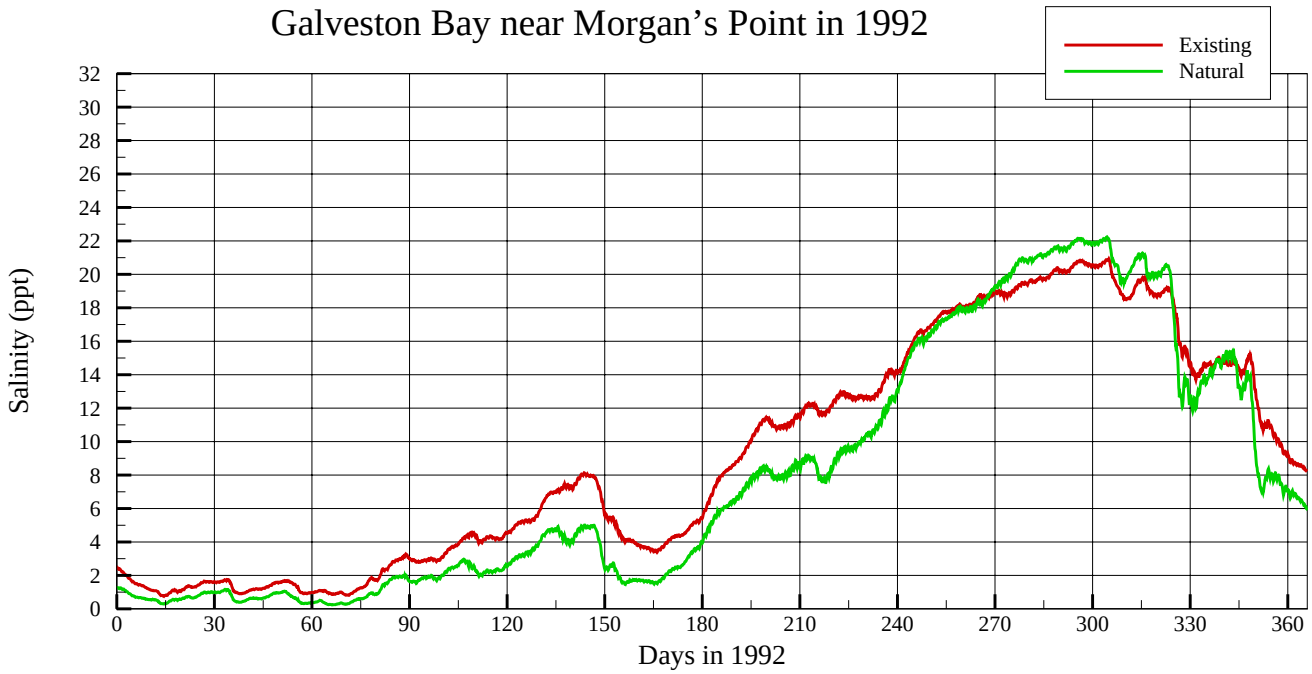

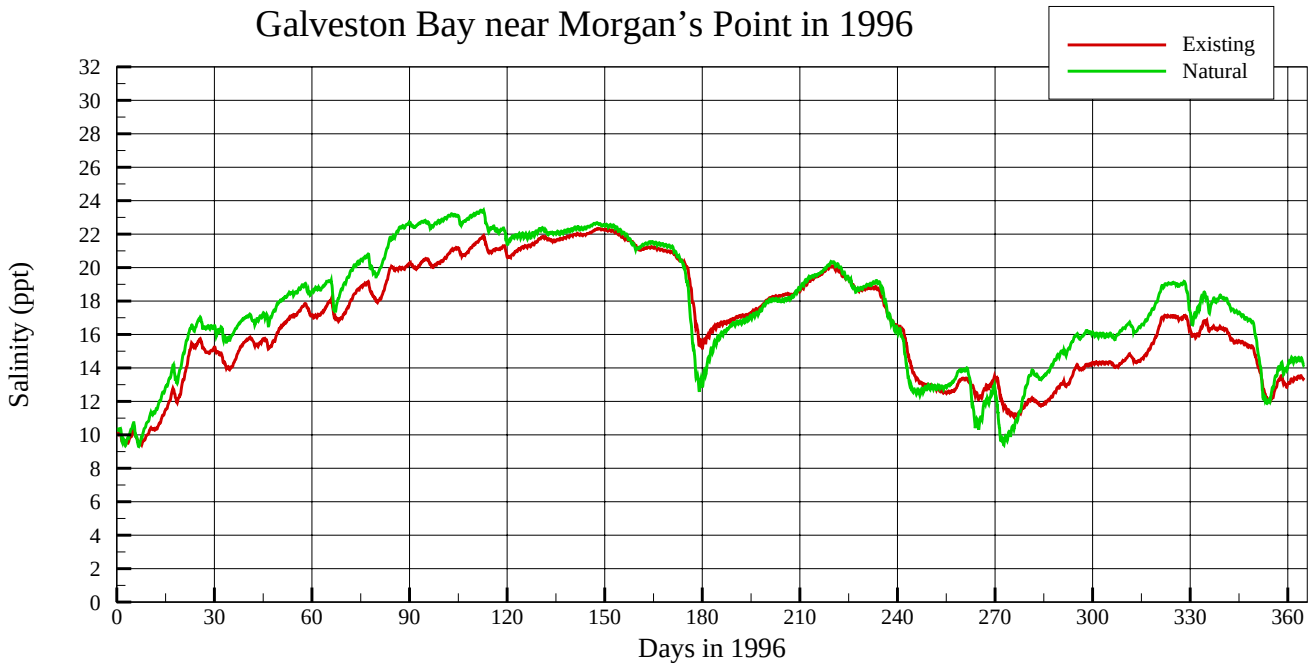

Figure 8.24 Comparison of simulated salinity near Morgan's Point; Existing case (red line) and Natural case (green)

Table 8.1 Galveston Bay monthly average salinity under existing condition

Year	Month	Upper Galvstn	Trinity Bay	Redfish Reef	East Bay	Chrstms Bay	West Bay	TxCity Chnnl	OffClr Lake
1992	1	1.26	0.33	2.58	6.75	21.18	12.22	9.30	1.84
1992	2	1.26	0.39	2.42	6.27	20.78	12.17	8.71	1.74
1992	3	1.58	0.50	3.10	6.64	21.74	14.79	9.75	2.26
1992	4	3.86	2.47	5.59	9.23	20.63	14.97	11.78	4.46
1992	5	6.75	5.18	8.51	11.52	20.25	16.58	13.89	7.32
1992	6	4.42	2.71	6.27	9.63	23.05	17.74	13.04	5.15
1992	7	10.09	8.17	12.50	15.72	29.39	26.80	20.87	11.00
1992	8	13.56	12.39	15.87	19.39	30.31	25.95	22.54	14.20
1992	9	17.97	16.40	19.92	22.77	30.72	27.73	25.26	18.45
1992	10	20.20	18.89	21.80	24.11	29.48	27.35	25.77	20.53
1992	11	18.29	16.69	20.20	22.64	28.15	25.57	24.69	18.53
1992	12	12.32	9.22	14.84	18.44	26.81	23.24	20.85	13.46
1996	1	12.34	10.51	14.75	17.50	26.94	23.25	20.82	12.95
1996	2	15.99	14.51	17.81	20.48	28.59	25.60	23.00	16.47
1996	3	18.64	17.11	20.49	23.07	29.32	26.51	25.03	19.07
1996	4	20.80	18.90	22.36	24.65	29.95	28.12	26.39	21.17
1996	5	21.74	20.19	22.96	24.50	28.05	27.38	26.14	21.93
1996	6	20.33	18.71	21.56	22.83	25.05	24.55	23.97	20.60
1996	7	17.74	16.10	19.39	21.53	27.29	25.82	23.73	18.16
1996	8	18.53	16.59	20.09	22.03	29.75	27.28	25.28	18.75
1996	9	13.20	11.59	15.09	17.92	30.03	24.91	21.77	13.47
1996	10	12.87	10.95	15.12	18.20	28.22	23.69	21.48	13.67
1996	11	15.77	14.09	17.69	19.99	26.34	23.77	22.05	16.31
1996	12	14.17	10.82	16.49	20.05	28.45	25.20	22.57	15.25

Year	Month	CtyChnl TrngBsn	TrntyRv Mouth	Cedar Bayou	HSC Morgns	Tabbs Bay	HSC BayTnnl	HSC Junctn	Coolng Pond
1992	1	9.30	0.00	0.69	1.26	1.05	0.54	0.06	0.47
1992	2	8.72	0.00	0.46	1.16	0.98	0.45	0.05	0.44
1992	3	9.74	0.00	0.79	1.52	1.29	0.66	0.08	0.60
1992	4	11.78	0.47	2.15	3.46	3.17	1.56	0.16	2.31
1992	5	13.89	1.80	4.35	6.16	5.82	3.15	0.44	4.82
1992	6	13.04	0.64	2.34	4.04	3.65	1.87	0.22	2.54
1992	7	20.89	4.61	7.53	9.50	8.96	5.44	0.96	7.71
1992	8	22.55	9.61	9.87	12.41	11.76	7.32	1.66	11.16
1992	9	25.27	13.54	13.80	17.40	16.93	13.34	6.59	15.12
1992	10	25.77	16.54	15.68	19.69	19.26	16.19	10.01	17.38
1992	11	24.70	10.51	11.35	17.26	16.59	12.46	5.69	14.65
1992	12	20.88	3.40	8.08	11.57	10.73	6.63	1.40	8.80
1996	1	20.80	7.33	7.73	11.78	11.29	8.68	3.93	9.34
1996	2	23.00	11.32	12.41	15.49	15.05	11.98	6.04	13.43
1996	3	25.03	14.02	13.99	18.08	17.63	14.56	8.42	15.66
1996	4	26.40	13.49	15.76	20.48	20.09	17.21	10.85	17.44
1996	5	26.16	15.77	17.84	21.41	21.17	17.84	10.67	18.91
1996	6	24.00	12.18	13.26	19.78	19.05	15.98	9.27	16.44
1996	7	23.74	11.03	14.25	17.25	16.82	13.38	6.88	15.04
1996	8	25.30	10.50	12.86	18.06	17.54	14.11	7.50	14.98
1996	9	21.78	7.30	7.84	12.37	11.77	8.16	2.84	10.02
1996	10	21.49	8.62	7.73	12.45	11.83	9.24	4.64	9.63
1996	11	22.04	10.50	9.95	15.31	14.80	12.19	7.02	12.49
1996	12	22.59	2.96	8.01	13.98	13.17	10.29	4.88	9.89

Table 8.2 Monthly salinity differences (ppt): existing - no diversion

Year	Month	Upper Galvstn	Trinity Bay	Redfish Reef	East Bay	Chrstms Bay	West Bay	TxCity Dike	OffClr Lake
1992	1	0.01	0.01	0.02	0.02	0.01	0.02	0.02	0.01
1992	2	0.01	0.01	0.01	0.01	0.01	0.00	0.00	0.00
1992	3	0.01	0.02	0.01	0.01	0.00	0.00	0.01	0.00
1992	4	0.04	0.07	0.04	0.02	0.00	0.01	0.02	0.02
1992	5	0.07	0.16	0.07	0.05	0.00	0.02	0.04	0.06
1992	6	0.07	0.11	0.07	0.06	0.01	0.04	0.05	0.05
1992	7	0.11	0.21	0.11	0.08	0.00	0.02	0.06	0.09
1992	8	0.13	0.31	0.14	0.11	0.01	0.06	0.08	0.10
1992	9	0.21	0.37	0.18	0.13	0.01	0.06	0.10	0.17
1992	10	0.19	0.33	0.18	0.14	0.02	0.07	0.11	0.17
1992	11	0.19	0.42	0.19	0.13	0.01	0.06	0.10	0.16
1992	12	0.17	0.28	0.18	0.13	0.02	0.09	0.11	0.14
1996	1	0.16	0.31	0.15	0.10	0.01	0.05	0.08	0.13
1996	2	0.22	0.39	0.21	0.14	0.02	0.06	0.11	0.18
1996	3	0.25	0.44	0.24	0.17	0.03	0.09	0.13	0.21
1996	4	0.30	0.50	0.26	0.17	0.02	0.07	0.13	0.25
1996	5	0.35	0.55	0.29	0.19	0.00	0.04	0.13	0.29
1996	6	0.38	0.66	0.34	0.23	0.01	0.04	0.14	0.32
1996	7	0.38	0.57	0.34	0.26	0.01	0.08	0.17	0.32
1996	8	0.40	0.65	0.36	0.25	0.02	0.08	0.18	0.34
1996	9	0.31	0.51	0.31	0.25	0.03	0.14	0.21	0.28
1996	10	0.22	0.35	0.22	0.17	0.04	0.13	0.14	0.20
1996	11	0.21	0.38	0.20	0.15	0.02	0.07	0.11	0.19
1996	12	0.24	0.41	0.24	0.18	0.02	0.09	0.14	0.21

Year	Month	CtyChnl TrnBasn	TrntyRv Mouth	Cedar Bayou	HSC Morgns	Tabbs Bay	HSC BayTnnl	HSC Junctn	Coolng Pond
1992	1	0.02	0.00	0.00	0.00	0.00	-0.01	0.00	0.01
1992	2	0.01	0.00	0.00	-0.01	0.00	-0.02	0.00	0.01
1992	3	0.00	0.00	0.00	0.00	0.00	-0.02	0.00	0.01
1992	4	0.02	0.06	0.00	0.00	0.00	-0.04	-0.01	0.04
1992	5	0.04	0.26	0.03	0.02	0.02	-0.07	-0.03	0.11
1992	6	0.05	0.09	0.02	0.01	0.02	-0.04	-0.02	0.07
1992	7	0.06	0.58	0.04	0.04	0.04	-0.09	-0.05	0.14
1992	8	0.08	1.11	0.02	0.01	0.00	-0.16	-0.10	0.19
1992	9	0.10	1.34	0.10	0.11	0.10	-0.16	-0.34	0.26
1992	10	0.11	1.18	0.08	0.11	0.09	-0.16	-0.41	0.24
1992	11	0.10	1.21	0.06	0.06	0.05	-0.19	-0.30	0.28
1992	12	0.11	0.38	0.05	0.06	0.05	-0.09	-0.07	0.20
1996	1	0.08	0.92	0.07	0.08	0.08	-0.08	-0.18	0.21
1996	2	0.11	1.25	0.12	0.13	0.13	-0.09	-0.25	0.27
1996	3	0.13	1.39	0.14	0.16	0.15	-0.07	-0.31	0.32
1996	4	0.13	1.43	0.18	0.21	0.21	-0.05	-0.35	0.36
1996	5	0.12	1.63	0.24	0.27	0.28	-0.02	-0.36	0.42
1996	6	0.15	1.78	0.20	0.25	0.26	-0.09	-0.42	0.47
1996	7	0.18	1.31	0.25	0.28	0.28	0.02	-0.22	0.43
1996	8	0.18	1.67	0.19	0.26	0.24	-0.12	-0.42	0.46
1996	9	0.21	1.12	0.12	0.18	0.16	-0.10	-0.19	0.35
1996	10	0.14	0.99	0.09	0.12	0.11	-0.08	-0.24	0.25
1996	11	0.11	1.14	0.09	0.13	0.11	-0.12	-0.34	0.27
1996	12	0.14	0.42	0.08	0.13	0.12	-0.10	-0.25	0.29

Table 8.3 Minimum and maximum salinity differences (ppt): existing - no diversion

Year	Month	Min	node	Max	node
1992	1	-0.02	4197	0.03	1088
1992	2	-0.02	4219	0.02	2748
1992	3	-0.02	4241	0.02	2715
1992	4	-0.04	4219	0.1	3616
1992	5	-0.08	4276	0.27	3803
1992	6	-0.05	4288	0.12	3461
1992	7	-0.11	4291	0.64	4004
1992	8	-0.18	4323	1.46	4075
1992	9	-0.45	4766	1.94	4166
1992	10	-0.56	4801	1.99	4179
1992	11	-0.39	4743	1.33	4003
1992	12	-0.11	4266	0.38	3878
1996	1	-0.25	4773	1.06	4030
1996	2	-0.36	4786	1.64	4075
1996	3	-0.46	4839	1.95	4152
1996	4	-0.56	4845	1.66	4052
1996	5	-0.57	4829	2.11	4100
1996	6	-0.64	4822	1.91	3975
1996	7	-0.35	4849	1.44	4004
1996	8	-0.59	4773	1.77	3975
1996	9	-0.24	4702	1.22	4030
1996	10	-0.33	4815	1.29	4075
1996	11	-0.48	4815	1.46	4100
1996	12	-0.33	4773	0.52	3667

Table 8.4 Monthly salinity differences (ppt): existing - no power

Year	Month	Upper Galvstn	Trinity Bay	Redfish Reef	East Bay	Chrstms Bay	West Bay	TxCity Dike	OffClr Lake
1992	1	0.10	0.04	0.12	0.08	0.03	0.09	0.11	0.19
1992	2	0.09	0.01	0.11	0.09	0.03	0.08	0.09	0.17
1992	3	0.13	0.05	0.15	0.10	0.02	0.08	0.11	0.25
1992	4	0.19	0.00	0.20	0.15	0.03	0.11	0.15	0.28
1992	5	0.17	-0.12	0.16	0.13	0.02	0.09	0.14	0.25
1992	6	0.12	-0.13	0.08	0.04	0.01	0.05	0.07	0.21
1992	7	0.37	-0.03	0.34	0.24	0.01	0.07	0.21	0.51
1992	8	0.27	-0.54	0.23	0.20	0.04	0.15	0.19	0.39
1992	9	-0.04	-0.77	-0.04	0.02	0.02	0.05	0.05	0.05
1992	10	-0.40	-1.31	-0.37	-0.22	-0.01	-0.06	-0.14	-0.30
1992	11	-0.77	-1.97	-0.76	-0.47	-0.04	-0.19	-0.36	-0.72
1992	12	-0.50	-1.11	-0.57	-0.48	-0.08	-0.31	-0.40	-0.41
1996	1	-0.50	-1.13	-0.46	-0.36	-0.06	-0.19	-0.28	-0.39
1996	2	-0.55	-1.24	-0.50	-0.37	-0.05	-0.17	-0.28	-0.43
1996	3	-0.61	-1.48	-0.57	-0.40	-0.05	-0.20	-0.29	-0.50
1996	4	-0.80	-1.63	-0.72	-0.47	-0.06	-0.19	-0.35	-0.71
1996	5	-0.89	-1.65	-0.75	-0.50	-0.03	-0.10	-0.31	-0.81
1996	6	-0.80	-2.15	-0.81	-0.54	-0.02	-0.09	-0.34	-0.83
1996	7	-0.87	-1.80	-0.80	-0.61	-0.03	-0.15	-0.39	-0.75
1996	8	-0.72	-1.66	-0.75	-0.51	-0.04	-0.16	-0.36	-0.78
1996	9	-0.82	-1.94	-0.92	-0.68	-0.09	-0.32	-0.55	-0.85
1996	10	-0.58	-1.33	-0.54	-0.42	-0.12	-0.31	-0.36	-0.41
1996	11	-0.74	-1.61	-0.64	-0.44	-0.06	-0.21	-0.33	-0.58
1996	12	-0.67	-1.24	-0.62	-0.49	-0.07	-0.25	-0.38	-0.53

Year	Month	CtyChnl TrnBasn	TrntyRv Mouth	Cedar Bayou	HSC Morgns	Tabbs Bay	HSC BayTnnl	HSC Junctn	Coolng Pond
1992	1	0.10	0.00	0.36	0.13	0.12	0.06	0.01	0.14
1992	2	0.09	0.00	0.19	0.11	0.11	0.04	0.01	0.01
1992	3	0.11	0.00	0.32	0.16	0.14	0.07	0.01	0.12
1992	4	0.15	0.00	0.85	0.23	0.23	0.11	0.01	-0.20
1992	5	0.14	0.00	1.77	0.26	0.31	0.15	0.02	-0.59
1992	6	0.07	0.00	1.17	0.20	0.26	0.12	0.01	-0.41
1992	7	0.21	0.00	3.15	0.48	0.53	0.30	0.05	-0.47
1992	8	0.20	-0.29	4.11	0.44	0.54	0.30	0.06	-1.79
1992	9	0.05	-0.49	4.34	0.14	0.25	0.18	0.09	-2.04
1992	10	-0.14	-0.95	4.67	-0.18	-0.03	-0.04	-0.01	-2.85
1992	11	-0.36	-0.95	3.36	-0.48	-0.25	-0.23	-0.09	-4.22
1992	12	-0.40	-0.37	3.06	-0.24	-0.07	-0.09	-0.03	-2.02
1996	1	-0.28	-0.68	1.84	-0.35	-0.27	-0.23	-0.10	-2.28
1996	2	-0.28	-0.85	3.73	-0.35	-0.24	-0.22	-0.11	-2.34
1996	3	-0.29	-1.04	3.95	-0.40	-0.28	-0.25	-0.14	-2.95
1996	4	-0.35	-1.00	4.36	-0.58	-0.44	-0.39	-0.22	-3.20
1996	5	-0.31	-1.13	5.49	-0.68	-0.52	-0.46	-0.25	-3.02
1996	6	-0.33	-1.12	5.20	-0.46	-0.05	-0.20	-0.16	-4.66
1996	7	-0.38	-1.12	5.09	-0.59	-0.39	-0.32	-0.14	-2.98
1996	8	-0.36	-0.86	5.06	-0.46	-0.12	-0.21	-0.14	-3.43
1996	9	-0.54	-1.04	3.45	-0.49	-0.15	-0.18	-0.06	-3.77
1996	10	-0.36	-0.89	1.63	-0.37	-0.30	-0.23	-0.11	-2.62
1996	11	-0.32	-1.02	1.82	-0.54	-0.47	-0.39	-0.22	-3.25
1996	12	-0.38	-0.28	1.20	-0.49	-0.43	-0.34	-0.15	-2.51

Table 8.5 Minimum and maximum salinity differences (ppt): existing - no power

Year	Month	Min	node	Max	node
1992	1	0.00	1	1.09	3576
1992	2	-0.02	3944	0.87	3576
1992	3	0.00	1	1.49	3576
1992	4	-0.56	3944	1.03	3576
1992	5	-1.45	3944	1.87	4324
1992	6	-0.86	3944	1.29	4314
1992	7	-1.26	3944	3.22	4333
1992	8	-3.89	3944	4.21	4333
1992	9	-4.37	3944	4.40	4342
1992	10	-5.69	3944	4.74	4342
1992	11	-8.51	3944	3.50	4315
1992	12	-3.44	3944	3.17	4325
1996	1	-4.55	3944	1.92	4325
1996	2	-4.28	3944	3.77	4342
1996	3	-5.67	3944	4.02	4334
1996	4	-6.08	3944	4.44	4334
1996	5	-5.37	3944	5.53	4343
1996	6	-9.01	3944	5.40	4325
1996	7	-4.87	3944	5.15	4342
1996	8	-6.71	3944	5.26	4324
1996	9	-6.75	3944	3.72	4314
1996	10	-5.19	3944	1.70	4333
1996	11	-6.61	3944	1.88	4333
1996	12	-5.07	3944	1.25	4333

Table 8.6 Monthly salinity differences (ppt): existing - Texas City Dike removal

Year	Month	Upper Galvstn	Trinity Bay	Redfish Reef	East Bay	Chrstms Bay	West Bay	TxCity Dike	OffClr Lake
1992	1	0.02	0.01	0.07	0.15	0.58	1.69	2.17	0.04
1992	2	0.02	0.00	0.04	0.11	0.64	1.76	2.27	0.03
1992	3	0.06	0.02	0.14	0.23	0.51	1.69	2.26	0.09
1992	4	0.14	0.09	0.19	0.31	0.42	1.40	2.04	0.16
1992	5	0.21	0.17	0.28	0.35	0.29	1.06	1.81	0.24
1992	6	0.10	0.07	0.15	0.24	0.37	1.27	2.15	0.12
1992	7	0.30	0.24	0.38	0.52	0.25	1.10	3.09	0.33
1992	8	0.30	0.29	0.36	0.46	0.47	1.62	2.39	0.31
1992	9	0.36	0.33	0.40	0.46	0.30	1.11	1.83	0.37
1992	10	0.33	0.31	0.36	0.39	0.26	0.83	1.35	0.34
1992	11	0.29	0.26	0.34	0.36	0.20	0.81	1.48	0.30
1992	12	0.17	0.13	0.24	0.33	0.30	1.26	1.88	0.20
1996	1	0.40	0.32	0.55	0.59	0.29	1.10	2.10	0.45
1996	2	0.55	0.51	0.61	0.62	0.38	1.34	2.15	0.57
1996	3	0.53	0.50	0.59	0.57	0.36	1.25	1.73	0.54
1996	4	0.52	0.49	0.54	0.53	0.27	0.91	1.65	0.52
1996	5	0.41	0.41	0.39	0.39	0.08	0.44	1.34	0.40
1996	6	0.18	0.18	0.17	0.18	0.04	0.25	0.88	0.17
1996	7	0.12	0.11	0.16	0.22	0.11	0.49	1.39	0.13
1996	8	0.17	0.15	0.19	0.24	0.17	0.75	1.86	0.17
1996	9	0.10	0.09	0.13	0.21	0.40	1.40	2.36	0.11
1996	10	0.20	0.16	0.28	0.35	0.56	1.62	2.14	0.23
1996	11	0.37	0.32	0.45	0.47	0.21	0.79	1.36	0.40
1996	12	0.34	0.26	0.42	0.51	0.28	1.24	2.14	0.38

Year	Month	CtyChnl TrnBasn	TrntyRv Mouth	Cedar Bayou	HSC Morgns	Tabbs Bay	HSC BayTnnl	HSC Junctn	Coolng Pond
1992	1	3.07	0.00	0.01	0.02	0.02	0.01	0.00	0.01
1992	2	3.08	0.00	0.00	0.02	0.02	0.00	0.00	0.01
1992	3	3.04	0.00	0.03	0.06	0.05	0.02	0.01	0.03
1992	4	2.77	0.01	0.07	0.12	0.10	0.05	0.01	0.08
1992	5	2.43	0.06	0.14	0.20	0.19	0.08	0.01	0.16
1992	6	2.94	0.01	0.05	0.09	0.07	0.03	0.00	0.06
1992	7	4.06	0.13	0.22	0.29	0.26	0.14	0.02	0.23
1992	8	3.12	0.22	0.21	0.26	0.24	0.13	0.02	0.25
1992	9	2.42	0.27	0.28	0.35	0.33	0.24	0.09	0.30
1992	10	1.78	0.28	0.24	0.32	0.30	0.22	0.11	0.29
1992	11	2.00	0.17	0.17	0.26	0.25	0.16	0.06	0.23
1992	12	2.55	0.05	0.09	0.15	0.12	0.06	0.00	0.12
1996	1	2.75	0.22	0.24	0.38	0.35	0.24	0.09	0.28
1996	2	2.70	0.39	0.43	0.53	0.51	0.38	0.17	0.47
1996	3	2.19	0.41	0.40	0.52	0.49	0.39	0.20	0.45
1996	4	2.07	0.35	0.40	0.51	0.50	0.42	0.25	0.44
1996	5	1.68	0.32	0.35	0.41	0.41	0.33	0.18	0.38
1996	6	1.16	0.12	0.13	0.17	0.17	0.13	0.07	0.16
1996	7	1.86	0.07	0.10	0.11	0.11	0.06	0.00	0.11
1996	8	2.45	0.10	0.11	0.16	0.15	0.10	0.03	0.13
1996	9	3.10	0.05	0.04	0.08	0.07	0.02	0.00	0.07
1996	10	2.82	0.13	0.11	0.19	0.17	0.12	0.05	0.14
1996	11	1.83	0.24	0.23	0.36	0.34	0.26	0.13	0.28
1996	12	2.79	0.07	0.18	0.34	0.30	0.21	0.08	0.23

Table 8.7 Minimum and maximum salinity differences (ppt): existing - Texas City Dike removal

Year	Month	Min	node	Max	node
1992	1	-0.07	223	3.25	2677
1992	2	-0.13	495	3.24	2677
1992	3	-0.07	562	3.20	2677
1992	4	-0.02	40	2.92	2677
1992	5	-0.02	494	2.56	2677
1992	6	-0.01	562	3.10	2677
1992	7	0.00	1	4.25	2677
1992	8	0.00	1	3.27	2677
1992	9	-0.01	418	2.55	2677
1992	10	0.00	1	1.87	2677
1992	11	-0.01	40	2.11	2677
1992	12	-0.01	4725	2.68	2677
1996	1	-0.01	78	2.89	2677
1996	2	0.00	1	2.81	2677
1996	3	0.00	1	2.29	2677
1996	4	0.00	1	2.15	2677
1996	5	-0.04	223	1.75	2677
1996	6	0.00	1	1.21	2677
1996	7	-0.01	562	1.95	2677
1996	8	-0.09	2503	2.57	2677
1996	9	-0.10	2503	3.25	2677
1996	10	0.00	1	2.96	2677
1996	11	-0.03	41	1.93	2677
1996	12	0.00	1	2.92	2677

Table 8.8 Monthly salinity differences (ppt): existing - HSC removal

Year	Month	Upper Galvstn	Trinity Bay	Redfish Reef	East Bay	Chrstms Bay	West Bay	TxCity Dike	OffClr Lake
1992	1	0.41	0.10	0.37	0.24	-0.34	1.20	1.50	0.43
1992	2	0.37	0.08	0.25	-0.02	-0.58	0.94	1.64	0.33
1992	3	0.47	0.13	0.41	0.22	-0.26	0.80	1.58	0.50
1992	4	0.95	0.44	0.43	-0.07	-0.45	0.46	1.17	0.74
1992	5	1.80	1.12	1.11	0.49	-0.23	0.52	1.48	1.50
1992	6	1.49	0.81	1.04	0.62	-0.34	0.59	1.77	1.35
1992	7	1.45	0.98	0.49	-0.23	-0.23	-0.09	1.51	1.05
1992	8	1.78	1.56	0.62	0.04	-0.26	0.34	1.17	1.23
1992	9	0.09	0.14	-0.41	-0.62	-0.32	-0.16	0.33	-0.11
1992	10	-0.92	-0.79	-1.03	-0.87	-0.25	-0.28	-0.18	-0.96
1992	11	0.02	-0.40	-0.67	-0.76	-0.32	-0.13	0.05	-0.32
1992	12	1.22	0.52	0.33	-0.15	-0.26	0.24	0.94	0.81
1996	1	-0.73	-0.59	-1.37	-1.38	-0.51	-0.91	-0.68	-1.01
1996	2	-1.16	-1.11	-1.51	-1.44	-0.48	-0.46	-0.34	-1.30
1996	3	-1.28	-1.17	-1.65	-1.43	-0.37	-0.45	-0.58	-1.42
1996	4	-1.34	-1.37	-1.46	-1.29	-0.31	-0.40	-0.31	-1.37
1996	5	0.01	-0.15	-0.18	-0.31	-0.10	0.07	0.58	-0.04
1996	6	0.73	0.38	0.40	0.18	-0.04	0.22	0.80	0.55
1996	7	0.80	0.77	0.42	0.21	-0.15	0.16	0.93	0.65
1996	8	0.32	0.20	-0.15	-0.29	-0.22	0.09	0.90	0.10
1996	9	0.62	0.28	-0.29	-0.63	-0.64	-0.01	0.80	0.21
1996	10	-1.09	-0.85	-1.73	-1.63	-0.70	-0.72	-0.56	-1.35
1996	11	-1.28	-1.25	-1.58	-1.40	-0.40	-0.79	-0.77	-1.39
1996	12	-0.76	-0.68	-1.36	-1.40	-0.41	-0.61	-0.19	-1.06

Year	Month	CtyChnl TrngBsn	TrntyRv Mouth	Cedar Bayou	HSC Morgns	Tabbs Bay	HSC BayTnnl	HSC Junctn	Coolng Pond
1992	1	9.30	0.00	0.69	1.26	1.05	0.54	0.06	0.47
1992	2	8.72	0.00	0.46	1.16	0.98	0.45	0.05	0.44
1992	3	9.74	0.00	0.79	1.52	1.29	0.66	0.08	0.60
1992	4	11.78	0.47	2.15	3.46	3.17	1.56	0.16	2.31
1992	5	13.89	1.80	4.35	6.16	5.82	3.15	0.44	4.82
1992	6	13.04	0.64	2.34	4.04	3.65	1.87	0.22	2.54
1992	7	20.89	4.61	7.53	9.50	8.96	5.44	0.96	7.71
1992	8	22.55	9.61	9.87	12.41	11.76	7.32	1.66	11.16
1992	9	25.27	13.54	13.80	17.40	16.93	13.34	6.59	15.12
1992	10	25.77	16.54	15.68	19.69	19.26	16.19	10.01	17.38
1992	11	24.70	10.51	11.35	17.26	16.59	12.46	5.69	14.65
1992	12	20.88	3.40	8.08	11.57	10.73	6.63	1.40	8.80
1996	1	20.80	7.33	7.73	11.78	11.29	8.68	3.93	9.34
1996	2	23.00	11.32	12.41	15.49	15.05	11.98	6.04	13.43
1996	3	25.03	14.02	13.99	18.08	17.63	14.56	8.42	15.66
1996	4	26.40	13.49	15.76	20.48	20.09	17.21	10.85	17.44
1996	5	26.16	15.77	17.84	21.41	21.17	17.84	10.67	18.91
1996	6	24.00	12.18	13.26	19.78	19.05	15.98	9.27	16.44
1996	7	23.74	11.03	14.25	17.25	16.82	13.38	6.88	15.04
1996	8	25.30	10.50	12.86	18.06	17.54	14.11	7.50	14.98
1996	9	21.78	7.30	7.84	12.37	11.77	8.16	2.84	10.02
1996	10	21.49	8.62	7.73	12.45	11.83	9.24	4.64	9.63
1996	11	22.04	10.50	9.95	15.31	14.80	12.19	7.02	12.49
1996	12	22.59	2.96	8.01	13.98	13.17	10.29	4.88	9.89

Table 8.9 Minimum and maximum salinity differences (ppt): existing - HSC removal

Year	Month	Min	node	Max	node
1992	1	-0.84	1172	2.74	2677
1992	2	-1.06	1172	2.75	2677
1992	3	-0.53	1171	2.63	2677
1992	4	-0.77	1172	2.15	2677
1992	5	-0.47	1172	3.34	4022
1992	6	-0.63	1172	2.85	2677
1992	7	-1.25	2417	4.22	4174
1992	8	-0.95	2503	4.53	4174
1992	9	-1.24	2503	2.20	4291
1992	10	-1.26	2503	0.92	4861
1992	11	-1.16	2503	3.24	4218
1992	12	-0.68	2503	4.13	4185
1996	1	-2.07	2503	1.38	4302
1996	2	-2.07	2503	1.34	4702
1996	3	-1.92	2503	1.28	4787
1996	4	-1.61	2503	1.36	4835
1996	5	-0.62	2503	2.09	4709
1996	6	-0.11	1171	2.94	4241
1996	7	-0.39	2417	2.11	4298
1996	8	-1.01	2417	2.99	4266
1996	9	-1.58	2503	3.83	4264
1996	10	-2.51	2503	1.16	4716
1996	11	-1.74	2503	1.32	4759
1996	12	-1.99	2503	1.74	4288

Table 8.10 Monthly salinity differences (ppt): existing - natural

Year	Month	Upper Galvstn	Trinity Bay	Redfish Reef	East Bay	Chrstms Bay	West Bay	TxCity Dike	OffClr Lake
1992	1	0.47	0.11	0.46	0.30	-0.32	1.27	1.58	0.59
1992	2	0.43	0.09	0.34	0.05	-0.56	1.01	1.73	0.48
1992	3	0.56	0.15	0.53	0.29	-0.25	0.87	1.68	0.73
1992	4	1.07	0.38	0.58	0.05	-0.43	0.56	1.31	0.99
1992	5	1.90	0.93	1.23	0.58	-0.22	0.59	1.59	1.72
1992	6	1.56	0.68	1.11	0.66	-0.33	0.64	1.84	1.57
1992	7	1.74	0.84	0.78	-0.03	-0.22	-0.02	1.73	1.56
1992	8	1.80	0.84	0.69	0.12	-0.24	0.43	1.28	1.48
1992	9	-0.14	-0.60	-0.54	-0.67	-0.31	-0.16	0.32	-0.18
1992	10	-1.47	-2.01	-1.44	-1.11	-0.26	-0.36	-0.36	-1.38
1992	11	-0.90	-2.25	-1.43	-1.20	-0.36	-0.32	-0.33	-1.16
1992	12	0.63	-0.62	-0.26	-0.61	-0.32	-0.04	0.56	0.35
1996	1	-1.23	-1.53	-1.74	-1.65	-0.54	-1.03	-0.88	-1.36
1996	2	-1.72	-2.17	-1.94	-1.72	-0.50	-0.59	-0.57	-1.73
1996	3	-1.93	-2.47	-2.14	-1.74	-0.41	-0.60	-0.82	-1.93
1996	4	-2.08	-2.69	-2.05	-1.65	-0.34	-0.55	-0.62	-2.02
1996	5	-0.78	-1.51	-0.81	-0.72	-0.12	-0.02	0.28	-0.75
1996	6	-0.04	-1.26	-0.29	-0.27	-0.06	0.12	0.45	-0.21
1996	7	-0.01	-0.70	-0.27	-0.29	-0.17	0.03	0.56	-0.01
1996	8	-0.31	-0.95	-0.69	-0.62	-0.23	-0.01	0.63	-0.54
1996	9	-0.23	-1.41	-1.08	-1.15	-0.68	-0.24	0.34	-0.58
1996	10	-1.67	-1.99	-2.16	-1.93	-0.75	-0.91	-0.80	-1.71
1996	11	-2.06	-2.67	-2.13	-1.74	-0.42	-0.92	-1.05	-1.98
1996	12	-1.45	-1.67	-1.89	-1.78	-0.45	-0.79	-0.50	-1.57

Year	Month	CtyChnl TrnBasn	TrntyRv Mouth	Cedar Bayou	HSC Morgns	Tabbs Bay	HSC BayTnnl	HSC Junctn	Coolng Pond
1992	1	2.61	0.00	0.54	0.70	0.67	0.49	0.06	0.22
1992	2	2.66	0.00	0.33	0.63	0.62	0.40	0.05	0.09
1992	3	2.56	0.00	0.55	0.81	0.77	0.57	0.08	0.23
1992	4	2.12	0.12	1.47	1.68	1.79	1.39	0.16	0.18
1992	5	2.31	0.51	2.90	2.84	3.04	2.64	0.42	0.48
1992	6	2.73	0.21	1.73	2.11	2.16	1.59	0.21	0.44
1992	7	2.86	0.91	4.49	2.96	3.29	3.86	0.87	0.38
1992	8	2.10	1.58	5.40	2.96	3.33	4.02	1.04	-0.40
1992	9	0.91	0.73	4.47	0.29	0.46	0.93	0.54	-1.87
1992	10	0.01	-0.57	4.01	-1.34	-1.26	-1.65	-1.98	-3.56
1992	11	0.13	-0.08	3.55	0.26	0.71	1.87	0.62	-4.55
1992	12	1.26	0.06	4.08	2.16	2.55	3.49	0.90	-1.52
1996	1	-0.22	-0.13	1.67	-0.79	-0.57	0.17	0.20	-2.68
1996	2	-0.07	-0.43	3.22	-1.37	-1.17	-0.55	-0.33	-3.29
1996	3	-0.46	-0.64	3.31	-1.62	-1.45	-1.23	-1.18	-3.96
1996	4	-0.28	-0.50	3.68	-1.82	-1.63	-1.69	-1.79	-4.30
1996	5	0.58	0.27	5.70	-0.38	-0.15	-0.10	-0.44	-2.92
1996	6	0.71	0.89	5.47	0.61	1.01	1.21	-0.03	-3.81
1996	7	1.03	0.62	5.67	0.40	0.62	0.80	0.24	-1.89
1996	8	1.23	0.95	5.31	0.20	0.60	1.08	0.41	-2.75
1996	9	1.11	0.21	3.83	0.95	1.49	2.86	1.44	-3.24
1996	10	-0.15	-0.56	1.22	-1.29	-1.15	-0.51	-0.29	-3.26
1996	11	-0.67	-0.77	1.19	-1.72	-1.61	-1.23	-1.05	-4.35
1996	12	0.11	-0.01	1.01	-0.94	-0.70	0.30	0.17	-2.99

Table 8.11 Minimum and maximum salinity differences (ppt): existing - natural

Year	Month	Min	node	Max	node
1992	1	-0.82	1172	2.82	2677
1992	2	-1.04	1172	2.84	2677
1992	3	-0.51	1171	2.74	2677
1992	4	-0.74	1172	2.29	2677
1992	5	-0.45	1172	3.31	4022
1992	6	-0.62	1172	2.92	2677
1992	7	-1.01	2417	4.74	4314
1992	8	-2.50	3944	5.67	4315
1992	9	-4.20	3944	4.54	4333
1992	10	-6.40	3944	4.04	4351
1992	11	-8.84	3944	3.73	4324
1992	12	-2.94	3944	4.35	4314
1996	1	-4.95	3944	1.73	4334
1996	2	-5.23	3944	3.24	4351
1996	3	-6.68	3944	3.34	4343
1996	4	-7.18	3944	3.72	4343
1996	5	-5.27	3944	5.76	4343
1996	6	-8.17	3944	5.70	4325
1996	7	-3.78	3944	5.76	4334
1996	8	-6.03	3944	5.55	4324
1996	9	-6.22	3944	4.20	4303
1996	10	-5.83	3944	1.24	4334
1996	11	-7.71	3944	1.20	4343
1996	12	-5.55	3944	1.04	4333

Table 8.12 Simulated average daily salinity (ppt)

	Existing		NoDiversion		NoPower		DikeRemoval		HSCrmvl		Natural	
location	mean	std	mean	std	mean	std	mean	std	mean	std	mean	std
HSCBayTunnel	7.74	4.88	7.79	4.90	7.65	4.99	7.59	4.81	6.11	5.47	6.52	5.84
TrinityBay	8.84	5.73	8.64	5.63	9.37	6.26	8.65	5.63	8.92	6.17	9.44	6.65
upprGalvestn	10.83	5.67	10.71	5.61	10.88	5.91	10.59	5.57	10.71	6.30	10.83	6.56
offClearLake	11.54	5.53	11.44	5.48	11.50	5.78	11.28	5.44	11.61	6.17	11.60	6.43
midGalvestn	12.75	5.70	12.64	5.65	12.82	5.93	12.45	5.61	13.10	6.33	13.18	6.55
EastBay	15.77	5.29	15.68	5.26	15.81	5.44	15.40	5.23	16.30	5.78	16.35	5.91
offTxCtyChnl	18.48	5.09	18.41	5.07	18.49	5.19	16.53	5.30	17.93	5.84	17.95	5.94
WestBay	21.31	4.69	21.27	4.68	21.31	4.73	20.13	4.82	21.35	5.14	21.36	5.18
ChristmasBay	25.01	4.13	25.00	4.13	25.01	4.14	24.68	4.13	25.34	4.22	25.34	4.22

Differences: existing - scenario case

	NoDiversion		NoPower		DikeRemoval		HSCrmvl		Natural	
location	mean	std	mean	std	mean	std	mean	std	mean	std
HSCBayTunnel	-0.05	-0.02	0.09	-0.11	0.15	0.07	1.63	-0.59	1.22	-0.96
TrinityBay	0.20	0.10	-0.53	-0.53	0.19	0.10	-0.08	-0.44	-0.60	-0.92
upprGalvestn	0.12	0.06	-0.05	-0.24	0.24	0.10	0.12	-0.63	0.00	-0.89
offClearLake	0.10	0.05	0.04	-0.25	0.26	0.09	-0.07	-0.64	-0.06	-0.90
midGalvestn	0.11	0.05	-0.07	-0.23	0.30	0.09	-0.35	-0.63	-0.43	-0.85
EastBay	0.09	0.03	-0.04	-0.15	0.37	0.06	-0.53	-0.49	-0.58	-0.62
offTxCtyChnl	0.07	0.02	-0.01	-0.10	1.95	-0.21	0.55	-0.75	0.53	-0.85
WestBay	0.04	0.01	0.00	-0.04	1.18	-0.13	-0.04	-0.45	-0.05	-0.49
ChristmasBay	0.01	0.00	0.00	-0.01	0.33	0.00	-0.33	-0.09	-0.33	-0.09

9. CONCLUSIONS

The purpose of the Galveston Bay Modeling Project is to study the effect of structures and practices on the circulation and salinity in Galveston Bay. Five Cases were studied: the *no diversion* case examined the effect of diversions from the Trinity River to the San Jacinto River; the *no power* case examined the effect of power plant withdrawal and discharge of bay water for cooling; the *Texas City Dike removal* case examined the effect of the Texas City Dike; the Houston Ship Channel (HSC) *removal* case examined the effect of the Houston Ship Channel; and the *natural* case examined the condition in which all these practices and structures are removed.

TxBLEND-2D model was used to simulate the circulation and salinity pattern in Galveston Bay. The model was run to simulate the eight years from 1989 to 1996. The results of simulations for the 1992 wet period and the 1996 dry period were closely examined by comparing the scenario cases with the existing condition. Residual water velocity vectors were computed to see the net movement of the bay water. Net flows through sections and passes were computed to find the major pathways of freshwater through the bay system.

Total annual freshwater inflow is 17.0 million ac-ft on average over the eight year period, of which 5% goes through Rollover Pass, 20% through San Luis Pass and 75% through the entrance channel to the Gulf. About 92% of freshwater flows down to Bolivar Roads, then 9% goes to West Bay through the Texas City Dike section (mainly the City Channel) and 8% through Galveston Channel. These latter two make up the 17% that goes through West Bay.

The residual vectors for the existing condition indicate that the HSC serves as a main conveyor of Gulf water into Galveston Bay and the upper HSC area. That is, the HSC brings in more Gulf water than it sends bay water Gulf-ward. As a result more salt is brought into the bay and to the upper HSC area by the ship channel.

The effect of diversion between river basins on circulation is minimal because of its relatively small volume (624 thousand ac-ft was diverted on average over 1990-2000 out of 9.4 million ac-ft total inflow from Trinity River to the bay, roughly 7%). The diversion's effect on salinity is insignificant during the wet period of simulation. During the dry period, it has more of an influence but it is still mostly local. The *no diversion* case reduces salinity by 2 ppt near the mouth of Trinity River and by 0.7 ppt in Trinity Bay, but raises salinity by 0.6 ppt in the upper HSC area (these salinity differences are given on a monthly average basis, while the percent differences in the net flow are compared to the total annual inflow).

The *no power* case reduces the flow in the mid section (Eagle Point-Smith Point section) by 7%, but the impact on the entrance channel, San Luis Pass, and Rollover Pass is minimal. The power plant operation has a salinity-leveling effect by promoting the

mixing of bay water in withdrawing and discharging the cooling water. This leveling is more effective during dry periods than wet periods. During wet periods it mostly affects the water intake and discharge sites and their vicinity. In Trinity Bay the reduction in salinity is nearly zero but in the mid-Galveston Bay near Redfish Reef and off Clear Lake salinity will be about 0.5 ppt lower. The effect is more pronounced during dry periods, when the salinity in Trinity Bay will be higher by 2.5 ppt and in Galveston Bay by 1 ppt.

Contrary to expectations, the flow in West Bay will not increase noticeably if the Texas City Dike is removed. However, its composition will be changed. In the *dike removal* case, the net flow through the entrance channel will be reduced by 1% and the net flow through West Bay, San Luis Pass, and Rollover Pass will increase by 0.6%. The composition of the West Bay flow will change from 8% Galveston Channel and 9% Texas City Dike section for the existing condition to 7% Galveston Channel and 11% Galveston Bay for the dike removal case. The removal of Texas City Dike has an effect on salinity in both wet and dry periods. The major effect occurs in and near the Texas City Ship Channel and in West Bay. Salinity in the turning basin will be lower by 4 ppt and in the mid West Bay by 2 ppt. Salinity in Galveston Bay and Trinity Bay will be lower by 0.6 ppt.

The *removal of the Houston Ship Channel* will increase net flow through the entrance channel by 5%, decrease the West Bay and San Luis Pass by 4%, and decrease Rollover Pass by 1.5%. Because more Gulf water is carried to upper estuary through the HSC it also acts as a salinity-leveling device. Without the HSC, low salinity during wet periods lasts longer and high salinity during dry periods tends to get higher. The removal of the HSC will mostly affect the upper Galveston Bay and upper HSC area. During a wet period, salinity will be lower by as much as 4 ppt near the Bay Tunnel and by 3 ppt near Morgan's Point, and it will be 1 to 2 ppt lower in Galveston Bay and Trinity Bay. During a dry period, salinity will be 1 to 2 ppt higher in both Galveston Bay and Trinity Bay.

The *natural* case brings back the Galveston Bay system to a state where human activities are no longer a factor. This includes removing the impacts due to the salinity-leveling mechanisms of power plant operation and the ship channel, as well as removing the Texas City Dike and stopping diversion of river flows. The combined effects resulted in the largest reduction or rise in salinity compared to existing conditions. As in the HSC removal case, salinity is as much as 4 ppt lower near the Bay Tunnel; 3 ppt lower near Morgan's Point and 1 to 2 ppt lower in Galveston Bay and Trinity Bay during wet periods. But during dry periods, salinity is higher than shown in the HSC removal case. Under the natural scenario, salinities are 2 to 3 ppt higher in Galveston Bay and Trinity Bay than under existing conditions.

10. REFERENCES

Berger, R.C., R.T. McAdory, W.D. Martin, J.H., Schmidt, Houston-Galveston Navigation Channels, Texas Project, Report 3, Three-Dimensional Hydrodynamic Model Verification, US Army Corps of Engineers, Waterways Experiment Station, 1995.

Brandes, R.J., Masch, F.D., Tidal Hydrodynamic and Salinity Models for San Antonio and Matagorda Bays, Texas, F.D. Masch and Associates, 1971.

Brandes, R.J., Masch, F.D., Tidal Hydrodynamic and Salinity Models for Coastal Bays—Evaporation Consideration, F.D. Masch and Associates, 1972.

Espey, W.H., A.J. Hays, Jr., W.D. Bergman, J.P. Buckner, R.J. Huston, G.H. Ward, Jr., Galveston Bay Project, Water Quality Modeling and Data Management, Phase II Technical Progress Report, Submitted to Texas Water Quality Board, 1971.

Fischer, H.B. (Ed.), Mixing in Inland and Coastal Waters, Academic Press, 1980.

Ippen, A.T. (Ed.), Estuary and Coastal Hydrodynamics, McGraw-Hill, 1966

Kinmark, I.P.E., The Shallow Water Equations: Formulation, Analysis, and Application, Lecture Notes in Engineering, Springer-Verlag, 15, 1986.

Kolar, R.L., Gray, W.G., Westerink, J.J., An Analysis of Mass Conserving Properties of the Generalized Wave Continuity Equation, Computational Methods in Water Resources IX, Russell et al (eds) Computational Mechanics Publications/Elsevier Applied Science, 537-544, 1992.

Longley, W.L.(ed), Freshwater Inflows to Texas Bays and Estuaries: Ecological Relationships and Methods for Determination of Needs. Prepared by Texas Water Development Board and Texas Parks and Wildlife Department. Published by Texas Water Development Board, 1994.

Lynch, D.R., and Gray, W.G., A Wave Equation Model for Finite Element Tidal Computations, Computers and Fluids, 7, 3:207-228, 1979.

Masch, F.D., N.J. Shankar, M. Jeffrey, R.J. Brandes, W.A. White, A Numerical Model for the Simulation of Tidal Hydrodynamics in Shallow Irregular Esturies, Hydraulic Enginnering Laboratory, Department of Civil Engineering, The University of Texas, 1969.

Matsumoto, J., Powell, G.L., Longley, W.L., Brock, D.A., Effects of Structures and Practices on the Circulation and Salinity Patterns of the Corpus Christi Bay National Estuary Program Study Area, Corpus Christi Bay National Estuary Program, CCBNEP-19, 1997.

Matsumoto, J., User's manual for the Texas Water Development Board's hydrodynamic and salinity model, TxBLEND. Texas Water Development Board, 1993.

Matsumoto, J., User's manual for the Texas Water Development Board's Rainfall-Runoff Model, TxRR. Texas Water Development Board, 1992.

Officer, C.B., Physical Oceanography of Estuaries, John Wiley & Sons, 1976.

Reid, R.O., B.R. Bodine, Numerical Model for Storm Surges in Galveston Bay, Journal of the Waterways and Harbors Division, Proceeding of the ASCE, pp33-57, 1968.

Schmalz, Jr., R.A., Development of a Nowcast/Forecast System for Galveston Bay, Estuarine and Coastal Modeling, Proceedings of the fifth international conference, 1997.

Solis, Ruben, Calibration of a Circulation and Salinity Transport Model for Galveston Bay, Texas Water Development Board staff report, 1994.

Texas Department of Water Resources, Trinity-San Jacinto Estuary: An Analysis of Bay Segment Boundaries, Physical Characteristics, and Nutrient Processes, LP-86, 1982.

Texas Department of Water Resources, Trinity-San Jacinto Estuary: A Study of the Influence of Freshwater Inflows, LP-113, 1981.

Texas Parks and Wildlife Department, Freshwater Inflow Recommendation for the Trinity-San Jacinto Estuary of Texas, 2001.

Wang, Keh-Han, Study of the Circulatory Change and Alteration of Salinity in Galveston Bay by Using a Three-Dimensional Hydrodynamic and Transport Modeling, Department of Civil and Environmental Engineering, University of Houston, 1993.

APPENDIX I. TxBLEND MODEL

TxBLEND is a two dimesional finite element model for simulating water circulation and salinity conditions in estuaries, based on the generalized wave continuity equation (Lynch and Gray 1979, Kinmark 1986, Kolar et al 1992) with linear triangular elements. TxBLEND is also capable of simulating an inundation and dewatering or wetting and drying process. There are three major partial differential equations solved numerically by the model. They are the continuity equation, the momentum equation, and the convective-diffusion equation or the conservative transport equation. The following explains how these equations are solved. A complete description of the model can be found in the user's manual (Matsumoto 1993).

Continuity Equation

The generalized wave continuity equation can be written as (Kinnmark 1986, Kolar et al 1992)

$$\frac{\partial^2 \zeta}{\partial t^2} + G\frac{\partial \zeta}{\partial t} - \nabla \bullet \left\{ \nabla \bullet (H\mathbf{V}\mathbf{V}) + gH\nabla\zeta + \frac{gH^2}{2\rho}\nabla\rho + \mathbf{f} \times H\mathbf{V} - H\mathbf{A} \right\}$$
$$+(G-\tau)\nabla \bullet (H\mathbf{V}) - H\mathbf{V} \bullet \nabla\tau = G \cdot (r-e) \qquad \text{(A.1)}$$

where ζ is the water surface elevation above reference level; H is the total depth and equal to $h+\zeta$, h is the bathymetry; $\boldsymbol{V}$ is the velocity vector consisting of u and v; u is the x-component velocity; v is the y-component velocity; g is the gravitational acceleration; ρ is the density; f is the Coriolis parameter; τ is the bottom friction parameter--computed by $(g \cdot n^2 \cdot \sqrt{u^2+v^2})/(2.208 \cdot H^{4/3})$; n is Manning's roughness coefficient; $\boldsymbol{A}$ represents the wind stress vector consisting of A_x and A_y, where $A_x = (K \cdot V_w^2 \cdot \cos\alpha)/H$ and $A_y = (K \cdot V_w^2 \cdot \sin\alpha)/H$, in which K is the wind stress coefficient; V_w is the wind speed; α is the wind direction; r is the precipitation; and e is the evaporation. The parameter G in (A.1) is referred to as bigG in TxBLEND. This is a nonphysical parameter and represents the degree by which the primitive continuity equation is reflected in the wave continuity equation. The larger the bigG, the more the primitive continuity equation is incorporated, but also the more the oscillative nature of the primitive equation is manifest. The smaller the bigG, the smoother the solution may become, but enforcement of continuity may become weaker. The actual value of bigG depends on the application and is usually determined by test runs.

In TxBLEND the nonlinear term in the wave continuity equation is assumed negligible. The weighted residual form of Equation (A.1) becomes

$$\int_\Omega \left(\frac{\partial^2\zeta}{\partial t^2} + G\frac{\partial\zeta}{\partial t}\right)\cdot\phi_i\cdot dA + \int_\Omega \left(gH\nabla\zeta + \frac{gH^2}{2\rho}\nabla\rho + \mathbf{f}\times H\mathbf{V} - H\mathbf{A}\right)\cdot\nabla\phi_i\cdot dA$$
$$+\int_\Omega \{(G-\tau)\nabla\bullet(H\mathbf{V}) - H\mathbf{V}\bullet\nabla\tau\}\cdot\phi_i\cdot dA = -\int_\Gamma \left(\frac{\partial H\mathbf{V}}{\partial t} + \tau H\mathbf{V}\right)\bullet\mathbf{n}\phi_i\, ds \qquad \text{(A.2)}$$

where Ω represents the domain, Γ the boundary, and ϕ_i is the basis function for a linear triangular element--expressed as $\phi_i = a_i + b_i x + c_i y$ (Pinder and Gray 1977). The second integral in (A.2) is the gravity term to which Green's formula for integration by parts was applied to reduce the second order derivative to first order derivative. The right hand side of (A.2) is the boundary integral which is zero except at an inflow point where it is evaluated by $0.5\cdot(\partial Q/\partial t + \tau Q)$. After spatial discretization, the numerical equation can be written for node-*i* of element-*e* consisting of nodes *i*, *j*, and *k* as

$$\sum_{e\in EL_i}\left(\frac{\partial^2\zeta}{\partial t^2} + G\frac{\partial\zeta}{\partial t}\right)\frac{A_e}{3} + (Gravity) + \sum_{e\in EL_i}\{(G-\tau)_i\,(DQXDX_e + DQXDY_e\}\frac{A_e}{3}$$
$$-\sum_{e\in EL_i}(DTAUDX_e\cdot QX_i + DTAUDY_e\cdot QY_i)\frac{A_e}{3} = 0 \qquad \text{(A.3)}$$

where A_e is the element area, EL_i is the set containing the element number surrounding node *i*, $DQXDX_e$, etc. represent the computed values for $\partial q_x/\partial x$, etc. (note $Hu = q_x$). In (A.3) the time derivative term is lumped and the gravity term is treated specially. The gravity term is divided into two parts (Lynch and Gray, 1979), one associated with the bathymetry and the other with the water surface elevation:

$$gH\nabla\zeta \approx w\cdot gH_{t+\Delta t}\cdot\nabla\zeta_{t+\Delta t} + (1-w)\cdot gH_t\cdot\nabla\zeta_t$$
$$= w\cdot gh\cdot\nabla\zeta_{t+\Delta t} + w\cdot g\zeta_{t+\Delta t}\cdot\nabla\zeta_{t+\Delta t} + (1-w)\cdot g(h+\zeta)_t\cdot\nabla\zeta_t \qquad \text{(A.4)}$$

where *w* represents the weight, 1 being a totally implicit scheme; *t* is the current time level and $t+\Delta t$ is the future time level. The gravity term associated with the bathymetry is integrated as follows.

$$\int_\Omega gh\nabla\zeta\cdot\nabla\phi\, dA = \sum_{e\in EL_i}\int_{\Omega_e} gh\nabla\zeta\cdot\nabla\phi\, dA = \sum_{e\in EL_i}\int_{\Omega_e} gh\left(\frac{\partial\zeta}{\partial x}\frac{\partial\phi_i}{\partial x} + \frac{\partial\zeta}{\partial y}\frac{\partial\phi_i}{\partial y}\right) dA$$
$$\approx \sum_{e\in EL_i}\int_{\Omega_e} g\left(\sum_{j\in ND_e} h_j\phi_j\right)\left\{\left(\sum_{j\in ND_e}\zeta_j\, b_j\right)\cdot b_i + \left(\sum_{j\in ND_e}\zeta_j\, c_j\right)\cdot c_i\right\} dA$$
$$= \sum_{e\in EL_i} g\cdot smh_e\cdot\left\{\left(\sum_{j\in ND_e}\zeta_j\, b_j\right)\cdot b_i + \left(\sum_{j\in ND_e}\zeta_j\, c_j\right)\cdot c_i\right\}\frac{A_e}{3} \qquad \text{(A.5)}$$

where Ω_e represents the element *e*, ND_e is the set containing the node numbers that constitutes element *e*, and smh_e is the elemental sum of the bathymetries.

The time derivative term can be discretized by central differences as

$$(\zeta_{t+\Delta t} - 2\zeta_t + \zeta_{t-\Delta t})/\Delta t^2 + G\cdot(\zeta_{t+\Delta t} - \zeta_{t-\Delta t})/2\Delta t \qquad \text{(A.6)}$$

which is termed here the three-time level scheme. The two-time level scheme which is adopted in TxBLEND uses the present and future time levels for the first order derivative:

$$(\zeta_{t+\Delta t} - 2\zeta_t + \zeta_{t-\Delta t})/\Delta t^2 + G\cdot(\zeta_{t+\Delta t} - \zeta_t)/\Delta t \qquad \text{(A.7)}$$

Because TxBLEND internally iterates twice, the time derivative term can be positioned at the half time step into the future, $t + \Delta t/2$, at the second internal iteration as in the two-time level scheme (A.7). This positioning improved the numerical accuracy and stability in test examples.

After multiplying (A.7) by Δt^2, the time derivative term and the gravity term of (A.5) associated with the water surface elevation of the future time level are combined to form the left hand side of the numerical equation. This is equivalent to the nonzero element of the coefficient matrix, expressed by

$$\left\{(1 + G\cdot\Delta t) + \Delta t^2 \cdot g \cdot smh_e \cdot (b_i b_j + c_i c_j)\right\}\frac{A_e}{3} \qquad \text{(A.8)}$$

for the main diagonal element; for the off diagonal element, the $(1 + G\cdot\Delta t)$ term is dropped.

The remaining part of the gravity term and the time derivative term are shifted to the right hand side. They are:

$$\left\{(2 + G\cdot\Delta t)\zeta_t - \zeta_{t-\Delta t}\right\}\frac{A_e}{3} - (1-w)\Delta t^2 \cdot g \cdot smH_{e,t}\cdot(DZDX_e \cdot b_i + DZDY_e \cdot c_i)_t \cdot \frac{A_e}{3}$$
$$+ w\cdot\Delta t^2 \cdot g \cdot smz_{e,t+\Delta t}\cdot(DZDX_e \cdot b_i + DZDY_e \cdot c_i)_{t+\Delta t} \cdot \frac{A_e}{3} \qquad \text{(A.9)}$$

where $smH_{e,t}$ is the elemental sum of total depths at time *t*, and $smz_{e,t+\Delta t}$ is the elemental sum of the water surface elevations at time $t + \Delta t$ --which are unknown, so approximations are used. The right-hand-side of the numerical equation for the wave continuity equation consists of the time derivative term and the gravity term as in (A.9) with the divergence term and the friction term which are the second and third summations in (A.3).

Notice the coefficient matrix is stationary because the nonzero elements (A.8) are stationary. One of the advantages of the wave continuity equation approach is the decoupling of the continuity equation and the momentum equation so that they can be solved sequentially, whereas in the primitive continuity equation they have to be solved simultaneously. Since the coefficient matrix is stationary, matrix inversion or matrix decomposition is required only once at the beginning of the simulation, which contributes to computational efficiency. (Latest version re-inverts the coefficient matrix at each iteration for a better accuracy and stability.) As explained in the next section, the momentum equation is solved without matrix operation and

thus as a whole the model is efficient from a computational point of view. (For a wet/dry version, the coefficient matrix is re-inverted whenever the dryness condition changes.)

Momentum Equation

The conservation form of the momentum equation for the *x*-direction can be expressed as

$$\frac{\partial q_x}{\partial t} + \frac{\partial u q_x}{\partial x} + \frac{\partial v q_x}{\partial y} + gH\frac{\partial \zeta}{\partial x} + \tau q_x = r_x \qquad \text{(A.10)}$$

where q_x is the unit flow in the *x*-direction, and r_x represents other terms shifted to the right hand side, such as the wind stress term and the Coriolis term. The gravity term in (A.10) can be treated implicitly or explicitly by weighting the values at two time levels:

$$w \cdot (gH \cdot \partial\zeta / \partial x)_{t+\Delta t} + (1-w) \cdot (gH \cdot \partial\zeta / \partial x)_t \qquad \text{(A.11)}$$

where *w*=1 corresponds to a totally implicit scheme, *w*=0 to an explicit scheme, and *w*=0.5 to a Crank-Nicholson scheme. Because the continuity equation is solved separately before the momentum equation, ζ at $t+\Delta t$ is available when the momentum equation is solved. Therefore the gravity terms for both current and future time levels are evaluated as if it were an explicit scheme.

The nonlinear terms are treated by the Picard iteration (Carey and Oden, 1986) in which there are two internal iterations at each time step. At the first internal iteration the solution is taken as an approximation to the future time level. For the second internal iteration the values at the half time step in the future can be approximated by

$$\zeta_{t+\Delta t/2} = (\zeta_t + \zeta^*_{t+\Delta t})/2 \quad \text{and} \quad q_{x,t+\Delta t/2} = (q_{x,t} + q^*_{x,t+\Delta t})/2 \qquad \text{(A.12)}$$

where the ones with * indicate solutions calculated in the first internal iteration. These values at the half time step are used for the nonlinear terms in the momentum equation and the divergence terms in the wave continuity equation. Notice that the two-time level scheme (A.7) for the first order time derivative is also positioned at the half time step in the future.

Using two time levels, the numerical equation for the momentum equation (A.10) can be written as

$$(q_{x,t+\Delta t} - q_{x,t})/\Delta t + 0.5 \cdot \{(\tau q_x)_{t+\Delta t} + (\tau q_x)_t\} = \bar{r}_x \qquad \text{(A.13)}$$

where $\bar{r}_x$ represents all the terms shifted to the right hand side. Then by rearrangement,

$$q_{x,t+\Delta t} = \{(1 - 0.5 \cdot \tau_t) \cdot q_{x,t} + \Delta t \cdot \bar{r}_x\}/(1 + 0.5 \cdot \Delta t \cdot \tau_{t+\Delta t}) \qquad \text{(A.14)}$$

where $\tau_{t+\Delta t}$ is the bottom friction factor at the future time level for which an approximation is used, which is calculated at the end of the first internal iteration.

Convective Diffusion Equation

The convective diffusion equation is expressed as

$$\frac{\partial C}{\partial t} + u\frac{\partial C}{\partial x} + v\frac{\partial C}{\partial y} - \frac{\partial}{\partial x}\left(D_x \frac{\partial C}{\partial x}\right) - \frac{\partial}{\partial y}\left(D_y \frac{\partial C}{\partial y}\right) = s \qquad \text{(A.15)}$$

where C is concentration or salinity, D_x and D_y are diffusion coefficients in the *x* direction and the *y* direction, and *s* is the source term. After applying Green's theorem to reduce the second order derivatives to the first order, the weighted residual form of Equation (A.15) becomes

$$\int_\Omega \frac{\partial C}{\partial t} \cdot \phi_i \cdot dA + \int_\Omega \left(u\frac{\partial C}{\partial x} + v\frac{\partial C}{\partial y}\right) \cdot \phi_i \cdot dA$$

$$+ \int_\Omega \left(D_x \frac{\partial C}{\partial x} + D_y \frac{\partial C}{\partial y}\right) \cdot \nabla \phi_i \cdot dA = \int_\Omega s \cdot \phi_i \cdot dA \qquad \text{(A.16)}$$

Equation (A.16) is converted to a numerical equation by the finite element procedure. A fully implicit scheme is used to solve the system of equations in which the convective terms and the diffusion terms are treated implicitly. For an element *e* consisting of nodes *i*, *j*, and *k*, the nonzero element on the diagonal can be written as

$$\{1 + \Delta t \cdot (\bar{u}_i \cdot b_i + \bar{v}_i \cdot c_i) + \Delta t \cdot (smD_x \cdot b_i \cdot b_i + smD_y \cdot c_i \cdot c_i)\} \cdot A_e / 3 \qquad \text{(A.17)}$$

where the time derivative term is lumped, $\bar{u}_i$ and $\bar{v}_i$ are the weighted averages of *u* and *v*, and smD_x and smD_y are the elemental sums of diffusion coefficients. The weighted average is computed by $\bar{u}_i = (2 \cdot u_i + u_j + u_k)/4$. For the off-diagonal nonzero elements, the equation is silmilar to (A.17) without the time derivative term. The contribution to the right-hand-side from node i of element e becomes $\bar{s}_i \cdot A_e / 3$.